

NEW YORK STATE GEOLOGICAL ASSOCIATION

60th Annual Meeting
October 8 & 9, 1988

FIELD TRIP GUIDEBOOK

James F. Olmsted
EDITOR

HOSTED BY:
THE CENTER FOR EARTH AND ENVIRONMENTAL SCIENCES
AND
THE CENTER FOR LIFELONG LEARNING

STATE UNIVERSITY COLLEGE
PLATTSBURGH, NEW YORK

NEW YORK STATE GEOLOGICAL ASSOCIATION

60th Annual Meeting

October 8 & 9, 1988

FIELD TRIP GUIDEBOOK

JAMES F. OLMSTED
EDITOR

HOSTED BY:

THE CENTER FOR EARTH AND ENVIRONMENTAL SCIENCES
AND
THE CENTER FOR LIFELONG LEARNING

STATE UNIVERSITY COLLEGE
PLATTSBURGH, NEW YORK

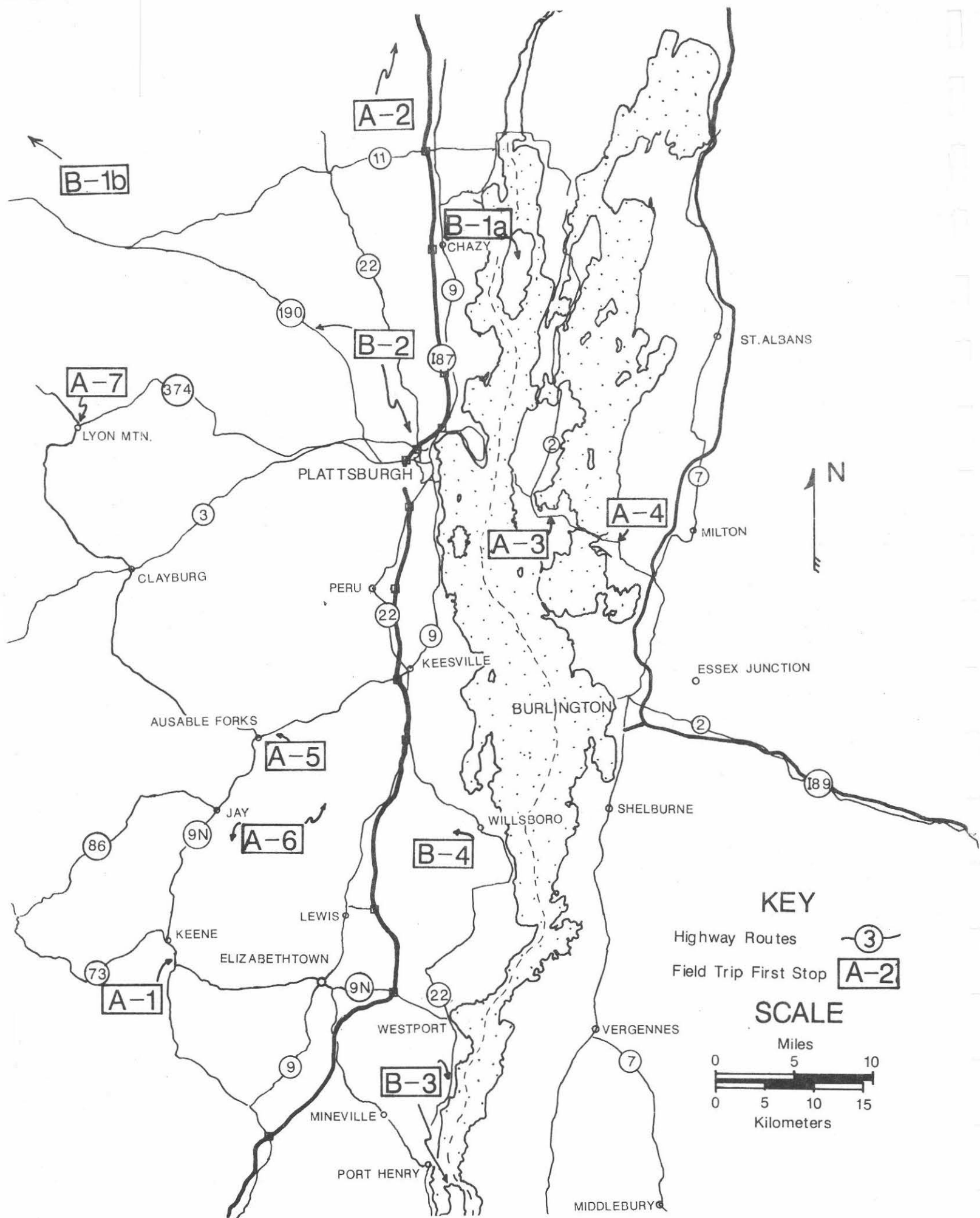
PREFACE

Upon recalling my first thoughts of a teaching job at SUNY at Plattsburgh two impressions seem to have been important to me. One was the prospect of living in a pleasant place with interesting landscape and variable climate and secondly some interesting geology at the doorstep. Someone who considers himself a field petrologist is certain to be impressed with the notion of living and teaching with the Green Mountains a few miles to the east and the Adirondacks nearby in the other direction. Those thoughts could not begin to represent the richness and variety of the geology and its history to be found in the Champlain Valley. The fact alone that this college is hosting the NYSGA for the second time in less than twenty years is evidence of the interest in the geology of the Lake Champlain region.

All of the trips that are offered here reflect work that has been accomplished within the last ten years. Many of these works include efforts of students who have surely benefitted greatly as have the authors and, we hope, so will you. That this region continues to be a spectacular geological laboratory is supported by the variety of descriptions included herein.

I would like to thank all of those who contributed to this volume, in particular Dave Franzi who personally prepared much of two of the trips and solicited another and helped me in many other ways. Thanks is also due to Carolyn Turner who assisted with some of the typing and to Dave Lawrence who supervised production of the volume. Thanks is also due to the other faculty in the CENTER who helped in many ways and to Yngvar Isachsen who provided the cover design. Finally recognition is due to Tom Wolosz of our department, current NYSGA president and to Kate Chilton of the Center for Lifelong Learning, Plattsburgh State who ran the meeting. One does not have to read very far to realize that a number of important conclusions are reported here. The authors are to be commended, and I also wish to thank them here.

Finally that this is the SIXTIETH annual meeting of this organization attests to the vitality of the NYSGA and of geology as a profession in New York State. In reviewing previous guidebooks I am impressed with them as a resource of geological literature for New York and adjacent areas. The NYSGA provides important academic and professional service to the region and truly deserves this recognition.



KEY

- Highway Routes 3
- Field Trip First Stop A-2

SCALE

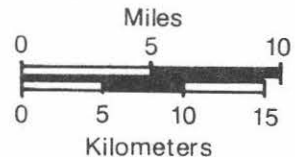


TABLE OF CONTENTS

SATURDAY

A-1	DIEMER, John A. & David A. FRANZI Aspects of the Glacial Geology of Keene and Lower Ausable Valleys, Northeastern Adirondack Mountains, New York.	1-27
A-2	EBY, G. Nelson Geology and Petrology of Mounts Johnson & St.Hilaire, Monteregian Hills Petrographic Province.	29-43
A-3	STANLEY, Rolfe S. Foreland Deformation as seen in Western Vermont,	45-82
A-4	MEHRTENS, Charlotte J. The Cambrian Platform and Platform Margin in Northwestern Vermont.	83-106
A-5	JAFFE, Elizabeth B. & Howard W.JAFFE Grenville Calc-silicate, Anorthosite, Gabbro and Iron- Rich Syenitic Rocks from the Northeastern Adirondacks.	107-131
A-6	WHITNEY, Philip R. & James F. OLMSTED Metasedimentary and Metavolcanic Rocks of the Ausable Syncline, Northeastern Adirondacks.	133-147
A-7	DAWSON, James C., MORAVEK, John R., GLENN, Morris F. & Gordon C. POLLARD Iron Industry of the Eastern Adirondack Region.	149-174

SUNDAY

- B-1a FRANZI, David A. & Thomas M. CRONIN 175-200
Late Wisconsin Lacustrine and Marine Environments in
the Champlain Lowland, New York and Vermont.
- B-1b RODRIGUES, Cyril G. 201-214
Late Quaternary Glacial to Marine Successions in the
Central St. Lawrence Lowland
- B-2 ISACHSEN, Y.W., KELLEY, W.A., SINTON, C.,
COISH, R.A. and M.T. HEISLER 215-243
Dikes of the Northeast Adirondack Region: Their
Distribution, Orientation, Mineralogy, Chronology,
Chemistry and Mystery.
- B-3 SELLECK, Bruce W. & David MacLEAN 245-261
Middle Ordovician Stratigraphy and Sedimentology -
Southern Lake Champlain Valley
- B-4 OLMSTED, James F. & Paul W. OLLILA 263-278
Geology of the Willsboro Wollastonite Mine

ASPECTS OF THE GLACIAL GEOLOGY OF KEENE AND LOWER AUSABLE VALLEYS, NORTHEASTERN ADIRONDACK MOUNTAINS, NEW YORK

JOHN A. DIEMER

Department of Geography and Earth Sciences
University of North Carolina at Charlotte
Charlotte, NC 28223

DAVID A. FRANZI

Center for Earth and Environmental Science
State University of New York at Plattsburgh
Plattsburgh, NY 12901

INTRODUCTION

The existence of Late Quaternary proglacial lakes in the Adirondacks has long been suspected (Taylor, 1897; Kemp, 1898; Ogilvie, 1902; Alling, 1916, 1919; Denny, 1974; Craft, 1976; Gurrieri, 1983; Diemer, *et al.*, 1984; Gurrieri and Musiker, 1988). Sedimentary deposits interpreted as dropstone-bearing varves and landforms interpreted as incised outlet channels, deltas and wave-formed beaches have been used as evidence for the existence of these intermontane proglacial lakes. On this trip, we propose to document some of these features in Keene and lower Ausable Valleys of the northeast Adirondacks. We will also discuss some constraints on the history of deglaciation of this region. Much work on the glacial geology of the northeast Adirondacks remains to be done and we hope you find this trip to be provocative.

FIELD AREA

Keene Valley extends northward 35 km (22 mi) from St. Huberts to Au Sable Forks (Figure 1). Waters from the Upper and Lower Ausable Lakes feed the East Branch of the Ausable River which flows northward through Keene Valley. The elevation of the valley floor is 340 m (1117 ft) at St. Huberts (Figure 2), 254 m (833 ft) at Keene (Figure 3), and 170 m (558 ft) at Au Sable Forks (Figure 4). The West Branch of the Ausable River originates to the south of Lake Placid (Figure 1). It drops in elevation from 488 m (1600 ft) to 305 m (1000 ft) as it flows through Wilmington Notch. At Haselton (Figure 5), the elevation is approximately 254 m (832 ft). The confluence with the East Branch of the Ausable River is at the town of AuSable Forks. Below the confluence, the Ausable River flows east-northeast for 25 km (15.5 mi) through the lower Ausable Valley and empties into Lake Champlain (elevation 29 m (95 ft)) at Ausable State Park.

The mountains bordering Keene Valley are highest at the southern end (e.g. Giant Mountain to the east of St. Huberts is 1410 m (4627 ft)) and decrease in elevation northward (e.g. Bald Mountain southeast of Au Sable Forks is 652 m (2139 ft) (Figure 1)). Major cols along the drainage divides separating Keene Valley from adjacent watersheds occur along lineaments. Two prominent sets of lineaments trend approximately NE-SW and NW-SE. The elevations of the cols decrease northward.



Figure 1. Location map taken from Lake Champlain 1:250,000 contour map, USGS (1949). Field trip stops are numbered. The areas covered by Figures 2 (St. Huberts), 3 (Keene), 4 (Au Sable Forks), and 5 (Black Brook) are indicated.

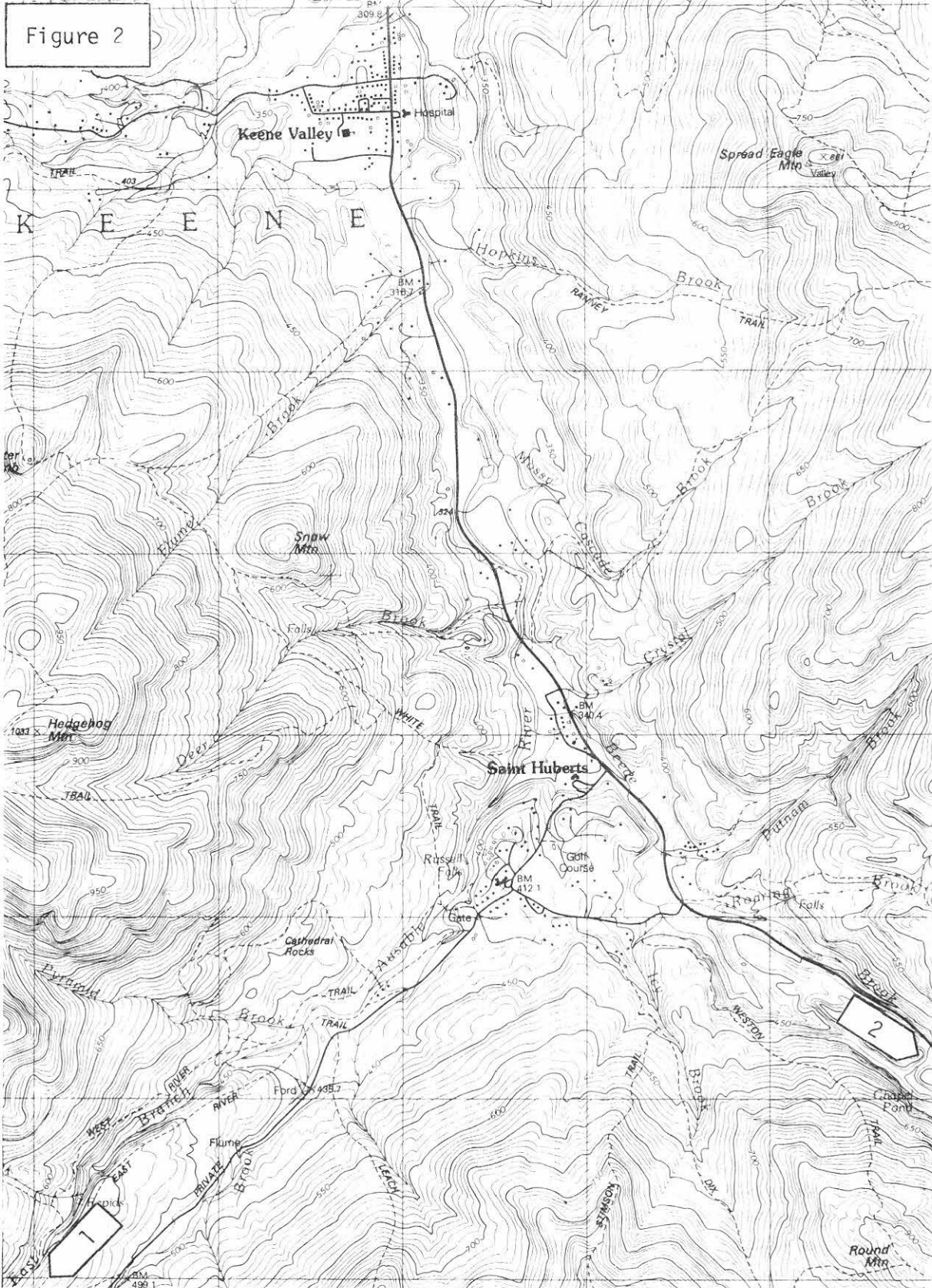


Figure 2. St. Huberts area in south end of Keene Valley, from Keene Valley, NY 1:25,000 metric map, USGS (1979). Grid overlay is 1 km by 1 km. Possible outlet channels and paleoflow directions are indicated by arrows.

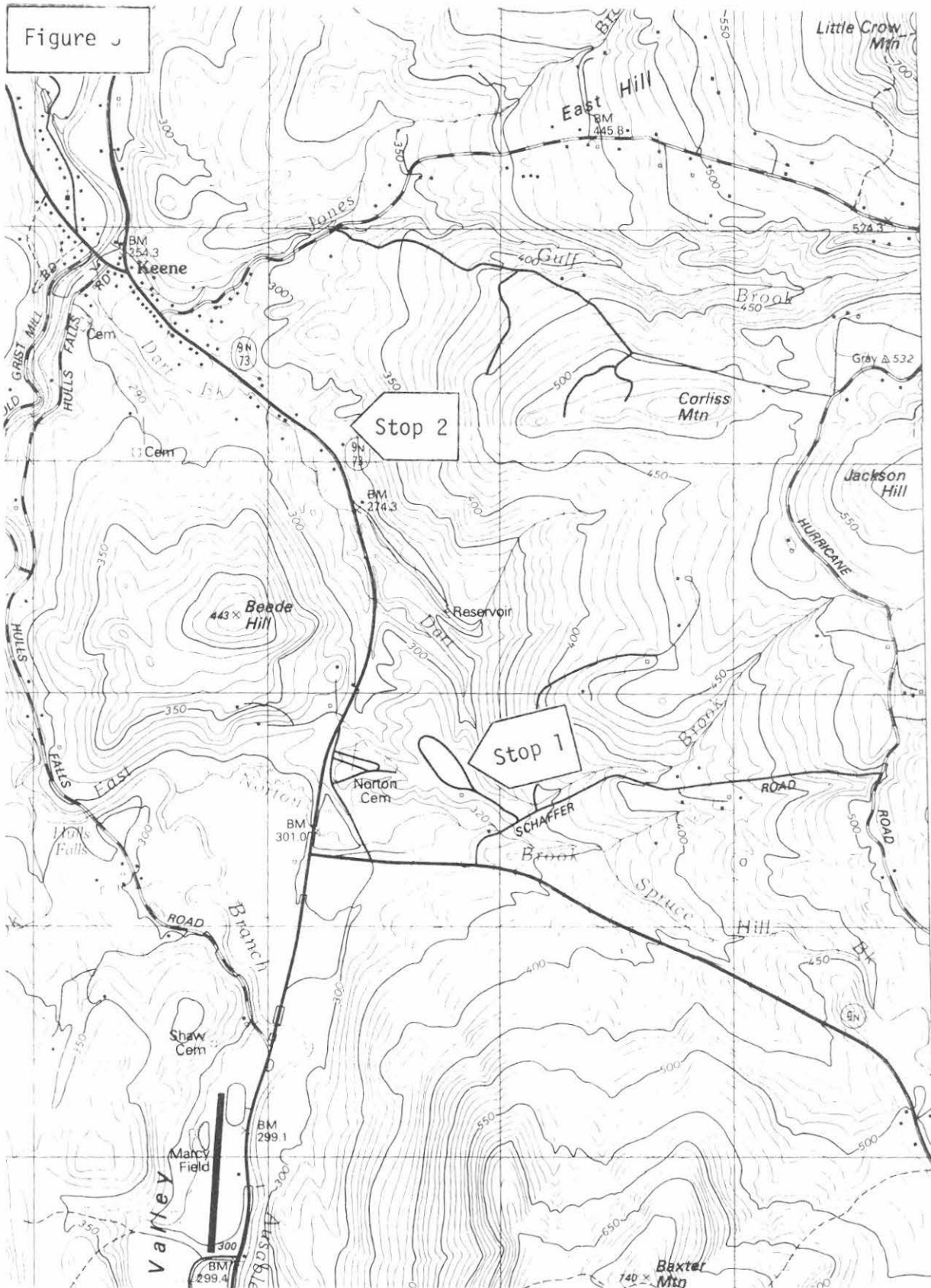


Figure 3. Keene area including Norton Cemetery, from Keene Valley, NY and Lake Placid, NY 1:25,000 metric maps, USGS (1979). Grid overlay is 1 km by 1 km. Stops 1 and 2 are indicated by large arrows.

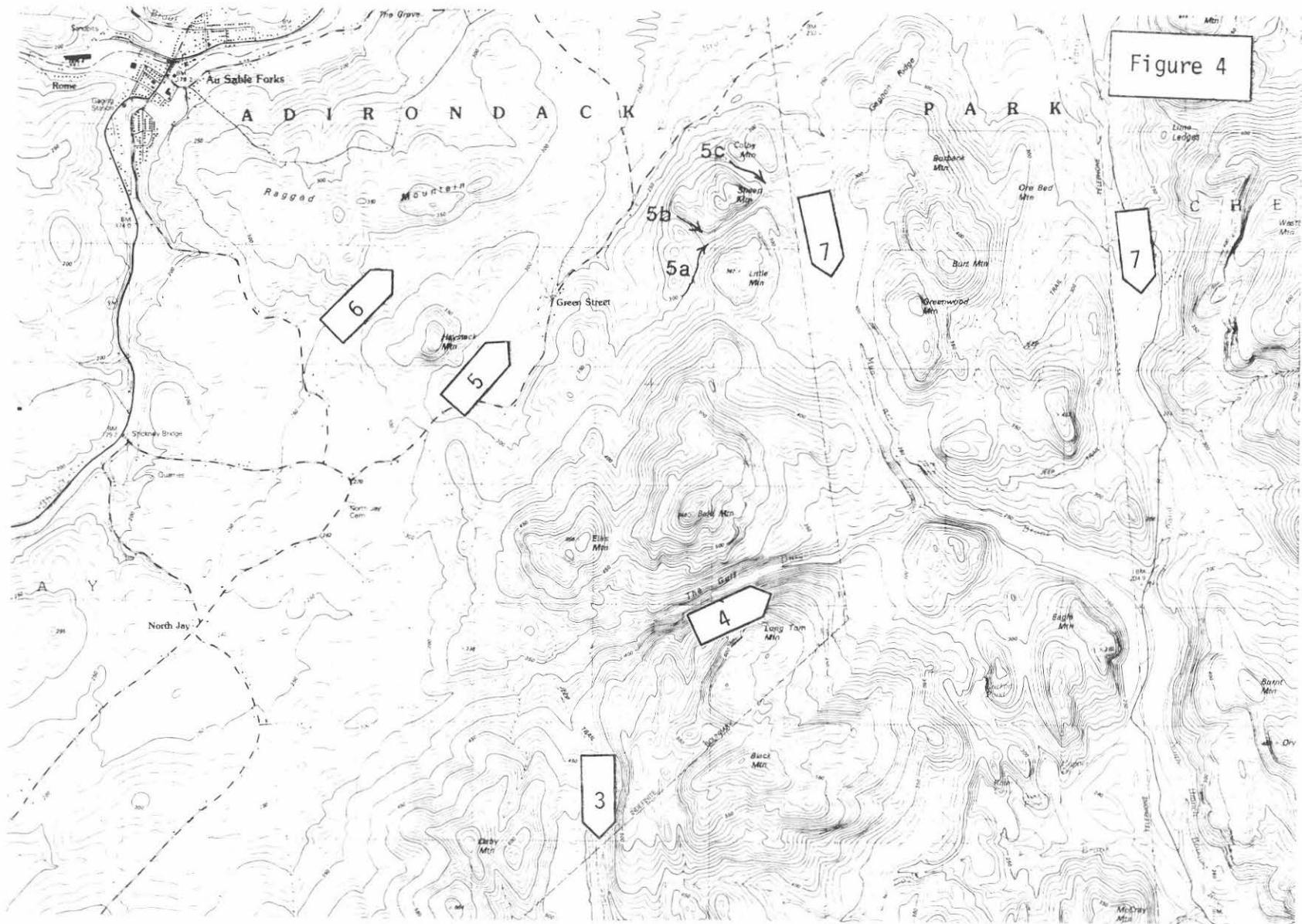


Figure 4. Ausable Forks area in northeastern Keene Valley, from Au Sable Forks, NY 1:25,000 metric map, USGS (1978). The grid overlay is 1 km by 1 km. Possible outlet channels and paleoflow directions are indicated by arrows.

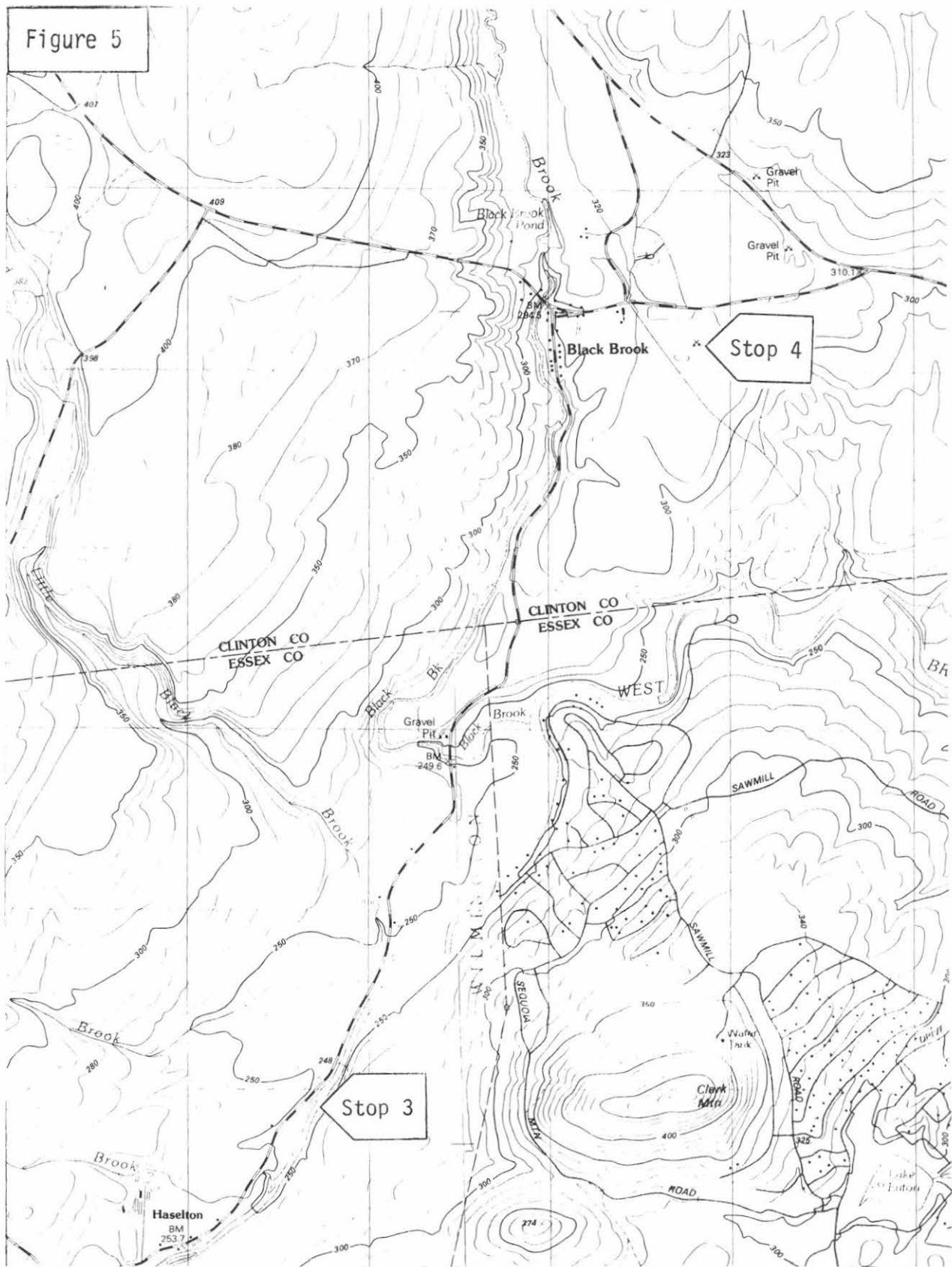


Figure 5. Black Brook and Haselton area in northwestern Keene Valley, from Au Sable Forks, NY and Wilmington, NY 1:25,000 metric maps, USGS (1978). Grid overlay is 1km by 1 km. Stops 3, 4 and 5 are indicated by large arrows.

PREVIOUS WORK

Alling (1916) argued that proglacial lakes existed in the central Adirondacks. Using altimeters to measure elevations, he correlated shoreline features such as deltas, wave-cut notches, beach ridges and lake outlet channels throughout Keene, Elizabethtown and Lake Placid valleys. He identified several lake stages, and proposed outlet channels for the Keene Valley lakes through the Ausable Lakes to the southwest (drainage channel 1 of Figures 2 and 6), Wilmington Notch and Newman Pass to the west, Chapel Pond to the southeast (drainage channel 2 of Figures 2 and 6), the South Gulf and Gulf to the east (drainage channels 3 and 4 of Figures 4 and 6), and several channels in the vicinity of Haystack and Ragged Mountains to the east (drainage channels 5, 6 and 7 of Figures 4 and 6). Alling (1916) proposed that outlet channels opened (in the order presented above) at progressively lower elevations as ice tongues occupying Keene and Elizabethtown Valleys retreated northward.

Denny (1974) worked mainly to the north of the area of this field trip. However, he mapped two ice front positions that trend southeast to the lower Ausable River Valley (ice-front positions 2 and 3; Denny, 1974). He argued that these NW-SE trending ice fronts resulted in ice-contact glaciofluvial deposits (e.g. at Black Brook), incised channels and proglacial lakes in northward draining valleys (e.g. Keene Valley). Denny (1974) proposed that Saranac River waters were diverted southward by the ice front (position 2) into the lower Ausable River Valley and were responsible for large deltaic deposits between the towns of Ausable Forks and Clintonville. He tentatively correlated these deltaic deposits to Lake Coveville. Denny (1974) identified broad terraces along the Ausable River at Keeseville and interpreted them as deltaic deposits that were built into Lake Fort Ann and the Champlain Sea.

Craft (1976) addressed the question of whether there was local glaciation in the Adirondacks during the Late Wisconsinan. He worked primarily in the High Peaks region at elevations above 610 m (2,000 ft). He found evidence for local glaciation in the form of striations and pebble orientations at high angles to regional ice flow directions, numerous cirques and associated moraines, and locally derived tills. Craft (1976) identified several high-elevation moraines produced by local valley glaciers in the High Peaks. He mapped only one moraine below an elevation of 610 m (2,000 ft). According to Craft (1976), part of this moraine can be traced northwestward from an elevation of 732 m (2400 ft) in Roaring Brook Valley (on the west side of Giant Mountain) down to an elevation of 366 m (1200 ft) near the village of Keene Valley (Figure 2). He interpreted the moraine complex as a product of a local glacier flowing west down Roaring Brook into the Keene Valley. Craft (1976) included a prominent bench at St. Huberts (approximate elevation 412 m (1350 ft), Figure 2) as part of the moraine complex.

Craft (1976) also noted the presence of lacustrine sediments, deltas and beaches at various locations in Keene Valley. An example of a delta mapped by Craft is at the outlet of Johns Brook on the north side of the village of Keene Valley (Figures 1 and 2). He proposed that local glaciers, including the one which occupied Johns Brook valley, flowed into the lake in Keene Valley and produced icebergs. He suggested this calving-terminus mechanism to explain the scarcity of local-glacier moraines at elevations below 610 m (2000 ft) in Keene Valley.

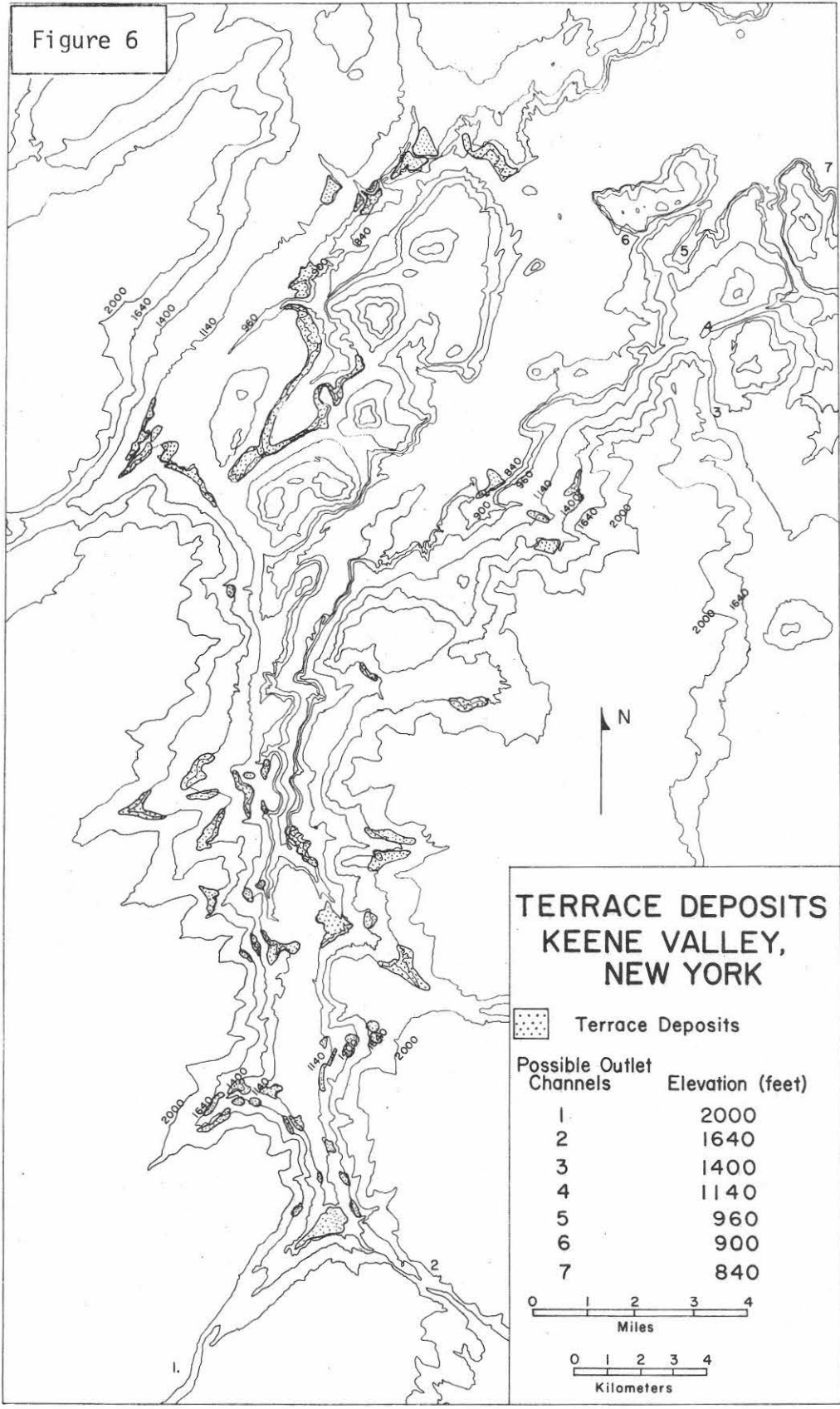


Figure 6

THIS STUDY

Terraces

Working from topographic maps and aerial photographs, Diemer *et al.* (1984) mapped constructional terraces on the side walls of Keene Valley (Figure 6). The purpose of the study was to evaluate whether the terraces recorded proglacial lake levels in Keene Valley as proposed by Alling (1916). The terraces are gently sloping features of variable size, commonly located along tributaries to both branches of the Ausable River. The range of surface elevations of some deposits with multiple terraces is large (e.g. the deposits at St. Huberts, Figures 2 and 6), however, relief on individual terrace treads is generally less than 10 meters. The surfaces of major terraces cluster near elevations of approximately 500 m (1640 ft), 427 m (1400 ft), 348 m (1140 ft), 293 m (960 ft), 274 m (900 ft) and 256 m (840 ft) (Figure 6). The maximum and minimum terrace elevations decrease northward (Figure 6). Terraces in the Ausable River floodplain (presumably Holocene in age) were not mapped.

Outlet Channels

Diemer *et al.* (1984) identified several deeply incised cols along the Ausable River drainage divide (Figure 6; Table 1), which they interpreted as outlet channels for proglacial lakes in the Keene Valley. Additional cols near Colby, Sheep, and Little mountains, which have threshold elevations of approximately 315 m (1033 ft), 308 m (1010 ft) and 296 m (970 ft), probably also acted as outlet channels (Figure 4). The distal ends of most of the outlet channels open onto broad, gently sloping sand plains (e.g. The Plains in the North Branch of the Bouquet River valley, 5 km (3 mi) north of Exit 32 on I-87). The distal ends of other channels are characterized by bedrock-lined lakes, interpreted by Alling (1916) as plunge pools (e.g. Copper, Nesbit and Round Ponds on the east flank of Black Mountain, Figure 4). The elevations of the outlet-channel thresholds generally correspond to the elevations of the terraces and also decrease northward (Figure 6; Table 1).

Facies

The terraces that have been examined contain a variety of facies (Diemer *et al.*, 1984). In places, horizontally bedded, interlaminated muds and clays in millimeter to centimeter thick laminae (i.e. rhythmites) occur at the bases of terrace deposits. Rhythmites are most common at elevations near the floor of Keene Valley. The overlying terrace deposits are composed of stratified sand and gravel that show a general increase in grain size and scale of sedimentary structures up-section. Near the base of the sand and gravel facies, the grain size is generally fine to very fine sand, sorting is moderate, and sedimentary structures include planar bedding, climbing ripple cross-laminations, and deformed bedding. In the upper part of the section, moderately well-sorted, planar bedded and trough cross-stratified, fine to medium sands are common. Climbing ripple cross-laminations and soft sediment deformation features are locally abundant. At the top of terrace deposits, trough cross-stratified and channelized, poorly sorted, coarse sands to gravels are common.

Table 1. Outlet channel locations and threshold elevations (from Diemer, *et al.*, 1984; see Figure 6).

Drainage Outlet	Location	Elevation	
		(meters)	(feet)
1	Upper Ausable Lake	610	2000
2	Chapel Pond	500	1640
3	South Gulf	427	1400
4	Gulf	348	1140
5	Southeast of Haystack Mountain	293	960
6	Between Haystack & Ragged Mts.	274	900
7	Mud Brook/Trout Pond	256	840

The coarse-grained deposits are typically separated from underlying fine-grained deposits by major erosion surfaces. Decimeter-scale, rounded, laminated mud clasts occur locally in the coarse-grained, channelized facies and in the underlying moderately sorted, medium sand facies.

Rhythmite exposures on the floor of Keene Valley that are not associated with terraces were also examined (Diemer, *et al.*, 1984). These rhythmites contain dropstones, soft sediment deformation features, and laminated sand layers. The latter have sharp basal contacts and grade upward from horizontally bedded sand to cross-laminated sands and asymmetrical ripples. The ripples are commonly draped by rhythmites. The rhythmites conformably overlie diamictons, composed of mud to boulder-size material, at some localities.

Origin of Terraces and Channels

The terraces examined to date are interpreted as deltaic deposits that prograded into proglacial lakes. The rhythmites found at the base of some terraces are interpreted as proximal lacustrine deposits. The moderately to well sorted, fine-grained sand deposits represent deltaic foreset beds. The poorly sorted, coarser-grained, upper portions of terraces are interpreted as fluvial topset beds, possibly formed in braided stream. The rounded mud clasts are reworked rhythmites from higher elevation lacustrine deposits, or reworked fine-grained floodplain material. The rhythmites which are not associated with terrace deposits are interpreted as distal glaciolacustrine deposits, possibly varves. The laminated sand beds within some rhythmite sequences are interpreted as tubidites. The diamictons underlying the rhythmites are either glacial tills or debris-flow deposits associated with a retreating ice front.

It is important to note that not all stratified terrace deposits are deltaic in origin. For example, some terraces are not located along side valley tributaries. An alternative depositional environment is subaqueous or subaerial glacial outwash, possibly in contact with ice. These deposits may resemble deltas, and thus, the sedimentology of the deposits must be understood to correctly interpret their origin. Distinguishing features of ice-contact outwash deposits are faults (due to melting of buried or adjacent ice), coarse grain size, and interbedded

diamictons (interpreted as glacial tills or sediment gravity flows originating from a nearby ice front). Furthermore, paleoflow indicators of glacial outwash would tend to be parallel to valley trend whereas paleoflow indicators of delta deposits would tend to be normal to the main valley trend.

If it is assumed that most of the mapped terraces are deltaic in origin, the northward decrease of terrace elevations can be interpreted as a product of ice front retreat of an ice lobe in Keene Valley. As the ice front retreated, progressively lower outlet channels were opened, allowing drawdown of the lake level to the elevations of the outlet channels. The falling lake levels controlled the elevations of active delta construction at the mouths of side valley streams. Deltas at higher elevations would therefore be older than deltas at lower elevations.

Outlet channels deeply incised into bedrock probably carried large (catastrophic?) discharges immediately after the channels opened. Sand plains at distal ends of outlet channels probably formed where flow diverged, either on outwash plains or into proglacial lakes.

The sequence of channels which opened as the ice front retreated as interpreted here is similar to the sequence proposed by Alling (1916). The first outlet channel drained southwestward through the valley presently occupied by the Ausable Lakes (drainage channel 1, Figure 2). Although we have not mapped terraces at the 610 m (2000 ft) level anywhere in Keene Valley, Alling (1916) does report the existence of terraces at that elevation restricted to the valley occupied by the Ausable Lakes. When the ice front retreated sufficiently to open the valley presently occupied by Chapel Pond, drainage switched to a southeastward flow (drainage channel 2, Figure 2). The lake elevation presumably dropped from 610 m (2000 ft) to 500 m (1640 ft) (using present-day elevations and not correcting for isostatic rebound).

The 500 m (1640 ft) lake level persisted until the ice front retreated northward sufficiently to open a channel through the South Gulf (drainage channel 3 (427 m (1400 ft)), Figure 4) and then the Gulf (drainage channel 4 (348 m (1140 ft)), Figure 4). The ice front then retreated to positions east of Au Sable Forks where outlets near Colby, Sheep, Little and Haystack mountains (drainage channels 5a (315 m (1030 ft)), 5b (308 m (1010 ft)), 5c (296 m (970 ft)) and 6 (274 m (900 ft)), Figure 4) controlled lake levels. Meltwater from proglacial lakes in the Saranac River watershed may have built the terraces in the vicinity of Black Brook (Figure 5) at the time the ice occupied these positions.

The ice front then retreated down the lower Ausable River Valley sufficiently so that the drainage channels along Mud Brook and Trout Pond (drainage channel(s) 7 (256 m (840 ft)), Figure 4) controlled the lake level. Ice recession from the highlands south of Keeseville allowed the regional proglacial lakes (and later the Champlain Sea) in the Champlain Valley to inundate the lower Ausable Valley. Terraces at 195 to 207 m (640 to 680 ft) near Clintonville and 152 to 165 m (500 to 540 ft) near Keeseville correspond to lakes Coveville and Fort Ann, respectively (Denny, 1974). Terraces at elevations below 107 m (350 ft), northeast of Keeseville, were graded to levels of the Champlain Sea (Chapman, 1937; Denny, 1974).

DISCUSSION

We agree with Alling (1916) that the cols near Ausable Lakes and Chapel Pond were early outlet channels for proglacial lakes in the Keene Valley. We have not, however, found evidence for westward drainage of the Keene Valley lakes through Wilmington Notch. The ice tongue occupying the West Branch of the Ausable River may have prevented westward drainage until after lower outlet channels opened at Chapel Pond, the South Gulf and the Gulf. A single lake occupying both the South Meadows/Lake Placid region and Keene Valley with a connection through Wilmington Notch, as proposed by Alling (1916), probably did not exist.

Westward drainage through Wilmington Notch was restricted to discharge from local, high-level proglacial impoundments or ice-marginal meltwater streams in the upper West Branch of the Ausable River when ice occupied the eastern end of the notch. This drainage interval is recorded by meltwater channels with plunge pools (e.g. Marsh, Winch, Cooperas, Warren, Coldspring and Owens ponds) east of Lake Placid. Ice recession from Wilmington Notch initiated eastward drainage from the Lake Placid area to proglacial lakes in the Keene Valley.

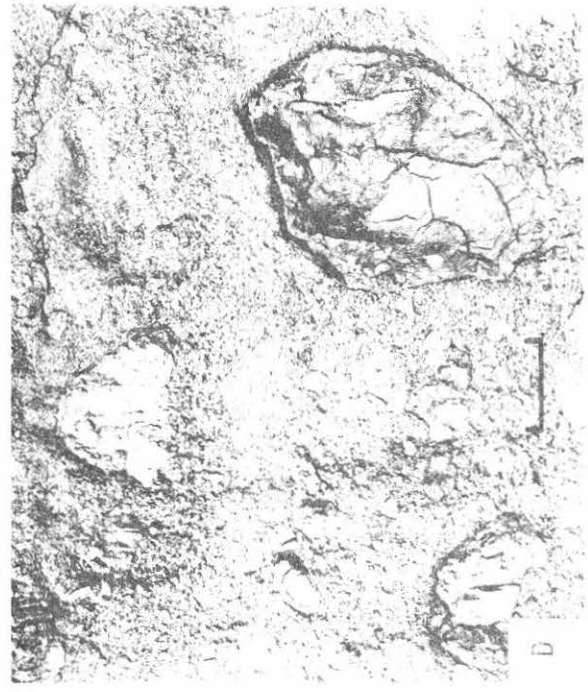
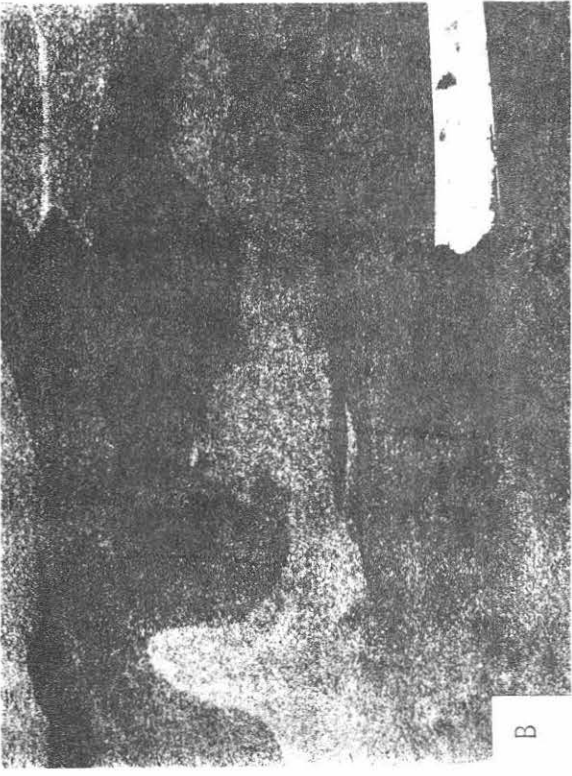
In contrast to Craft (1976), we interpret the terraces in the vicinity of St. Huberts as deltaic in origin rather than part of a moraine complex (Figures 2 and 6). These terraces could have been built where northward-flowing streams from the Ausable Lakes valley entered Keene Valley. The South Gulf outlet channel may have controlled the lake level into which the deltas were built. We did not recognize terraces above the 500 meter (1640 foot) level in the St. Huberts area. The features mapped by Craft (1976) at elevations above 500 meters in the Roaring Brook Valley on the west side of Giant Mountain may be debris-slide levees or lateral moraines associated with local alpine glaciation. The calving terminus mechanism proposed by Craft (1976) may have prevented the formation of alpine glacier moraines at lower elevations along Roaring Brook.

The evolution of the proglacial lakes occupying Keene and lower Ausable Valleys as interpreted here is based upon data acquired primarily from aerial photographs and topographic maps. Only a few terraces have been field-checked to date. Additional terraces need to be examined in order to determine their sedimentology. Only when the sedimentology is known can confident interpretations be made concerning the origins of the terraces and the deglaciation history of the region.

DESCRIPTIONS OF FIELD TRIP LOCALITIES

STOP 1. NORTON CEMETERY (Figures 1 and 3)

The borrow pits in the eastern part of the Norton Cemetery terrace contain stratified sand and gravel deposits. In the lower parts of the pits, horizontally stratified, trough cross-stratified and cross-laminated fine to medium sands in bedsets decimeters thick are common (Figure 7A). Soft sediment deformation features are locally abundant (Figure 7B). The terrace deposit coarsens upward to trough cross-stratified and channelized sands and gravels (Figure 7C). Channels are decimeters to a meter or so deep and meters wide. Channels are filled with either stratified or massive sands and gravels (e.g. Figure 7C). Channel margins have variable dips including nearly vertical (Figure 7C).



Near the top of the Norton Cemetery terrace deposit, a sharp erosion surface is overlain by trough and planar cross-stratified sands and boundary gravels filling small channels. The channels intercut and are decimeters deep and meters wide. A concentration of boulders occurs immediately above the sharp erosion surface. Rounded, laminated, mud clasts occur locally both above and below the sharp erosion surface (Figure 7D).

The terrace deposits are interpreted as a upwardly coarsening delta deposit. The lower part of the sequence consists of delta foreset beds with subaqueous channels, partly filled by sediment gravity flow deposits, at their upper ends. Steeply dipping channel margins may be due to channel incision into a frozen substrate. The prominent erosion surface is interpreted as the contact between delta foreset and fluvial topset beds. The trough and planar cross-stratification above the erosion surface are interpreted as the product of deposition by migrating dunes and small bars. The abundant intercutting channel forms and bar remnants suggest a braided stream origin. Rounded, laminated mud clasts are interpreted as either reworked, higher-level, lacustrine rhythmites or as floodplain muds.

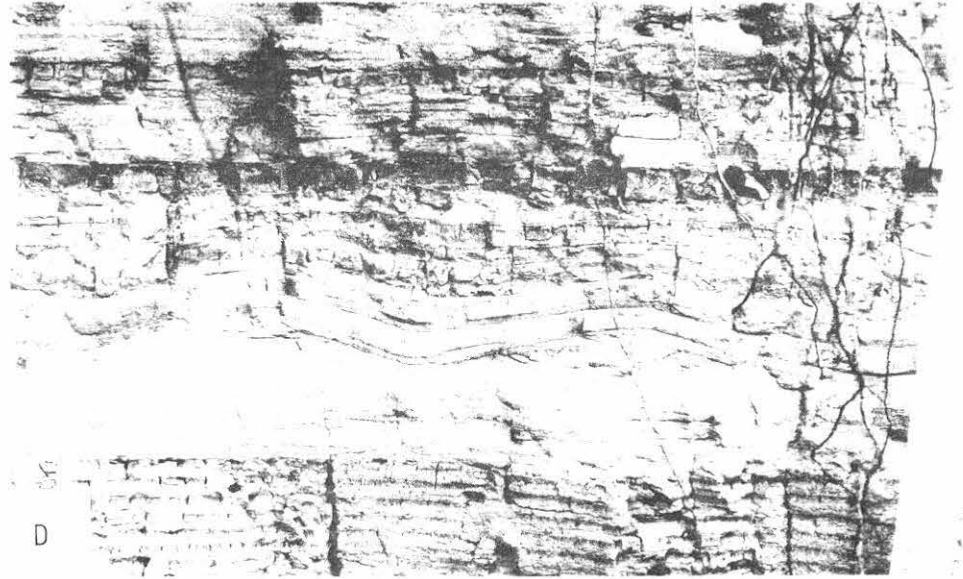
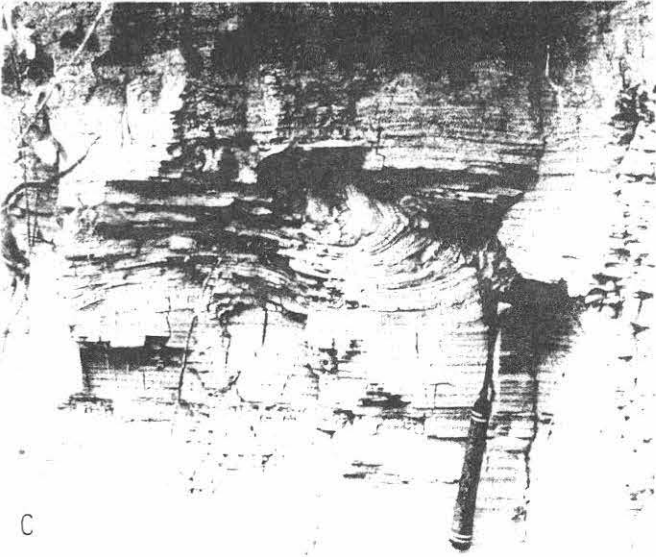
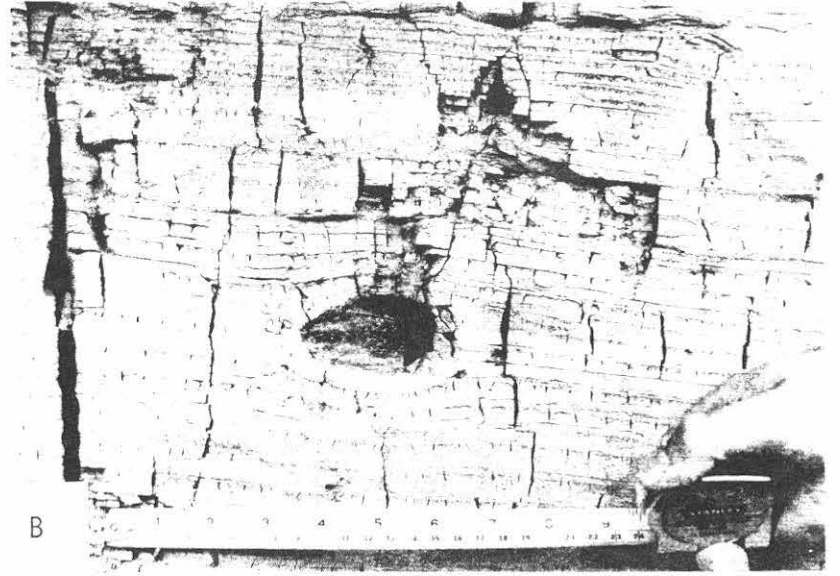
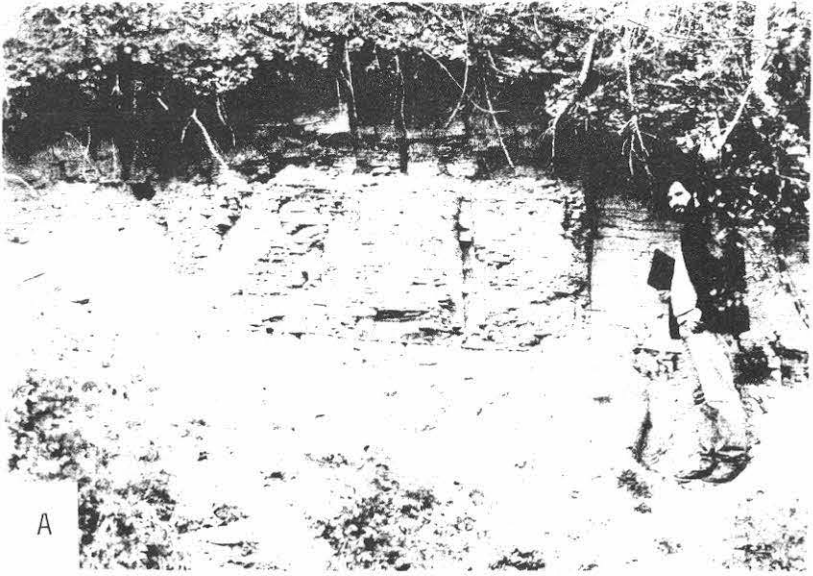
A second locality at Stop 1 is at the end of the access road to Norton Cemetery. The access road to the south of the cemetery entrance has been closed as a result of slumping. In the landslide scar, climbing ripple cross-laminated very fine sand with abundant mud drapes can be seen. The bedding has been disturbed, either by soft-sediment deformation or by road construction. These sediments are the lowest accessible terrace deposits and are interpreted as the distal portion of delta foresets. A spring line marking the contact with underlying interlaminated muds and clays (rhythmites) is located a few meters downslope. The rhythmites are centimeter-scale and interpreted as lacustrine deposits formed in a setting close to a sediment source (i.e. a side valley tributary). Hence the rhythmites are interpreted as delta toset beds.

Figure 7A: Horizontally stratified, trough cross-stratified and cross-laminated fine to medium sand coarsening up to stratified very coarse sand and gravel. Photo is from lower part of borrow pit, east side of Norton Cemetery terrace. Scale bar is 10 cm.

Figure 7B: Soft sediment deformation features in fine to medium sands. Location and scale is the same as for Figure 7A.

Figure 7C: Coarsening upward sequence in borrow pit, east side of Norton Cemetery. Note cross-stratified fine sand at base of outcrop, large channel form midway up outcrop, and stratified sand and gravel near top of outcrop. The channel form has low slope margin on left and steep margin on right. A prominent erosion surface truncates the massive channel fill and is overlain by a concentration of rounded boulders. Scale bar is 1 m.

Figure 7D: Rounded, mud clasts in a stratified sand and gravel deposit. Location is a small pit used as a trash dump to the north of the borrow pit in Figures 7A, 7B and 7C. Scale bar is 10 cm.



STOP 2. D.O.T. SAND AND GRAVEL PIT, KEENE, N.Y. (Figure 3)

The Department of Transportation operates a sand and gravel pit 1 km to the south of Keene, N.Y. The sediments are composed of stratified sands and gravels interbedded with diamictons. Grain size ranges from sand to boulders in both the stratified gravels and the diamicton. These sediments are interpreted as ice-contact glacial outwash in origin.

STOP 3. RHYTHMITE SEQUENCE AT HASELTON, N.Y. (Figure 5)

The sediments at Stop 3 are composed of a diamicton overlain by a rhythmite sequence. The diamicton contains boulders as large as 1 meter (Figure 8A). The top of the diamicton has decimeters of relief and is conformably overlain by millimeter to centimeter thick interlaminations of mud and clay (rhythmites). Dropstones are common (Figure 8B). The rhythmites are typically horizontally bedded, but may be locally deformed (Figure 8C). In places, rhythmites are interbedded with cross-laminated sands which have sharp basal contacts and grade upward to asymmetrical ripple forms draped by mud laminations (Figure 8D). The sediments at this stop are interpreted as glacial till or debris-flow deposits at the base (diamicton), overlain by lacustrine sediments (rhythmites). The rhythmites may have accumulated in a setting distant from a sediment source as they are fine grained. The interbedded cross-laminated sand layers may be due to turbidity currents. The deformed bedding may be a result of soft-sediment deformation on a low slope.

Figure 8A: Roadcut on Black Brook Road 100 meters south of private airfield. Sequence comprises diamicton (at feet of geologist) overlain by rhythmite sequence (at knees of geologist). Rhythmites are horizontally bedded and approximately 1 meter thick at this locality.

Figure 8B: Dropstone in rhythmites. Same location as Figure 8A. Scale is in inches and centimeters.

Figure 8C: Deformed bedding in rhythmite sequence. View is parallel to the fold axis. Overlying rhythmites are undeformed. Same location as Figure 8A. Hammer for scale.

Figure 8D: Laminated sand bed interbedded with rhythmites. Base of sand is sharp. Sand is horizontally laminated at base and grades up to cross-laminations and asymmetrical ripple forms. Rhythmites drape ripple forms. Same location as Figure 8A. Scale is in inches and centimeters.

STOP 4. BLACK BROOK SAND PLAIN (Figure 5)

The Black Brook sand plain is a terraced accumulation of stratified drift at the distal end of a bedrock gorge north of the village of Black Brook. The surface of the sand plain is roughly triangular in map view and ranges in elevation from 329 m (1080 ft) at the mouth of the gorge to 275 m (902 ft) at the West Branch of the Ausable River.

The exposures in a gravel pit 0.64 km (0.4 mi) east of Black Brook contain meter-scale beds of coarse sandy gravel to boulder gravel (Figure 9). The working face of the pit is oriented east-west and is approximately 40 m (130 ft) long and 4 to 6 m (13 to 20 ft) high. The surface elevation of the sand plain at this location is approximately 315 m (1033 ft). The lower unit consists of horizontally stratified, and trough and planar cross-stratified sandy gravel, the base of which is obscured by slumping. The sandy gravel is overlain by a 2.0 to 2.5 m (6.6 to 8.2 ft) thick, massively bedded, very coarse boulder gravel layer. The gravel contains boulders over 1.5 m (5.0 ft) in diameter, some of which are crudely imbricated. The gravel unit can be traced laterally across the working face of the pit. The gravel is overlain by 1.0 to 1.2 m (3.0 to 4.0 ft) of cross-stratified sandy gravel. The cross strata are centimeters to decimeters thick and commonly extend from the top to the bottom of the unit. Paleocurrent indicators indicate southward to southeastward flow throughout the section.

The Black Brook terrace deposits are interpreted as a fluviodeltaic complex that was built into falling levels of proglacial lake in the lower Ausable Valley (Figure 10). Base level was probably controlled by the outlet channels in the vicinity of Colby, Sheep, Little, and Haystack mountains (outlet channels 5a, 5b, 5c, and 6, Figure 4).

The sand and gravel deposits at Stop 4 are probably glaciofluvial in origin and may represent deltaic topset beds. The sandy gravel facies probably represents fluvial deposition under near average meltwater discharges through the bedrock channel north of Black Brook. The boulder gravel facies is interpreted as a high-energy, catastrophic flood deposit. Discharge of this magnitude may have been produced by the diversion of outflow from lakes in the Saranac Valley through the Black Brook channel (i.e. a limnic hlaup).

STOP 5. (OPTIONAL) DIAMICTONS NEAR AUSABLE FORKS (Figure 5)

This stop includes roadside exposures along Ausable Drive, approximately 2.4 km (1.5 mi) southwest of Ausable Forks. The sediments consist of massive to crudely stratified diamicton with thin sand, gravel and silt interbeds. The diamicton beds are commonly decimeters to meters thick, light colored and have sandy matrices. The sandy interbeds are thin (centimeter-scale) and discontinuous and are either nonstratified or contain horizontal or ripple-drift laminations. The bedding is subhorizontal but may be deformed locally. These deposits probably accumulated in a ice-marginal, subaqueous environment.

STOP 6. DELTAIC DEPOSITS NEAR CLINTONVILLE (Figure 1)

The gravel pit at Stop 6 is located on an extensive sand plain on the north side of the Ausable Valley between Clintonville and Ausable Forks (Figure 1). The surface of the sand plain slopes southward from approximately 204 m (670 ft) at its northern margin to 198 m (650 ft) near the Ausable River.

The lower portion of the pit contains approximately 5 to 6 m (16 to 20 ft) of southwardly dipping, fine to medium sand and sandy silt foreset beds. The bedsets are centimeters to decimeters thick and commonly contain horizontal laminations

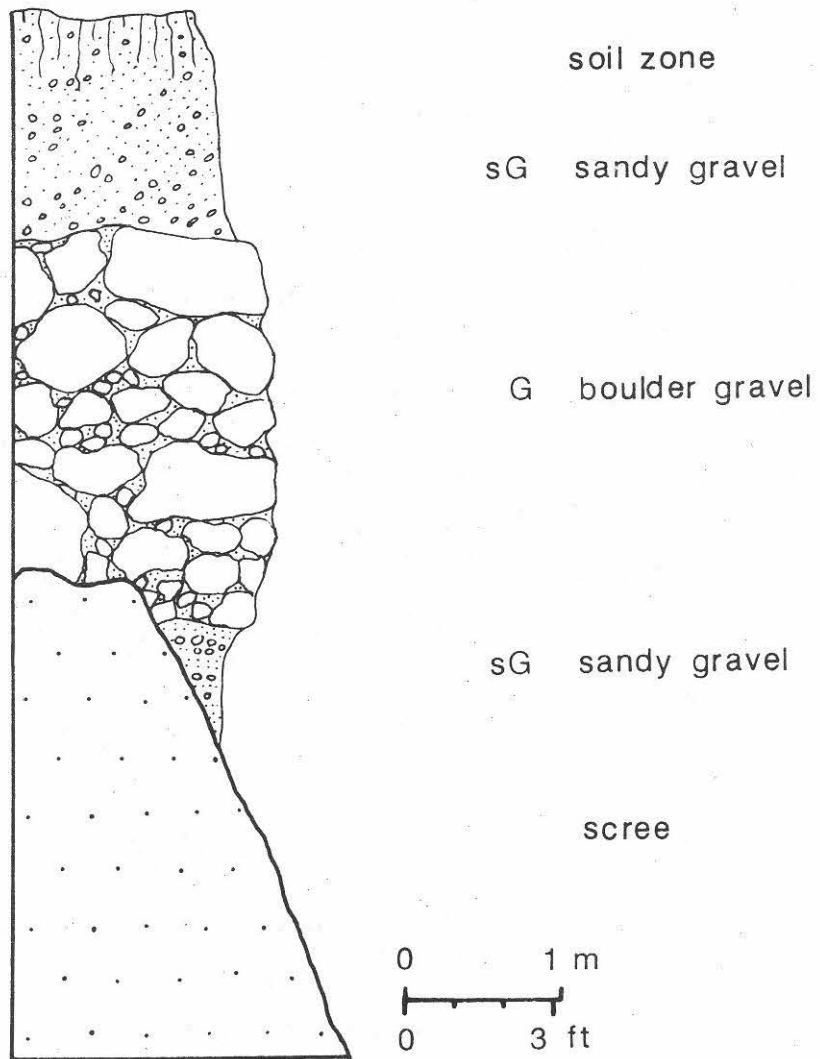


Figure 9. Stratigraphy at the gravel pit near Black Brook.

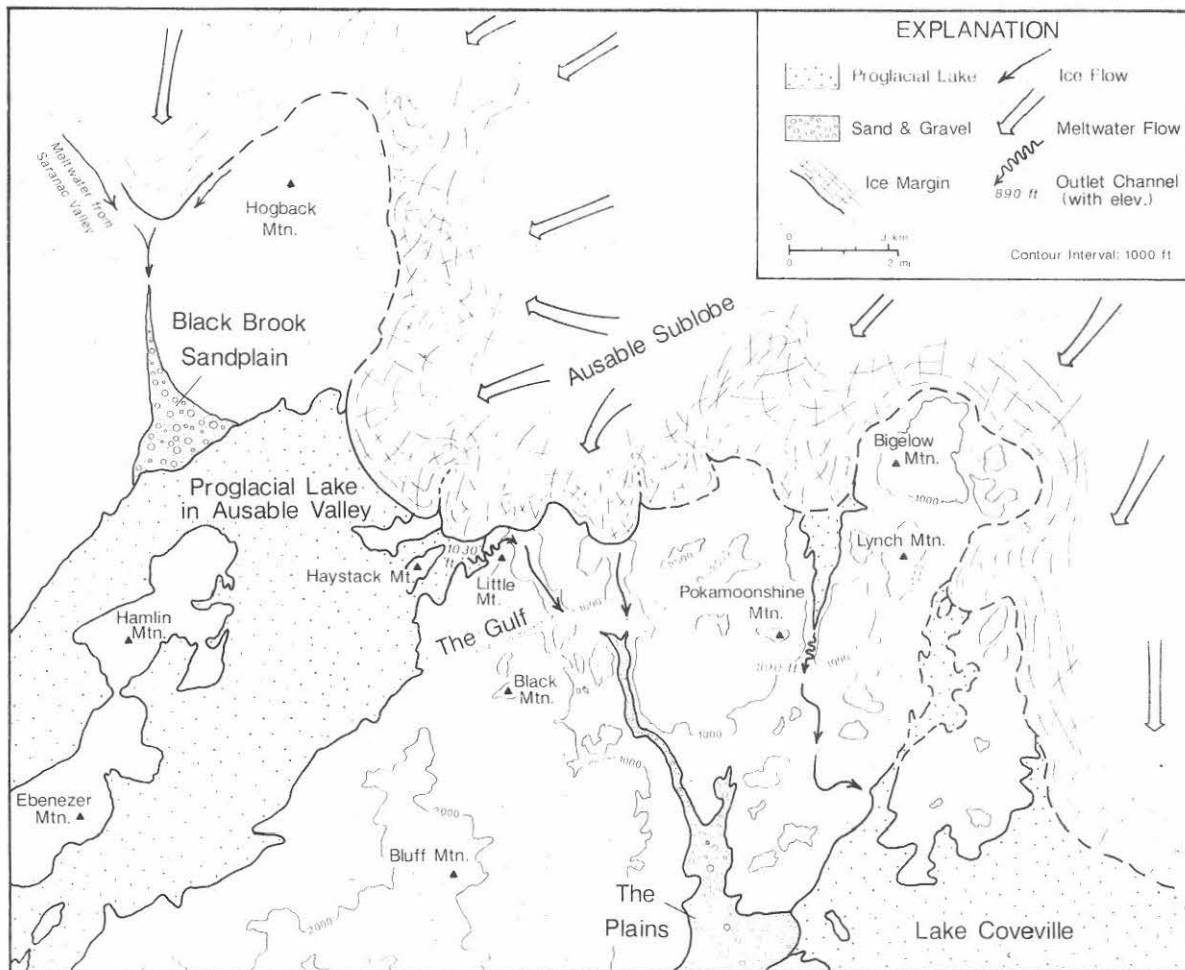


Figure 10. Inferred distribution of proglacial lakes and ice margins during the deposition of the Black Brook sand plain. Lake level in the Ausable Valley is controlled by an outlet channel north of Little Mountain. Meltwater from lakes in the Ausable Valley probably contributed to deltaic sedimentation at The Plains in the North Branch of the Bouquet River Valley.

and ripple-drift cross-laminations. Thin silty deposits occur locally as draped laminae over ripple forms. The upper portions of the foreset beds are truncated and overlain by 1.0 to 1.5 m (3.0 to 5.0 ft) of horizontally stratified and trough and planar cross-stratified sand and gravel.

The sediments at the Clintonville gravel pit are interpreted as deltaic in origin. The erosional surface between the lower sandy facies and the upper gravel facies represents the contact between the subaqueous foreset beds and the fluvial topset beds. The elevation of the topset-foreset contact is approximately 198 m (650 ft) which indicates that deltaic sedimentation was graded to the level of Lake Coveville in the Champlain Valley (Denny, 1974). Southward-flowing meltwater streams from ice in the Little Ausable drainage basin north of Arnold Hill (Figure 1) provided much of the deltaic sediment in the eastern portion of the sand plain. The western portion of the sand plain was probably built by eastwardly flowing streams from the upper Ausable drainage basin. Southward drainage from proglacial lakes in the Saranac River Valley into the lower Ausable Valley via the Black Brook channel (Stop 4) may have contributed to delta construction near Ausable Forks (Denny, 1974).

STOP 7. LANDSLIDE SCAR ON THE AUSABLE RIVER AT KEESEVILLE (Figure 1)

The section at Keeseville is exposed in a landslide scar on the south bank of the Ausable River at Keeseville. The river is deeply incised into deltaic terrace deposits which Denny (1974) correlated with Lake Fort Ann in the Champlain Valley. The surface elevation of the terrace is approximately 155 m (510 ft).

The base of the section consists of massive, compact, calcareous, gray diamicton with a silty to clayey silt matrix. The base of the diamicton is obscured by colluvium. The upper surface of the unit has a few centimeters of relief and is draped by 0.3 to 0.5 m (1.0 to 1.5 ft) of silt and clay rhythmites. The rhythmite sequence contains 11 silt-clay sediment couplets. The rhythmites are conformably overlain by approximately 6 m (20 ft) of fine to medium sand which coarsens upward to gravelly sand near the terrace surface. Spring sapping at the sand-rhythmite contact is responsible for slumping in the overlying sand unit.

The sediments at the Keeseville section record the ice recession from the mouth of the Ausable Valley. The diamicton is interpreted as a basal till and thus represents an interval of ice cover. The rhythmites are interpreted as varved lacustrine deposits that record the initial, deglaciation of the lower Ausable Valley and its subsequent inundation by Lake Coveville. The rhythmites, therefore, were probably deposited contemporaneously with the Lake Coveville deltas near Clintonville (Stop 6).

The overlying sandy deposits represent deltaic sedimentation by eastward-flowing streams from the Ausable Valley into Lake Fort Ann. Regional lake level fell approximately 43 m (140 ft) in the Champlain Valley with the initiation of Lake Fort Ann. If the rhythmites are assumed to be Lake Coveville varves and the overlying sandy facies to be part of the Lake Fort Ann delta, then the time between the deglaciation of the mouth of the Ausable Valley and the initiation of Lake Fort Ann was about 11 years. The ice-front in the Champlain Valley may have receded northward to the mouth of the Saranac River at the time Lake Fort Ann was established (Denny, 1974).

ACKNOWLEDGEMENTS

We thank Jim Olmsted and Bob Dineen for helpful comments in the field. Critical readings by Lawrence Gillett, Kate Collie and Dorothy Merritts are much appreciated. Field work was supported by Franklin and Marshall College and SUNY-Plattsburgh.

REFERENCES CITED

- ALLING, H.L., 1916, Glacial lakes and other glacial features of the central Adirondacks: Geol. Soc. America Bull., v.27, p.645-672.
- , 1919, Pleistocene geology of the Lake Placid Quadrangle: N.Y. State Museum Bulletin, v.211-212, p.71-95.
- CRAFT, J.L., 1976, Pleistocene local glaciation in the Adirondack Mountains, New York (Ph.D. dissert.): University of Western Ontario, 226p.
- DENNY, C.S., 1974, Pleistocene geology of the northeast Adirondack region, New York: U.S. Geol. Surv. Prof. Paper 786, 50p.
- DIEMER, J.A., OLMSTED, J.F., and SUNDERLAND, L., 1984, The evolution of a high-altitude glacial lake, Keene Valley, New York: Geol. Soc. Amer. Abstr. with Prog., v.16, No.1, p.12.
- GURRIERI, J.T., 1983, Surficial geology of the Saranac Lake Quadrangle, New York (M.S. thesis): University of Connecticut, 86p.
- GURRIERI, J.T., and MUSIKER, L.B., 1988, Late Wisconsinan deglaciation in the lake belt region of the northern Adirondack Mountains, New York: Geol. Soc. Amer. Abstr. with Prog., V.20, No.1, p.24.
- KEMP, J.F., 1898, The geology of the Lake Placid region: N.Y. State Museum Bulletin, v.21, p.21.
- OGILVIE, I.H., 1902, Glacial phenomena in the Adirondacks and Champlain Valley: Jour. Geol., v.10, p.397-412.
- TAYLOR, F.B., 1897, Lake Adirondack: Am. Geol., V.19, p.392-396.

ROAD LOG

CUM. MILES	MILES F.L.P.*	DESCRIPTION
0.0	0.0	Assemble in the west parking lot of Hudson Hall on the P.S.U.C. campus. Leave the parking area, turn right at the entrance and proceed northwestward on Broad St.
0.4	0.4	Intersection of Broad and Cornelia streets. Bear left onto Cornelia and proceed westward.
1.1	0.7	Junction I-87 (Northway) North; Continue westward on Cornelia St. under Northway overpass.
1.3	0.2	Junction I-87; Turn left onto entrance ramp and follow the signs for I-87 South. Proceed southward on I-87 to Exit 31 at Elizabethtown (Approximately 45 mi). Turn right onto the exit ramp and proceed to Route 9N. Reset road log at the junction of the Exit 31 ramp and Route 9N.
0.0	0.0	Turn right at the end of the exit ramp and proceed westward on Route 9N toward Elizabethtown.
3.8	3.8	Cross Bouquet River.
4.2	0.4	Intersection of Routes 9N and 9 in Elizabethtown. Continue westward on Route 9N.
14.1	9.9	Intersection of Route 9N and Schaffer Rd. Turn right onto Schaffer Rd. and proceed northward for 0.2 mi to the entrance of the gravel pit (STOP 1) on the west side of the road.
14.3	0.2	STOP #1. Norton Cemetary. Following the discussions turn around and proceed southward on Schaffer Road to Route 9N.
14.5	0.2	Intersection of Schaffer Rd. and Route 9N. Turn right onto Route 9N and proceed westward.
14.9	0.4	Intersection of Routes 9N and 73. Turn right and proceed northward on Routes 9N and 73 (combined).

*From last point

CUM. MILES	MILES F.L.P.	DESCRIPTION
16.1	1.2	STOP #2. D.O.T. Gravel Pit. Continue northward on Routes 9N and 73 following the discussions at this stop.
16.7	0.6	Routes 9N and 73 diverge. Bear right and proceed northward on Route 9N.
19.7	3.0	Cross Styles Brook. Continue northward on Route 9N.
22.7	3.0	Enter the village of Upper Jay. Follow Route 9N through the village.
25.8	3.1	Enter the village of Jay. Continue northward on Route 9N.
26.2	0.4	Intersection of Routes 9N and 86. Turn left onto Route 86 and proceed northwestward toward Wilmington.
28.2	2.0	View of Beaver Bk. Valley and Whiteface Mt. Continue northwestward on Route 86.
29.1	0.9	Intersection of Route 86 and Bilhuber Rd. Turn right onto Bilhuber Rd. and proceed northward.
30.9	1.8	Intersection of Bilhuber Rd. and unmarked road. Turn right onto unmarked road and proceed northeastward. The road follows the West Branch of the Ausable River.
32.6	1.7	STOP #3. Rhythmites at Haselton. This will also be the LUNCH STOP. Continue northeastward toward Black Brook after lunch.
33.9	1.3	Cross Black Brook. The road turns northward to the village of Black Brook.
35.6	1.7	Intersection of unmarked road and Silver Lake Rd. at Black Brook. Turn right and proceed eastward on Silver Lake Rd.
35.7	0.1	Stop sign, continue eastward on Silver Lake Rd.
36.1	0.4	STOP #4. Black Brook sand plain. The entrance to the gravel pit is on the south side of the road. Continue eastward on Silver Lake Rd. to Ausable Forks after the discussions at this stop.

CUM. MILES	MILES F.L.P.	DESCRIPTION
---------------	-----------------	-------------

39.6	3.5	Intersection of Silver Lake and Golf Course roads. Follow inset road log to optional stop #5 or turn left onto Golf Course Rd. and follow main road log.
------	-----	--

CUM. MILES	MILES F.L.P.	DESCRIPTION
---------------	-----------------	-------------

0.0	0.0	Turn right onto Golf Course Road and proceed southward.
-----	-----	---

0.2	0.2	Intersection Golf Course Road and Route 9N at Ausable Forks. Continue southward on Route 9N.
-----	-----	--

0.4	0.2	Intersection of Route 9N and Church St. Turn right and proceed westward on Church St.
-----	-----	---

1.2	0.8	Intersection Church St. and Ausable Drive. Turn left and proceed southward on Ausable Drive.
-----	-----	--

2.0	0.8	STOP #5. (OPTIONAL) Diamicton Exposures. Turn around and follow the inset road log in reverse order to the intersection of Golf Course and Silver Lake roads.
-----	-----	---

41.5	1.9	Intersection of Golf Course and Palmer Hill roads. Bear right and proceed eastward on Palmer Hill Road. The road traverses the Lake Coveville deltas described by Denny (1974).
------	-----	---

43.4	1.9	STOP #6. Lake Coveville Delta. The entrance to the gravel pit is on the south side of the road. Continue eastward on Palmer Hill Rd. after the discussions at this stop.
------	-----	--

44.4	1.0	Intersection of Palmer Hill and Harkness-Clintonville roads. Turn right (sharply) and proceed southward to Clintonville.
------	-----	--

45.6	1.2	Intersection of the Harkness-Clintonville Rd. and Route 9N. Turn left and proceed eastward on Route 9N.
------	-----	---

45.8	0.2	Intersection of Route 9N and small road to the village of Clintonville. Turn right onto the side road and proceed to the bridge across the Ausable River.
------	-----	---

CUM. MILES	MILES F.L.P.	DESCRIPTION
46.2	0.4	Bridge across the Ausable River at Clintonville. Turn right across the bridge to the Dugway Road intersection (0.1 mi).
46.3	0.1	Dugway Road Intersection. Turn left and proceed eastward on Dugway Road.
51.3	5.0	Intersection of Dugway and Augur Lake roads. Turn left and continue eastward on Augur Lake Road.
51.6	0.6	I-87 overpass. Continue eastward on Augur Lake Rd. to the entrance of Keeseville Industrial Park (0.1 mi) on the north side of the road.
51.7	0.1	STOP #7. Landslide scar on the Ausable River. Continue eastward on Augur Lake Rd. after the discussions at this stop.
52.0	0.3	Intersection of Augur Lake Road and Route 9. Turn left and proceed northward on Route 9 to Plattsburgh.
54.7	3.0	Ausable Chasm
55.1	0.4	Surface of Champlain Sea delta (upper marine limit).
55.7	0.6	Surface of Champlain Sea delta (Port Kent Stage).
56.9	1.2	Entrance to Ausable Point State Park on the delta of the present Ausable River.
64.7	7.8	Skyway Plaza and Plattsburgh Air Force Base. Continue on northward on Route 9 to next traffic light.
65.0	0.3	Intersection of Route 9 and Elizabeth St. Turn left onto Elizabeth St. and proceed westward for 0.1 mi. Bear right onto Platt St. and continue westward.
65.4	0.4	Intersection of Platt and South Catherine streets. Turn right onto Catherine St. and proceed northward across the Saranac River.
65.9	0.5	Intersection of South Catherine and Broad streets. Turn left onto Broad St. and proceed westward toward the P.S.U.C. campus.
66.3	0.4	Intersection of Broad and Beckman streets. Hudson Hall is on the northwest corner of the intersection.

END LOG

GEOLOGY AND PETROLOGY OF MOUNTS JOHNSON & ST.-HILAIRE,
MONTEREGIAN HILLS PETROGRAPHIC PROVINCE

G. NELSON EBY
Department of Earth Sciences
University of Lowell
Lowell, MA 01854

INTRODUCTION

The Monteregian Hills petrographic province consists of a group of small igneous intrusions and associated dikes and sills which lie along a more or less linear East-West trend extending from the Oka carbonatite complex located 30 km west of Montreal to Mounts Shefford and Brome 70 km east of Montreal (Figure 1). These plutons cut a number of terranes: the Precambrian Grenville, the St. Lawrence Lowlands, and the folded rocks of the Appalachian orogen. Mount Megantic lies 100 km east of Mounts Shefford and Brome and its assignment to the Monteregian Hills province is somewhat problematical. Petrographically and chemically Mount Megantic shows stronger affinities with the White Mountain igneous province than with the Monteregian Hills. On this field trip we will visit two plutons located in the central part of the province which are representative of some of the major magmatic trends in the Monteregian Hills.

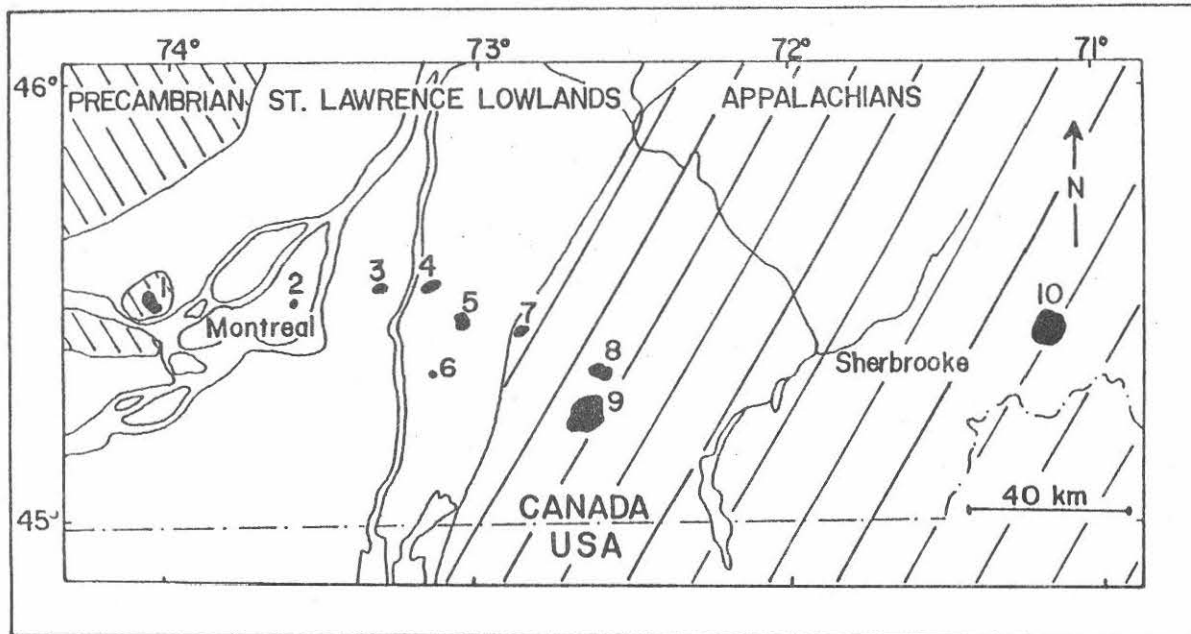


Figure 1. Location and generalized geologic setting of the Monteregian plutons. 1-Oka carbonatite complex, 2-Mt. Royal, 3-Mt. St. Bruno, 4-Mt. St.-Hilaire, 5-Mt. Rougemont, 6-Mt. Johnson, 7-Mt. Yamaska, 8-Mt. Shefford, 9-Mt. Brome, 10-Mt. Megantic

GEOLOGY AND GEOCHEMISTRY OF THE MONTEREGIAN HILLS

Geology and Petrography

Igneous activity in the Monteregian Hills is represented by a variety of magma types ranging from strongly silica undersaturated to silica saturated. There is a geographic pattern to the magmatism in that strongly silica undersaturated rocks are concentrated in the western half of the province while silica saturated rocks generally occur in the eastern half of the province. The general geology of the province has been described by a number of authors (e.g. Philpotts, 1974; Eby, 1987).

The Oka carbonatite complex is located at the western end of the province and consists of a core carbonatite which has been intruded by a variety of strongly silica-undersaturated rocks: okaite, melteigite, ijolite, and urtite. Alnoitic rocks also intrude the complex and the alnoitic phase of magmatism is confined to the Oka area. A recent review of the Oka complex, and a field trip guide for the Oka area, can be found in Gold et al. (1986).

Mounts Royal, Bruno, Rougemont, and Yamaska are mafic to ultramafic in character. The dominant lithologies are pyroxenite and gabbro, and in the field these two lithologies tend to be interlayered. This interlayering generally occurs at the outcrop scale so that map units show the dominant lithology. Mappable gabbroic units occur in all of these plutons and they often represent the later stages of igneous activity. None of the pyroxenite and gabbro units carry nepheline, although they are often slightly nepheline normative due to locally abundant amphibole, and quartz occasionally occurs in contact zones due to crustal contamination. Layering is often prominent due to the alignment of pyroxenes and plagioclases. This layering is at moderate to steep angles which has led to the conclusion that the rocks represent crystallization of the magma, in a convecting system, from the walls inward. There is occasional evidence for movement of material in the partly molten state, although the bulk of the rocks seem to have crystallized at their current level of emplacement. At Mounts Royal and Yamaska the gabbro-pyroxenite sequence is intruded by essexites and nepheline-bearing syenites which define a late stage, strongly silica undersaturated, period of magmatism. A recent review of the geology of Mounts Royal and Bruno can be found in Eby (1984). Detailed geologic maps for Mounts Bruno and Rougemont were published by Philpotts (1976). Field trip guides for Mounts Royal (Gelinas, 1972) and Rougemont (Philpotts, 1972) were prepared for the 1972 International Geological Congress.

At Mounts St.-Hilaire, Johnson, Shefford, and Brome the dominant mafic lithologies are gabbro, essexite, and diorite, pyroxenites are either absent or occur as minor components. Syenitic units, either quartz-bearing or nepheline-bearing are important components of these plutons. Mount St.-Hilaire can be conveniently divided into a western half consisting largely of gabbro and an eastern half consisting largely of nepheline- and sodalite-bearing syenites. Mount Johnson largely consists of essexite with an outer annulus of syenite and nepheline-bearing syenite. Mounts Shefford and Brome are found in close proximity and are geologically similar.

Shefford has a large central core which is predominately diorite. The diorites are intruded by arcuate bodies of syenite (pulaskite and foyaite) and quartz-bearing syenite (nordmarkite). The core of Mount Brome is pulaskite. To the south this core is partly surrounded by a large, layered, arcuate gabbro body. The gabbro can be divided into a number of zones which apparently represent cycles of magmatic activity. Quartz-bearing syenites are found along the outer edges of the pluton. The central syenite is intruded by late stage nepheline-bearing diorites and syenites. Recent information on the geology of these plutons can be found in Eby (1984, 1985a) and Currie et al. (1986). Philpotts (1972) and Woussen & Valiquette (1972) have published field trip guides for Mounts Johnson, Shefford, and Brome.

Mount Megantic is located at the extreme eastern end of the province and its assignment to the Montereian Hills is questionable. The core of the pluton consists of a two-feldspar granite plug which is surrounded by a gabbro-diorite unit and an outer ring dike of nordmarkite. The central granite is very similar in appearance and mineralogy to the "Conway" granite of the White Mountains. The gabbros often carry two pyroxenes, which is common for White Mountain mafic rocks but rare in the case of the Montereian Hills. A recent review of this pluton can be found in Eby (1985a).

The plutons of the Montereian Hills are intruded by a variety of mafic and felsic dikes. Dikes are also widely distributed in the country rocks. These dikes tend to lie along a northwest trend. The mafic dikes can be classified as lamprophyres (alnoites, monchiquites, and camptonites), alkali olivine basalts, and basanites. The felsic dikes can be classified as bostonites, solvsbergites, nepheline syenites, and tinguaites. The strongly silica undersaturated dikes are concentrated towards the western end of the province.

Dike nomenclature used in the Montereian Hills is as follows. By definition, lamprophyres must be porphyritic rocks which do not have feldspar phenocrysts. Alnoites contain melilite and biotite as essential minerals and are feldspar free. Monchiquites have a groundmass of glass, analcime or nepheline, and ferromagnesian silicates. Camptonites have a groundmass of labradorite, amphibole, pyroxene, and subordinate alkali feldspar, nepheline, and/or leucite. In the monchiquites phenocrysts are commonly olivine or pyroxene while in the camptonites phenocrysts are commonly amphibole. The basanites are mineralogically similar to the monchiquites while the alkali olivine basalts are similar to the camptonites, but these dikes do not carry phenocrysts. The bostonites are texturally distinctive felsic rocks which have a trachytic or flow texture in which lath-shaped feldspar grains are arranged in rough parallelism or in radiating patterns. Tinguaites are equivalent to phonolites and in the Montereian Hills often contain sparse feldspar phenocrysts.

Geochronology, Geochemistry, and Isotope Geology

A number of geochronologic techniques have been applied to the dating of Montereian igneous activity. Ages determined by Rb-Sr whole-rock methods,

conventional K-Ar biotite and amphibole methods, and fission-track methods (apatite and sphene) for the main plutons and dikes are summarized in Eby (1987). These data indicated that there were two distinct periods of igneous activity in the Montereian province, one centered around 132 Ma and the other around 120 Ma. These ages also seemed to have a petrogenetic significance in that strongly silica-undersaturated rocks were confined to the younger period of igneous activity. Recently Foland et al (1986) have reported the results of Ar-40/Ar-39 geochronology on several of the Montereian plutons which indicate that the plutons had a short emplacement history centered around 125 Ma. These data, while internally consistent, are at variance with the data obtained from other radiometric methods. Further work is required to rationalize these apparent discrepancies.

Chemically the rocks of the Montereian Hills, with the exception of some cumulates, plot in the alkali field on a total alkalis versus silica diagram. Most of the rocks are nepheline normative, although the nepheline normative character of the cumulate rocks is due to the presence of abundant amphibole, rather than the occurrence of nepheline. In the strongly undersaturated series of rocks there is a strong enrichment trend in total alkalis with respect to silica which is mirrored by the occurrence of abundant modal nepheline. REE abundance patterns show moderate to strong enrichment in the LREE with respect to the HREE, with the strongly silica undersaturated rocks showing the greatest enrichment. In agreement with alkaline rocks from other parts of the world, the Montereian rocks are relatively enriched in alkalis and high-charge-density cations.

Both Sr and Pb isotopic data have been reported for the various Montereian plutons by Eby (1985b) and Grunenfelder et al (1985). These data suggest the presence of a depleted subcontinental lithosphere which served as the source of the Montereian magmas. During the ascent of the magmas to their level of crystallization interactions occurred with the country rocks. The nature of the isotopic contamination was quite varied since in some cases the country rocks were of Grenville age whereas in other cases they were Lower Paleozoic in age. As a general rule, the rocks emplaced last in any particular pluton show the most primitive isotopic signatures, an observation which is generally explained by the earlier formed magmas coating the magma conduits and isolating the later magmas from the country rocks.

Petrogenesis

A variety of magmatic sequences can be identified in the Montereian Hills and the details of their petrogenesis can be found in Eby (1984, 1985a, 1987). In brief the following sequences are delineated:

1. Carbonatite and possibly related (through liquid immiscibility) nepheline-rich rocks plus alnoitic dike rocks.
2. Pyroxenite - gabbro - diorite sequences which occur as significant components in a number of the plutons. These rocks are largely cumulate in nature, and calculated magma compositions indicate that they formed from alkali picrites.

3. Gabbro - diorite - syenite sequences and chemically similar camptonitic dikes. These rocks apparently represent the crystallization products of alkali olivine basalts.

4. Nepheline-bearing diorites and syenites and chemically similar mochiquite dikes. These rocks were apparently derived from basanitic magmas.

5. Quartz-bearing syenite and granite.

Chemical, isotopic, and experimental data have been used to outline possible petrogenetic histories for each of these sequences. The carbonatites and related rocks are inferred to have been derived from a carbonated garnet lherzolite mantle. The alkali picrite magmas are inferred to have arisen by moderate degrees of partial melting of a garnet lherzolite mantle. The basanitic and alkali olivine basalt magmas are believed to have arisen by increasing degrees of partial melting of a spinel lherzolite mantle. Given the strong enrichment in incompatible elements found for the initial melts, and the depleted mantle signature shown by the isotopic systems, it is concluded that mantle metasomatism occurred either immediately before, or during, melting. During ascent these magmas underwent various degrees of interaction with the crust producing residua enriched in silica. Some of the quartz-bearing syenites and the granite appear to have a crustal origin. In general, increasing degrees of silica saturation (or decreasing silica undersaturation) are marked by increasing initial strontium isotopic ratios, indicating the degree of crustal interaction.

GEOLOGY OF MOUNTS JOHNSON AND ST-HILAIRE

Mount Johnson

Mount Johnson, the smallest of the Monteregeian plutons, is roughly circular in plan with an approximate diameter of 680 meters (Figure 2). The bulk of the pluton consists of essexite with an outer annulus of syenite. The major lithologies can be subdivided into a number of units which are arranged concentrically around the core. Pajari (1967) divided the pluton into a core series (370 m in diameter) and a peripheral series. The central part of the core series consists of a fine-grained essexite which grades into a coarser-grained essexite carrying sparse pyroxene and plagioclase phenocrysts. The mineralogy and bulk chemistry of the core series is essentially constant with the exception of the disappearance of olivine in the outer portion of the series. Pajari (1967) concluded that the contact of the core series with the peripheral series is erosive in nature, indicating the intrusion of the core series into the pre-existing peripheral series. A small arcuate body of kaersutite-rich essexite, found within the core series, may represent the pre-existing material. The peripheral series passes outward through an essexite with abundant cumulus oligoclase, melanocratic essexite, transitional essexite, anhedral feldspar porphyry, biotite pulaskite porphyry, and nepheline syenite porphyry. In the peripheral series pyroxene is largely replaced by amphibole, presumably indicating elevated water pressure during the crystallization of this series. Spene is also found as an accessory in the peripheral series, but is absent in the core series. The surrounding Ordovician Lorraine silstones have been metamorphosed to the hornblende hornfels facies and near the

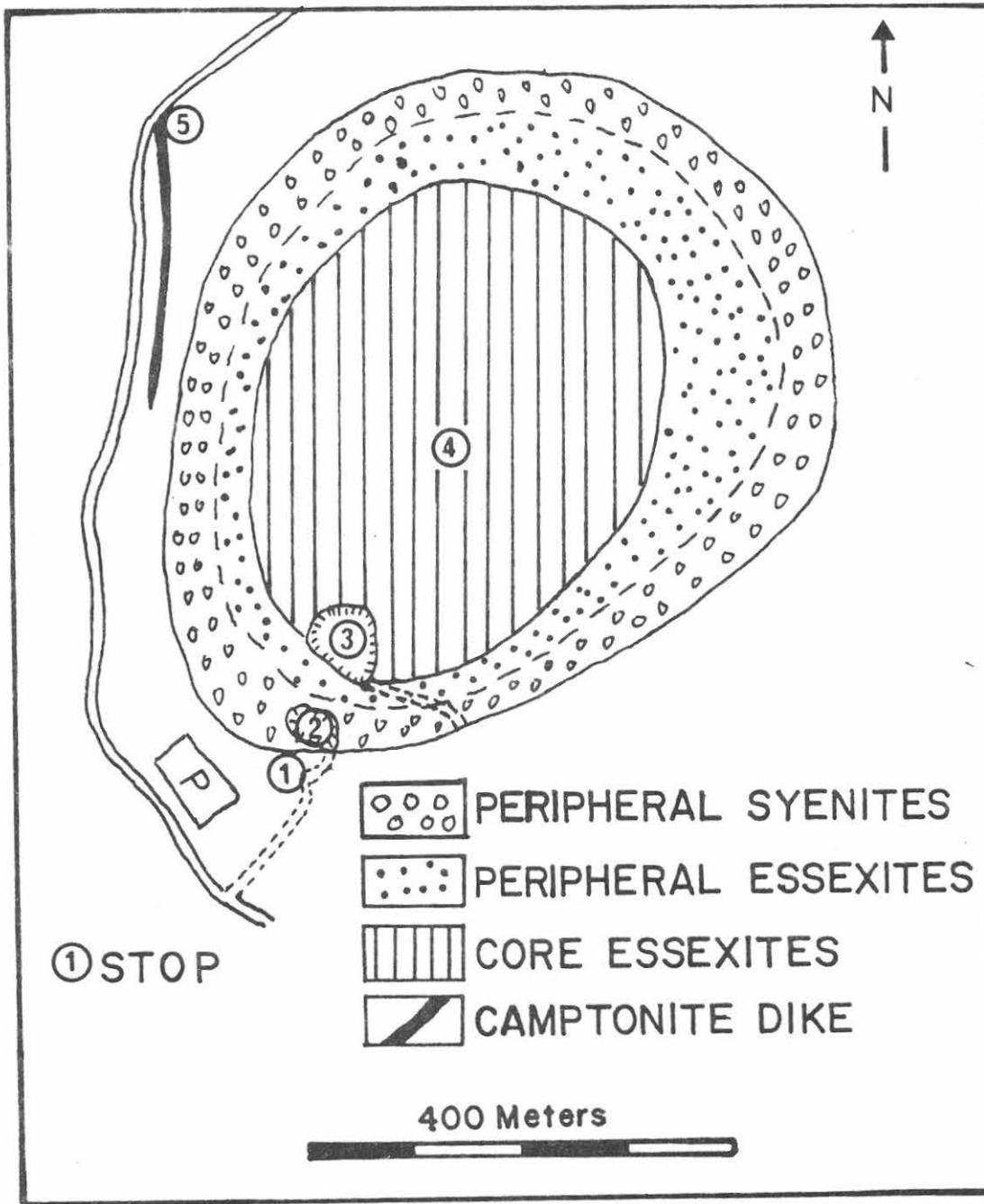


Figure 2. Geologic map (after Philpotts, 1972) showing field trip stops.

intrusion the hornfels dips in toward the contact.

All of the units of the pluton show a well-developed fabric. This fabric consists of vertically aligned feldspar laths, concentric layering, and cross-bedding in the essexites. These features indicate that the pluton consists of a series of vertical shells centered about the core, and that crystallization proceeded from the margins inward. Locally the

essexite contains feldspar crystals which dip toward the center of the intrusion giving an imbricate structure. This structure may be due to the flow of magma down the walls of the magma chamber. Except for the anhedral feldspar porphyry, in which fractured feldspar crystals show evidence of movement in the solid state, all of the units appear to have been passively emplaced. The fine-grained nature of the central portion of the core unit suggests that the magma chamber may have been vented to the surface during the emplacement of this unit.

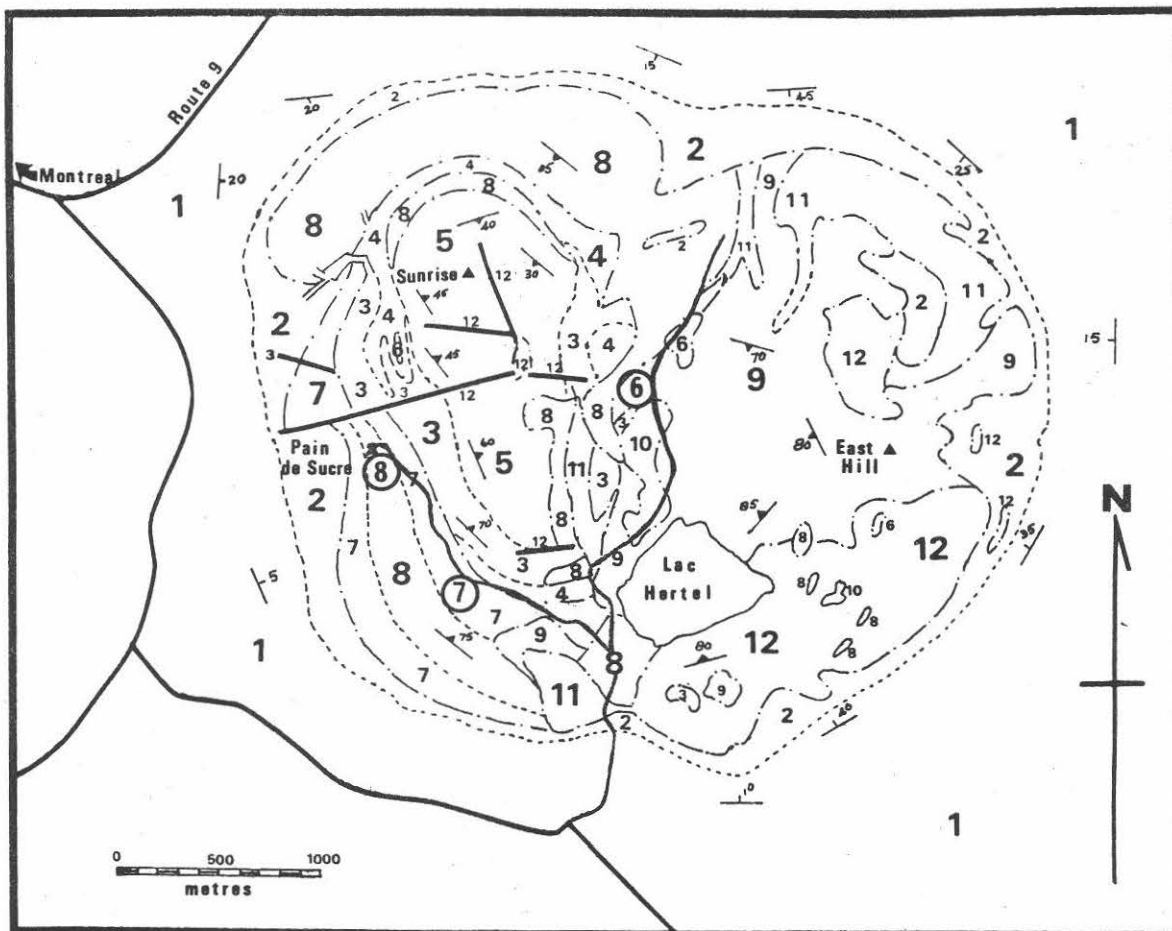
Despite its small size and apparent geologic simplicity, the Mount Johnson pluton has spawned a number of petrogenetic models. Wahl (1946) suggested that the pulaskite resulted from the diffusion of felsic components of the magma towards the cooler wall of the intrusion. Bhattacharji (1966) suggested that the operative process was flowage differentiation with the early crystallizing phases migrating towards the center of the conduit forming the olivine essexite core. Pajari (1967) envisioned the presence of two magmas, one which underwent crystal fractionation in the conduit to produce the syenites and essexites of the peripheral series and a second magma, of similar composition to the first, which formed the core series rocks. Philpotts (1968) suggested that the two major lithologies, essexite and syenite, were the result of the movement of two immiscible liquids up the conduit, the mafic liquid being preceded by the felsic liquid. Eby (1979) suggested that trace element data would support a silicate-liquid immiscibility process, although he envisioned two magmas being involved in the formation of the pluton. The first magma behaved immiscibly forming the syenites and essexites of the peripheral series while the second magma formed the core series. In the field sharp contacts are not seen between the various units, an observation which creates difficulties for most of the above petrogenetic models.

Mount St.-Hilaire

The Mount St.-Hilaire pluton (Figure 3) intrudes upper Ordovician shales, silstones, and limestones. The pluton is surrounded by a narrow biotite hornfels aureole. The low grade of contact metamorphism is somewhat anomalous considering the apparently high temperatures of the magmas. Near the contact the hornfels dips inward at moderate to steep angles suggesting passive emplacement of the magmas into collapsed material.

Currie (1983) and Currie et al (1986) divided the rocks of the pluton into several suites. The Sunrise and Pain de Sucre suites consist of mafic to intermediate rocks and form the western half of the pluton while the East Hill suite consists of peralkaline syenites and forms the eastern half of the pluton. The contact between the western and eastern halves consists of a variety of breccias including igneous and diatrema-like breccias.

The Sunrise suite is apparently the oldest of the igneous groups and consists of pyroxenites and gabbros, with gabbro as the dominant lithology. The rocks are strongly foliated, medium grained, and consist of poikilitic amphibole, clinopyroxene, calcic plagioclase, and accessory minerals. Although the rocks are nepheline normative, nepheline is not found in any of the units. There is a regular variation in the mineralogy marked by the



CRETACEOUS

MONT SAINT HILAIRE PLUTON (Units 3-12)

East Hill suite (units 9-12, not necessarily in order of emplacement)

- 12 Fine grained nepheline syenite, nepheline syenite porphyry and phonolite with trachytoid feldspar, nepheline and sodalite phenocrysts and xenocrysts; locally contains inclusions of units 3-8 and 11; grades to unit 9 by increase in proportion of inclusions
- 11 Coarse grained peralkaline nepheline syenite and pegmatite with feldspar, nepheline and sodalite phenocrysts; interstitial phonolite
- 10 Breccia, predominantly of units 2-8 with minor amounts of 9, 11 and 12; fragments well rounded, and locally somewhat altered
- 9 Igneous breccia; rounded to contorted fragments and xenocrysts of units 3-12 in a trachytoid, opaque-charged matrix similar to 12

Pain de Sucre suite (units 7-8)

- 8 Nepheline diorite and monzonite; medium- to coarse-grained rocks with tabular to granular plagioclase rimmed by alkali feldspar, interstitial nepheline, and mafic clots containing titanite, kaersutite, biotite and olivine
- 7 Biotite, trachygabbro; lath-like plagioclase with minor alkali feldspar rims, intergrown titanite and biotite, olivine and kaersutite

Sunrise suite (suites 3-6)

- 6 Anorthositic gabbro and leucogabbro; labradorite-rich, foliated titanite-magnetite gabbro
- 5 Amphibole gabbro: strongly foliated coarse grained rocks with minor titanite and biotite
- 4 Amphibole-pyroxene gabbro; moderately to weakly foliated granoblastic rocks with subequal amounts of kaersutite and titanite
- 3 Pyroxene melagabbro and jacupirangite; strongly to moderately foliated medium grained rocks with colour index greater than 60 and abundant magnetite; pyroxenite and perknite
- 2 Hornfels and metasomatic hornfels; fine grained to aphanitic grey to black quartz-rich, commonly containing abundant dykes

ORDOVICIAN

RICHMOND GROUP

- 1 Calcareous siltstone and shale, siltstone, minor limestone
Strike and dip of bedding
Strike and dip of igneous foliation
Geological contact, defined-approximate, gradational

Geology by K.C. Rajasekaran 1966, H.M. Aarden 1970, K.L. Currie 1971, 1972

Figure 3. Geologic map of Mount St.-Hilaire from Currie (1983) showing field trip stops and paths of the Gault Estate.

replacement of pyroxene by amphibole. These rocks are obviously cumulates and originally occurred as a funnel-shaped mass near the center of the pluton. Currie (1983) defined an igneous stratigraphy for this suite on the basis of a regular decline in color index with distance from the contact.

The Pain de Sucre suite occurs as thick ring dike intruding the Sunrise suite. The rocks are massive, slightly laminated, nepheline gabbros (essexites), diorites, and monzonites. Variations within the suite are gradational. Nepheline and occasional olivine occur along with amphibole, biotite, pyroxene, sodic to intermediate plagioclase, and alkali feldspar.

The East Hill suite consists of peralkaline nepheline syenites and porphyries. An early phase of this suite was a coarse-grained nepheline-sodalite syenite which is now found as xenoliths in the younger, flow-banded, nepheline syenites and phonolites. Actinitic pyroxenes and Na-rich amphiboles are the major mafic phases. Ilmenite and magnetite are rich in Mn, and both nepheline and/or sodalite are significant minerals, locally comprising as much as 40% of the rock. Elpidite, eudialite, and astrophyllite have been identified in a few specimens.

Currie et al. (1986) outlined a petrogenetic history for Mount St.-Hilaire which required two separate magmatic events. The first magma was believed to be an alkali picrite from which crystallized the cumulus rocks of the Sunrise suite. The second magma was hypothesized to be basanitic in composition and the nepheline gabbro - monzonite sequence was formed from this magma through fractional crystallization of pyroxene, magnetite, apatite, and plagioclase. For the East Hills suite they made the rather provocative suggestion that these rocks were the result of the interaction of a basanitic magma with a saline brine at crustal depths. This brine would be rich in Na and Cl, which would explain why nepheline and sodalite are abundant in the syenites. Because their age data indicated a significant hiatus between the emplacement of the Sunrise suite and the other suites, they hypothesized that the magmas were derived by successive melts formed in response to the upward progression of a thermal anomaly.

REFERENCES CITED

- Bhattacharji, S., 1966, Flowage differentiation in Mount Johnson stock, Monteregian Hills, Canada: Transactions of the American Geophysical Union, v. 47, p. 196-197.
- Currie, K. L., 1983, An interim report on the geology and petrology of the Mont Saint Hilaire pluton, Quebec: Current Research, Part B, Geological Survey of Canada, Paper 83-1B, p. 39-46.
- _____, 1986, The petrology of the Mont Saint Hilaire complex, southern Quebec: An alkaline gabbro-peralkaline syenite association: Lithos, v. 19, p. 65-81.
- Eby, G. N., 1979, Mount Johnson, Quebec - An example of silicate-liquid immiscibility: Geology, v. 7, p. 491-494.
- _____, 1984, Monteregian Hills I. Petrography, major and trace element geochemistry, and strontium isotopic chemistry of the western intrusions: Mounts Royal, St. Bruno, and Johnson: Journal of Petrology, v. 25, p. 421-452.

- 1985a, Monteregian Hills II. Petrography, major and trace element geochemistry, and strontium isotopic chemistry of the eastern intrusions: Mounts Shefford, Brome, and Megantic: *Journal of Petrology*, v. 26, pp. 418-448.
- 1985b, Sr and Pb isotopes, U and Th chemistry of the alkaline Monteregian and White Mountain provinces, eastern North America: *Geochimica et Cosmochimica Acta*, v. 49, p. 1143-1154.
- 1987, The Monteregian Hills and White Mountain alkaline igneous provinces, eastern North America, in J. G. Fitton and B. G. J. Upton, eds., *Alkaline igneous rocks: Geological Society Special Publication No. 30*, p. 433-447.
- Foland, K. A., Gilbert, L. A., Sebring, C. A., and Jiang-Feng, C., 1986, Ar-40/Ar-39 ages for plutons of the Monteregian Hills, Quebec: Evidence for a single episode of Cretaceous magmatism: *Geological Society of America Bulletin*, v. 97, p. 966-974.
- Gelinas, L., 1972, Geology of Mount Royal: 24th International Geological Congress, Excursion B-12, 44 p.
- Gold, D. P., Eby, G. N., Bell, K., and Vallee, M., 1986, Carbonatites, diatremes, and ultra-alkaline rocks in the Oka area, Quebec: Geological Association of Canada, Mineralogical Association of Canada, Canadian Geophysical Union, Joint Annual Meeting, Ottawa '86, Field Trip 21 Guidebook, 51 p.
- Grunenfelder, M. H., Tilton, G. R., Bell, K., and Blenkinsop, J., 1985, Lead and strontium isotope relationships in the Oka carbonatite complex, Quebec: *Geochimica et Cosmochimica Acta*, v. 50, p. 461-468.
- Pajari, G. E., Jr., 1967, The mineralogy and petrochemistry of Mount Johnson: Unpublished PhD dissertation, University of Cambridge, Cambridge, England, 208 p.
- Philpotts, A. R., 1968, Igneous structures and mechanism of emplacement of Mount Johnson, a Monteregian intrusion, Quebec: *Canadian Journal of Earth Sciences*, v. 5, p. 1131-1137.
- 1972, Monteregian Hills: Mounts Johnson and Rougemont: 24th International Geological Congress, Excursion B-14, 18 p.
- 1974, The Monteregian province, in H. Sorenson, ed., *The alkaline rocks*: New York, John Wiley, p. 293-310.
- 1976, Petrography of Mounts Saint-Bruno and Rougemont, Quebec: *Ministere des Richesses Naturelles, Report ES-16*: Quebec City, Quebec, 106 p.
- Wahl, W. A., 1946, Thermal diffusion-convection as a cause of magmatic differentiation. Pt. 1: *American Journal of Science*, v. 244, p. 417-441.
- Woussen, G. and Valiquette, G., 1972, The geology of the Brome and Shefford igneous complexes: 24th International Geological Congress, Excursion B-13, 16 p.

ROAD LOG FOR MOUNTS JOHNSON AND ST.-HILAIRE

Note: To avoid unnecessary delay at Canadian customs, foreign nationals in the United States should be sure to have credentials to reenter the United States.

CUMULATIVE MILEAGE	MILES FROM LAST POINT	ROUTE DESCRIPTION
0.0	0.0	Leave Holiday Inn assembly point. Turn right on Rt. 3.
0.05	0.05	Turn right into entrance ramp north of Rt. I-87.
7.25	7.3	Exit 40 N. Y. Rt. 345, Spellman Road. Continue on I-87.
16.5	23.8	Canadian Customs, I-87 becomes P. Q. Rt. 15.
13.1	36.9	Exit 21. Leave Rt. 15.
0.4	37.3	Turn right on P. Q. Rt. 219 toward Napierville.
2.6	39.9	Turn left in Napierville and continue on Rt. 219.
12.2	52.1	Enter St. Jean and continue east on Rt. 219, St. Jacques Street.
2.0	54.1	Turn right on Richelieu Street.
0.1	54.2	Turn left on St. Georges Street.
0.1	54.3	Turn left on Place du Quai.
0.1	54.4	Turn onto bridge crossing Richelieu River.
0.3	54.7	Enter Iberville.
0.1	54.8	Turn left at first traffic light off bridge onto 1st Street.
0.2	55.0	Turn right (east) onto 9th Avenue.
0.7	55.7	Turn left, cross RR, then right onto Rt. 104 (east). (You will see Rt. 104 signs in about 1/4 mile.)
0.4	56.1	Pass under P. Q. Rt. 35. Continue east on Rt. 104.

- | | | |
|-----|------|---|
| 3.9 | 60.0 | Village of Mont. St. Gregoire. Rt. 104 turns east. Continue straight (north). |
| 1.1 | 61.1 | Turn left on road that runs along the south and west sides of Mount Johnson (Mt. St. Gregoire). |
| 0.4 | 61.5 | STOP 1: Turn right into small parking lot across road from Vasseur Campground. Please note that this is private property that is made available to the public through the generosity of the owners. Walk up the marked trail to the right of the information booth. |

STOP 1. EXPOSURES OF HORNFELS COLLAR

Walk up the trail to the base of the waste-rock pile. Along the trail are numerous exposures of the Lorraine siltstone, now metamorphosed to the hornblende hornfels facies. The hornfels dips northward into the intrusion with increasing steepness as the base of the waste-rock pile is approached. Climb up the waste-rock pile to the first quarry.

STOP 2. QUARRY IN PULASKITE

Excellent exposures of the pulaskite are found in this small quarry. The strong vertical foliation is clearly evident in the quarry wall. Climb up through this quarry to a slightly larger quarry located at higher elevation. Note the increase in the amount of amphibole in climbing from the first to second quarry. The rock apparently grades from pulaskite to essexite.

STOP 3. QUARRY IN RHYTHMICALLY LAYERED ESSEXITE

This quarry is located in the coarse-grained, layered essexite, that comprises the outer edge of the core series. Along the road leading into this quarry are outcrops of hornblende-rich essexite which are typical of the essexite found in the peripheral series. This hornblende-rich essexite contains sphene while the essexite in the quarry does not carry sphene. In the quarry are found excellent exposures of rhythmically layered essexite with cross-beds and trough-like structures. Climbing up out of the quarry note the disappearance of the rhythmic layering. Continue on to the summit. Note the decrease in grain size as the summit is approached.

STOP 4. SUMMIT OF MOUNT JOHNSON

At the summit the fine-grain size makes it difficult to distinguish the foliation which was clearly visible on the climb from Stop 3 to Stop 4. With the exception of the presence of olivine, the essexite at the summit and in the quarry at Stop 3 is petrographically and chemically identical. To the north of the summit is found an arcuate body of coarse-grained, amphibole-rich essexite. On a clear day the summit of Mount Johnson provides an excellent view of the Monteregian Hills. Return by the same route to the parking lot. It is once again worthwhile to look at the rocks

to see if it is possible to distinguish any clear breaks between the various petrographic units.

0.6	62.1	STOP 5. Turn right out of the parking lot and continue northwesterly along the road to a lamprophyre dike cutting the Lorraine siltstone. Park on the west side of the road.
-----	------	--

STOP 5. CAMPTONITE DIKE

The dike trends north-south along the western margin of Mount Johnson. It is of somewhat older age than the main pluton but may be petrogenetically related to the Mount Johnson magmas. The dike consists of phenocrysts of titanite, partly altered to a mixture of green amphibole, brown biotite and chlorite, and kaersutite in an intergranular groundmass of plagioclase, biotite, kaersutite, opaques, apatite, and trace sphene.

2.0	64.1	Continue northerly to the Juncture of P. Q. Rt. 227. Turn left onto Rt. 227 north.
1.9	66.0	Cross P. Q. Rt. 10. Continue on Rt. 227. Mount St.-Hilaire is directly ahead.
1.5	67.5	Marieville. Continue on Rt. 227.
0.5	68.0	Stop sign. Continue on Rt. 227.
0.5	68.5	Juncture P. Q. Rt. 112. Continue straight across Rt. 112 on Rt. 227.
5.9	74.4	Juncture P. Q. Rt. 229. Rougemont Road to the right. Continue north on Rtes. 227 & 229 toward Mount St.-Hilaire.
0.6	75.0	Turn left on Rt. 229. Proceed west along Rt. 229 toward Mt. St.-Hilaire
0.3	75.3	Rt. 229 turns right. Continue straight (westerly).
1.7	77.0	Road turns sharply left with side road to the right. Turn right.
0.1	77.1	Take second road to left. Note sign indicating this is the Gault Estate, Center for Nature Conservation, McGill University. Park on left. Admission is \$1.00 Canadian

NOTE: The Gault Estate is a nature preserve and the eastern half of the mountain is closed to the general public. Permission for any collecting on the Estate should be obtained from: Executive Director, Gault Estate, 422, rue des Moulins, Mont-Saint Hilaire, Quebec, J3G 4S6, Canada.

STOP 6. EXPOSURES OF IGNEOUS AND DIATREME BRECCIAS

Proceed north along the main trail which follows the valley between the two halves of the mountain. Pass Lac Hertel. On the left (west side) of the trail are scattered outcrops and boulders of both the igneous and diatrema-like breccias. Most of the lithologies of the pluton can be found as blocks and fragments in these breccias.

STOP 7. GABBROS AND DIORITES OF THE SUNRISE SUITE

Retrace your path southwards to the intersection with the Pain de Sucre trail. Proceed up this trail (west) towards the summit of Pain de Sucre. Outcrops of gabbro and diorite of the Sunrise suite are exposed along this trail. In places the rocks are extremely coarse-grained and outcrops are found to carry clots of large radiating amphiboles. Foliation is generally poorly developed in this part of the suite.

STOP 8. NEPHELINE DIORITES AND MONZONITES OF THE PAIN DE SUCRE SUITE

Continue on to the summit of Pain de Sucre. In the immediate vicinity of the summit is an almost continuous exposure of relatively leucocratic coarse-grained rocks of the Pain de Sucre suite. The rocks usually have a bluish cast and visible laths of alkali feldspar. Olivine is present locally and nepheline occurs as an interstitial phase. Return to the parking lot.

- | | | |
|-----|------|--|
| 0.1 | 77.2 | The following road log guides you around the north side of Mt. St.-Hilaire to a quarry presently owned by R. Poudrette. Earlier literature referred to this as the Unimix Quarry. The remainder of the route will return you to Plattsburgh via routes P. Q. Rt. 15 and I-87 without retracing the route through Iberville and St. Jean. Care must be exercised or you will end up in downtown Montreal via the Victoria Bridge. Turn right as you leave the Gault Estate. |
| 0.1 | 77.3 | Turn left (easterly). |
| 1.0 | 78.3 | Sharp right then left, continue easterly. |
| 0.9 | 79.2 | Turn left onto Rt. 229 north. |
| 3.2 | 82.4 | Bear left and continue northwesterly on Rt. 229. |
| 2.3 | 84.7 | Left on road into Poudrette Quarry. |
| 0.7 | 85.4 | Quarry gate. Obtain permission to enter quarry. |
| 0.7 | 86.1 | Turn left onto Rt. 229. |

0.6	86.7	Intersection with P. Q. Rt. 116. Turn left (west) on Rt. 116 toward Montreal through the village of Mont St.-Hilaire.
3.9	90.6	Cross Richelieu River. Continue west on Rt. 116 (Blvd. Laurier) through the villages of Beloeil and Basile.
8.5	99.1	Village of St. Bruno. Mt. St. Bruno on right.
0.8	99.9	Jct. with Rte. 30. Continue on Rt. 116.
3.0	102.9	Jct. Rt. 112 east. Continue west on Rt. 116.
0.6	103.5	Rt. 112 west merges with Rt. 116. Continue west on Rts. 112 & 116.
2.3	105.8	Rt. 116 ends. Keep right for Rt. 112.
0.6	106.4	City of St. Lambert. Continue on Rt. 112.
0.6	107.0	Keep right for Rt. 132 north. If you want to go into Montreal continue on Rt. 112 to the Victoria bridge.
0.1	107.1	Right on Riverside Street. Must go north for about two blocks to get Rt. 132 south towards the U.S.A.
0.75	107.85	Turn left on Notre Dame under the bridge.
0.1	107.95	Turn left beneath bridge for ramp to Rts. 132 & 20 south.
0.15	108.1	Enter Rts. 132 & 20 south.
2.4	110.5	Jct. with Rt. 15 south. Rts. 10, 15, & 20 cross Champlain bridge for Montreal. Continue south on Rts. 15 & 132 for U.S.A. and I-87.
34.6	145.1	No stop at Canadian Customs. Continue south about 1/4 mile for U. S. Customs. South on I-87 about 24 miles to Plattsburgh.

FORELAND DEFORMATION AS SEEN IN WESTERN VERMONT

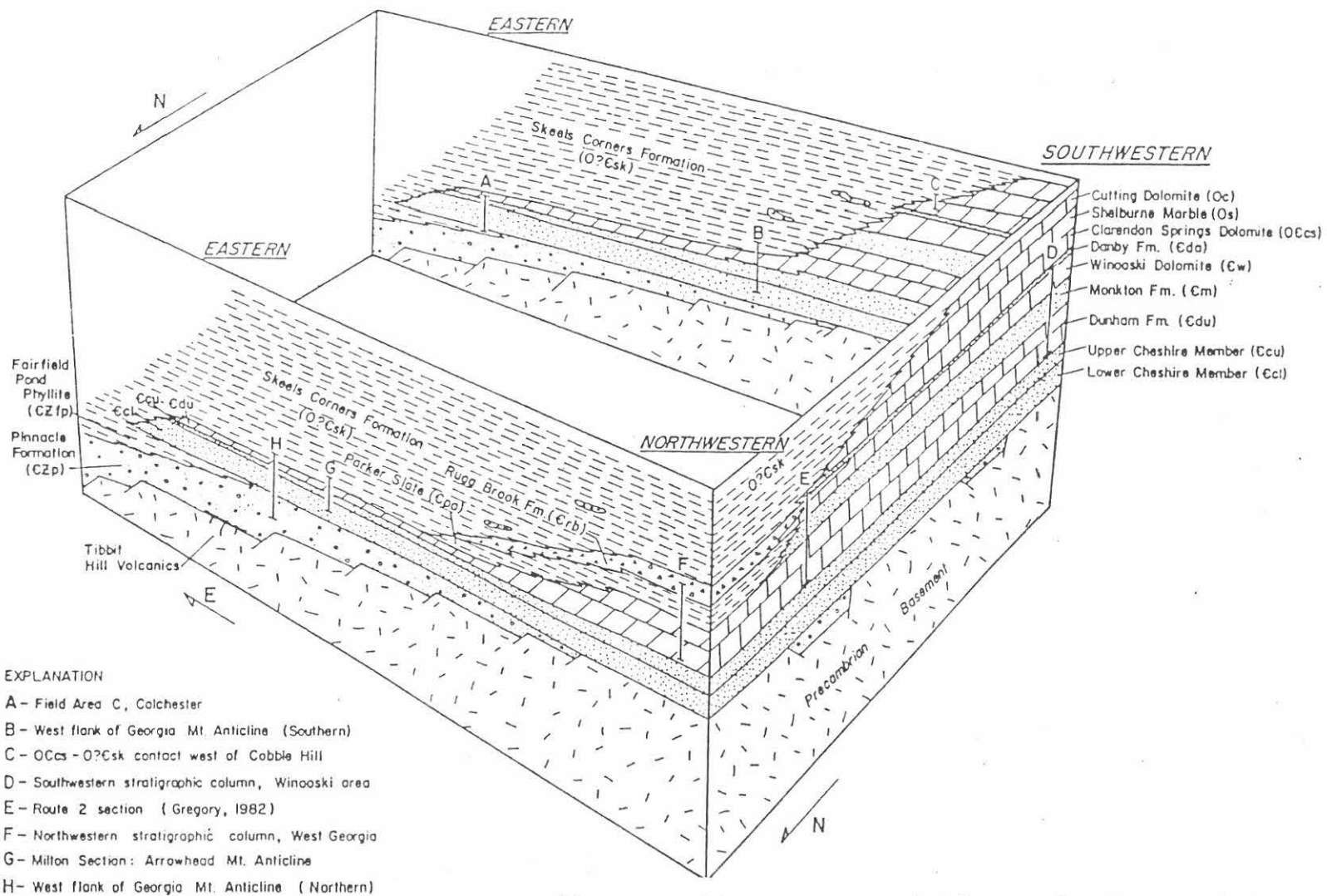
by

Rolfe S. Stanley
Department of Geology
University of Vermont
Burlington, Vermont, 05405

INTRODUCTION

Western Vermont is underlain by three distinctive sequences of rocks that range in age from Late Proterozoic to Middle Ordovician and are typical of the western part of the Appalachian Mountains. The lowest most sequence, which rest with profound unconformity on the Middle Proterozoic of the Green Mountain and Lincoln massifs, largely consists of metawackes, mafic volcanic rocks and phyllites that represent a rift clastic sequence. These rocks grade upward into siliciclastic and carbonate rocks of the platform sequence which in turn are overlain by Middle Ordovician shales of the foreland basin sequence. The boundary between the two sequences is the based of the Cheshire Formation (fig. 1). North of Burlington, Vermont the platform sequence grades into shales, breccias and conglomerates of the ancient platform margin and eastern basin. These sequences have been studied by a number of workers in the past (Cady, 1945; Cady and others, 1962; Hawley, 1957; Erwin, 1957; Welby, 1961; Stone and Dennis, 1964, for example) and are receiving current attention by Mehrrens (1985, 1987) and her students (Gregory, 1982; Myrow, 1983; Teetsel, 1985; Bulter, 1986; MacLean, 1986, 1987). Agnew (1977), Carter (1979), Tauvers (1982), DiPietro (1983) and Dorsey and others (1983) have reexamined parts of the rift clastic sequence while Doolan and his students are currently working in the same sequence in northern Vermont and Quebec (Doolan and others, 1987; Colpron and others, 1987). Figures 1 and 2 illustrate the representative stratigraphic columns for western Vermont north of the latitude of the Lincoln massif where the field conference will be held. Additional information can be found in Welby (1961) and Doll and others (1961).

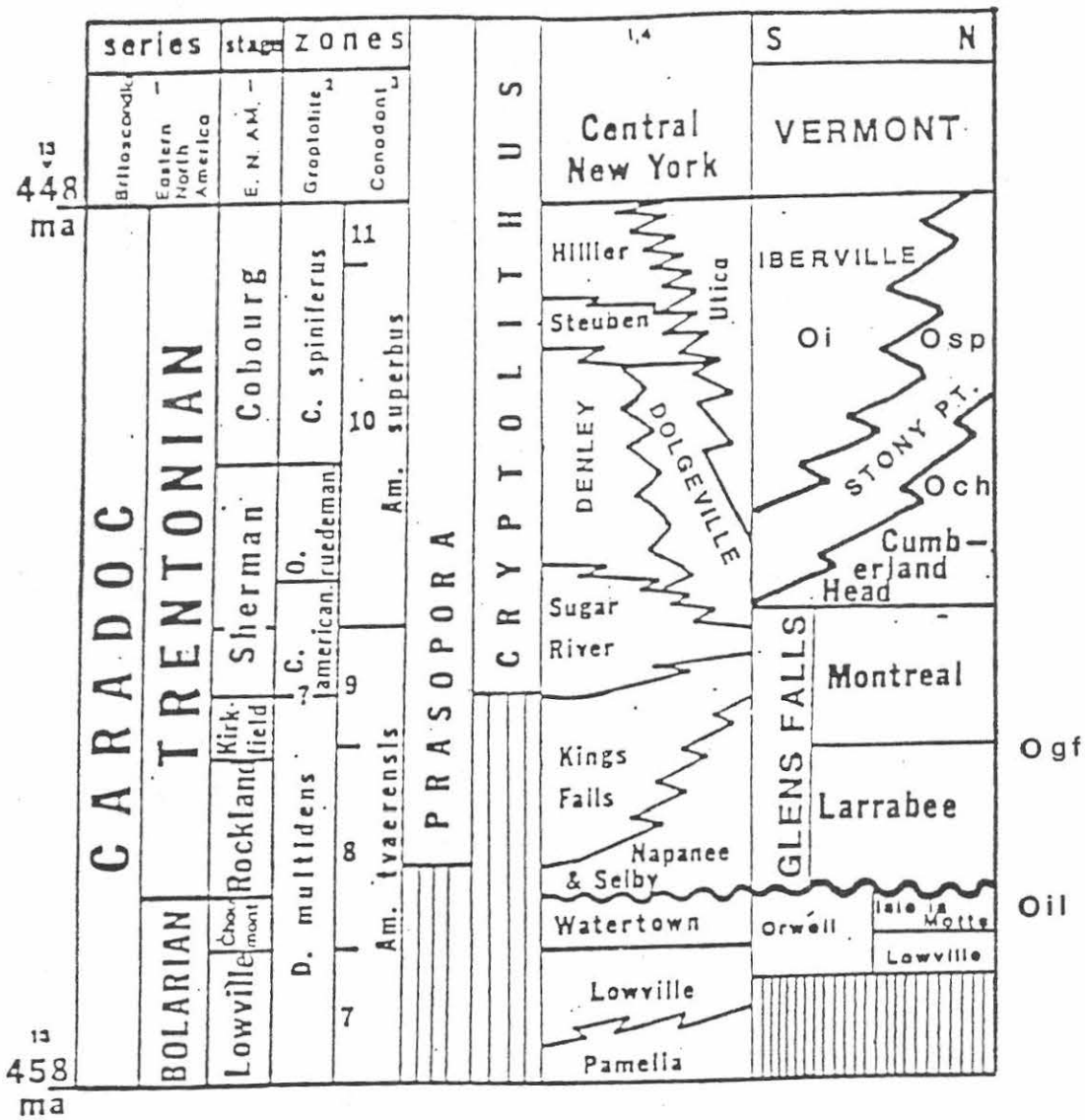
The structure of western Vermont is dominated by major, north-trending folds and imbricate thrust faults which are well displayed on the Geologic Map of Vermont (Doll and others, 1961). The rift clastic and platform sequences have each been displaced westward on major thrust faults that extend through much of Vermont. The larger of the two, the Champlain thrust, extends from southern Quebec to Albany, New York and places the older platform sequence over the younger foreland basin sequence. Estimates of westward displacement range from 15 km to 100 km. The smaller of the two, the Hinesburg thrust, places transitional and rift clastic rocks over the platform sequence and as such forms a boundary between the synclinal rocks of western Vermont and the



- Diagrammatic representation of the original depositional protolith for the Milton quadrangle reconstructed from stratigraphic information in the indicated areas.

Figure 1

Dorsey and others (1983)



MacLean 1986, 1987

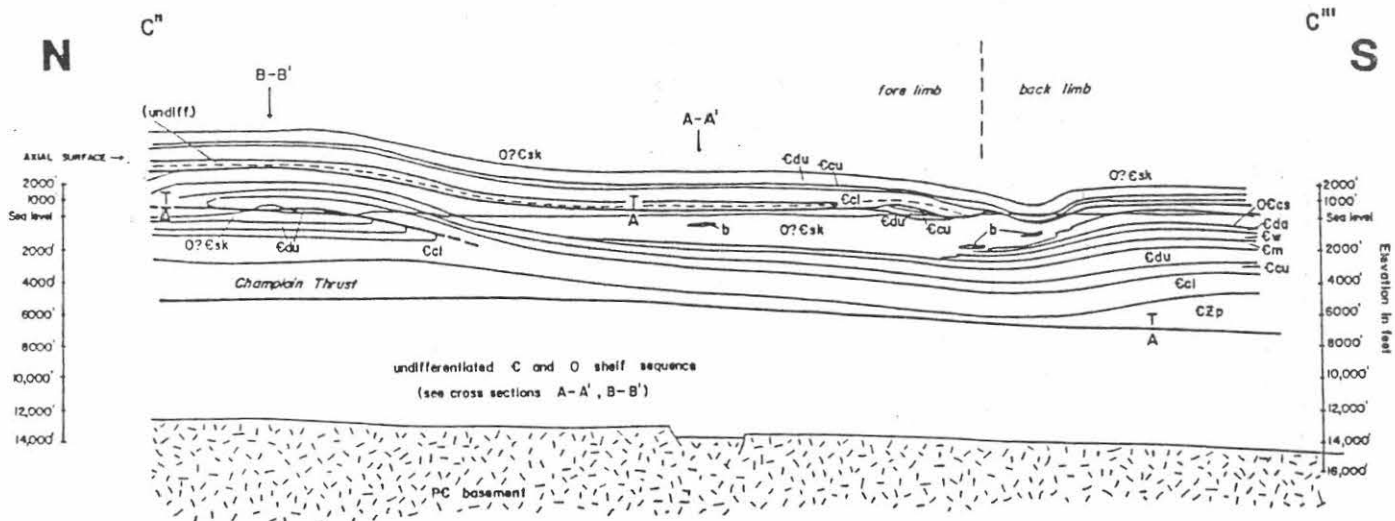
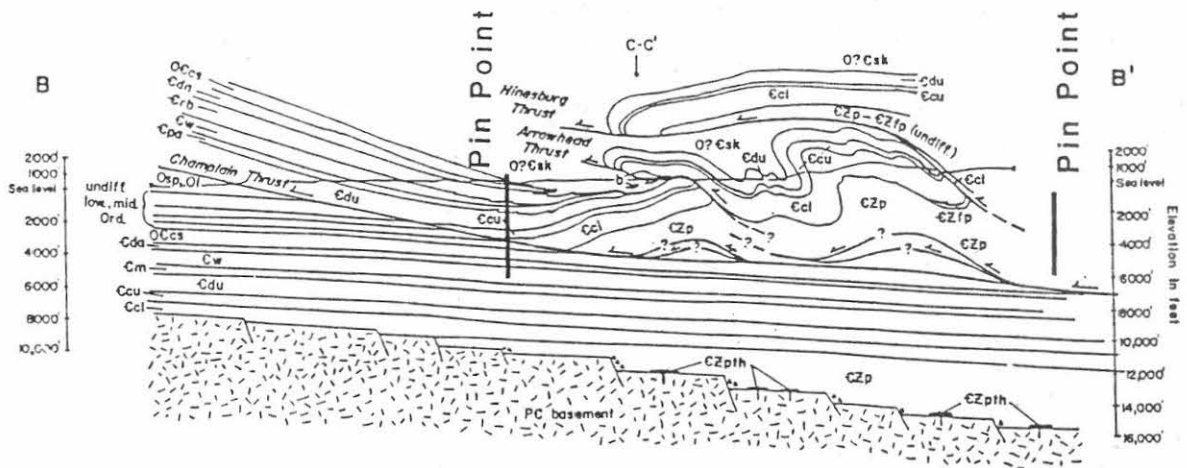
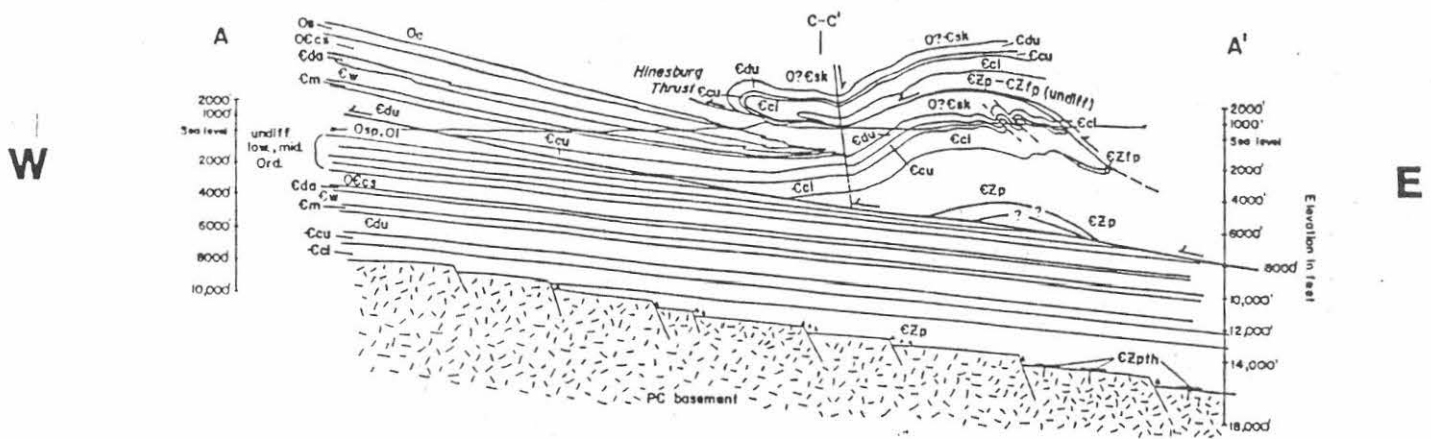
Figure 2 - Stratigraphic column for the western Vermont and Central New York. For further stratigraphic discussion read Erwin (1957) and Hawley (1957, 1972).

Green Mountain anticlinorium. Dorsey and others (1983) have demonstrated that the Hinesburg thrust developed along the overturned limb of a large recumbent fold (fault-propagation fold of Suppe, 1985) and therefore is quite different from the geometry of the Champlain thrust fault. Westward displacement is estimated to be 6 km.

Recent seismic traverses across western Vermont demonstrate that the Champlain thrust dips eastward at approximately 15 degrees beneath the Green Mountain anticlinorium and that the major folds of western Vermont are formed by duplexes and related structure on this and other thrust faults which are present both within the platform and the foreland basin sequences. High angle normal faults have been mapped along the Champlain thrust fault and in many parts of the foreland basin sequence (Welby, 1961; Doll and others, 1961). Seismic information shows that some of the faults are older than the Champlain thrust fault whereas others are younger. Stanley (1980) has shown that several of the faults that cut the eastern part of the platform sequence are Mesozoic in age.

The structure of western Vermont in the Burlington region is best illustrated by the recent work of Dorsey and others (1983) in the Milton quadrangle (fig. 3) and Leonard (1985) in South Hero Island. The cross sections for this region show that the Champlain thrust fault is essentially planar which is consistent with recent seismic studies at this latitude. Detailed surface mapping, however, has shown that the overlying thrust faults are folded. Dorsey and others (1983) therefore suggest that these folds are related to duplexes in the Champlain slice (fig. 4). Based on this configuration the highest fault, the Hinesburg thrust, is the oldest and the Champlain thrust is the youngest. Thus the thrust sequence developed from the hinterland (east) to the foreland. Shortening as measured between the pin points in section B-B' (fig. 4) is in the order of 55 percent with 6 km of displacement on the Hinesburg thrust and 0.85 km of movement on the Arrowhead Mountain thrust. The Milton cross sections clearly show the change in structural style and fabric that occurs as one crosses from the foreland to the hinterland.

The foregoing conclusions are consistent with the character of each of the fault zones. The Champlain thrust fault is marked by gouge, welded breccias and pressure solution features (Stanley, 1987). An estimate of the confining pressure based on the stratigraphic thickness (2700 m) of the hangingwall block is 0.73 kbars which corresponds to approximately 2.5 km below the earth's surface. This assumes the fault is a Taconian feature. At this depth the temperature would be in the order of 100⁰ C assuming a geothermal gradient of 20⁰ to 30⁰ C/ km. (Strehle and Stanley, 1986, fig. 5). The gouge and cataclastic features are consistent with these estimates and suggest that if the



Dorsey and Stanley (1983)

CROSS SECTIONS OF THE MILTON QUADRANGLE WESTERN VERMONT

Figure 4

hangingwall block at the longitude of Lone Rock Point did involve a repeated section or tectonic load, the additional section was small. The Arrowhead Mountain thrust fault, on the other hand, is another story. The shaley dolostone slivers in the fault zone are welded cataclasites that contain a later, fault-related, pressure-solution cleavage. In the quartzite near the fault surface the quartz shows undulose extinction, deformation lamellae, and, limited recrystallization whereas the feldspar is fractured and twinned. Oriented sericite occurs along cleavage surfaces in the quartzite (Strehle and Stanley, 1986). Because the stratigraphy of the hangingwall block is only slightly thicker (2900 m.) than the Champlain slice the fault-zone fabric along the Arrowhead Mountain thrust fault should be similar to the Champlain thrust. The fabric at Arrowhead Mountain, however, has clearly formed at an higher temperature and pressure because it involves recrystallization of quartz and the growth of sericite. Strehle and Stanley (1986, fig. 5) suggest temperatures in the order 200⁰ C to 250⁰ C which is in agreement with oxygen and carbon isotope temperatures of 210-295⁰ C from calcite and dolomite assemblages in the weakly metamorphosed carbonate rocks directly west of the Lincoln massif 40 km to the south. These temperatures correspond to pressures of approximately 2.5 kbars or 7.5 - 8.0 km. These fabrics and the corresponding estimates indicate that the Arrowhead Mountain thrust must have carried a tectonic load of more than double the standard stratigraphic section. This load would correspond to the hangingwall block of the Hinesburg thrust (fig. 4).

The story for the Hinesburg thrust fault is again similar to that of the Arrowhead Mountain thrust. At Hinesburg the quartzite within 25 m. of the fault has been extensive recrystallized and mylonitic textures become progressively well developed as the fault contact is approached. An ultramylonite marks the fault surface. Feldspar grains are fractured and bent but show little signs of recrystallization. Sericite, chlorite, and stilpnomelane are present along the fault - related cleavages. The deformation features in quartz and feldspar indicate that deformation occurred below 450⁰ C (Voll, 1976). Strehle and Stanley (1986; fig. 5) suggest temperatures in the order of 350⁰ C which would correspond to pressures in the order of 3.5 km or 11 to 12 km. Clearly the upper plate of the Hinesburg thrust must have carried older thrust faults that rooted in the pre-Silurian section to the east (Underhill slice of Stanley and Ratcliffe, 1985, fig 2A, pl. 1). Thus the fabrics along the Champlain, Arrowhead Mountain and Hinesburg thrust faults developed under progressive more ductile conditions as a result of higher temperatures and pressures generated by an increasing tectonic load.

Most of the deformation in western Vermont occurred during

the Taconian Orogeny. This conclusion is based on regional considerations (Stanley and Ratcliffe, 1985) and the analysis of available isotopic data (Sutter and others, 1985). Mesozoic deformation in the form of extensional faults and igneous activity clearly affected the region (McHone and Bulter, 1984; Stanley, 1980). Available evidence, however, can not rule out limited Acadian or even Alleghenian deformation.

Participants of this field trip will see the change in structure and fabric as they cross the foreland from South Hero Island to the western margin of the hinterland at the Hinesburg thrust fault at Mechanicsville, Vermont.

ITINERARY

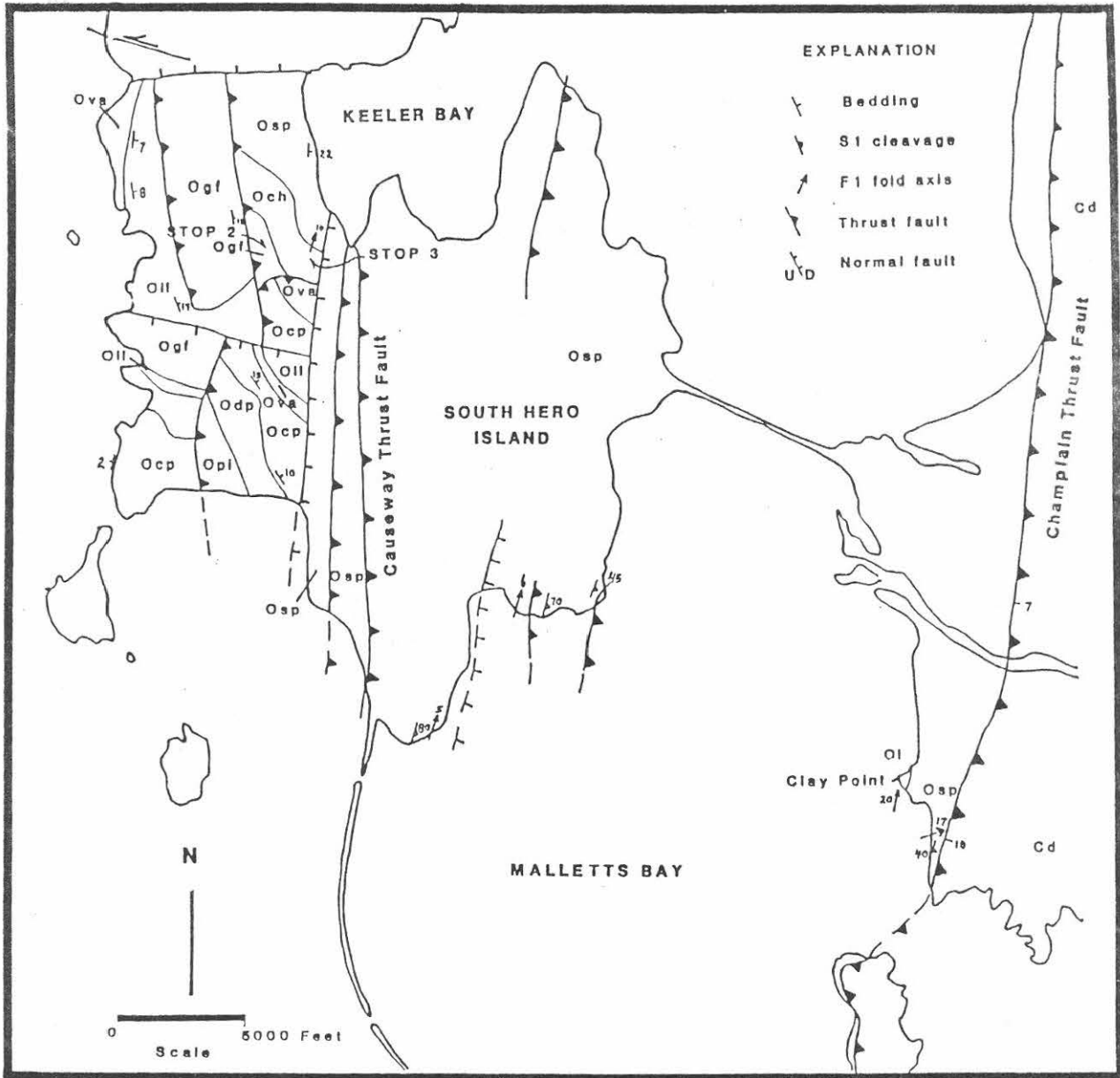
ALL STOPS ARE LOCATED ON GEOLOGIC OR TOPOGRAPHIC MAPS. A MILEAGE LOG IS NOT INCLUDED.

Assemble at the Apple Store on the south side of Route 2 in the village of South Hero at 8:30 AM. The first three stops will be on South Hero Island (fig. 5). PLEASE DO NOT USE HAMMERS ON THIS TRIP. LEAVE THEM IN THE CAR.

STOP 1 - West Shore of South Hero Island. This stop illustrates the low level of deformation that characterizes much of the west shore of the Champlain Islands and the eastern shore of New York in the area of Plattsburg. Local areas of moderate deformation, however, do exist where bedding plane faults and high-angle faults cut the bedrock. These outcrops of shale and thin micrite beds are in the Stony Point Shale. Note that the bedding, which is nearly horizontal, is cut by a poorly developed cleavage that is only developed in the shale beds. The cleavage dips very gently to the east and is interpreted to result from simple shear parallel to the bedding. Thin layers of calcite are present on some of the beds. Those layers that are marked by prominent slickenlines are bedding plane faults. As we will see at other outcrops today, the larger faults are marked by thicker layers of lineated calcite.

STOP 2 - Lessor's Quarry (fig. 6) - This quarry is located in the fossiliferous Glens Falls Limestone. The quarry contains some of the finest evidence of pressure solution in western Vermont. The cleavage (S1), which is discontinuous and wavy, is a classical pressure solution feature with well developed selvages that truncate fossils and offset bedding. A small anticline at the south edge of the quarry contains adjustment faults at its hinge that end along cleavage zones with thick clay selvages.

The major structures in the quarry are bedding-plane thrust faults. These faults are marked by calcite layers with west-trending slickenlines and a fault-zone cleavage (St).



Bedrock Geology of South Hero Island, Vermont

Leonard (1985), Erwin (1957)

Figure 5

Near the larger faults the S1 cleavage is rotated (Sr) toward the plane of the fault. Note that both St and Sr dip gently to the east and indicate that movement on the bedding faults was to the west. The St cleavage forms as a result of simple shear on the faults. The anticline along the southwall and edge of the quarry is formed from a small duplex. Unfortunately, the best evidence for this duplex has been excavated.

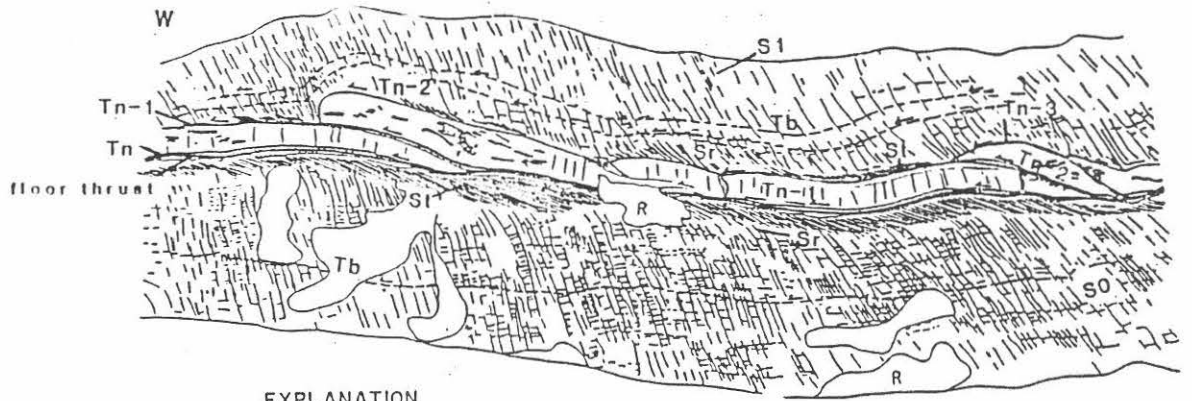
On the northeast side of the quarry (fig. 6) a syncline and an associated blind, synformal thrust fault are truncated by the major thrust fault that is continuous across the north wall of the quarry. The origin of this structure is not clear, but it is thought to be associated with a duplex or ramp below the level of the quarry floor.

STOP 3 - "THE BEAM" - THIS IS A SUPERB OUTCROP THAT SERVES AS A FIELD LABORATORY FOR RESEARCH AND TEACHING OF FORELAND DEFORMATION. PLEASE STUDY IT. USE YOUR CAMERAS BUT NOT YOUR HAMMERS. REFER TO FIGURES 7, 8, AND 9.

The outcrop is located in the Cumberland Head Formation approximately 5 miles (8 km.) west of the exposed front of the Champlain thrust fault or approximately 4600 ft. (1400 m.) below the restored westward projection of the thrust surface. The major questions that will be discussed are: 1. How do ramp faults form?, 2. Are there criteria to determine if imbricate thrust faults develop toward the foreland or hinterland?, 3. What is the relation between faulting and cleavage development?, 4. What processes are involved in the formation of fault zones?, 5. Are there criteria that indicate the relative importance and duration of motion along a fault zone?, 6. Is there evidence that abnormal pore pressure existed during faulting?, and finally 7. What is the structural evolution of the imbricate faults? The first six questions will be largely addressed by direct evidence at the outcrop. The last question will be answered by palinspastically restoring the imbricated and cleaved sequence to its undeformed state (fig. 9).

THE OUTCROP

Five imbricate thrust faults and associated ramps are exposed in profile section in a foot thick bed of micrite that extends 14 m along an azimuth of N 80 E (fig. 7a). The imbricate fault can be further classified as a central duplex of three horsts that are separated from two simple ramps at either end of the outcrop by approximately 2.5 m of flats. The micrite bed is surrounded by at least 1.5 m of well-cleaved calcareous shale. Bedding plane faults are present along the upper and lower surface of the micrite where they merge with ramp faults that cut across the micrite bed at an angle of approximately 30 degrees. The lower bedding plane fault or floor thrust is relatively planar and



EXPLANATION

- S₀ Bedding
- S₁ Pressure solution cleavage
- S_r Thrust zone cleavage
- T_b Bedding plane thrust in shale
- Calcite veins & layers
- En schelon fractures
- Rubble
- Thrust fault, showing relative motion

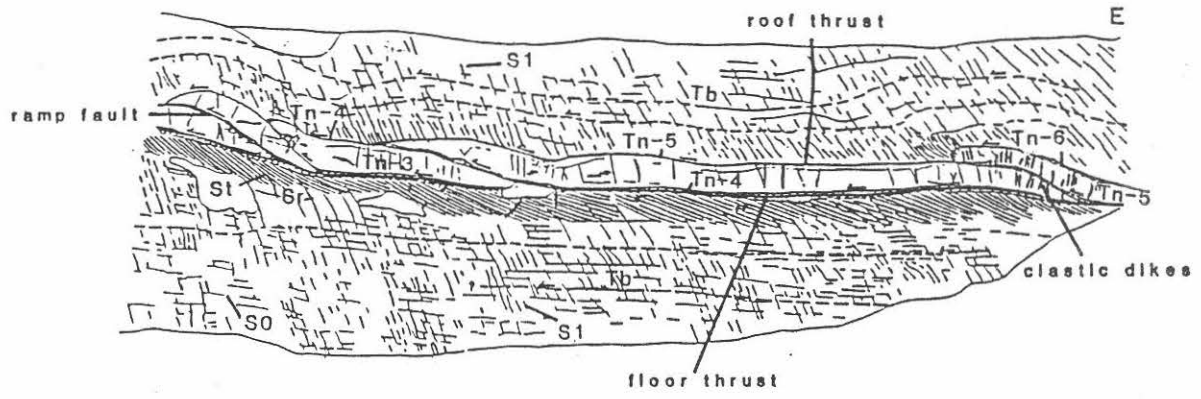


Figure 7a

Stanley 1985

DEFORMATION OF THE CUMBERLAND HEAD FORMATION
SOUTH HERO, VERMONT

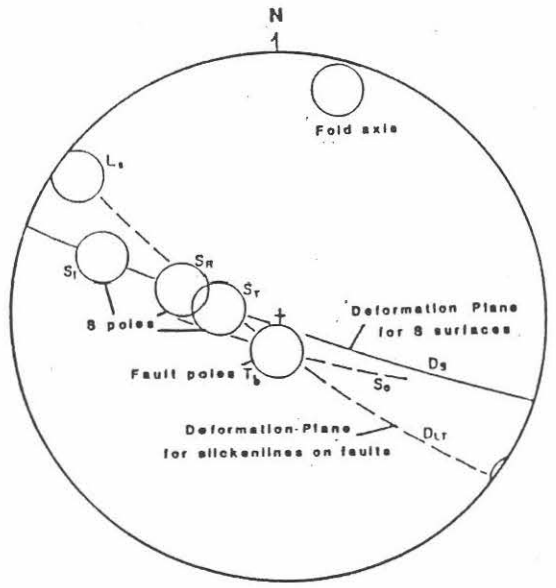


Figure 7b

the fault zone is thick compared to the upper bedding plane faults which are folded in the ramp areas, cut by ramp faults, and the fault zones are thin. The upper bedding plane fault forms the roof thrust for the central duplex. Along the intervening flats the upper faults are generally planar although they are cut by the S1 cleavage in many places. The lower bedding plane fault is the major decollement across the outcrop. Older bedding plane faults are also present throughout the shale where they are offset by the penetrative S1 cleavage.

All the fault surfaces are covered by layers of sparry calcite that vary in thickness from several millimeters to 4-6 cm. The thickest zone is found along the decollement or floor thrust whereas the thinnest zone is found along the older bedding plane faults in the calcareous shale (fig. 7a). In all but the thinnest layers, the calcite is arranged in distinct layers that are separated by discontinuous selvage of dark gray shale. Each of the layers are marked by grooves or slickenlines that trends N 56 W and are essentially parallel from layer to layer (7b). In sections oriented perpendicular to the layering and parallel to the slickenlines the shale selvages are more parallel to each other than in sections cut perpendicular to the slickenlines where the selvages either anastomose or conform to the cross section of the grooves. In the parallel sections, however, some of the selvage layers are truncated by more continuous surfaces. One of these can be traced for 1.5 m or more along the decollement. At a number of places along the different fault zones small dikes of sparry calcite have intruded the lower part of the calcite-shale layers. The fault-zone fabrics are most clearly displayed along the decollement where the calcite-selvage layers are more abundance.

Fractures are common throughout the micrite bed where they are oriented at either a high angle or low angle to the bedding. Most fractures are filled with sparry calcite. The most prominent fractures are arranged in an echelon arrays that climb either to the west or the east. Most of these arrays are located in ramp areas and along the west-facing limbs or small flexures. A few are present in the flat regions of the bed. The fractures in many of the arrays in the ramp regions are folded and some are cut by younger generations of an echelon fractures. In the eastern ramp the hangingwall and footwall are cut by near-vertical fractures that are filled with fragments of the surrounding micrite embedded in sparry calcite so as to form clastic dikes.

Two, well developed, pressure-solution cleavages are present throughout the calcareous shale. The first and most conspicuous one, S1, strikes N 20 E and dips 60 to the east (fig. 7b). This orientation is an average based on measurements taken across the vertical face of the outcrop

because the individual S1 surfaces are quite wavy along strike. As a result they form a distinct diamond-shape pattern on the bedding surface. The acute angle of the diamond pattern is approximately 30 degrees in the shale and 50 degrees in the micrite bed. This geometry indicates a moderate level of cleavage development according to the scheme of Alvarez and others (1976). S1 surfaces are covered by a black, carbon-rich selvage of illite and kaolinite which is less than 0.5 cm thick. Although many of the cleavage surfaces are vertically continuous through the shale, some of them are short and discontinuous with tapered ends. The thickest selvage occurs on the most continuous surfaces. The surfaces of the selvage are not lineated although some are polished. The S1 cleavage offsets bedding and the older bedding-plane thrust faults with a down-to-the-east sense throughout much of the outcrop. This displacement is greatest where a selvage is the thickest and it gradually is reduced to zero as a selvage thins toward the tapered ends of the shorter cleavage surfaces. The average width of the microlithons between the S1 surfaces is 5.6 cm thick. The S1 cleavage not only cuts the older bedding-plane faults but cuts across most of the roof faults on top of the micrite bed.

A second, well developed cleavage, St, is restricted to a foot-thick zone directly below the decollement (fig. 7a). The individual cleavage surfaces are thinner (about 1 mm thick), more closely spaced (about 1 cm or more), and are covered with a thin selvage (less than 1 mm). Furthermore, St dips to the east at only 6 degrees compared to the steeper dip of S1. St is also developed along the roof thrust of the micrite bed, but the zone is thinner and it is more difficult to recognize because the roof faults have been folded in the ramp areas and deformed by S1. The St cleavage is definitely related to movement of the thrust faults because it is only found near the faults and it is absent away from them.

In the zone near the decollement and the roof faults the S1 cleavage is rotated eastward so that the steeper 60 degree dip in the shale is reduced to 25 degrees (fig. 7b). The strike of the rotated S1 (hereafter referred to as Sr) is the same as S1 away from the faults. The counterclockwise rotation of S1 through an angle of shear of 35 degrees indicates that movement on the decollement was east-over-west along a direction of N 56 W as indicated by the slickenlines along the decollement. This sense of displacement is consistent with the orientation of St since the normal to St would correspond to the direction of maximum finite compressive strain.

Cleavage, similar to S1 and St, is totally absent from the micrite bed. In a few places, however, a very thin (less 1 mm), stylitic to very irregular cleavage is oriented perpendicular to bedding in the micrite. This cleavage is

not developed uniformly throughout the micrite. Where it is formed the cleavage surfaces are separated from each other by at least 6-10 cm. The form, orientation and limited distribution of this cleavage indicates that it formed very early in the deformation sequence while compression was essentially parallel to the planar micrite bed.

RAMP FAULTS

All the east-dipping ramp faults develop from arrays of west-climbing, en echelon fractures. Although a few of the fractures are cavities covered by terminated calcite crystals, most of them are completely filled with sparry calcite. The sequence by which these faults develop is well displayed in a few gently folded parts of the micrite bed and in the ramp regions where the en echelon arrays are folded or cut by continuous ramp faults. These arrays appear to nucleate along the west-facing limbs of slightly asymmetrical buckle folds. The individual extension fractures within the arrays dip more steeply to the west by values of 7 to 11 degrees than the nearby bedding at the boundary of the micrite bed. The sequence continues with the rotation of the extension fractures by distributed shear strain along the west-climbing array. The individual fracture continued to grow as the older central parts of the fractures were rotated counterclockwise to produce S shaped fractures. Shear strains along these arrays were calculated using equation 2.3 of Ramsay and Huber (1983) and are in the order of 1.4 (54 degrees). These strains indicate that at least 5.6 cm of displacement occurs across the arrays before they fail along a ramp fault. During this time new arrays of planar fractures were developed over the older arrays thus producing a weakened zone along the trend of the array. As generations of fractures were superposed they eventually coalesced and developed into ramp faults as demonstrated by deformed fracture arrays in the footwall and hangwall which are truncated by the ramp faults. The presence of sparry calcite and cavities in the fractures indicates that the fractures opened rapidly and at a shallow enough level in the crust so that the micrite bed was strong enough to support the shape of the cavities.

East-climbing, en echelon fracture arrays are also present in the micrite where they tend to concentrate in the ramp regions. Unlike the fractures in the west-climbing arrays, the individual extension fractures in the east-climbing arrays are either parallel to or dip more steeply to the east than bedding. These angular relations are important because they indicate that the east-climbing arrays were not formed at the same time as the west-climbing arrays. Although some of the fractures in these arrays are deformed into Z shapes, none of the arrays developed into west-over-east faults or backthrusts. Calculated shear strains along these arrays give a maximum value of 1.1 (47 degrees). I suggest that

they formed as a result of continued compression after the ramp faults were locally locked and before failure developed in another ramp zone farther to the west.

The orientation of the extension, or perhaps true tension, fractures in the micrite bed are important because they indicate the relative position of the bedding relative to the direction of maximum compressive stress (Σ_1) which was essentially horizontal during deformation. During the early stage of deformation bedding was essentially parallel to Σ_1 because the stylonitic cleavage, which forms perpendicular to Σ_1 , is perpendicular to bedding. The bedding then rotated eastward so that the extension fractures in the west-climbing arrays formed at a more-westerly inclined angle than bedding. East-over-west displacement in bedding plane faults could occur at this time because the finite shear stress was now high enough to overcome frictional resistance. Subsequent formation of ramp faults and their evolution led to the development of the east climbing arrays as a result continued compression. The orientation of these extension fractures is then controlled by the local orientation of Σ_1 in the ramp regions. Single, bed-parallel fractures in the flat regions of the micrite bed could have formed any time during the deformation sequence.

FAULT CHRONOLOGY

The discussion here will concentrate on the chronology of faults that are present within and in direct contact with the micrite bed. The bedding plane faults in the surrounding shales are clearly older than these faults because they are cut and offset by the S_1 cleavage. Although the bedding plane faults that are in direct contact with the micrite bed may have formed originally at this time there is abundant evidence that they certainly were active long after those in the shale. Their average age therefore is younger. Furthermore, they play an essential role in the development of the ramp faults.

The evidence for the relative age of each of the faults is found in the regions where the ramp faults merge with the roof and floor faults. For example, in the western part of figure 7a the ramp fault (T_{n-1}) cuts across the upper-bedding plane fault (T_{n-2}) of the hangingwall block but merges asymptotically with the floor fault (T_n) of the footwall block. Furthermore, the roof fault of the hangingwall block is folded and cut by S_1 cleavage. At the junction of the ramp fault and the floor fault, the quasiplanar slip surfaces in the calcite-shale fault zone cut across the fault zone of the ramp fault. The relative age relations therefore are clear - the oldest fault of the three is the roof thrust and is designated T_{n-2} . The youngest fault is the floor thrust

(Tn). This same relative chronology applies to all the ramps and duplexes to the east.

Several important conclusions result from this analysis. First, the imbricate faults which comprise the roof, ramp, and floor fault system become younger to the west or the foreland for the Northern Appalachians. This conclusion is based on direct evidence and not an assumption on the fault sequence. Second, the floor fault is continually reactivated during the evolution of the fault system. The average age of the fault zone therefore becomes younger to the west. It is a time transgressive structure in very sense of the word. Furthermore, it is the most continuous fault in the outcrop. This second conclusion explains why the fault zone for the floor fault is thicker than the fault zones along the ramp or roof faults. The floor fault has been active for a longer period of time than any of the other faults. The thickness and continuity of a fault zone therefore are directly related to the duration of motion of a given fault. How far this relationship can be carried to faults in other sequence is uncertain. It does seem to hold true for the shale section in western Vermont.

The geometry of the westward-younging faults in the micrite bed is distinctive - a flat, continuous floor fault with folded roof faults that are cut by ramp faults along their steeper west-facing limbs (fig. 7a). This is the standard "piggyback" sequence described for many mountain chains in which the thrust faults young toward the foreland (Boyer and Elliot, 1982; for example). Would the geometry, however, be different for an eastward-younging sequence or, in this case of the Northern Appalachians, a sequence that would young toward the hinterland? As shown in figure 8, the answer is yes. Here the roof fault can take on various configurations as irregularities caused by earlier ramp anticlines are eliminated by continued movement on the roof fault zone. Note that each of the ramp faults are truncated by the younger roof thrust. The floor faults are irregular and are cut successively by each of the ramp faults to the east. Ramps and duplexes with this geometry have not been recognized in the shales of western Vermont.

FAULT-ZONE DEPOSITS

With our understanding of fault chronology and importance, I now consider the processes by which the sparry calcite and shale are formed along the fault zones. Because the floor fault has been active throughout the development of the imbricate system one can find the most complete history there compared to the other faults where the history has been shorter and less complex. The fact that the average age of the fault zone along the floor fault is older to the east than the west, further suggests that more of its history will be recorded at the eastern part of the outcrop than the

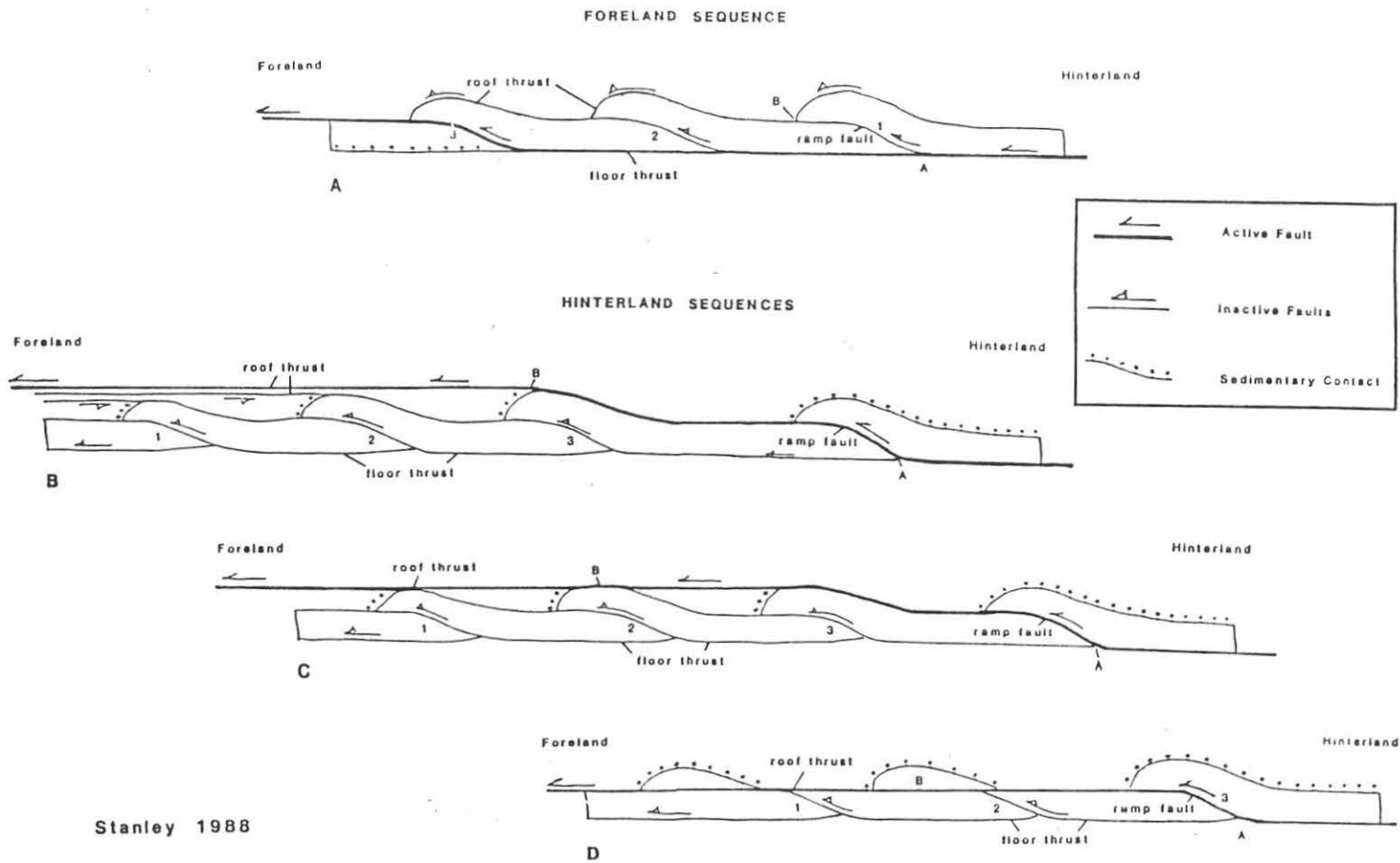


Figure 8 Comparison between imbricate thrust faults that become younger toward the foreland (foreland sequence) and those that become younger toward the hinterland (hinterland sequences). In all models the ramp faults are numbered 1, 2, and 3 in the direction of the ramp with the youngest age. In **A**, the foreland sequence, the older roof thrusts are cut by the younger ramp faults (loc. **B**) whereas the ramp faults are cut by the floor thrust nearest the foreland (loc. **A**). The age and the fault-zone fabric along the floor thrust become older and more complex toward the hinterland. In the hinterland sequences each floor thrust toward the foreland is cut by the ramp fault with the next higher number toward the hinterland (loc. **A**, for example). The roof thrusts must cut across folded bedding (not shown) along the limb facing the foreland (loc. **B**) in **B** and **C**. **D** is considered an unlikely possibility in nature because the roof thrust must cut across the strong rocks of the "beam" rather than follow the weak layer between the "beam" and the

overlying shale. In all hinterland sequences the age and fault-zone fabrics along the roof thrust become older and more complex toward the foreland. In **C** the number of roof thrusts increases toward the foreland. Their individual fault fabrics may be relatively simple since they may not be involved with repeated movement during each imbrication. The position of the sedimentary contacts, here defined as a contact that is not involved with shortening of the "beam", is a very important criterion that separates foreland from hinterland sequences. In the hinterland sequences either the anticlinal limb facing the foreland (**B** and **C**) or the full ramp anticline (**D**) are sedimentary contacts. In the foreland sequence the ramp thrust caps all the anticlines. A basic assumption in all these models is that faults that have undergone repeated movement during their evolution will be planar or geometrically simple. These faults are the labelled the "active faults" in the models.

western part. The fabric along the floor fault, however, appears to be just as complex to the west as it is to the east. I have not been able to identify any feature that can be correlated directly with age. Other such factors as fault junctions in the ramp or duplex areas and broad flexures along the intervening flats control the thickness and complexity of the fault zone and, hence, overshadow any age-related fabric that might be preserved along the length of the fault. Leonard (1985) studied the fault zones in the field and in oriented thin sections cut parallel and perpendicular to the slickenlines.

The important facts that bear on the evolution of the fault-zones are the following:

1) All the fault zones are filled with veins of sparry calcite and minor quartz which are generally oriented either parallel or at a low angle to the fault surface. Vertical veins, which commonly join sills higher in the fault zone, are more common in the lowest layers of the fault zone and in the shale directly beneath the fault zone. Here in the shale some of the thinnest veins are filled with fibrous calcite and shale chips which are aligned parallel to the vein walls in the typical "crack-seal" pattern of Ramsay (1980).

2) Discontinuous, dark, stylolitic clay laminae with concentrations of quartz adjacent to or within the laminae are interlayered with the calcite in all but thinnest zones. The laminae are identical in appearance to the selvages on the S1 cleavage surfaces. Some of the clay laminae are continuous with chips of shale which are either completely enclosed within a calcite layer or occur at the boundary between two calcite veins. These shale chips preserve varying degrees of pressure solution. For example, some of the chips are similar to the undeformed shale in microlithons away from fault zones whereas others have dark, thin selvages within the chip and along their edges.

3) A relative planar surface decorated with shale laminae cuts older surfaces in the fault-zone deposit and is continuous for 1.5 or 3 m along the floor fault. Such surfaces as this are called slip surfaces.

4) The size of the sparry calcite is directly proportional to vein width. Most grains are bladed in form, but their long axes is not preferentially aligned. The calcite in all the layers is twinned with the greatest density occurring in the thinner layers between shale laminae where the grains are turbid and small. The larger grains in thicker layers nearest the planar slip surface are generally more twinned than are those grains in veins further away.

5) Quartz occurs in a variety of forms. Large euhedral quartz crystals are found here and there in the middle of wide calcite veins. The quartz is deformed by fracture

whereas the calcite is twinned. Small crystals occur along the edges of selvages. Very small grains with oriented C axes and indistinct borders are oriented parallel to some vein boundaries. In other areas calcite and quartz appear to be randomly intergrown with indistinct and irregular boundaries. The quartz in the microlithons in the shale away from faults is equant whereas it is elliptical in the well cleavage zone within a foot of the floor fault.

6) The slickenlines on each of the vein layers are formed by grooves rather than calcite fibers.

7) The calcite-shale layers tend to be more parallel in sections cut parallel to the slickenlines rather than they are in sections cut perpendicular to the slickenlines where the layers are irregular or anastomose.

It is clear from the foregoing information that the calcite has been intruded along the faults after the initial cohesion had been broken along the shale-shale or shale-micrite contacts where the strength contrast is the greatest and the cohesive strength the weakest. Once such a zone has developed and is filled with calcite, it becomes a zone of weakness. Subsequent failure likely occurred along the calcite-shale interface and resulted in scabs and chips of the shale being incorporated into the fault zone. Other shale fragments may have been sheared in along faults or carried in along thick veins. During renewed movement the calcite and quartz were dissolved from the shale to form the black selvages which are interlayered with the calcite and decorate the slip surfaces. These boundaries then formed weak planes along which subsequent movement occurred within the fault zones. As the fault zone thickened movement could occur along planar surfaces (slip surfaces) which smoothed out the irregular geometry formed by ramp zones and broad folds in the intervening flat regions of the micrite bed. Movement therefore was no longer restricted to the calcite-shale boundaries of thin fault zones, but could occur along any favorably situated calcite-selvedge boundary. The resulting clay selvedge then acted as a catalyst that facilitated solution of calcite from the selvedge-calcite boundary of the surrounding veins. This process resulted in the stylolitic form of the selvedge. Leonard (1985) suggested that preferential solution in the direction of fault movement produced the slickenline grooves and the stylolitic selvages best seen in sections cut perpendicular to the slickenlines.

Because the floor fault was continually active during the evolution of the imbricate system, it is not surprising to find evidence for repeated vein injection in the form of numerous crosscutting veins in the thick fault zone deposit. During each of these events the influx of fluid and the subsequent crystallization were relatively rapid so that

sparry calcite formed rather than fibered calcite. As the fault zone thickened with layers of calcite and clay selvage, new veins could form along any surface of weakness within the fault zone rather than being confined to the outer borders with the country rock. As movement continued across the fault zone, the calcite in the older veins became heavily twinned and severely strained. Repeated solution of calcite along their boundaries with the adjacent clay selvages reduced their thickness and produced the common observation that calcite in many of the thinner veins are heavily twinned.

The senario that has been inferred from the fault zone fabrics and the relative age relations among the faults suggests that fault movement was intermittent with each event occuring rapidly. During the intervening time deformation in the fault zone may have been restricted to twinning in the calcite.

SHORTENING AND CLEAVAGE DEVELOPMENT

The shortening across the outcross is conveniently recorded by the folds in the ramps areas and structural overlap across the faults. The displacement on each of the faults in the micrite bed ranges from 7.6 to 48.3 cm which adds up to a total displacement of 134 cm (1.34 m) over a present horizontal distance of 10.7 m. The five anticlines over ramps and the broad folds along the flats account for approximately 12.7 cm of additional shortening so that the total shortening equal 146.7 cm (1.47 m). These values correspond to a shortening of 13.7 percent of which folding only accounts for 8.7 percent of the total reduction in length.

In the shale the corresponding shortening is provided by volume reduction across the cleavage surfaces, S1 and to a far lesser degree St. It is clear that these cleavages formed by pressure solution because they are marked by insoluble residue. Furthermore the abundance of calcite and minor quartz in fractures and along the faults indicates that these two minerals were dissolved from the calcareous shale and deposited in nearby openings. In order to see if the shortening determined from the micrite bed is comparable to the shortening in the shale, an independent estimate therefore was made for the shale by determining the percentage of insoluble material. Samples of suitable material from four different microlithons where immersed in hydrochloric acid until all the soluble material was eliminated. The final average residue was 36 percent of the original mass (a range of 32% to 39% for 4 samples). The number of cleavage selvages was then counted across a present outcrop width of 7.9 m measured perpendicular to the cleavage. The total width of the selvages (a range of 35.4 to 54 cm) was then multiplied by 2.8 to given an estimate of

the original width now represented by the cleavages (99 to 152 cm). The original length of the present 7.9 m width was then estimated to be 8.8 to 9.5 cm. Shortening was then calculated to be in the range of 11 to 16 percent. Although this range overlaps the shortening value determined from the "beam", the shale value is less accurate because there is more error in estimating the thickness and number of the cleavage selvages.

I therefore conclude that the formation of the cleavage and consequent shortening in the shale occurred during imbricate faulting in the micrite bed. Although this conclusion may seem intuitively obvious, it does have important implications for the evolution of the cleavage. Because I have already proven that the faults represent a time-transgressive sequence that developed from east to west, I must also conclude that the cleavage in the surrounding shales developed in a similar manner. Unlike my earlier conclusion, this relation is far from obvious if my observations were restricted just to the cleaved shale. In fact it is the existence of the micrite bed and its fault geometry that allows me to conclude that the cleavage in the shale is indeed a time transgressive phenomena.

The next problem is the origin of Sr, the rotated cleavage, and St the finely spaced cleavage below the floor thrust. Because Sr is simply the dominant S1 cleavage that has been rotated in simple shear near the floor and roof faults, it had to form during subsequent displacement on these faults. Measurements of cleavage rotation taken at 8 locations below the micrite bed averaged 36 degrees whereas similar measurements taken at 7 locations above the micrite bed averaged 27 degrees (Table 1). These line rotations correspond to angular shear strains of 51 degrees for the floor thrust and 33 degrees for the various roof thrusts using equation 2.3 of Ramsay and Huber (1983) in which Γ , the shear strain = $\cot \alpha - \cot \alpha'$. In this equation α and α' are the angles of S1 and St respectively from the fault surface. The fact that the Sr cleavage below the thrust has been rotated in most cases through a greater angle of shear than Sr above the thrust is consistent with my earlier conclusion that the floor thrust was active throughout deformation whereas the individual roof faults are short lived and are only active during the time interval between the formation of each of the imbricate faults.

The St cleavage clearly formed after Sr because it cuts across Sr at a low angle and is not folded or rotated near any of the faults. Although St is best developed below the floor thrust, it is also present just above the roof thrusts where the cleavage is less distinct and occupies a thinner zone compared to the comparable cleavage along the floor thrust. Because the St cleavage is confined to a narrow zone near the faults, it most likely developed as a result of

simple shear which rotated the S1 cleavage. In order to test this hypothesis the angle between St and the nearby fault, O' , was measured and compared with a calculated value predicted by the Ramsay equation $\tan 2O' = 2/\gamma$ (Ramsay and Huber, 1983, equation 2.4; Table 1, this paper). The values of γ were calculated from the rotation of the cleavage using the equation described in the foregoing paragraph (Ramsay and Huber, 1983, eq. 2.3). This equation predicts the acute angle, O' , between the plane defined by λ_1 and λ_2 of the strain ellipsoid (long axis of the strain ellipse in 2 dimensions) and the plane of simple shear which in this case is the fault surface. In the ideal case of simple shear the St cleavage will be parallel to the λ_1 - λ_2 principal plane of the strain ellipsoid. Thus the calculated and observed values should be the same within the margin of error providing no mechanism other than simple shear was involved. Along the floor fault the calculated angle between St and the fault is an average of 29 degrees for 8 separate locations. The observed value, however, was an average of 21 degrees. Along the higher roof thrust the calculated angle between St and the nearby fault was an average of 37 degrees for 6 locations whereas the observed value was 32 degrees. Although the sample population was small and the corresponding standard deviations large for both the calculated and observed values, the differences do suggest two important relations. First, the angle O' between the St cleavage and the fault is larger along the roof thrust than it is for the floor thrust. This relation simply reflects the smaller shear strain along the roof thrust compared to the floor thrust. Second, and more importantly, the calculated angle O' between St and the nearby faults is consistently larger than the observed angle by values that range from 8 degrees for the floor thrust to 5 degrees for the roof thrust. This relation is important because it suggests either that the St cleavage has been subsequently flattened by some sort of vertical loading after simple shear or that the volume reduction, which has occurred during the formation of the St cleavage, has indeed reduced the O' angle. The volume reduction associated with the formation of the St cleavage was probably less than the 10 percent calculated for the S1 because the St surfaces are much thinner than S1 although they are more numerous.

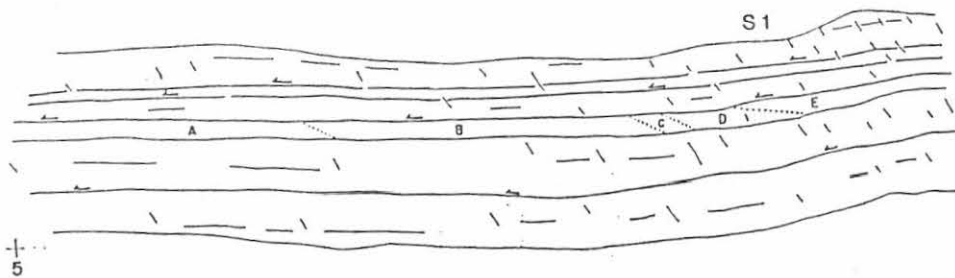
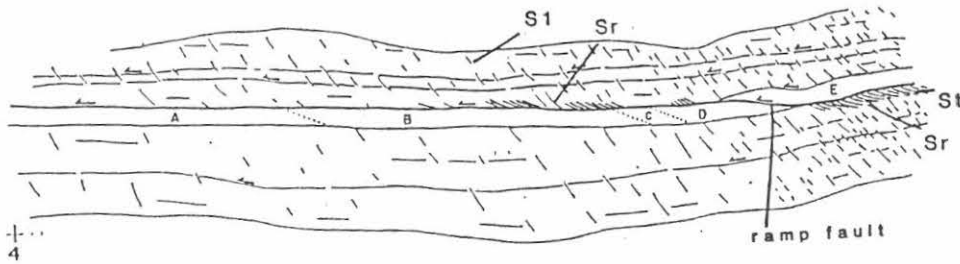
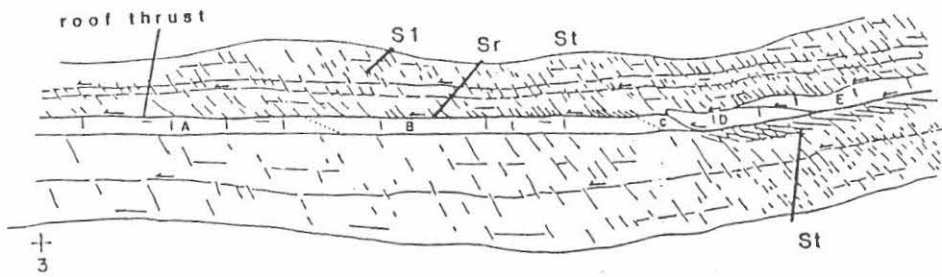
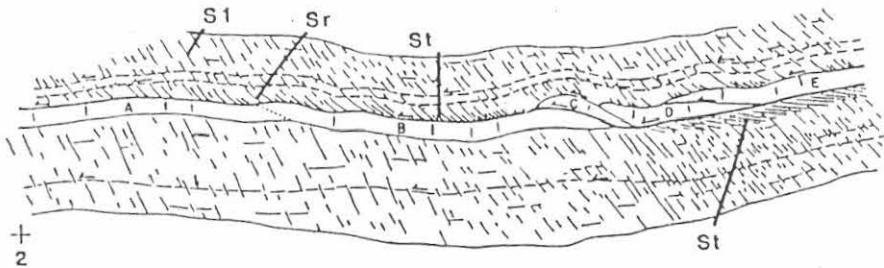
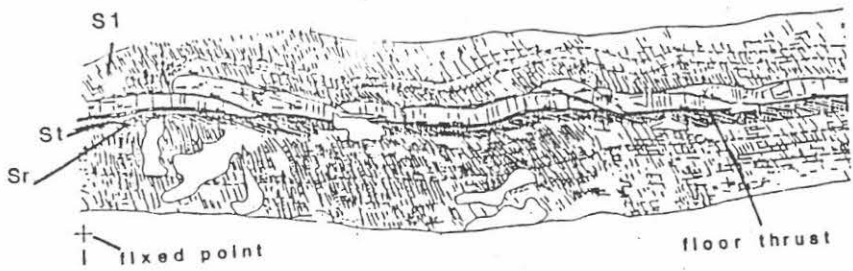
Are Sr and St time transgressive? Because I have demonstrated earlier that the floor fault and the respective roof faults are time transgressive, it must follow that both Sr and St are also time transgressive to the west. This conclusion suggests that the amount of rotation of Sr should also increase to the east particularly along the floor thrust where the displacement is larger and has taken place over a longer period of time. Although this feature was evaluated across the outcrop, I could not detect within the error of my measurements any such relation for Sr. This observation suggests that the process by which the S1 cleavage is bent

essentially work hardens and another deformational mechanism progressively takes over as the angle of line rotation increases during simple shear. This process appears to be the formation of the pressure-solution St cleavage because it is confined to the fault zone and is not bent like the older Sr cleavage. My measurements suggest that the St cleavage probably developed when the S1 cleavage was rotated somewhere in the neighborhood of 35 degrees.

EVOLUTION OF STRUCTURES

The evolution of the imbricate faults and the various cleavages described in the foregoing section is illustrated in a series of retrodeformed sections in figure 9. Section 1 shows the outcrop at South Hero in its present state. Section 2 is developed by reversing the deformation associated with the youngest ramp fault at the western part of the outcrop. The remaining four sections are formed by systematically unroofing the micrite bed from west to east in the reverse order of their formation. For example, in section 2 the hanging wall block (B, section 2) is unfolded as it is returned to its original position east of the footwall block (A, section 2). During this time the active fault which carried the eastern sequence westward was the floor thrust below segments D and E, the ramp fault just below segment C, and the roof thrust above segments B and A, which were then undeformed. In the shale above and below this active fault the S1 cleavage is shown in a flatter position (Sr) as a result of rotation generated by east-over-west simple shear. Note that the rotated cleavage, Sr, is absent below blocks A and B since, at this time, the micrite bed is attached to the underlying shale. The fault-zone cleavage, St, is also shown in the shale along the active fault. I believe that this cleavage developed during the evolution of the imbricate structures rather than after all the imbricate faults had formed because St is present, although poorly developed, along the roof thrust above each segment of the micrite bed. If the fault-zone cleavage had formed after all the imbricate faults had moved into place, then it (St) would only be found along the floor thrust. The St cleavage therefore must have developed during the formation of each imbricate fault.

As a consequence of reversing the displacement on the fault and unfolding the ramp fold, the volume in the adjacent shale must be increased by eliminating much of the cleavage below segments A and B of the micrite bed. Note, however, that the density of S1 cleavage in the thrust plate above segments A and B is essentially the same across section 2. This diagram is drawn in this way because I believe that the upper plate of the active fault was probably being shortened as a result of ramps or irregularities along the fault surface farther to the west. In actual fact, however, the density of S1 in the upper plate must decrease to the west because, first, this is



RETRODEFORMED SECTION OF THE CUMBERLAND HEAD FORMATION

Figure 9

SOUTH HERO, VERMONT

Stanley, 1987

what is observed to the west across South Hero Island and, second, the overall stress intensity during deformation in theoretical models diminishes from the hinterland to the foreland (for example, Hubbert, 1951; Chapple, 1979; Davis and others, 1982). Thus at any one time the cleavage density not only diminishes toward the foreland but it also changes in the same way from the upper plate to the lower plate (compared sections 2 through 5). As deformation progresses older cleavage surfaces continue to grow in thickness and lateral extent and younger surfaces nucleate in older microlithons and grow essentially parallel to the older S1 surfaces. In the end the S1 cleavage is uniformly developed across the outcrop and appears to the casual observer to be coeval across the outcrop because its style and orientation are the same. As can be seen in these series of sections, however, that the S1 cleavage is clearly a time transgressive structure.

Sections 3, 4 and 5 show the retrodeformation continuing to the east and are constructed in the same manner as section 2. Thus the evolution of the imbricate system and its associated structures can be seen by studying diagrams 5 through 1. Clearly all the structures are time transgressive from east to west as they are traced through sections 5 to section 1. During deformation the floor thrust or basal decollement undergoes repeated west-directed movement. As a result the Sr cleavage is rotated to a larger angle along the floor thrust than it is along the roof thrusts. When this angle reaches values in the range of 30 to 35 degrees, it appears that pressure solution takes over as the dominant shortening mechanism and the fault-zone cleavage, St, begins to be developed. Because the floor thrust continually moves the St cleavage is better developed there than along the higher roof faults.

STOP 4 - THE CHAMPLAIN THRUST FAULT AT LONE ROCK POINT, BURLINGTON, VERMONT - The following discussion is reprinted from The Centennial Field Guide, Volume 5, of the Geological Society of America in 1986. All the figure numbers for this stop refer to those figures in the reprint. The reprinted discussion appears in Appendix 1. Figure 10 is a regional map showing the location of the Champlain thrust fault in western Vermont. The Long Rock Point locality is identified as "LRP". The Arrowhead Mountain thrust fault is located east of the Champlain thrust fault and is identified by the letters "AMTF".

STOP 5 - THE HINESBURG THRUST FAULT AT HINESBURG, VERMONT - This is the classic and best exposed locality for the Hinesburg thrust fault (fig. 10, "HTFM"). It contains many fault related fabrics that have recently been studied by Strehle (1985) and published by Strehle and Stanley (1986) in a bulletin of the Vermont Geological Survey (Studies in

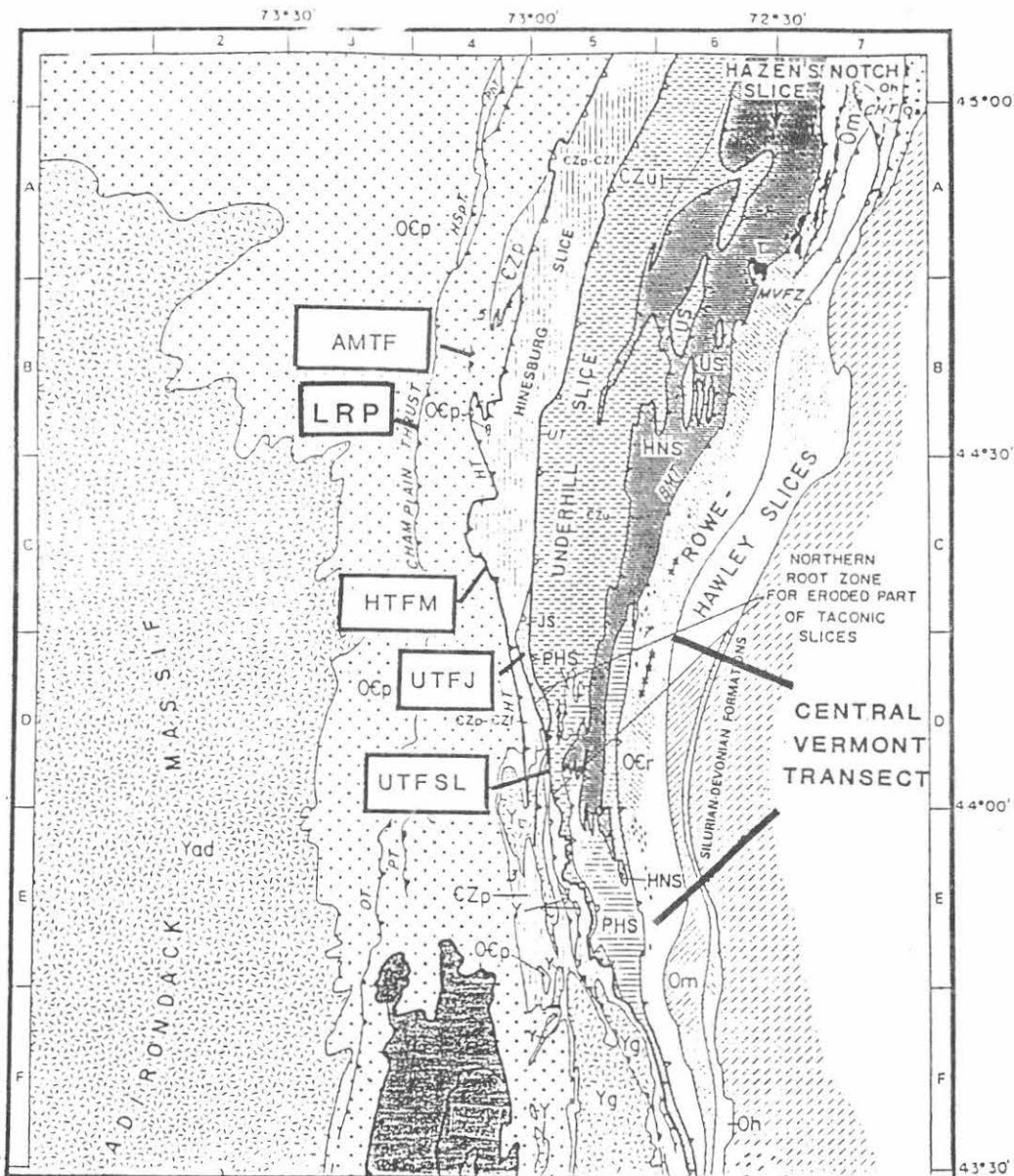


Figure 10 Interpretative Tectonic Map of Vermont and eastern New York showing the general location of the Arrowhead Mountain thrust fault (AMTF), the Hinesburg thrust fault at Mechanicsville (HTFM), and the Underhill thrust fault at Jerusalem (UTFJ), and South Lincoln (UTFSL). The geological map is taken from Stanley and Ratcliffe (1985, Pl. 1, figure 2a). Symbol \bar{T} in A6 is a glaucophane locality at Tilliston Peak. Short line with x's (Worcester Mountains) and line with rhombs (Mount Grant) in C6 and D5 mark the Ordovician kyanite-chloritoid zones of Albee (1968). Widely-spaced diagonal lines in northcentral Vermont outline the region that contains medium-high pressure amphibolites described by Laird and Albee (1981b). Irregular black marks are ultramafic bodies. Open teeth of thrust fault symbols mark speculative thrust zones. The following symbols are generally listed from west to east. *Yad*, Middle Proterozoic of the Adirondack massif; *Yg*, Middle Proterozoic of the Green Mountain massif; *YL*, Middle Proterozoic of the Lincoln massif; *Y*, Middle Proterozoic between the Green Mountain massif and the Taconic slices, Vermont; *OCp*, Cambrian and Ordovician rocks of the carbonate-siliciclastic platform; rift-clastic sequence of the Pinnacle (*CZp*) and Fairfield Pond Formations (*CZf*) and their equivalents on the east side of the Lincoln and Green Mountain massifs, *PhT*, Philipsburg thrust; *HSpT*, Highgate Springs thrust; *PT*, Pinnacle thrust; *OT*, Orwell thrust, *UT*, Underhill thrust; *HT*, Hinesburg thrust; *U*, ultramafic rocks; *CZu*, Underhill Formation; *CZuj*, Jay Peak Member of Underhill Formation; *OCr*, Rowe Schist; *Om*, Moretown Formation; *Oh*, Hawley Formation and its equivalents in Vermont; *JS*, Jerusalem slice; *US*, Underhill slice; *HNS*, Hazens Notch slice; *MVFZ*, Missisquoi Valley fault zone; *PHS*, Pinney Hollow slice; *BMT*, Belvidere Mountain thrust; *CHT*, Coburn Hill thrust; *Qa*, Ascot-Weedon sequence in grid location 7A.

Vermont Geology No.3). This publication also contains analyses of other fault zones of western Vermont which will not be seen during this conference. The reader is referred to this paper or an earlier NEIGC trip by Gillespie and others (1972).

The Hinesburg thrust fault separates the Cambrian-Ordovician rocks of the platform sequence from the older, highly deformed metamorphic rocks of the eastern hinterland. As shown in figure 4, the Hinesburg thrust fault developed along the overturned, sheared limb of a large recumbent fold. This fault probably broke out from the overturned limb of a fault-propagation fold (Suppe, 1985) and therefore is similar in origin to the Arrowhead Mountain thrust fault. To the south the Hinesburg thrust fault dies out somewhere in the overturned limb of the Lincoln massif (Tauvers, 1982; DiPietro, 1983; DelloRusso and Stanley, 1986).

At the Mechanicsville locality the lower 40 m. of the Cheshire Quartzite is structurally overturned along the base of the upper plate of the Hinesburg thrust fault. Higher up the cliff the quartzite grades into the Fairfield Pond Formation of Tauvers (1982). The lower plate rocks, which are poorly exposed, consist of carbonates of the Lower Ordovician Bascon Formation. Slivers of dark gray phyllite of the Brownell Mountain Phyllite are found at several localities along the fault trace. Chlorite, muscovite, and stilpnomelane are present in the quartzite. Muscovite and chlorite are present in the schist. Quartz is thoroughly recrystallized, but feldspar grains are fractured and bent.

The following features should be studied here:

- 1) The change in fabric as the fault surface is approached. The quartzite grades from a protomylonite away from the fault to an ultramylonite near the fault. In thin section quartz becomes finer grained and quartz porphyroclasts decrease in number toward to fault.

- 2) The presence of east-over-west or "S" shaped asymmetrical folds. These folds are related to simple shear along the fault and are not related to the overturned limb of the older Hinesburg nappe. Parasitic minor folds related to this older structure would show a west-over-east or "Z" shaped asymmetry.

- 3) The prominent compositional layering. This layering is not bedding but represents the axial surface schistosity of the older parasitic folds related to the Hinesburg nappe. It is overprinted by a younger schistosity that is associated with the east-over-west folds. These two schistosities become a composite mylonitic schistosity as the fault surface is approached.

4) The prominent mineral lineation consisting of elongate quartz and quartz clusters.

5) "Z" shaped quartz veins that are associated with beds of quartzite. These structures are particularly interesting because the record progressive shear strain and mylonitization along the fault. The veins are confined to the metasandstone and metasiltstone layers and occur in at least 3 orientations. The least deformed veins are oriented either perpendicular to the layering or dip steeply to the west. They are filled with straight quartz fibers oriented perpendicular to the vein walls and show no signs of recrystallization except where they cross older "Z" shaped veins (Warren, 1988, pers. comm.). Here the fibers are reduced to smaller, nearly equant grains with undulose extinction. The most deformed veins are "Z" shaped and dip to the east. The older quartz fibers are completely replaced by fine grained, recrystallized quartz that forms a mylonite with distinct whitish layers oriented essentially parallel to the vein boundary. The third set is intermediate in orientation and deformation between the other two. The "Z" pattern develops because the shear strain (8.5 or an angle of shear of 84°) is higher in the pelitic units that surround the metasandstones where the shear strain is 1.48 (angle of shear of 56°). Strehle and Stanley (1986) suggested that these veins developed as shear fractures during east-over-west shear. This interpretation is not consistent with the fact that the youngest veins are vertical and consist of quartz fibers orientated essentially parallel to the layering (Warren, 1988, pers. comm.). It therefore appears that the veins formed as extension fractures during periods of vertical or near vertical loading. These periods of flattening (pure shear) were then followed by longer periods of east-over-west simple shear during which the veins were rotated westward and the characteristic "Z" pattern developed. The quartz, which was originally fibered, became progressively mylonitized as the extension veins were rotated into the favorable, east-dipping, shear position. Movement on these east-dipping veins continued even after they were cut by younger, unrotated veins because the fibered segments of the younger veins are deformed and recrystallized.

6) Rare west-dipping shear bands. These structures deform the younger schistosity which is parallel to the axial surfaces of the "S" shaped folds.

7) Westward displacement (N 75 W) of the upper plate of the Hinesburg thrust is documented by "S" shaped folds, "Z" shaped-quartz veins, quartz porphyroclasts, and late shear bands.

8) Late fractures and associated en echelon fracture arrays. These structures thought to be related to Mesozoic normal faults which cut the Champlain and Hinesburg slices.

One of these faults is located about 1000 m. directly west of this locality.

The interpretation of these structures and the thin sections fabrics are discussed in Strehle and Stanley (1986).

ACKNOWLEDGEMENTS

Many students have helped in the collection of data and the discussions that have resulted in my interpretations at the "beam", the Hinesburg thrust fault, and western Vermont. Although each has contributed in their own way, I would like to mention a few who have contributed above and beyond the "call to duty". At the "beam" John Humphrey provided data and calculations for shortening in the shale. John Delphia was one of the first to retrodeform the beam and demonstrate the time-transgressive nature of the cleavages. Vinnie DelloRusso supplied much of the data for figure 7b. Steve Taylor analyzed the quartz-fiber geometry associated with late pyrite at the Hinesburg thrust. Tom Armstrong stimulated revision of my earlier interpretations on the composition layering and the "S" shaped folds. Marian Warren provided important information on the "Z" shaped quartz veins at Hinesburg. Her work is still continuing. The work from South Hero was part of Kitty Leonard's Master of Science thesis (1985) while the Hinesburg thrust was part of Dick Gillespie's thesis in 1972. Barbara Strehle's work on the Arrowhead Mountain and Hinesburg thrust faults was very important to our present understanding of the transition from foreland to hinterland fault-zone fabrics. Last, but far from least, was the critical work and synthesis of Becky Dorsey. Her success was in part a result of earlier "pioneer" work by Eric Rosencranz, Paul Agnew, and Craig Carter. To all of these students and those that I have failed to mention - "thanks for the memories".

REFERENCES

- Agnew, P.C., 1977, Reinterpretation of the Hinesburg thrust in northwestern Vermont: M. S. thesis, University of Vermont, Burlington, Vermont, 82p.
- Alvarez, Walter, Engelder, J. T., Geiser, P. A., 1978, Classification of solution cleavage in pelagic limestone: *Geology*, v. 6, p. 263-266.
- Butler, R. G., Jr., 1986, Sedimentation of the Upper Cambrian Danby Formation of western Vermont; an example of mixed siliciclastic and carbonate platform sedimentation: M. S. thesis, University of Vermont, Burlington, Vermont, 137p.
- Cady, W. M., 1945, Stratigraphy and structure of west-central Vermont: *Geological Society of America Bulletin*, v. 56, p. 515-587.
- Cady, W. M., Albee, A. L., and Murphy, J. F., 1962, Bedrock geology of the Lincoln Mountain quadrangle, Vermont: U. S. Geological Survey Geologic Quadrangle Map, GQ - 164, scale 1:62,500.
- Carter, C. M., 1979, Interpretation of the Hinesburg thrust north of the Lamoille River, northwestern Vermont: M. S. Thesis, University of Vermont, Burlington, Vermont, 84 p.
- Chapple, W. M., 1979, Mechanics of thin-skinned fold and thrust belts: *Geological Society of America Bulletin*, v. 89, p. 1189-1198.
- Davis, Dan, Suppe, John, and Dahlen, D. A., 1983, Mechanics of fold and thrust belts and accretionary wedges: *Journal of Geophysical Research*, v. 88, p. 1153-1172.
- DiPietro,-----, 1983, Geology of the Starksboro area, Vermont: Vermont Geological Survey Special Bulletin No. 4, 14 p.
- Doll, C. G., Cady, W. M., Thompson, J. B., Jr., and Billings, M. P., 1961, Centennial Geologic Map of Vermont: Montpelier, Vermont, Vermont Geological Survey, Scale 1:250,000.
- Dorsey, R. L., Agnew, P. C., Carter, C. M., Rosencrantz, E. J., Stanley, R. S., 1983, Bedrock geology of the Milton quadrangle, northwestern Vermont: Vermont Geological Survey Special Bulletin No. 3, 14 p.
- Erwin, R.B., 1957, The geology of the limestone of Isle La Motte and South Hero Island, Vermont: Vermont Geological Survey Bulletin No. 9, 94p.

- Gregory, G. J., 1982, Paleoenvironments of the Dunham Dolomite (Lower Cambrian) of northwestern Vermont: M. S. thesis, University of Vermont, Burlington, Vermont, 180p.
- Gillespie, R. P., Stanley, R. S., Barton, T. E., and Frank, T. K., 1972, Superposed folds and structural chronology along the southeastern part of the Hinesburg synclinorium: in Doolan, B.D., and Stanley, R. S., eds., Guidebook to field trips in Vermont, New England Intercollegiate Geological Conference 64th Annual Meeting, University of Vermont, Burlington, Vermont, p. 151 - 166.
- Hawley, David, 1957, Ordovician shales and submarine slide breccias of northern Champlain Valley in Vermont: Geological Society of America Bulletin, v. 68, p. 155-194.
- , 1972, Sedimentation characteristics and tectonic deformation of Middle Ordovician shales of northwestern Vermont north of Malletts Bay: in Doolan, B.D., and Stanley, R. S., eds., Guidebook to field trips in Vermont, New England Intercollegiate Geological Conference 64th Annual Meeting, University of Vermont, Burlington, Vermont, p. 151 - 166.
- Hubbert, M. K., 1951, Mechanical basis for certain familiar geologic structures: Geological Society of America Bulletin, v. 62, p. 355-372.
- Laird, Jo, 1987, Metamorphism of pre-Silurian rocks, Central Vermont, in Westerman, D. S., ed., Guidebook for Field Trips in Vermont, Volume 2, New England Intercollegiate Geological Conference 79th Annual Meeting, Montpelier, Vermont; p. 339-344.
- Leonard, Katherine, 1985, Foreland folds and thrust belt deformation chronology, Ordovician limestone and shale, northwestern Vermont: M. S. thesis, University of Vermont, Burlington, Vermont, 120p.
- McHone, J. G. and Bulter, J. R., 1984, Mesozoic igneous provinces of New England and the opening of the Atlantic: Geological Society of America Bulletin, V. 95, p. 757-765.
- McLean, D. A., 1986, Depositional environments and stratigraphic relationships of the Glens Falls Limestone, Champlain Valley, Vermont and New York: M. S. thesis, University of Vermont, Burlington, Vermont, 170p.
- , 1987, Facies relationships within the Glen Falls Limestone of Vermont and New York, in Westerman, D. S., ed., Guidebook to field trips in Vermont, Volume 2, New England Geological Conference 79th Annual Meeting, Montpelier, Vermont, p. 53-79.

- Mehrtens, C. J., 1985, The Cambrian platform in northwestern Vermont: Vermont Geology, v. 4., p. E1-E16.
- Mehrtens, C. J., Parker, Ronald, and Butler, Robert, 1987, The Cambrian platform in northwestern Vermont in Westerman, D. S., ed., Guidebook to field trips in Vermont, Volume 2, New England Geological Conference 79th Annual Meeting, Montpelier, Vermont, p. 254-270.
- Myrow, Paul, 1983, Sedimentology of the Cheshire Formation in west-central Vermont: M. S. thesis, University of Vermont Burlington, Vermont, 177p.
- Ramsay, J. G., 1980, Shear zone geometry: a review: Journal of Structural Geology, v. 2, no. 1/2, p. 83-99.
- Ramsay, J. G. and Huber, M. I., 1984, The techniques of modern structural geology, vol. 1, Strain analysis: Academic Press, London, 306p.
- Stanley, R. S., 1980, Mesozoic faults and their environmental significance in western Vermont: Vermont Geology, v. 1, p. 22-32.
- , 1987, The Champlain thrust fault, Lone Rock Point, Burlington, Vermont: Geological Society of America, Centennial Field Guide for the Northeast Section, p. 67-72.
- Stanley, R. S., Ratcliffe, N. M., 1985, Tectonic synthesis of the Taconic orogeny in western New England: Geological Society of America Bulletin, v.96, p. 1227-1250.
- Sutter, J.F., Ratcliffe, N.M., and Mukasa, S.B., 1985
⁴⁰Ar/³⁹Ar and K-Ar data bearing on the metamorphic and tectonic history of western New England: Geological Society of America Bulletin, in press.
- Tauvers. P. R., 1982, Bedrock geology of the Lincoln area, Vermont: Vermont Geological Survey Special Bulletin No. 2, 8 p.
- Sheppard, S. M. F., and Schwarcz, H. P., 1970, Fractionation of carbon and oxygen isotopes and magnesium between coexisting metamorphic calcite and dolomite: Contributions to Mineralogy and Petrology, v. 26, p. 161-198.
- Stone, S. W. and Dennis, J. G., 1964, The geology of the Milton quadrangle, Vermont: Vermont Geological Survey Bulletin No. 26, 79p.
- Strehle, B. A. and Stanley, R. S., 1986, A comparison of fault zone fabrics in northwestern Vermont: Vermont

Geological Survey, Studies in Vermont Geology No. 3, 36 p.
and 4 plates.

Suppe, John, 1985, Principles of structural geology:
Prentice-Hall Inc., 537p.

Teetsel, M. B., 1984, Sedimentation of the Taconic foreland
basin shales in northwestern Vermont: M. S. thesis,
University of Vermont, Burlington, Vermont, 97p.

Voll, G., 1976, Recrystallization of quartz, biotite, and
feldspars from Erstfeld to the Leventina nappe, Swiss
Alps, and its geological significance; Schweiz. Mineral.
Petrogr. Mitt., v. 56, p. 641- 647.

Welby, C. W., 1961, Bedrock geology of the central Champlain
Valley of Vermont: Vermont Geological Survey Bulletin No.
14, 296p.

APPENDIX 1 - LONG ROCK POINT - REPRINT.

The Champlain thrust fault, Lone Rock Point, Burlington, Vermont

Rolfe S. Stanley, Department of Geology, University of Vermont, Burlington, Vermont 05405

LOCATION

The 0.6 mi (1 km) exposure of the Champlain thrust fault is located on the eastern shore of Lake Champlain at the north end of Burlington Harbor. The property is owned by the Episcopal Diocesan Center. Drive several miles (km) north along North Avenue (Vermont 127) from the center of Burlington until you reach the traffic light at Institute Road, which leads to Burlington High School, The Episcopal Diocesan Center, and North Beach. Turn west toward the lake and take the first right (north) beyond Burlington High School. The road is marked by a stone archway. Stop at the second building on the west side of the road, which is the Administration Building (low rectangular building), for written permission to visit the field site.

Continue north from the Administration Building, cross the bridge over the old railroad bed, and keep to the left as you drive over a small rise beyond the bridge. Go to the end of this lower road. Park your vehicle so that it does not interfere with the people living at the end of the road (Fig. 1). Walk west from the parking area to the iron fence at the edge of the cliff past the outdoor altar where you will see a fine view of Lake Champlain and the Adirondack Mountains. From here walk south along a footpath for about 600 ft (200 m) until you reach a depression in the cliff that leads to the shore (Fig. 1).

SIGNIFICANCE

This locality is one of the finest exposures of a thrust fault in the Appalachians because it shows many of the fault zone features characteristic of thrust faults throughout the world. Early studies considered the fault to be an unconformity between the strongly-tilted Ordovician shales of the "Hudson River Group" and the overlying, gently-inclined dolostones and sandstones of the "Red Sandrock Formation" (Dunham, Monkton, and Winoski formations of Cady, 1945), which was thought to be Silurian because it was lithically similar to the Medina Sandstone of New York. Between 1847 and 1861, fossils of pre-Medina age were found in the "Red Sandrock Formation" and its equivalent "Quebec Group" in Canada. Based on this information, Hitchcock and others (1861, p. 340) concluded that the contact was a major fault of regional extent. We now know that it is one of several very important faults that floor major slices of Middle Proterozoic continental crust exposed in western New England.

Our current understanding of the Champlain thrust fault and its associated faults (Champlain thrust zone) is primarily the result of field studies by Keith (1923, 1932), Clark (1934), Cady (1945), Welby (1961), Doll and others (1961), Coney and others (1972), Stanley and Sarkisian (1972), Dorsey and others (1983), and Leonard (1985). Recent seismic reflection studies by Ando and others (1983, 1984) and private industry have shown that the Champlain thrust fault dips eastward beneath the metamorphosed rocks of the Green Mountains. This geometry agrees with earlier interpretations shown in cross sections across central and

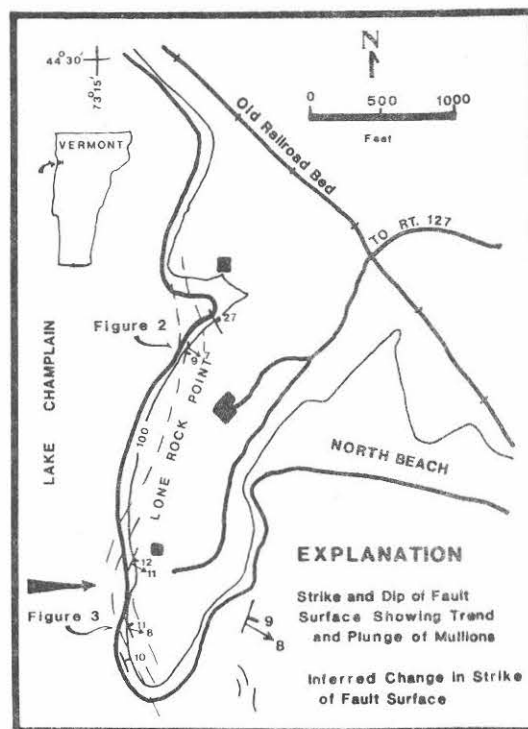


Figure 1. Location map of the Champlain thrust fault at Lone Rock Point, Burlington, Vermont. The buildings belong to the Episcopal Diocesan Center. The road leads to Institute Road and Vermont 127 (North Avenue). The inferred change in orientation of the fault surface is based on measured orientations shown by the dip and strike symbols. The large eastward-directed arrow marks the axis of a broad, late syncline in the fault zone. The location of Figures 2 and 3 are shown to the left of "Lone Rock Point." The large arrow points to the depression referred to in the text.

northern Vermont (Doll and others, 1961; Coney and others, 1972). Leonard's work has shown that the earliest folds and faults in the Ordovician sequence to the west in the Champlain Islands are genetically related to the development of the Champlain thrust fault.

In southern Vermont and eastern New York, Rowley and others (1979), Bosworth (1980), Bosworth and Vollmer (1981), and Bosworth and Rowley (1984), have recognized a zone of late post-cleavage faults (Taconic Frontal Thrust of Bosworth and Rowley, 1984) along the western side of the Taconic Mountains. Rowley (1983), Stanley and Ratcliffe (1983, 1985), and Ratcliffe (in Zen and others, 1983) have correlated this zone with the Champlain thrust fault. If this correlation is correct then the Champlain thrust zone would extend from Rosenberg, Canada, to the Catskill Plateau in east-central New York, a distance of 199 mi (320 km), where it appears to be overlain by Silurian and Devonian rocks. The COCORP line through southern Vermont

shows an east-dipping reflection that roots within Middle Proterozoic rocks of the Green Mountains and intersects the earth's surface along the western side of the Taconic Mountains (Ando and others, 1983, 1984).

The relations described in the foregoing paragraphs suggest that the Champlain thrust fault developed during the later part of the Taconian orogeny of Middle to Late Ordovician age. Subsequent movement, however, during the middle Paleozoic Acadian orogeny and the late Paleozoic Alleghenian orogeny can not be ruled out. The importance of the Champlain thrust in the plate tectonic evolution of western New England has been discussed by Stanley and Ratcliffe (1983, 1985). Earlier discussions can be found in Cady (1969), Rodgers (1970), and Zen (1972).

REGIONAL GEOLOGY

In Vermont the Champlain thrust fault places Lower Cambrian rocks on highly-deformed Middle Ordovician shale. North of Burlington the thrust surface is confined to the lower part of the Dunham Dolomite. At Burlington, the thrust surface cuts upward through 2,275 ft (700 m) of the Dunham into the thick-bedded quartzites and dolostones in the very lower part of the Monkton Quartzite. Throughout its extent, the thrust fault is located within the lowest, thick dolostone of the carbonate-siliciclastic platform sequence that was deposited upon Late Proterozoic rift-clastic rocks and Middle Proterozoic, continental crust of ancient North America.

At Lone Rock Point in Burlington the stratigraphic throw is about 8,850 ft (2,700 m), which represents the thickness of rock cut by the thrust surface. To the north the throw decreases as the thrust surface is lost in the shale terrain north of Rosenberg, Canada. Part, if not all, of this displacement is taken up by the Highgate Springs and Philipsburg thrust faults that continue northward and become the "Logan's Line" thrust of Cady (1969). South of Burlington the stratigraphic throw is in the order of 6,000 ft (1,800 m). As the throw decreases on the Champlain thrust fault in central Vermont the displacement is again taken up by movement on the Orwell, Shoreham, and Pinnacle thrust faults.

Younger open folds and arches that deform the Champlain slice may be due either duplexes or ramps along or beneath the Champlain thrust fault. To the west, numerous thrust faults are exposed in the Ordovician section along the shores of Lake Champlain (Hawley, 1957; Fisher, 1968; Leonard, 1985). One of these broad folds is exposed along the north part of Lone Rock Point (Fig. 2). Based on seismic reflection studies in Vermont, duplex formation as described by Suppe (1982) and Boyer and Elliot (1982) indeed appears to be the mechanism by which major folds have developed in the Champlain slice.

North of Burlington the trace of the Champlain thrust fault is relatively straight and the surface strikes north and dips at about 15° to the east. South of Burlington the trace is irregular because the thrust has been more deformed by high-angle faults and broad folds. Slivers of dolostone (Lower Cambrian Dunham Dolomite) and limestone (Lower Ordovician Beekmantown Group) can be found all along the trace of the thrust. The limestone represents

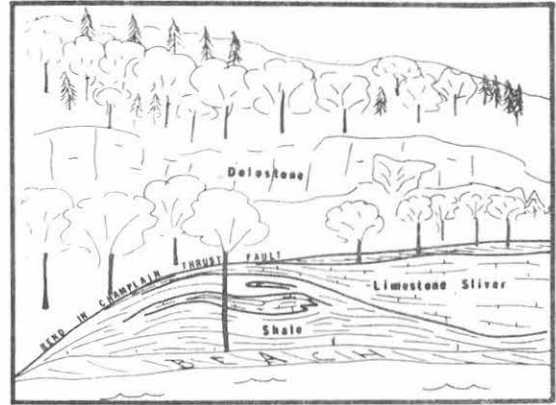


Figure 2. A sketch of the Champlain thrust fault at the north end of Lone Rock Point showing the large bend in the fault zone and the slivers of Lower Ordovician limestone. The layering in the shale is the S1 cleavage. It is folded by small folds and cut by many generations of calcite veins and faults. The sketch is located in Figure 1.

fragments from the Highgate Springs slice exposed directly west and beneath the Champlain thrust fault north of Burlington (Doll and others, 1961). In a 3.3 to 10 ft (1 to 3 m) zone along the thrust surface, fractured clasts of these slivers are found in a matrix of ground and rewelded shale.

Estimates of displacement along the Champlain thrust fault have increased substantially as a result of regional considerations (Palmer, 1969; Zen and others, 1983; Stanley and Ratcliffe, 1983, 1985) and seismic reflection studies (Ando and others, 1983, 1984). The earlier estimates were less than 9 mi (15 km) and were either based on cross sections accompanying the Geologic Map of Vermont (Doll and others, 1961) or simply trigonometric calculations using the average dip of the fault and its stratigraphic throw. Current estimates are in the order of 35 to 50 mi (60 to 80 km). Using plate tectonic considerations, Rowley (1982) has suggested an even higher value of 62 mi (100 km). These larger estimates are more realistic than earlier ones considering the regional extent of the Champlain thrust fault.

Lone Rock Point

At Lone Rock Point the basal part of the Lower Cambrian Dunham Dolostone overlies the Middle Ordovician Iberville Formation. Because the upper plate dolostone is more resistant than the lower plate shale, the fault zone is well exposed from the northern part of Burlington Bay northward for approximately 0.9 mi (1.5 km; Fig. 1). The features are typical of the Champlain thrust fault where it has been observed elsewhere.

The Champlain fault zone can be divided into an inner and outer part. The inner zone is 1.6 to 20 ft (0.5 to 6 m) thick and consists of dolostone and limestone breccia encased in welded, but highly contorted shale (Fig. 3). Calcite veins are abundant. One of the most prominent and important features of the inner fault zone is the slip surface, which is very planar and continuous throughout the exposed fault zone (Fig. 3). This surface is marked by very fine-grained gouge and, in some places, calcite slickenlines. Where the inner fault zone is thin, the slip surface is located

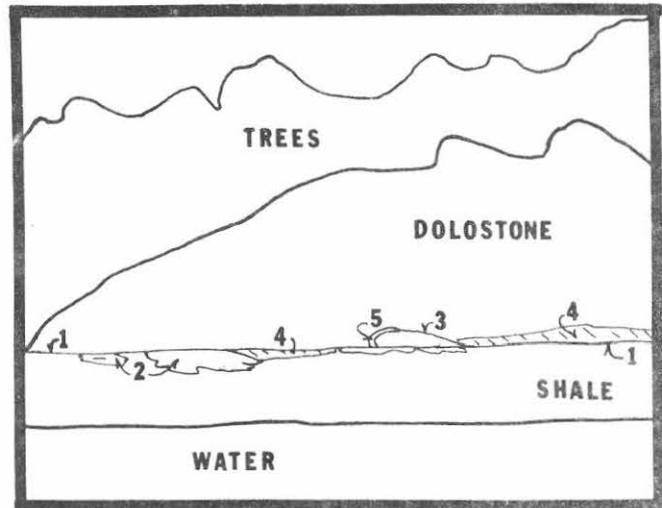
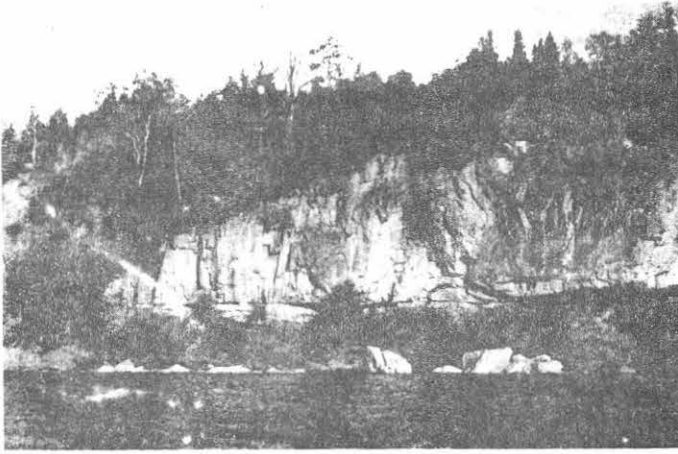


Figure 3. View of the Champlain thrust fault looking east at the southern end of Lone Rock Point (Fig. 1). The accompanying line drawing locates by number the important features discussed in the text: 1, the continuous planar slip surface; 2, limestone slivers; 3, A hollow in the base of the dolostone is filled with limestone and dolostone breccia; 4, Fault mullions decorate the slip surface at the base of the dolostone; 5, a small dike of shale has been injected between the breccia and the dolostone.

along the interface between the Dunham Dolomite and the Iberville Shale. Where the inner fault is wider by virtue of slivers and irregularities along the basal surface of the Dunham Dolomite, the slip surface is located in the shale, where it forms the chord between these irregularities (Fig. 3). The slip surface represents the surface along which most of the recent motion in the fault zone has occurred. As a consequence, it cuts across all the irregularities in the harder dolostone of the upper plate with the exception of long wave-length corrugations (fault mullions) that parallel the transport direction. As a result, irregular hollows along the base of the Dunham Dolomite are filled in by highly contorted shales and welded breccia (Fig. 3).

The deformation in the shale beneath the fault provides a basis for interpreting the movement and evolution along the Champlain thrust fault. The compositional layering in the shale of the lower plate represents the well-developed S1 pressure-resolution cleavage that is essentially parallel to the axial planes of the first-generation of folds in the Ordovician shale exposed below and to the west of the Champlain thrust fault (Fig. 4). As the trace of the thrust fault is approached from the west this cleavage is rotated eastward to shallow dips as a result of westward movement of the upper plate (Fig. 4). Slickenlines, grooves, and prominent fault mullions on the lower surface of the dolostone and in the adjacent shales, where they are not badly deformed by younger events, indicate displacement was along an azimuth of approximately N60°W (Fig. 4; Hawley, 1957; Stanley and Sarkesian, 1972; Leonard, 1985). The S1 cleavage at Lone Rock Point is so well developed in the fault zone that folds in the original bedding are largely destroyed. In a few places, however, isolated hinges are preserved and are seen to plunge eastward or southeastward at low angles (Fig. 4). As these F1 folds are traced westward from the fault zone, their hinges change orientation to

the northeast. A similar geometric pattern is seen along smaller faults, which deform S1 cleavage in the Ordovician rocks west of the Champlain thrust fault. These relations suggest that F1 hinges are rotated towards the transport direction as the Champlain thrust fault is approached. The process involved fragmentation of

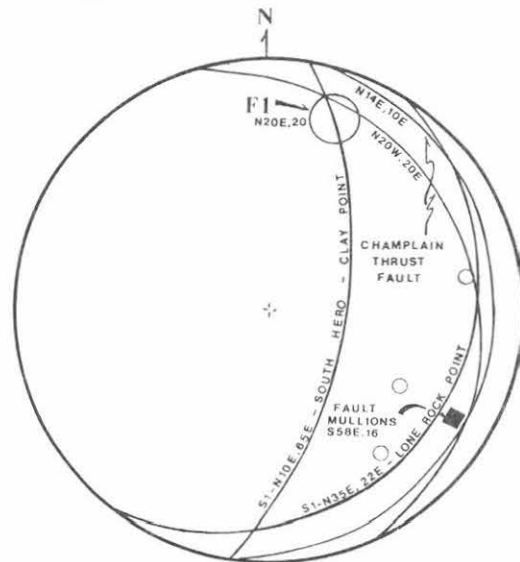


Figure 4. Lower hemisphere equal-area net showing structural elements associated with the Champlain thrust fault. The change in orientation of the thrust surface varies from approximately N20°W to N14°E at Lone Rock Point. The orientation of S1 cleavage directly below the thrust is the average of 40 measurements collected along the length of the exposure. S1, however, dips steeply eastward in the Ordovician rocks to the west of the Champlain thrust fault as seen at South Hero and Clay Point where F1 hinges plunge gently to the northeast. Near the Champlain thrust fault F1 hinges (small circles) plunge to the east. Most slickenlines in the adjacent shale are approximately parallel to the fault mullions shown in the figure.

the F1 folds since continuous fold trains are absent near the thrust. Much of this deformation and rotation occurs, however, within 300 ft (100 m) of the thrust surface. Within this same zone the S1 cleavage is folded by a second generation of folds that rarely developed a new cleavage. These hinges also plunge to the east or southeast like the earlier F1 hinges. The direction of transport inferred from the analysis of F2 data is parallel or nearly parallel to the fault mullions along the Champlain thrust fault. Stanley and Sarkesian (1972) suggested that these folds developed during late translation on the thrust with major displacement during and after the development of generation 1 folds. New information,

however, suggests that the F2 folds are simply the result of internal adjustment in the shale as the fault zone is deformed by lower duplexes and frontal or lateral ramps (Figs. 1, 2). The critical evidence for this new interpretation is the sense of shear inferred from F2 folds and their relation to the broad undulations mapped in the fault zone as it is traced northward along Lone Rock Point (Fig. 1). South of the position of the thick arrow in Figure 1, the inferred shear is west-over-east whereas north of the arrow it is east-over-west. The shear direction therefore changes across the axis of the undulation (marked by the arrow) as it should for a synclinal fold.

REFERENCES CITED

- Ando, C. J., Cook, F. A., Oliver, J. E., Brown, L. D., and Kaufman, S., 1983, Crustal geometry of the Appalachian orogen from seismic reflection studies, in Hatcher, R. D., Jr., Williams, H., and Zietz, I., eds., Contributions to the tectonics and geophysics of mountain chains: Geological Society of America Memoir 158, p. 83-101.
- Ando, C. J., Czuchra, B. L., Klemperer, S. L., Brown, L. D., Cheadle, M. J., Cook, F. A., Oliver, J. E., Kaufman, S., Walsh, T., Thompson, J. B., Jr., Lyons, J. B., and Rosenfeld, J. L., 1984, Crustal profile of mountain belt; COCORP Deep Seismic reflection profiling in New England Appalachians and implications for architecture of convergent mountain chains: American Association of Petroleum Geologists Bulletin, v. 68, p. 819-837.
- Bosworth, W., 1980, Structural geology of the Fort Miller, Schuylerville and portions of the Schaghticoke 7½-minute Quadrangles, eastern New York and its implications in Taconic geology [Ph.D. thesis]: Part 1, State University of New York at Albany, 237 p.
- Bosworth, W., and Rowley, D. B., 1984, Early obduction-related deformation features of the Taconic allochthon; Analogy with structures observed in modern trench environments: Geological Society of America Bulletin, v. 95, p. 559-567.
- Bosworth, W., and Vollmer, F. W., 1981, Structures of the medial Ordovician flysch of eastern New York; Deformation of synorogenic deposits in an overthrust environment: Journal of Geology, v. 89, p. 551-568.
- Boyer, S. E., and Elliot, D., 1982, Thrust systems: American Association of Petroleum Geologists Bulletin, v. 66, p. 1196-1230.
- Cady, W. M., 1945, Stratigraphy and structure of west-central Vermont: Geological Society of America Bulletin, v. 56, p. 515-587.
- , 1969, Regional tectonic synthesis of northwestern New England and adjacent Quebec: Geological Society of America Memoir 120, 181 p.
- Clark, T. H., 1934, Structure and stratigraphy of southern Quebec: Geological Society of America Bulletin, v. 45, p. 1-20.
- Coney, P. J., Powell, R. E., Tennyson, M. E., and Baldwin, B., 1972, The Champlain thrust and related features near Middlebury, Vermont, in Doolan, B. D., and Stanley, R. S., eds., Guidebook to field trips in Vermont, New England Intercollegiate Geological Conference 64th annual meeting: Burlington, University of Vermont, p. 97-116.
- Doll, C. G., Cady, W. M., Thompson, J. B., Jr., and Billings, M. P., 1961, Centennial geologic map of Vermont: Montpelier, Vermont Geological Survey, scale 1:250,000.
- Dorsey, R. L., Agnew, P. C., Carter, C. M., Rosencrantz, E. J., and Stanley, R. S., 1983, Bedrock geology of the Milton Quadrangle, northwestern Vermont: Vermont Geological Survey Special Bulletin No. 3, 14 p.
- Fisher, D. W., 1968, Geology of the Plattsburgh and Rouses Point Quadrangles, New York and Vermont: Vermont Geological Survey Special Publications No. 1, 51 p.
- Hawley, D., 1957, Ordovician shales and submarine slide breccias of northern Champlain Valley in Vermont: Geological Society of America Bulletin, v. 68, p. 155-194.
- Hitchcock, E., Hitchcock, E., Jr., Hager, A. D., and Hitchcock, C., 1861, Report on the geology of Vermont: Clairmont, Vermont, v. 1, 558 p.; v. 2, p. 559-988.
- Keith, A., 1923, Outline of Appalachian structures: Geological Society of America Bulletin, v. 34, p. 309-380.
- , 1932, Stratigraphy and structure of northwestern Vermont: American Journal of Science, v. 22, p. 357-379, 393-406.
- Leonard, K. E., 1985, Foreland fold and thrust belt deformation chronology, Ordovician limestone and shale, northwestern Vermont [M.S. thesis]: Burlington, University of Vermont, 138 p.
- Palmer, A. R., 1969, Stratigraphic evidence for magnitude of movement on the Champlain thrust: Geological Society of America, Abstract with Programs, Part 1, p. 47-48.
- Rodgers, J., 1970, The tectonics of the Appalachians: New York, Wiley Interscience, 271 p.
- Rowley, D. B., 1982, New methods for estimating displacements of thrust faults affecting Atlantic-type shelf sequences; With applications to the Champlain thrust, Vermont: Tectonics, v. 1, no. 4, p. 369-388.
- , 1983, Contrasting fold-thrust relationships along northern and western edges of the Taconic allochthons; Implications for a two-stage emplacement history: Geological Society of America Abstracts with Programs, v. 15, p. 174.
- Rowley, D. B., Kidd, W.S.F., and Delano, L. L., 1979, Detailed stratigraphic and structural features of the Giddings Brook slice of the Taconic Allochthon in the Granville area, in Friedman, G. M., ed., Guidebook to field trips for the New York State Geological Association and the New England Intercollegiate Geological Conference, 71st annual meeting: Troy, New York, Rensselaer Polytechnical Institute, 186-242.
- Stanley, R. S., and Ratcliffe, N. M., 1983, Simplified lithotectonic synthesis of the pre-Silurian eugeoclinal rocks of western New England: Vermont Geological Survey Special Bulletin No. 5.
- , 1985, Tectonic synthesis of the Taconic orogeny in western New England: Geological Society of America Bulletin, v. 96, p. 1227-1250.
- Stanley, R. S., and Sarkesian, A., 1972, Analysis and chronology of structures along the Champlain thrust west of the Hinesburg synclinorium, in Doolan, D. L., and Stanley, R. S., eds., Guidebook for field trips in Vermont, 64th annual meeting of the New England Intercollegiate Geological Conference, Burlington, Vermont, p. 117-149.
- Suppe, J., 1982, Geometry and kinematics of fault-related parallel folding: American Journal of Science, v. 282, p. 684-721.
- Welby, C. W., 1961, Bedrock geology of the Champlain Valley of Vermont: Vermont Geological Survey Bulletin No. 14, 296 p.
- Zen, E-an, 1972, The Taconide zone and the Taconic orogeny in the western part of the northern Appalachian orogen: Geological Society of America Special Paper 135, 72 p.
- Zen, E-an, ed., Goldsmith, R., Ratcliffe, N. M., Robinson, P., and Stanley, R. S., compilers, 1983, Bedrock geologic map of Massachusetts: U.S. Geological Survey; the Commonwealth of Massachusetts, Department of Public Works; and Sinnott, J. A., State Geologist, scale 1:250,000.

THE CAMBRIAN PLATFORM AND PLATFORM MARGIN
IN NORTHWESTERN VERMONT

Charlotte J. Mehrtens
Department of Geology
University of Vermont
Burlington, Vt. 05405

INTRODUCTION

The stratigraphy of northwestern Vermont is dominated by sedimentary rocks of the Cambro-Ordovician platform and basin sequence, which is part of an extensive belt of similar facies extending from Newfoundland to Alabama. These facies consist of carbonate and siliciclastic deposits characteristic of a shallow water platform, bordered to the east by a basinal sequence of shales and sedimentary breccias. Rodgers (1968) recognized this platform to basin transition as the margin of the Lower Paleozoic platform in eastern North America.

Cambro-Ordovician sediments were deposited on a passively subsiding shelf following late Precambrian rifting. These sediments accreted at a rate which kept pace with thermal subsidence as the shelf assumed the morphology of an accretionary rimmed platform during the Lower Cambrian. Examining the distribution of facies comprising the shallow water platform indicates that the interior regions were affected by tidal and wave processes whereas the shelf margin regions were subtidal and wave reworked (Gregory, 1982; Butler, 1986; Rahamanian, 1981; Myrow, 1983; Chisick and Friedman, 1982; Braun and Friedman, 1969). The adjacent deeper water basins accumulated talus, debris flows, and turbidites composed of detritus shed off the platform (Mehrtens and Dorsey, 1986; Mehrtens and Borre, 1987; Mehrtens and Hillman, in review).

The Cambro-Ordovician sequence in northwestern Vermont is unique in that the platform to basin sequence is intact and undissected by faults. Looking at the Cambro-Ordovician sequence throughout the Appalachians, only Pfeil and Read (1980) describe a platform to basin sequence, but it has been dismembered by faults and cannot provide information on the original geometric relations on the platform.

This field trip guide describes the facies and evolution of a portion of the Cambro-Ordovician carbonate platform in northern Vermont (Figure 1). The Cheshire Quartzite is the basal unit in the sequence (Figure 2),

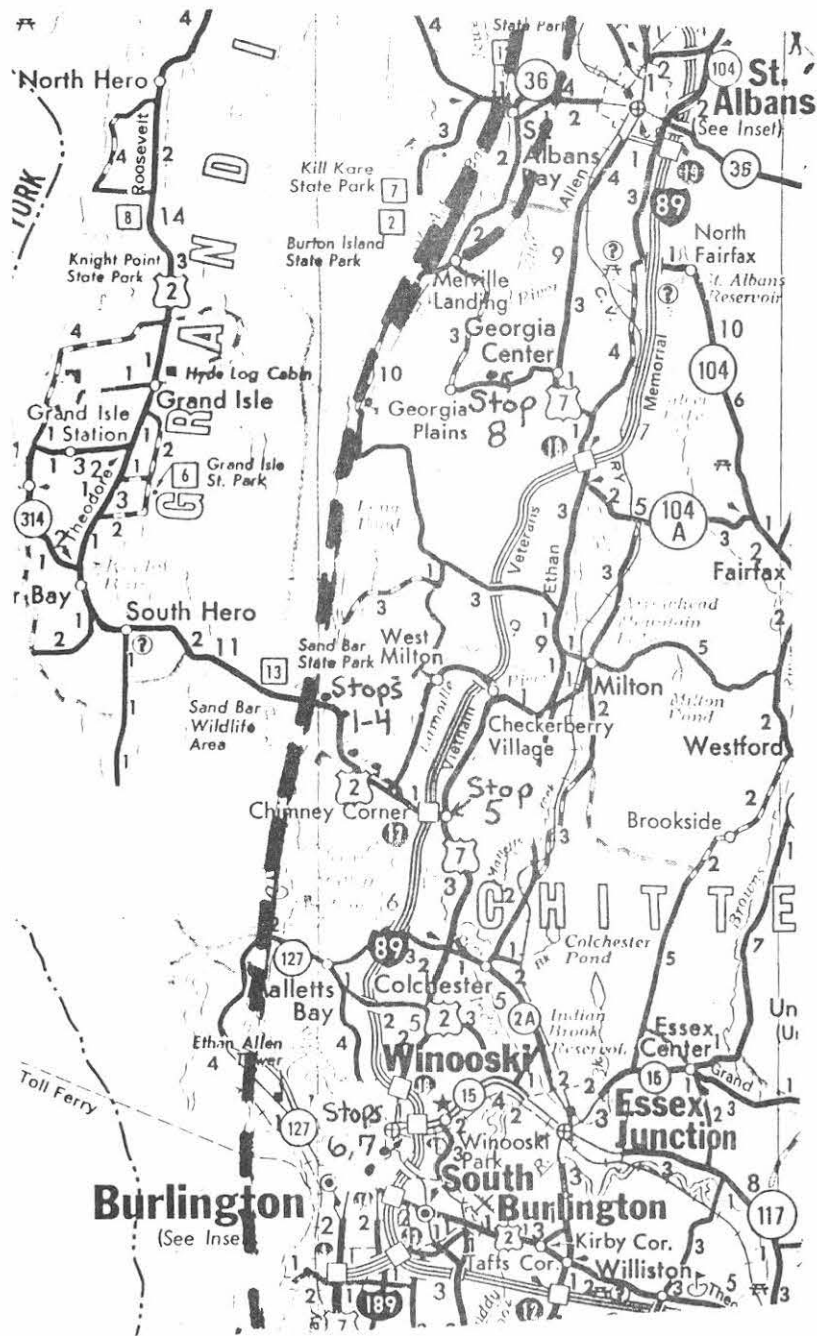


Figure 1. Locality map for stops 1-8. The trace of the Champlain Thrust is shown.

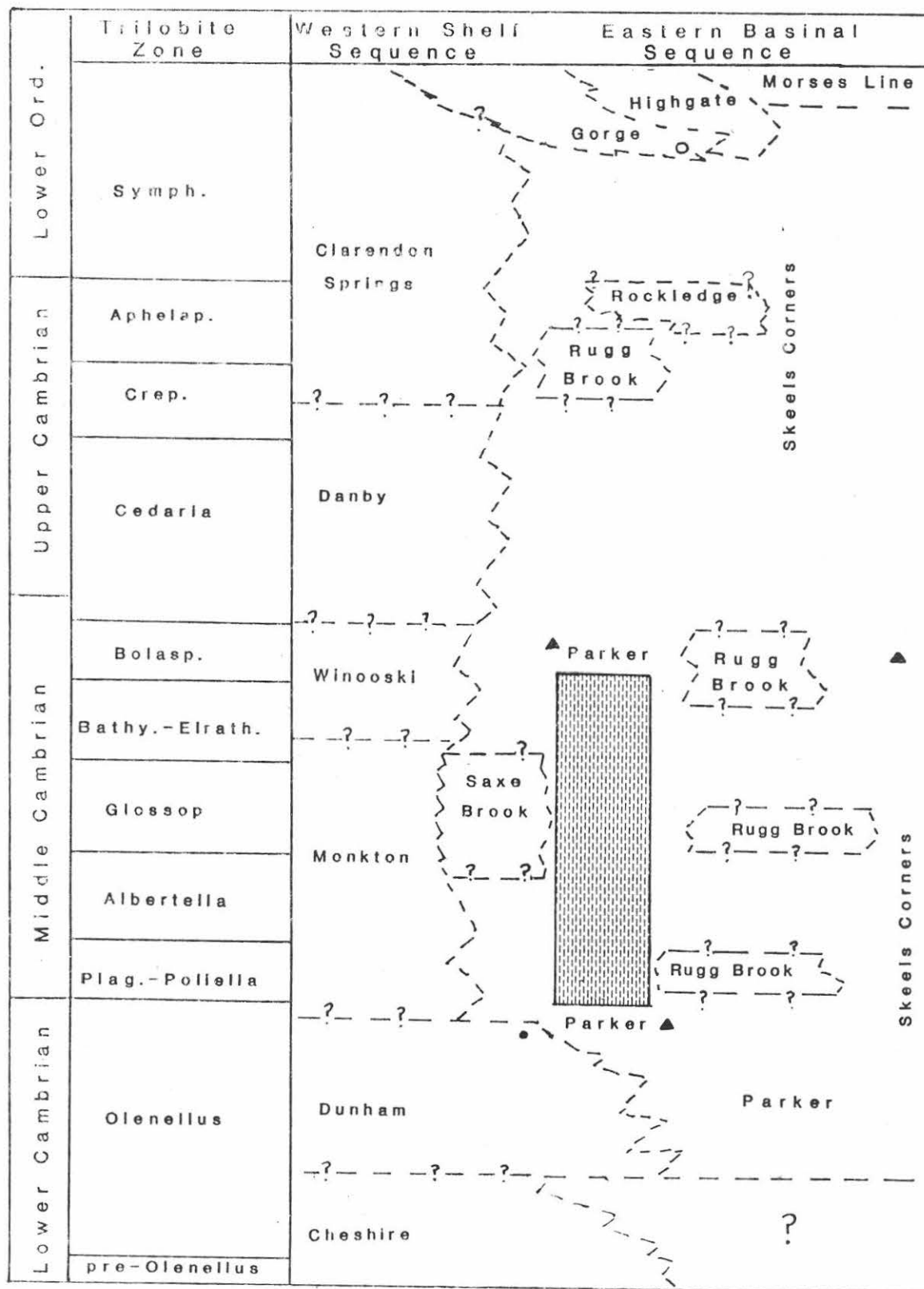


Figure 2. (previous page) Correlation chart for the Cambro-Ordovician strata of northwestern Vermont. Chart is based on biostratigraphic data by Palmer (1970), Palmer and James (1980), Landing (1983), and Mehrtens and Gregory (1984), and physical stratigraphic relationships by Mehrtens and Dorsey (1986) and Mehrtens and Borre (1987). Age relationships on the platform are approximate because they are based on intertonguing relationships with the basinal units. The Hawke Bay event is illustrated with shaded bar within the Parker Slate. Pods of Rugg Brook Dolomite extend from post-Dunham to Rockledge time. The Skeels Corners Slate has been dated as Bolaspidella zone in age but mapping relationships suggest it has a much broader age range.

overlying Eocambrian rift-related sediments of the Pinnacle and Fairfield Pond Formations (Tauvers, 1982), and it will not be examined on this trip. The Cheshire is in gradational contact with the overlying Lower Cambrian Dunham Dolomite (Myrow, 1984), a carbonate unit which records sedimentation in peritidal, subtidal and platform margin environments (Gregory, 1982). The facies distribution and paleogeography of the Dunham Dolomite influenced the platform geometry and evolution in subsequent Cambrian deposits, consequently it will be examined in detail.

Overlying the Dunham Dolomite is the lower Middle Cambrian Monkton Quartzite, a mixed siliciclastic/carbonate unit which also records tidal flat to platform margin sedimentation (Rahmanian, 1981). The Middle Cambrian Winooski Dolomite has not been studied in detail, but a review of sedimentary and biogenic structures suggests that it also records peritidal to platform margin environments of deposition. The Upper Cambrian Danby Quartzite overlies the Winooski and contains a diverse suite of sedimentary structures documenting tidal flat, shallow subtidal, and platform margin environments, with significant storm overprinting (Mehrtens and Butler, in review).

This field trip will look at each of these units and examine evidence for their interpretation as shallow water platform deposits. The trip will also examine one basinal unit, the Rockledge Formation (Upper Cambrian). The Rockledge Formation is a limestone-clast conglomerate unit with associated massive sandstones and laminated siltstones interpreted to represent high and low density turbidity currents (Mehrtens and Hillman, in review).

GEOLOGIC SETTING AND STRATIGRAPHY OF THE CAMBRO-ORDOVICIAN SEQUENCE

The Cambrian to Lower Ordovician stratigraphic sequence in western Vermont outcrops in a north-south trending belt, a region bordered on the east by the Green Mountain Anticlinorium, a belt of Precambrian rocks thought to represent the easternmost occurrence of the north American craton in the Lower Paleozoic (Rodgers, 1968). The north-south trending outcrop belt consists of several major fold belts (St. Albans and Middlebury Synclinoria) and thrusts (Champlain, Hinesburg, Pinnacle, Highgate Springs). The north-western portion of the outcrop belt is well suited for sedimentologic studies because it lies within the Quebec Reentrant (Thomas, 1978), which kept deformation and metamorphism associated with the Taconic and Acadian Orogenies to a minimum. The most complete exposures of the Lower Paleozoic are contained within thrust sheets in this region. Stratigraphy within the thrust sheets is coherent, which enables us to reconstruct original geographic relationships on the Cambro-Ordovician platform.

The Cambro-Ordovician stratigraphic sequence (Figure 2) in northwestern Vermont was divided into two sequences by Dorsey and others (1983). The Western Shelf Sequence is composed of alternating siliciclastic (Cheshire, Monkton, Danby Formations) and carbonate (Dunham, Winooski and Clarendon Springs Formations) units of the platform.

The Eastern Basinal Sequence consists of units which are coeval with the platform sequence, but were deposited in deeper water adjacent to the platform. This Sequence consists of shale (Parker and Skeels Corners Slates) and conglomerates and breccias (Rugg Brook, Rockledge Formations). Unlike the Western Shelf Sequence, correlations are well developed in the Eastern Basinal Sequence, with a trilobite zonation developed by Shaw (1959) and Palmer (1970) and physical stratigraphic relationships (Mehrtens and Dorsey, 1986) and Mehrstens and Borre (1987).

SUMMARY OF THE DEPOSITIONAL ENVIRONMENTS OF THE WESTERN SHELF SEQUENCE

Pre-Cheshire Units

The Pinnacle and Fairfield Pond Formations underly the Cheshire Quartzite in central Vermont. The stratigraphy and structure of these units was studied by Tauvers (1982) and their depo-tectonic setting described by Dorsey and

others (1983). The Pinnacle and Fairfield Pond Formations are interpreted as representing sediments which infilled grabens formed during Eocambrian rifting. Doolan and others (1982) have suggested that this rifting may have occurred around 560mybp. The proposed topography of the rift basin resulted in deposition of coarse-grained clastics, possibly alluvial fan in origin, overlain by finer-grained siliciclastic sediments of the Fairfield Pond Formation in marginal marine basins (Tauvers, 1982). The contact of the Fairfield Pond Formation was shown by Tauvers to be conformable. These units will not be seen on this trip.

In northern Vermont, the Eocambrian syn-rift sediments of the pre-Cheshire Oak Hill Group also record deposition in a marginal marine setting (Dowling, et al, 1987). These units will also not be seen on this trip.

Cheshire Quartzite

Myrow (1983) completed a study of the Cheshire Quartzite in west-central Vermont. He recognized eight lithofacies within the Cheshire, five within the lower Cheshire and three from the upper Cheshire. The lower Cheshire is composed of: (1) fine-grained, mottled grey, argillaceous arkose with extensive bioturbation, thin white rippled beds and shale partings; (2) fine-grained, white subarkosic and fine-grained arkosic beds with ripple bedding, wavy and lenticular bedding, thick and thinly interlayered bedding, parallel laminations, cross stratification, and U-shaped vertical burrows; (3) fine-grained, white subarkosic beds with thin clay drapes and massive parallel laminated and low angle tabular cross stratification, lenticular beds, low angle trough cross stratification, rippled beds, reactivation surfaces and low angle erosional surfaces; (4) thin, lenticular, structureless sand bodies with erosional bases and flat upper surfaces; (5) tabular sand beds characterized by planar, non-erosive bases and reworked tops.

The upper Cheshire is composed of: (1) a pink to white, moderately sorted massive fine-grained arkosic to quartz arenite sandstone; (2) shale clast conglomerate composed of interbedded quartzite; (3) massive quartzite beds, lenticular in shape, with large scale erosional surfaces at their bases and trough cross stratification.

Interpretation:

These eight lithofacies can be interpreted to represent sediments deposited on a newly formed shelf, at least in

part within wave base, and partially tidally influenced. The Cheshire Quartzite is thought to represent the marine shelf sand blanketing the underlying rift basin topography. Shelf sediments of the lower Cheshire exhibit periodic storm sedimentation, and are capped by the prograding strandline sediments of the upper Cheshire. These interpretations are based on: (1) the stratigraphic position of the Cheshire between the Eocambrian rift-related sediments and the overlying Dunham Dolomite; (2) the absence of any evidence of a supratidal environment; (3) a suite of sedimentary structures indicating wave working of the substrate, and the presence of tidal currents; and (4) bedforms indicative of episodic high energy events (storms?).

The Cheshire Quartzite will not be seen on this trip as the best exposures of this unit are in west-central Vermont. It is an important unit within the Cambro-Ordovician sequence, for its presence marks the transition from sedimentation associated with graben infilling to that of the newly formed shelf (rift-drift transition).

Dunham Dolomite

The Lower Cambrian Dunham Dolomite will be seen at Stops 1-3.

The lithofacies and depositional environments of the Dunham Dolomite were studied by Gregory (1982) and Mehrtens and Gregory (in review). These authors described the Dunham Dolomite as a 400 meter thick unit composed of four major lithofacies representing peritidal, channel, subtidal/open shelf, and platform margin environments. Both the lower and upper contacts with the Cheshire and Monkton Quartzites, respectively, are conformable.

The peritidal lithofacies of the Dunham is characterized by a bedding style termed "sedimentary boudinage", which describes the rhythmic interbedding of dolomite and dolomitic siltstone and subsequent differential compaction to produce beds which exhibit pods or boudins. This rhythmic interbedding is interpreted to be the result of deposition in a tidally-influenced regime, possibly a tidal flat. Bioturbation has disrupted the bedding, and early cementation lithified horizons enough to have formed intraclasts and local intraformational conglomerates. Cryptalgalaminites also occur in this facies.

The subtidal/open shelf lithofacies is characterized by shallowing-up cycles (SUC) 6 to 10 meters in thickness

which have at their base massive, structureless beds of bioturbated dolomite passing up into rhythmically interbedded dolomite and silt-rich dolomite of the peritidal lithofacies. The bulk of the Dunham Dolomite is composed of these shallowing-up cycles, indicating that tidal flats prograded across the adjacent platform.

The third lithofacies, the channel deposits, are interbedded with both the peritidal and subtidal/open shelf lithofacies. Channels are best exposed in outcrops that trend parallel to strike so they are not exposed at the Route 2 outcrop but they are found in the Georgia and St. Albans localities. A typical channel is several meters wide and 0.5 meters deep, with a lenticular shape and a down-cutting base. Channel sediments contain trough cross bedded quartz sand and both intraformational and exotic clasts.

Rocks characteristic of the platform margin lithofacies exhibit horizons of polymictic breccias within a quartz sand-rich dolomite matrix. These deposits are interpreted as talus deposits and debris flows accumulating off the edge of the Dunham platform. In the Milton, Georgia and St. Albans regions the Dunham breccias grade conformably into clast-rich horizons of the Parker Slate. Analysis of the distribution of the platform margin breccias is important in developing a model for the geometry of the Lower Cambrian carbonate platform, since these deposits very accurately place the position of the platform-to-basin transition. The Dunham Dolomite passes eastward, down dip into the Parker Slate and this facies change marks the passage into the shale basin and deeper water sediments of the Iapetus Ocean (seen for example at Arrowhead Mountain). Platform margin breccias also pass northward into a basin which Mehrrens and Dorsey (1986) proposed represents a foundered graben within the shelf. The distribution of platform margin facies defined the platform-to-basin transition and led to the definition of a horseshoe-shaped intrashelf basin, termed the St. Albans Reentrant (Mehrrens and Dorsey, 1986). We see the configuration of the St. Albans Reentrant maintained throughout the remainder of the Cambrian.

Montkton Quartzite

The Monkton has been dated as lower Middle Cambrian in age by Palmer and James (1980) and its lithofacies were first described by Rahmanian (1981). Seven lithofacies were recognized in the 300 meter thick Monkton. Shallowing-up cycles are characterized by repetitive packages of: (1) basal subtidal sand shoals and channels overlain by, (2) interbedded sand, silt, and carbonate intertidal flat

sediments, capped by (3) carbonate muds of the high intertidal and supratidal flat. These cycles are interpreted to represent prograding tidal flat deposits. Two siliciclastic lithofacies were recognized: (1) sand bars and tidal channels and (2) mixed rippled sands with mud drapes of the intertidal. These supra-, inter-, and shallow subtidal sediments exposed in the Burlington and Winooski areas pass downdip to the east and north into subtidal oolitic dolomites and platform margin breccias exposed along Route 2 and the Milton region.

The high degree of similarity between the environments of deposition and facies distribution of the Dunham Dolomite and Monkton Quartzite suggests that the morphology of the platform established in the Lower Cambrian was maintained into the Middle Cambrian. Although composition of the platform sediments changed from dominantly carbonate (Dunham) to mixed siliciclastic and carbonate (Monkton), the environments of deposition in which these sediments were deposited remained the same.

In the Burlington and Winooski areas the shallow water platform sediments of the Monkton Quartzite are gradually overlain by the Winooski Dolomite. In the Milton and Georgia areas the Monkton platform margin facies pass into the Rugg Brook Conglomerate and undifferentiated Parker and Skeels Corners Slates (Mehrtens and Borre, 1987) basinal deposits.

Winooski Dolomite

The environments of deposition and lithofacies of the Middle Cambrian Winooski Dolomite have not been studied in the detail of the other units, but initial studies indicate that it is approximately 300 meters thick and composed of the following lithofacies: (1) interbedded rippled fine-grained sand and silt with minor clay; (2) dolomite with planar cryptalgalaminite structures; (3) dolomite with LLH stromatolites; (4) dolomite with disseminated quartz sand; (5) quartz arenite beds with a dolomite matrix, and (6) polymictic breccia beds with a matrix of dolomite and quartz-rich dolomite.

Lithofacies 1 through 5 are arranged in a vertical stratigraphic sequence in Whitcomb's Quarry in Winooski. Lithofacies (1) and (2) are interbedded with the underlying Monkton Quartzite and are interpreted to represent peritidal deposits. Lithofacies (3), (4), and (5) overlie facies (1) and (2) and they make up the bulk of the Winooski stratigraphic sequence seen along the Winooski River (Stop 6). Due to an absence of any diagnostic

sedimentary structures and a position overlying lithofacies (1) and (2) these lithofacies are interpreted as shallow subtidal in origin. Lithofacies (4), (5) and (6) are recognized as composing the uppermost horizons of the Winooski Dolomite, and are interpreted as representing subtidal and platform margin deposits.

As also seen in the Dunham and Monkton, the Winooski exhibits significant north-south facies changes parallel to depositional strike. In the Burlington and Winooski region the Winooski is gradationally overlain by the platform deposits of the Danby Quartzite while along Route 2 and in the Milton area the Winooski is overlain by the basinal deposits of the Rugg Brook Conglomerate (Mehrtens and Borre, 1987). Thus, the platform geometry first observed in the Dunham Dolomite was maintained into the Middle Cambrian.

Danby Quartzite

The Danby Quartzite (Upper Cambrian) is a 35-80 meter thick mixed siliciclastic/carbonate unit. The Danby is composed of a basal un-named sand-rich unit and the upper Wallingford Member. Significant variations in sand--carbonate ratios occur from southern to northern Vermont; the Danby is thinner in northwestern Vermont and more carbonate-rich while to the south it is thicker and dominantly sandstone in composition. Four lithofacies have been recognized by Butler (1986): (1) intertidal to shallow subtidal; (2) subtidal, (3) open shelf sand shoals and (4) platform margin. The inter- to shallow subtidal facies is characterized by interbedded sandy dolomites, sandstone and shales with mudcracks, vertical burrows, wave and current ripples, cryptalgalaminites, and oncolites. The subtidal sediments are composed of thick-bedded sandy dolomites, and pure dolomite with herringbone cross stratification, oncolites, pinch and swell bedding, upbundling of ripples, and LLH stromatolites. These features will be seen at Stop 7 along the Winooski River. The open shelf facies is characterized by thick-bedded, coarse-grained dolomitic sandstones and sandstones with large scale tabular cross stratification interpreted as sand shoals.

Platform margin facies include polymictic breccias in a dolomite matrix and ball and pillow sands and shales.

The Danby Formation is characterized by complex facies mosaicing and compositional heterogeneity. Butler (1986) proposed that storms on the platform were a major factor influencing the distribution of sand.

The distribution of facies of the Danby is identical to that of the underlying units: platform margin facies are found in the Milton region, bordering the St. Albans Reentrant, while shallower water platform sediments occur to the south.

Rockledge and Rugg Brook Formations

Bedrock mapping by Mehrtens and Dorsey (1986) and Mehrtens and Borre (1987) documented the distribution of these units in northwestern Vermont. Previous workers had, on the basis of map patterns and dolomite lithology, interpreted the Rugg Brook to be a lateral equivalent of the Middle Cambrian Winooski Dolomite. Mehrtens and her coworkers documented, however, that the Rugg Brook is not a time-stratigraphic unit and it occurs at several horizons interbedded with the Parker and Skeels Corners Slates (Figure 2). The Rugg Brook was recognized as consisting of four lithofacies: dolomite with sparse dolomite clasts, dolomitic sandstone, sandy matrix dolomite clast conglomerate, and shaley-matrix dolomite clast conglomerate. All of these lithofacies are interpreted to represent various types of sediment gravity flows accumulating basinward of the shallow-water platform.

The distribution of the Rockledge Formation was also studied by Mehrtens and her coworkers. Previously thought to be confined to a narrow time-stratigraphic horizon (Shaw, 1958), Mehrtens was able to document its occurrence at several stratigraphic horizons. The Rockledge is an easily recognizable deposit of limestone clast conglomerates within undifferentiated Parker and Skeels Corners Slates. It is also interbedded with the Rugg Brook Formation. Mehrtens and Hillman (in review) described four lithofacies within the Rockledge, including: limestone clast conglomerate, massive sandstone, laminated and rippled siltstone, and structureless micrite. These lithofacies are all interpreted to represent sediment gravity flows formed along a slope apron adjacent to the platform. Because the clasts of the Rockledge are not dolomitized they have been valuable in describing the pre-dolomitization composition of the shallow water platform sediments from which they were derived. Five dominant clast compositions were recognized. These include: pelsparites, algal boundstone, oomicrites, calcareous sandstone and micrite, indicating that the Upper Cambrian shelf was characterized by agitated, shallow water conditions.

PLATFORM GEOMETRY

Figure 3, taken from Dorsey and others (1983) summarizes the geometry of the Cambrian platform in northwestern Vermont. Several important features are shown on this diagram, constructed from a view looking southeast. The St. Albans Reentrant, the shale basin lying along depositional strike in the shelf, is shown. Note also the north-to-south, and west-to-east facies changes present within every Cambrian platform deposit. The shallow water facies are present in the south, and they pass northward and eastward into subtidal and platform margin deposits, and ultimately into the shale basin. The diagram also shows the localization of the platform margin from Dunham through Danby time. This is important because it indicates that the platform was up-building throughout the Cambrian. Platform facies did not build out into the basin, nor did the platform founder to produce significant onlap of shales. What could have caused the localization of the platform margin? If the St. Albans Reentrant is indeed a graben within the shelf which foundered as a result of movement of an underlying Eocambrian rift-related lystric fault, then these localized deposits accumulated along the fault scarp. Sedimentation on the platform itself was able to keep pace with thermal subsidence on the young, hot, recently-rifted margin, and the sediment built vertically, with an abrupt pinchout into the adjacent basin. The timing of initial movement of the graben which formed the St. Albans Reentrant is thought to be late-to--post-Dunham time, based on the fact that the Dunham Dolomite is the only shelf unit which continues across what becomes the shale basin. Following deposition of the Dunham, the facies on the northern rim of the Reentrant are different than those to the south (Mehrtens and Dorsey, 1986).

Figure 3. (following page) Block diagram from Dorsey, et al (1983) illustrating the proposed paleogeography of the southern margin of the St. Albans Reentrant. Diagram shows the platform deposits pinching out to the east into the marginal Iapetus Ocean, and to the north into the St. Albans Reentrant; the latter platform margin is characterized by thick conglomerate and breccia deposits. The field trip will be viewing sections D (Winooski River) and E (Route 2).

REFERENCES

- Braun, M. and Friedman, G., 1969, Carbonate lithofacies and environments of the Tribes Hill Formation (Lower Ordovician) of the Mohawk Valley, New York, Jour. Sed. Pet., vol. 39, p. 113-135.
- Butler, R., 1986, Sedimentology of the upper Cambrian Danby Formation of western Vermont: an example of mixed siliciclastic and carbonate platform sedimentation unpub. M.S. Thesis, Univ. of Vermont, 137p.
- Chisick, S. and Friedman, G., 1982, Paleoenvironments and lithofacies of the Lower Ordovician Fort Cassin (Upper Canadian) and Providence Island (Upper Canadian-Lower Whiterockian) Formations of northeastern New York and adjacent southwestern Vermont, Geol. Soc. Am. Abstr. with Prog., vol. 14.
- Doolan, B., Gale, M., Gale, P., and Hoar, R., 1982, Geology of the Quebec Reentrant, possible constraints from early rifts and the Vermont-Quebec serpentine belt, in, St. Julien, P. and Hubert, C., eds., Major structural zones and faults of the northern Appalachians, Geol. Assoc. Can. Sp. Pap. no. 24, p. 87-115.
- Dorsey, R., Agnew, P., Carter, C., Rosencrantz, E., and Stanley, R., 1983, Bedrock geology of the Milton Quadrangle, northwestern Vermont, Vt. Geol. Surv. Sp. Bull. 3.
- Dowling, W., Colpron, M., Doolan, B., 1987, The Oak Hill Group, southern Quebec and Vermont: along strike variations across a late Precambrian rift margin, Geol. Soc. Am. Abstr. with Prog., vol. 19, p. 11.
- Greiner, G. 1982, Geology of a regressive peritidal sequence with evaporitic overprints: the subsurface Dunham Formation (Lower Cambrian), Franklin, Vermont, unpub. M.S. Thesis, Rensselaer Polytechnic Institute, 116p.
- Gregory, G., 1982, Paleoenvironments of the Dunham Dolomite (Lower Cambrian) of northwestern Vermont, unpub. M.S. Thesis, Univ. of Vermont, 180p.
- James, N. 1983, Facies models 10. Shallowing-upward sequences in carbonates, in, Walker, R., ed., Facies Models, Geosci. Canada, p. 109-119.
- Landing, E., 1983, Highgate Gorge: Upper Cambrian and Lower Ordovician continental slope deposition and biostrat-

igraphy, northwestern Vermont. Jour. Paleo. vol. 57, p. 1149-1187.

Mehrtens, C. and Gregory, G., 1983, An occurrence of Salterella conulata in the Dunham Dolomite (Lower Cambrian) of northwestern Vermont, and its stratigraphic significance, Jour. Paleo., vol. 58, p. 1143-1150.

Mehrtens, C. and Dorsey, R., 1986, Stratigraphy and bedrock geology of portions of the St. Albans and Highgate Quadrangles, northern Vermont, Vt. Geol. Surv. open file rpt.

Mehrtens, C. and Borre, M., 1987, Stratigraphy and bedrock geology of portions of the Colchester and Georgia Plains Quadrangles, Vermont, Vt. Geol. Surv. open file report

Mehrtens, C. and Hillman, D., in review, The Rockledge Formation: a Cambrian slope apron deposit in northwestern Vermont, Northeastern Geology.

Myrow, P., 1983, Sedimentology of the Cheshire Formation in west-central Vermont, unpub. M.S. Thesis, Univ. of Vermont, 177p.

Palmer, A., 1970, The Cambrian of the Appalachians and eastern New England regions, eastern United States, in, C. Holland, ed., The Cambrian of the New World, Wiley Interscience, New York, p. 170-214.

Palmer, A. and N. James, 1980, The Hawke Bay event: a circum-Iapetus regression near the lower Middle Cambrian boundary, in, Wones, D., ed. Proceedings of the Caledonides in the USA, I.G.C.P. Project 27: Caledonide orogen, Dept. of Geol. Science, V.P.I. and S.U. Memoir 2, p. 15-18.

Pfeil, R. and Read, J., 1980, Cambrian carbonate platform margin facies, Shady Dolomite, southwestern Virginia, Jour. Sed. Pet., vol. 50, p. 90-116.

Rahmanian, V., 1981, Mixed siliciclastic-carbonate tidal sedimentation in the Lower Cambrian Monkton Formation in west central Vermont, Geol. Soc. Am. Abstr. with Prog., vol. 13, p. 170-171.

Rodgers, J., 1968, The eastern edge of the North American continent during the Cambrian and Early Ordovician, in, Zen, E-An, White, W., Hadley, J. and Thompson, J., eds., Studies in Appalachian Geology, northern and maritime, Wiley Interscience, New York, p. 131-149.

Shaw, A., 1958, Stratigraphy and structure of the St. Albans area, northwestern Vermont, Geol. Soc. Am. Bull., vol. 69, p. 519-567.

Stone, S. and Dennis, J., 1964, The geology of the Milton Quadrangle, Vermont, Vt. Geol. Surv. Bull. no. 26, 79p.

Tauvers, P., 1982, Bedrock geology of the Lincoln area, Vt. Geol. Surv. Sp. Bull. no. 2, 8p.

Thomas, W., 1978, Evolution of the Ouachita-Appalachian continental margin, Jour. Geol., vol. 84, p. 323-342.

FIELD TRIP ITINERARY

Several stops require parking on the shoulders of roads, and space is often at a premium. Please try to condense into as few cars as possible. Visits to private farms (Stop 8) require permission.

Assembly point: Sand Bar State Park on Route 2, Vermont

Mileage

- 1.6 Stop 1- Abandoned quarry on the north side of Rt. 2.

Park on the southwest (right) shoulder, cross Rt 2, and ascend overgrown driveway into quarry. The Champlain Trust floors the quarry as the Dunham Dolomite is emplaced on the Middle Ordovician Stony Point Shale. The Dunham Dolomite exposed here is the basal facies of the Dunham, characterized by the rhythmic interbedding of dolomite (white) and silty dolomite (pink). This bedding style is interpreted to be the result of alternating sedimentation in a tidal flat setting, producing "ribbon bedding". Look for: undisturbed horizons of the dolomite and silt-rich dolomite, horizons of intraclasts, burrows, and cryptalgaminites. Note that many of the clasts show rips and tears in their margins, others are bent. Many clasts are cored by calcite. Greiner (1982) recorded occurrences of gypsum in this facies in sub-surface cores.

Return to cars and continue east on Route 2.

- 2.4 Stop 2 Shallowing-up cycles in the Dunham

This roadcut on the left (north shoulder) exposes 3 shallowing-up cycles within the Dunham. They are recognizable in the large roadcut because of the characteristic pink and white ribbon bedding of the peritidal caps of the SUC's. One SUC can be studied in detail on the northwest corner of the roadcut. The SUC (Figure 4) is composed of a basal subtidal dolomite overlain by the ribbon bedding of the peritidal cap. The cycles in the Dunham are similar to "muddy shallowing-up cycles" of James (1983) and they consist of 6-10 meters of bioturbated, sandy dolomite passing up into ribbon-bedded dolomite and silt-rich dolomite and local intra-formational conglomerate. What is the origin of the sand within the Dunham subtidal muds? SEM work led Gregory (1982) to suggest that frosting micro-textures on quartz grains recorded an eolian history to the sediment. However, channels within the Dunham are sand-filled, and provide a mechanism for the transport of sand across the platform. This is similar to the tidal channels of Shark Bay, western Australia, where channels are infilled with a mixture of carbonate mud and quartz sand from eroded Pleistocene bedrock.

Return to cars and continue driving east on Route 2.

3.1 Stop 3- Dunham subtidal and platform margin facies.

Pull off about 100 yards beyond the speed limit sign on this long roadcut. At the base of this outcrop (west end) there are good exposures of the subtidal facies of the Dunham with the characteristic mottled texture, thought to be produced by burrowing. Burrow mottles are irregular in shape, 1 to 8 cm in diameter, and lack sand. The segregation of siliciclastic material is one property that implies bioturbation produced this mottled texture. Between the white burrows the red matrix is very clay and sand-rich, and Stone and Dennis (1964) attribute this color variation to differing concentrations of trace metals. Specimens of Salterella conulata (Mehrtens and Gregory, 1983) were found in this facies. The platform margin facies is exposed on the east end of the same outcrop. This facies is composed of chaotically-bedded, laterally discontinuous horizons of breccia in a sand-rich dolomite matrix. Clast composition is highly variable, and includes chert pebbles, sandstones, sandy-dolostones, and dolomitic

SHALLOWING-UP CYCLES

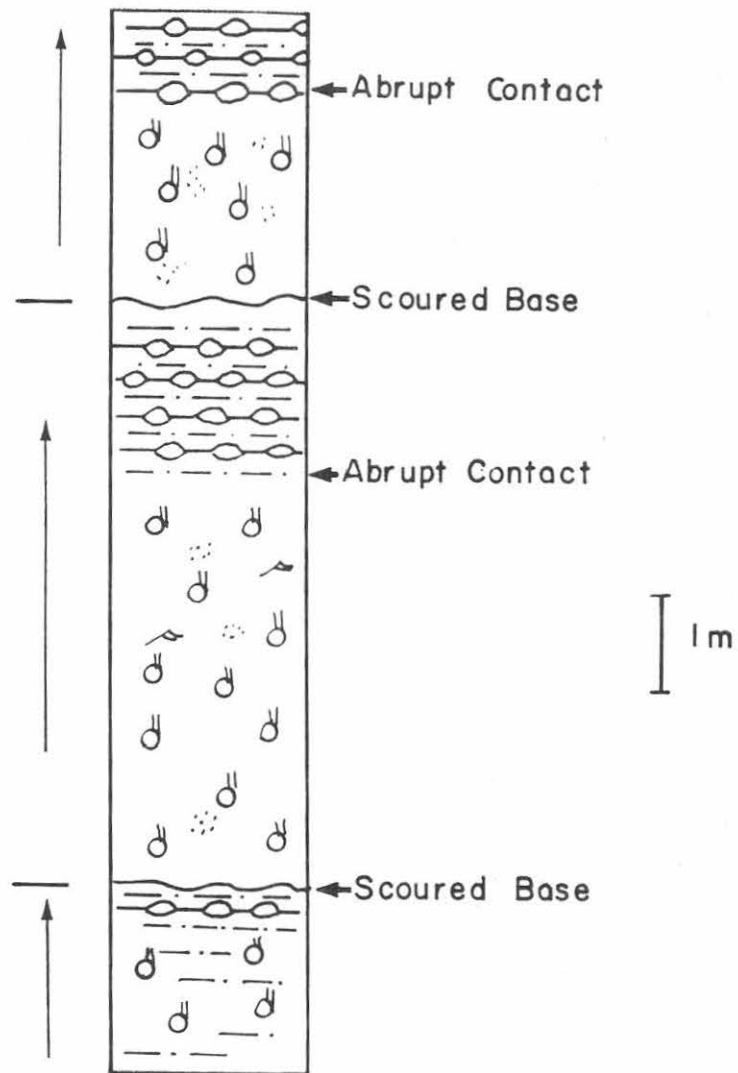


Figure 4. Shallowing-up-cycles in the Dunham Dolomite.

sandstones. Breccia beds are structureless and very poorly sorted. Graded beds of sandstone are also present.

Return to cars and continue east on Route 2.

3.8 Stop 4- Monkton Quartzite, subtidal and shelf edge facies

This roadcut exhibits the subtidal and shelf edge facies of the Monkton, as evidenced by the overall thickness of the individual beds, increasing amounts of shale between sandstone beds, presence of relict oolites in some dolomite horizons, and occurrences of large scale tabular cross stratification. Many of these beds probably represent shelf edge sand shoals. Note characteristics of the Monkton here for comparison to the shallower-water deposits seen at Stop 6.

Walk east 0.3 miles to the small knoll beyond the road sign. Here the polymictic breccia of the platform margin facies is exposed. The clasts are floating in a matrix of sandy dolomite and are interbedded with cross-bedded sandstones. Clast composition includes dolomite, sandstone and dolomitic sandstones. Beds are structureless and poorly sorted. These breccias are interpreted to represent talus deposits formed at the edge of the platform. These breccias can be traced to the north, where they form a rim around the St. Albans Reentrant. Mehrtens and Borre (1987) have documented that the Monkton passes laterally into the Rugg Brook Conglomerate within the basin.

Return to cars and continue east on Route 2.

4.7 T-intersection with Routes 2 and 7 at Chimney Corners.
Turn left.

4.8 Pull off into commuter parking lot.

Stop 5- Winooski platform margin facies

Walk from the parking lot back to, and across the intersection, to the outcrop on the southwest side. This is an exposure of recrystallized dolomite, cross-bedded, and in places oolitic, of the upper most Winooski. Cross the road to the low-lying outcrop on the east side of Route 7. Note the

variable clast composition and abundance of sand in the dolomite matrix in this Winooski platform margin breccia. These outcrops of Winooski at Chimney Corners and the adjacent I-89 exit ramps are the northernmost outcrops of Winooski Dolomite in northwestern Vermont. Immediately to the north on I-89 and Route 7 are exposures of the Rugg Brook Dolomite, a breccia deposit within the St. Albans Reentrant.

Return to cars and head south to Burlington.

- 5.1 Southbound entrance ramp on I-89. Outcrops of the Monkton Quartzite occur as roadcuts all along I-89.
- 11.1 First outcrop of Winooski Dolomite on the median of I-89
- 11.3 Exit off I-89, southbound onto Routes 2 and 7.
- 12.5 Intersection in Winooski with Routes 2, 7 and 15. Continue straight ahead on Routes 2 and 7.
- 12.7 Bridge over the Winooski River (Stop 6 is below us).
Bear right at the "Y".
- 12.9 Park in the small pull-off on the right, or if there are many cars, across the street in store parking lots.

Stop 6- Salmon Hole- tidal flat facies of the Monkton, Winooski and Danby Formations.

Descend the pathway down to the broad bedding planes of the Monkton in the south bank of the river. This beautiful outcrop of Monkton is in danger of being destroyed by dam construction. Examine the multitude of rippled surfaces, and note the multiple paleoflow directions. Examine these rippled beds in cross section and note that they are composed of rippled dolomite, silty dolomite, and fine-grained sandstone with shale drapes, a typical tidal bedding style. Examining bedding planes again, look for both vertical and horizontal burrows. Mudcracks can also be found. The thick, structureless buff-colored dolomite bed near the top of the Monkton is interpreted to be supratidal in origin (carbonate mud washed up onto the tidal flat during a storm?). This implies that the section of Monkton just examined would be the upper

portion of a shallowing-up cycle, which characterize the Monkton Quartzite. From having seen the subtidal and platform margin facies of the Monkton at Stop 4 you can now compare the features seen at the two outcrops. The tidal flat facies seen here and at other localities around the Burlington and Winooski areas were prograding northward towards the platform margin in the Milton region. The Monkton/Winooski contact is under water here but can be examined at Whitcomb's Quarry at the I-89 interchange. It is gradational over about 10 meters, with progressively decreasing amounts of sand up section into the Winooski.

Return to cars. Turn around to head back across the river.

- 13.4 Drive across the river to the entrance to the Winooski Mill shopping mall. Drive to the back parking lot adjacent to the river. Carefully descend to the river bank on the upstream side of the building.

Stop 7 - Danby Quartzite and Winooski Dolomite

You are now on the bedding planes of the shallow subtidal facies of the Danby Quartzite (Figure 5), which is a dolomitic sandstone at this exposure. There are many exposures of sedimentary structures at this outcrop, including hummocky cross stratification, complexly-woven ripple bundles, bedding planes with interference ripples, and graded beds. Biogenic structures include small LLH stromatolites and oncolites. Most of these features suggest that the sediments of the Danby were frequently reworked by storm action, resuspending and reworking the substrate, and rapidly depositing sediment during post-storm surge ebb flow.

During low water levels the entire Danby can be walked out from its contact with the Winooski on this side (upstream) of the bridge. The contact is gradational and is characterized by increasing amounts of quartz sand in dolomite until it becomes a dolomitic sandstone. The Winooski Dolomite does not exhibit many features but thin wisps of carbonaceous material with sand grains concentrated along the laminae are interpreted to be cryptalgalaminites.

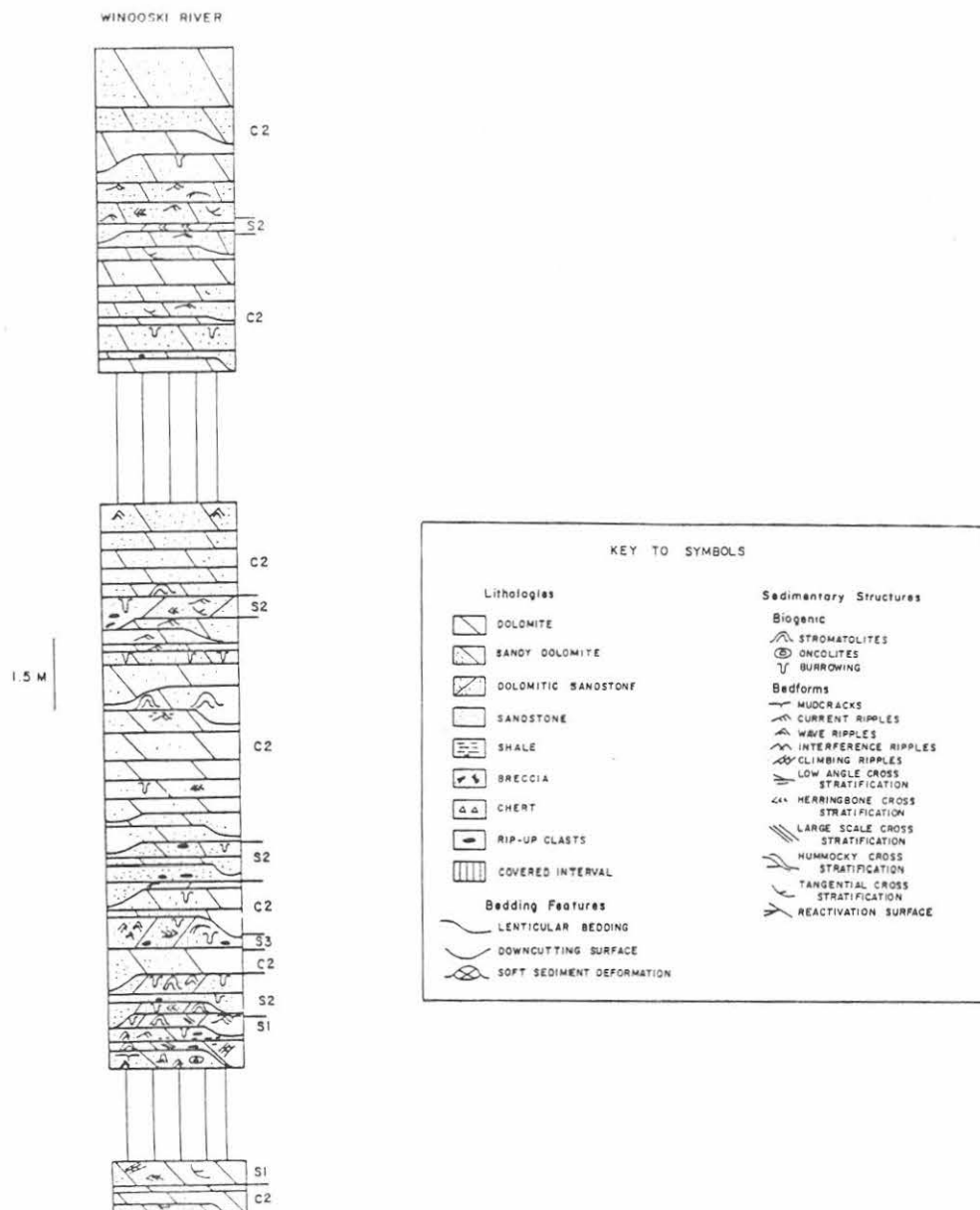


Figure 5. Measured stratigraphic section of the Danby Formation along the Winooski River.

Return to cars and exit shopping mall to Route 7.

- 14.8 Ascend Route 7 to I-89, passing Whitcomb's Quarry.
- 29.6 Head north on I-89, passing (at 23.3 miles) an exposure of Rugg Brook Conglomerate and at 25.1 and 25.7 miles, exposures of folded Skeels Corners Slate.
- Exit 18 Georgia Center/Fairfax.
- 32.3 Head north on Route 7 to Georgia Center
Left at Center Market towards Georgian Plains (west).
- 32.8 Go straight at Y in road. Knoll to your right (north) is Rockledge Conglomerate.
- 33.2 Knoll of Rockledge on the right. Pull off onto shoulder.

You must ask permission to visit this outcrop.

Stop 8- Rockledge Conglomerate

In the field immediately to the north of the road are scattered outcrops of the Rockledge Conglomerate limestone clast facies. Examine exposures of the conglomerate and the poor sorting and angularity of clasts, and the sandy limestone matrix. Pods of the conglomerate, interpreted as individual flows of high density turbidity currents, are surrounded by the laminated siltstones of the Skeels Corners Slate.

Time permitting, it is possible to continue west along this road and examine several facies of the Rugg Brook Formation.

- 34.2 Small ridges 100 yards to the north are composed of massive dolomitic sandstone facies of the Rugg Brook Formation.

Skeels Corners Slate occurs across the street to the west.

Turn right at the stop sign and head north

- 35.1 In the fields behind the yellow farm house are exposures of various facies of the Rugg Brook,

primarily the massive dolomite with scattered clasts and dolomitic sandstones.

Continue north

- 35.6 Turn Right
- 37.5 Intersection with Route 7. Turn right (south)
- 41.1 Intersection with I-89. Head southbound
- 49.9 Route 2 Champlain Islands exit ramp off I-89. Head west (right).
- 53.8 Return to Sand Bar State Park and meeting place for start of trip.

GRENVILLE CALC-SILICATE, ANORTHOSITE, GABBRO, AND IRON-RICH SYENITIC ROCKS FROM THE NORTHEASTERN ADIRONDACKS

By

ELIZABETH B. JAFFE and HOWARD W. JAFFE
Department of Geology and Geography
University of Massachusetts, Amherst

INTRODUCTION

The Marcy anorthosite massif is delineated by a major NW-SE-trending lobe and a smaller N-S-trending lobe which coalesce to the S to form a heart-shaped outcrop pattern covering 5000km². (Fig. 1). In section, the major NW-trending lobe approximates a piano bench or slab 3-4.5 km thick with two legs or feeder pipes extending at least 10 km down according to the geophysical model of Simmons (1964), whereas Buddington (1969) favored an asymmetrical domical shape based on extensive field mapping and other considerations. The massif consists of a coarsely crystalline core of apparently undeformed felsic andesine anorthosite thrust over a multiply deformed roof facies consisting of gabbroic-noritic anorthosite, gabbroic anorthosite gneiss, and quartz-bearing ferrosyenite-ferromonzonite facies (Pitchoff Gneiss). Remnants of a siliceous carbonate- and quartzite-rich metasedimentary sequence and associated garnet-pyroxene-microperthite granulites form discontinuous screens and xenoliths in the roof facies. Xenoliths of any kind are very rare inside the felsic anorthosite of the core, but abound in the gabbroic anorthosite of the roof facies.

We will visit ten outcrops which include all of the major rock types (Fig. 1) of the massif, and that lie principally in its multiply deformed roof facies.

That regional metamorphism took place at high pressure, in the range of 8-10 kbar at about 800^o, is indicated by the occurrence of orthoferrosilite, Fs95 + quartz, and the absence of any vestiges of fayalite in the ferrosyenite facies of the Pitchoff Gneiss (Jaffe et al., 1978). Because recent Sm147-Nd143 age dating yields 1288 M.Y. for the age of magmatic crystallization of the Marcy anorthosite (Ashwal and Wooden, 1983), and older Pb-U age dating by Silver (1969) yields about 1130 M.Y. for crystallization and about 1100-1020 for metamorphism, the Grenville orogeny may have spanned as much as 200 M.Y. and it is difficult to fix the peak of metamorphism with a specific thermal or tectonic event within this time span.

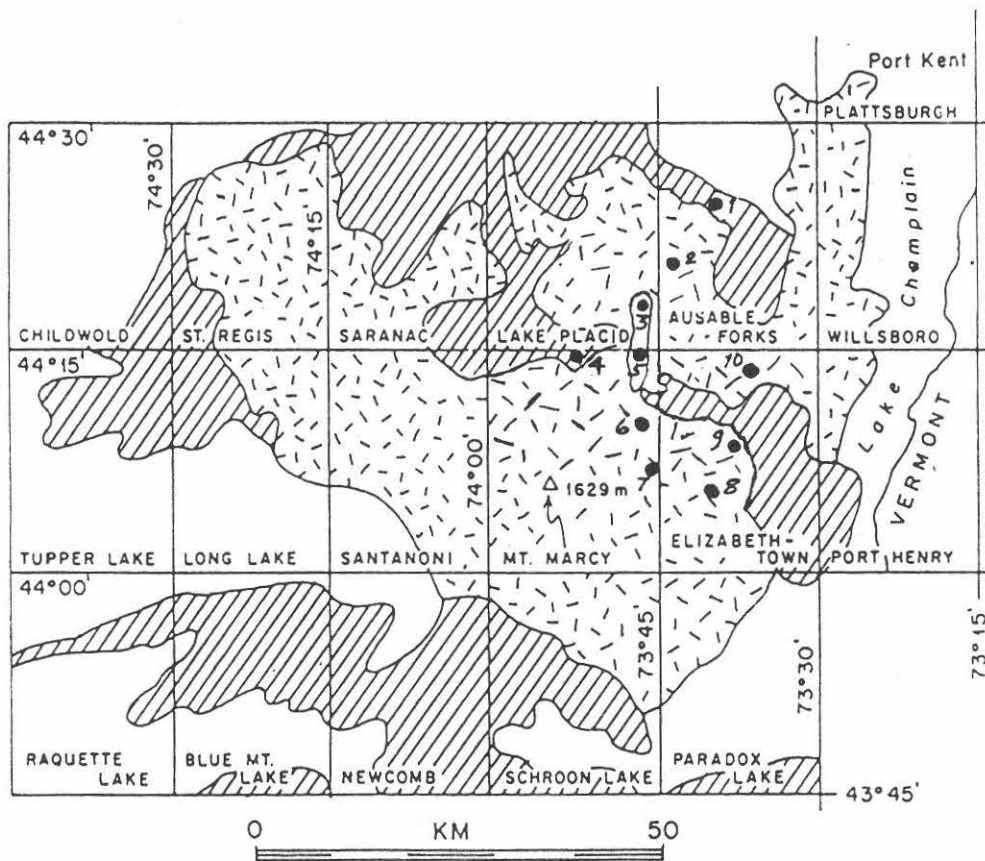


Figure 1. Generalized geologic map of the Marcy anorthosite massif and surrounding areas: anorthositic rocks , ferrosyenite-ferromonzonite gneiss , and Grenville metasediments . NYSGA - 1988 field trip stops 1-10.

Stop 1. FAYALITE-FERROHEDENBERGITE GRANITE, AUSABLE FORKS AREA, 15' AUSABLE FORKS QUADRANGLE, LOCALITY AF-1-A

Iron-rich granitic-syenitic-quartz monzonitic rocks, ascribed to a charnockitic gneiss series, are abundant in the northeastern and central Adirondacks, where they occur in close association with anorthositic and metasedimentary calc-silicate rocks in the Marcy Massif. Most of these contain iron-rich orthopyroxene (eulite or orthoferrosilite) with quartz, an assemblage stabilized at the high operable regional metamorphic pressure of about 8 kbar, with $T = 700-770^{\circ}\text{C}$ (Jaffe, Robinson, and Tracy, 1978; Bohlen and Boettcher, 1981). Other members of this alkali-feldspar-rich series contain fayalite and quartz in place of orthoferrosilite and quartz. From tables 1, 2, 3, 4, and Fig. 9 and Table 7 from Jaffe, Robinson and Tracy (1978), (Appendix I) it is reasonable to assume that both of these rock types were recrystallized under similar metamorphic conditions. Work by Bohlen and Essene (1978) and by Ollilla, Jaffe, and Jaffe (1988) indicate that these rocks had igneous precursors that crystallized above 900° .

JAFFE ET AL.: IRON-RICH PYROXENES (1978)

Table 1. Modes of pyroxene-micropertthite gneiss

	Po-13	SC-6	Po-17	FFG-6	AF-1A	Po-2
Quartz	4.1	9.1	13.8	18.4	69.1	1.5
Micropertthite	37.2*	46.5*	52.6*	69.2**	20.5	84.5
Plagioclase***	32.7	25.1	18.2	3.5	Trace	3.6
Augite	6.2	8.7	6.6	3.7	5.5	4.1
Orthopyroxene	3.9	2.4	1.9	None		2.4
Olivine	None	None	None	0.6	3.0	None
Hornblende	3.8	2.1	4.1	3.9	Trace	1.8
Garnet	7.1	3.6	1.7	None	None	0.8
Magnetite + Ilmenite	3.0	1.9	0.8	0.5	1.1	1.0
				Trace		
Zircon	0.2	0.3	0.1	0.1	0.3	Trace
Apatite	1.8	0.3	0.1	0.1	0.3	0.3
Fluorite					0.2	
	100.0	100.0	99.9	100.0	100.0	100.0
Color Index	26	19	15	9	10	15
Mole % An***	23	16	10	11	12	21
Mole % Fs	85-88†	92	95			83-9
Orthopyroxene	83-85††	89	91			
Mole % Fa†				99	99	
Olivine						

*Contains abundant exsolution lamellae of albite and is partially mixed to microcline micropertthite.
 **A micropertthite containing an oligoclase, An₁₁ component.
 ***An values for plagioclase host grains determined by measurement of the n index of refraction in oils. For probe analyses see Table 8.
 † $100(\text{Fe} + \text{Mn})/(\text{Fe} + \text{Mn} + \text{Mg})$.
 †† $100 \text{ Fe}/(\text{Ca} + \text{Fe} + \text{Mn} + \text{Mg})$ as used by Smith (1971a).

Table 2. Optical properties of iron-rich pyroxenes

	Po-13	SC-6	Po-17	FFG-6	Fe Augite**
Orthopyroxenes					
γ	1.7763	1.785	1.786	Z=pale blue-green	1.789
β	1.7765	1.774	1.774	Y=pink-yellow	1.780
α	1.7560	1.764	1.765	X=pale pink	1.772
$\gamma-\alpha$	0.0203	0.021	0.020		0.017
$2V_{\text{calc}}$	88°, (-)	88°, (+)	79°, (+)		86°, (+)
Disp.	r<v, strong r>v, strong r>v, strong				
Fe/Mn	.88	.92	.95		1.00
Fe/Mn+Mg					
Augites					
γ	1.7505	1.759	1.760	1.7645	(1.7646)
Fe/Mn	.83	.88	.93	.95	1.00
Fe/Mn+Mg					

*Indices as reported by Lindsley, Davis, and MacGregor, 1964. They report $2V = 58^{\circ}(+)$ which is inconsistent with their indices.
 **The value of γ for pure Fe augite is from the equation of Jaffe et al., 1975.

JAFFE ET AL. IRON-RICH PYROXENES (1978)

Table 3. Lattice parameters of natural and synthetic orthoferrosilite

	Synthetic FeSiO ₃		
	Po-17	Burnham (1965)	Sueno et al. (1973)
a (Å)	18.42	18.431	18.418
b (Å)	9.050	9.080	9.078
c (Å)	5.241	5.238	5.237
V (Å ³)	873.68	876.60	875.14

Table 4. Representative electron probe analyses of coexisting pyroxenes and olivine, and compositions of theoretical end members

	Po-13A	Po-13B	SC-6	Po-17	FFG-6	CaFeSi ₂ O ₆		Po-13A	Po-13B	SC-6	Po-17	FFG-6	FeSi ₂ O ₆		
Augite							Orthopyroxene							Fayalite Fe ₂ Si ₂ O ₆	
SiO ₂	47.81	47.84	48.51	48.69	47.66	48.44	SiO ₂	46.15	45.90	45.65	45.50	28.62	45.54		
Al ₂ O ₃	1.31	1.17	1.00	1.00	.65		Al ₂ O ₃	.30	.31	.27	.36	.08			
TiO ₂	.12	.10	.09	.14	.06		TiO ₂	.06	.08	.13	.11	.00			
Cr ₂ O ₃	.05	.05	.00	.06	.03		Cr ₂ O ₃	.06	.02	.05	.06	.03			
MgO	3.78	3.08	2.07	1.17	.91		MgO	4.62	3.52	2.48	1.36	.39			
ZnO	.09	.07	.14	.19	.01		ZnO	.28	.26	.38	.37	.31			
FeO	25.73	26.75	27.68	29.18	29.14	28.96	FeO	46.36	47.60	49.28	49.81	69.51	54.46		
MnO	.27	.38	.37	.43	.58		MnO	.51	.86	.72	1.10	1.57			
CaO	19.54	19.92	19.43	19.07	20.32	22.60	CaO	.80	.75	.79	.84	.05			
BaO				.00			BaO				.06				
Na ₂ O	.73	.72	.78	.72	.73		Na ₂ O	.00	.00	.00	.03				
K ₂ O	.00	.00	.00	.00			K ₂ O	.00	.01	.00	.00				
Total	99.43	100.08	100.07	100.65	100.09	100.00	Total	99.14	99.31	99.75	99.60	100.56	100.00		
Augite							Orthopyroxene							Fayalite Fe ₂ Si ₂ O ₆	
Si	1.926	1.925	1.965	1.977	1.949	2.000	Si	1.969	1.971	1.969	1.980	.964	2.000		
Al	.062	.056	.035	.023	.031		Al	.015	.016	.014	.019	.003			
Fe ³⁺	.012	.019			.020		Fe ³⁺	.016	.013	.017	.001	.033			
Total	2.000	2.000	2.000	2.000	2.000	2.000	Total	2.000	2.000	2.000	2.000	1.000	2.000		
Al			.013	.025			Ti	.002	.003	.004	.004				
Ti	.004	.003	.003	.004	.001		Cr	.002	.001	.002	.002	0			
Cr	.002	.002		.002	.000		Fe ³⁺	.025	.023	.022	.014	.036			
Fe ³⁺	.122	.124	.078	.044	.106		Mg	.294	.225	.159	.088	.019			
Mg	.227	.185	.125	.071	.054		Zn	.009	.008	.012	.012	.007			
Zn	.003	.002	.004	.006	.000		Fe ²⁺	1.613	1.674	1.739	1.798	1.892	2.000		
Fe ²⁺	.733	.757	.860	.947	.871	1.000	Mn	.018	.031	.026	.041	.045			
Mn	.009	.013	.013	.015	.020		Ca	.037	.035	.037	.039	.001			
Ca	.844	.859	.843	.830	.891	1.000	Ba				.001				
Na	.057	.056	.061	.057	.057		Na				.003				
Total	2.001	2.001	2.000	2.001	2.000	2.000	K		.001						
							Total	2.000	2.001	2.001	2.000	2.000	2.000		

Here, at Stop 1, we will visit outcrops of the fayalite-ferrohedenbergite granite and later, at Stop 4, we will visit a eulite-ferrohedenbergite syenite gneiss on Pitchoff Mt. in the 15' Mt. Marcy quadrangle.

A circular outcrop area, about 1 km in radius from the center of Ausable Forks village, was mapped by Kemp and Alling (1925) as an olivine-bearing quartz nordmarkite. They located several quarries within this outcrop area. On a fresh break, the rock shows the greenish cast typical of the ferrosyenites and charnockitic rocks of the northeastern and central Adirondack region. It is a medium-grained (1-5mm) hypersolvus granite, in places gneissic, with a color index of 5-15. Similar fayalite-bearing granitic rocks were described by Buddington and Leonard (1962) from the Cranberry Lake quadrangle, near Wanakena, from the St. Lawrence Co. magnetite district of the central Adirondacks. At Wanakena, and very likely at Ausable Forks, eulite- or orthoferrosilite-ferrohedenbergite granitic-quartz-monzonitic gneiss is closely associated with the fayalite-ferrohedenbergite granitic rock. Fayalite and ferrosilite, together with quartz, have not thus far been found in the same specimen; if they were it would provide a precise geobarometric value for the pressure of regional metamorphism. From Fig. 9 and Table 7, Jaffe, Robinson and Tracy, (1978) (see Appendix I) it will be seen that the assemblage orthoferrosilite + quartz gives a minimum P, whereas fayalite + quartz gives a maximum P. A range of 7-9 kbar at 600^o or 10-12 kbar at 800^o outlines the extremes of the metamorphic P-T conditions. Recent work by Ollila, Jaffe and Jaffe (1988) indicates that the orthoferrosilite in Pitchoff Mt. syenite gneiss is actually an inverted pigeonite crystallized from a magma above 9 kbar and 900^oc, conditions in excess of those accepted for the regional metamorphic peak.

In the Ausable Forks area, fayalite-ferrohedenbergite granite contains only trace amounts of hornblende: in outcrops where hornblende becomes abundant, fayalite is pseudomorphously altered to a brown fibrous serpentine or talc. The granitic rocks are cut by dikes of hornblende granite pegmatite and diabase.

The fayalite-ferrohedenbergite granite differs from the orthoferrosilite-ferrohedenbergite granitic-syenitic gneisses in several important aspects;

- 1) the fayalite granite is massive to poorly foliated, while the ferrosilite granitic gneiss is well foliated.
- 2) the fayalite granite is hypersolvus, carrying only a "strip" or "striped" microperthite that is slightly unmixed to sodic plagioclase and orthoclase, whereas the ferrosilite granitic gneiss is subsolvus, containing blebby and patchy microperthite more unmixed to sodic plagioclase and partly inverted to microcline, and this microcline microperthite coexists with an intermediate plagioclase,
- 3) the fayalite granite does not contain garnet because of the absence of intermediate plagioclase, whereas the ferrosilite granitic gneiss always carries garnet.

All of this suggests that the fayalite granite might be younger than the ferrosilite granitic gneiss. We concur with Buddington and Leonard (1962) who suggested that the fayalite granite could have originated from the fractional

remelting at depth of the pyroxene granitic gneisses, with its intrusion occurring during the waning stages of deformation.

Stop 2. ANORTHOSITE NEAR COVERED BRIDGE AT JAY, 15' AUSABLE FORKS QUADRANGLE

Outcrops just beyond a covered bridge about 0.32 km E of Ausable Forks center show the characteristic textures of anorthositic rocks along the margins of the Marcy Massif. In the roadcut, anorthositic block structure shows up to 2m blocks of coarse, cumulate-textured andesine anorthosite, and coarse hypersthene (to 25 x 15cm) enclosed in a gabbroic anorthosite. Dark layers, up to 2.5cm thick, occur within the country rock. Outcrops in the East Branch of the Ausable River are principally of coarse andesine anorthosite with a megacryst index of about 20-30 and a color index of only 1. Numerous shear veinlets crisscross the anorthosite, trending N40E and N10W for the most part.

Stop 3. GRENVILLE-ANORTHOSITE HYBRID GNEISS 3.4 KM S OF UPPER JAY ON RTE 9N IN THE 15' LAKE PLACID QUADRANGLE

We are located in a 6.4 x 1.6 km north-trending section of Grenville strata consisting largely of calc-silicate-amphibolite-marble assemblages. Graphitic marbles occur across the Ausable River to the W of this roadcut. All these have been intruded and pervaded by sills of gabbroic anorthositic composition, resulting in the formation of Grenville-anorthosite-hybrid gneisses. Subsequently these were intruded by a sill of gabbro that forms the center of the E side of the large road cut on Rte. 9N (Fig. 2).

The section may be divided into three parts:

- 1) a lower unit consists principally of a mottled granular black and white sphenc-augite-andesine calc-silicate gneiss discontinuously interlayered with black hornblendite-amphibolite lenses presumably of volcanic origin. The granular mottled host rock consists of white andesine, An₃₂₋₃₉, black augite, and 5-10% of red-brown to yellow-brown sphene. The black amphibolitic layers contain mostly brown hornblende along with white plagioclase now altered to prehnite and calcite.

2) a central unit is a biotite-hornblende-hypersthene-augite-garnet-plagioclase metagabbro sill. The abundance of garnet, 20%, suggests that the gabbro sill may have been olivine-rich. The sill shows sharp contacts above and below with the anorthosite-calc-silicate-hybrid gneiss.



Figure 2. Grenville calc-silicate anorthosite hybrid.

3) above the upper contact of the gabbro sill, the rock is augite-andesine An39-40 gabbroic anorthosite gneiss intercalated with dark amphibolite and calc-silicate layers.

Sporadic large garnets up to 6 cm in diameter occur along contacts of anorthositic and mafic layers.

The outcrop on the W side of the road shows a well-developed high strain pencil lamination, oriented N25E.

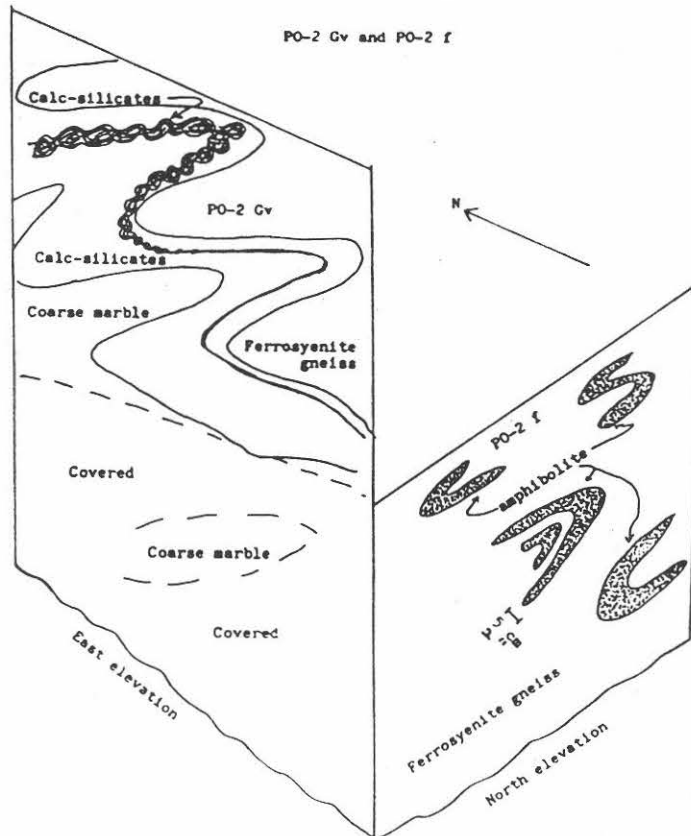
Stop 4. THE PITCHOFF GNEISS - FERROSYENITE FACIES, PO-2

Turn right (north) on Route 73, and go through Keene Village, where Route 73 turns west. Follow it about 4.5 miles (7.2 km) to the foot of Lower Cascade Lake. Park at the lakeside in the second parking area on the left, just past a sign **FALLEN ROCK 1 1/2 MILE**. Be very careful cutting across traffic: this is a busy high-speed highway. Recross the road on foot, again with great caution. Walk back toward the **FALLEN ROCK** sign, to a rough trail up the talus just short of the sign. The talus and cliff are both steep and full of loose rocks: be considerate of those below and behind.

The prominent, southeast-facing cliff we are climbing to is a ferrosyenite gneiss that crystallized from a melt prior to its metamorphism. It is one of a group of quartz-poor, alkali-feldspar- and ferroan-pyroxene-rich igneous rocks that acquired their gneissic fabric during an episode of isoclinal and recumbent folding associated with the Grenville orogeny at about 1100 M.Y. The persistent proximity and intimate intercalation of these gneisses with "Grenville" supracrustal rocks suggests that they may have initially been iron-rich felsic volcanics, or perhaps sills, interlayered with siliceous dolomites, calcareous quartzites, marls and basaltic flows comprising a Proterozoic series of rocks deposited about 1350 M.Y. This Grenville age is estimated from Ashwal's (1983) recent $\text{Sm}^{147}\text{-Nd}^{143}$ date of 1288 M.Y. believed to represent the age of crystallization of the Marcy anorthosite massif-core facies. Following the model of McLelland and Isachsen (1980) for the southern Adirondacks, we suggest that, in the High Peaks Region of the northeastern Adirondacks, a "typical" Grenville supracrustal sequence correlative with rocks of the Central Metasedimentary Belt (Wynne-Edwards, 1972) was buried in a plate-tectonic event or events to a depth of about 70 km (42 mi), that of a doubly thickened crust. Following Emslie (1977), we envisage the birth of an anorthositic magma from the fractionation of copious amounts of orthopyroxene from an already-fractionated Al-rich gabbroic magma. Under these deep-seated conditions, the high pressures and temperatures plus the availability of Grenville-strata-derived CO_2 -rich fluids initiated the formation of potassium- and iron-rich, relatively quartz-poor, melts of syenitic to monzonitic composition (Wendlandt, 1981). Ascent, intrusion, and emplacement of the syenitic melt at levels on the order of 25-35 km (15-21 mi) and temperatures of 800-900^o induced deep contact metamorphism of appropriate Grenville rock types. Here, at the easternmost part of the PO-2 outcrop, designated PO-2Gv (Fig. 3), a calc-silicate sequence infolded with the ferrosyenite contains the assemblage: wollastonite-diopside-grossular-quartz. Because anorthosite is absent, the contact-metamorphic origin of the wollastonite must be attributed to the intrusion of syenitic melt. Further, because

the ferrosyenite contains relict inverted pigeonite, which now consists of host orthoferrosilite, $100\text{Fe}/(\text{Fe}+\text{Mg})=85-92$, the melt must have crystallized at temperatures of $850-900^{\circ}$ (Lindsley, 1983 and Ollila, Jaffe and Jaffe, 1988). Alternatively, shallow emplacement with

Figure 3. PO-2gv. Folded amphibolite, marble, and wollastonite-bearing calc-silicate rock in ferrosyenite gneiss. Pitchhoff Mt. cliff, above north end of Lower Cascade Lake. Mt. Marcy quadrangle.



crystallization of fayalite and quartz, later deeply buried and converted to orthoferrosilite and quartz, is conceivable, yet unlikely, because no relict olivine, whatsoever, has been observed by Jaffe or by Ollila in quartz-bearing syenitic rocks of the Mt. Marcy and the Santanoni quadrangles. Fayalite (Fa_{95}) plus quartz, but with orthopyroxene absent, has been described from quartz-syenitic rocks in the Cranberry Lake quadrangle to the west (Buddington and Leonard, 1962, Jaffe et al. 1978) and in the Ausable Forks quadrangle to the northeast (Kemp and Alling, 1925 and Jaffe et al, 1978). A deep emplacement with high pressure crystallization is consistent with field observations and experimental data for all of these rocks.

At the PO-2 outcrop, we will split into several smaller groups: the footing can be a bit tricky. Remember not to step back for a better look at the outcrops. The first or westernmost cliff consists of strongly foliated ferrosyenite gneiss, N45E30W, with a large inclusion of shonkinite granulite (Fig. 4, Table 5). The foliation continues through the inclusion. The southwest end of the inclusion is sharply cut off by the gneiss but the northeast end fingers out. The inclusion is cut by a discordant vertical tongue of gneiss which becomes a subhorizontal pegmatite vein. At the northeast end of this cliff, the ferrosyenite gneiss is cut by an unfoliated aplite dike. Small amphibolite inclusions can be seen in the gneiss.

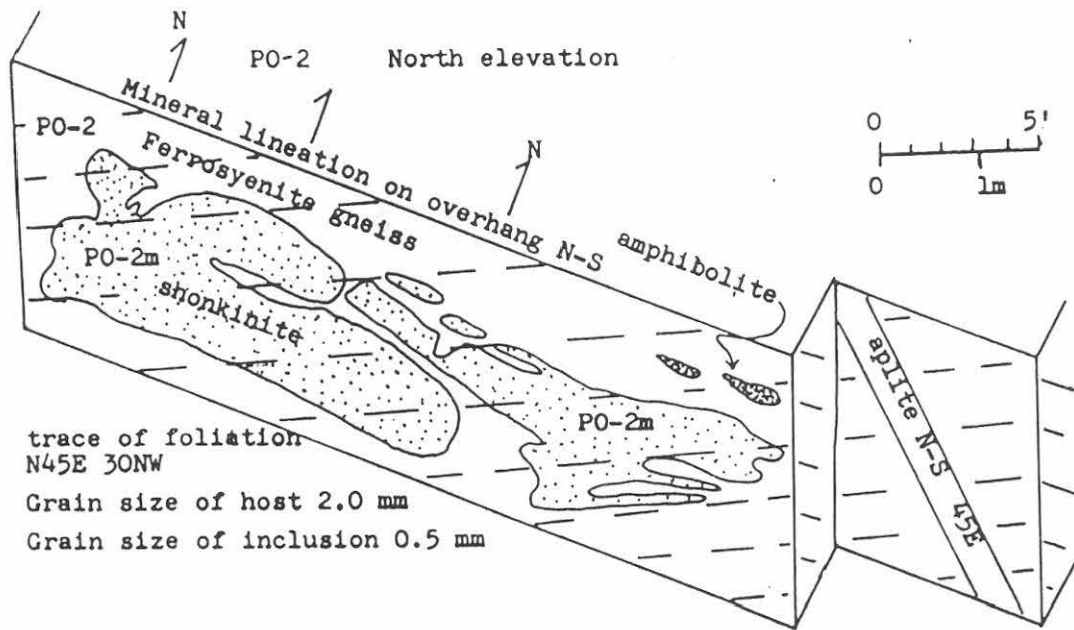


Figure 4. Xenolith of folded shonkinite layer PO-2m and amphibolite remnant in quartz ferrosyenite gneiss PO-2. Aplite dike cuts syenite gneiss. Pitchoff Mt. cliff above north end of Lower Cascade Lake, Mt. Marcy quadrangle.

TABLE 5. Modes of rocks at Stop 4, locality PO-2

	Ferrosyenite gneiss		Shonkinite	Amphibolite	Aplite
	PO-2 host rock		PO-2m inclusion	Inclusion	PO-2d dike
Q	1.5	2.0	-	-	23.0
Mp	84.5	84.0	50.0	-	60.0
Plag	3.6	4.0	13.0	30.0	16.0
Aug	4.1	4.0	12.7	-	-
Hy	2.4	2.0	16.6	-	-
Hb	1.8	2.0	4.1	58.0	0.9
Ore	1.0	1.0	2.6	+	0.1
Gt	0.8	1.0	+	-	0.0
Ap	0.3	+	1.0	2.0	tr
Zr	+	+	+	-	-
Bio	-	-	+	10.0	-
	100.0	100.0	100.0	100.0	100.0
An	21		21		
Fs(opx)	83-89		75		
CI	15		40	88	1

Mineral assemblages infolded in ferrosyenite gneiss
host rock at locality PO-2Gv.

Amphibolite: hornblende and altered plagioclase.

Calc-silicate: hedenbergite-plagioclase-quartz

hedenbergite-plagioclase-quartz-scapolite-sphene

diopside-grossular-quartz-sphene

wollastonite-diopside-grossular-quartz

wollastonite-calcite-prehnite

diopside-calcite

We will proceed cautiously about 300' (91.5 m) along the base of the cliff to the northeast, across a stream and a gully. Here we see several larger folded amphibolite inclusions in the ferrosyenite gneiss (Fig. 3). The axial planes of these folds are approximately parallel to the pervasive foliation. We will now crawl a few feet up the gully: in its east wall are exposed marbles and calc-silicates intimately infolded in the ferrosyenite gneiss. Wollastonite occurs in these calc-silicate beds (Fig. 3). If we make allowance for the plasticity of the marble, these folds are also approximately parallel to the pervasive foliation. There is a cave in the marble a little higher up this gully. On the opposite side of Lower Cascade Lake, in the anorthosite, another cave can be found a few hundred feet higher up. Caves are common in New York State, but these two must be among the few in Precambrian rocks.

Stop 5. GRENVILLE MARBLE-SYENITE-ANORTHOSITE SECTION SOUTH OF KEENE

Drive five miles (8 km) northeast on Route 73 to the first right turn after a Gulf gasoline station and almost into Keene village center. Turn right (south) on the westernmost of two small roads that parallel both sides of the East Branch of the Ausable River. Drive about 0.75 (1.2 km) miles south on this western side of Hulls Falls Road and park judiciously along the edge of this little travelled road. Descend about 25' (7.6 m) to the bank of the river watching out to avoid standing or sitting in Rhus toxicodendron which commonly grows in Grenville marble terrain. A fine river outcrop of folded Grenville marble consists of calcite (white), diopside (green), fluopargasite (black), and minor glistening flakes of phlogopite (brown) along with less abundant graphite. Pink quartz leucosyenite and black-streaked gray-white gabbroic anorthosite gneiss have been dragged into highly contorted syntectonic folds enhanced by the plasticity of the marble and the probable molten state of the quartz syenite and gabbroic anorthosite (Fig. 5). Occasional tongues of gabbroic anorthosite cross-cut the syenitic rocks. A major vertical fracture zone, the Keene Fault Zone

runs parallel to the river in a N-S direction, and is well exposed about one-half mile (0.8 km) south in a granulated anorthosite outcrop. The Keene Fault has dragged the preexisting, gently north dipping, isoclinally folded strata into fairly steeply plunging folds at this locality. A late, brittle stage of movement on the same fault has granulated and retrograded all of the brittle rock types. Feldspar in syenite is sericitized, intermediate plagioclase in gabbroic anorthosite has been albitized and veined by calcite, grossular-diopside calc-silicate rocks have been prehnitized and chloritized, but marble merely goes along for the glide.

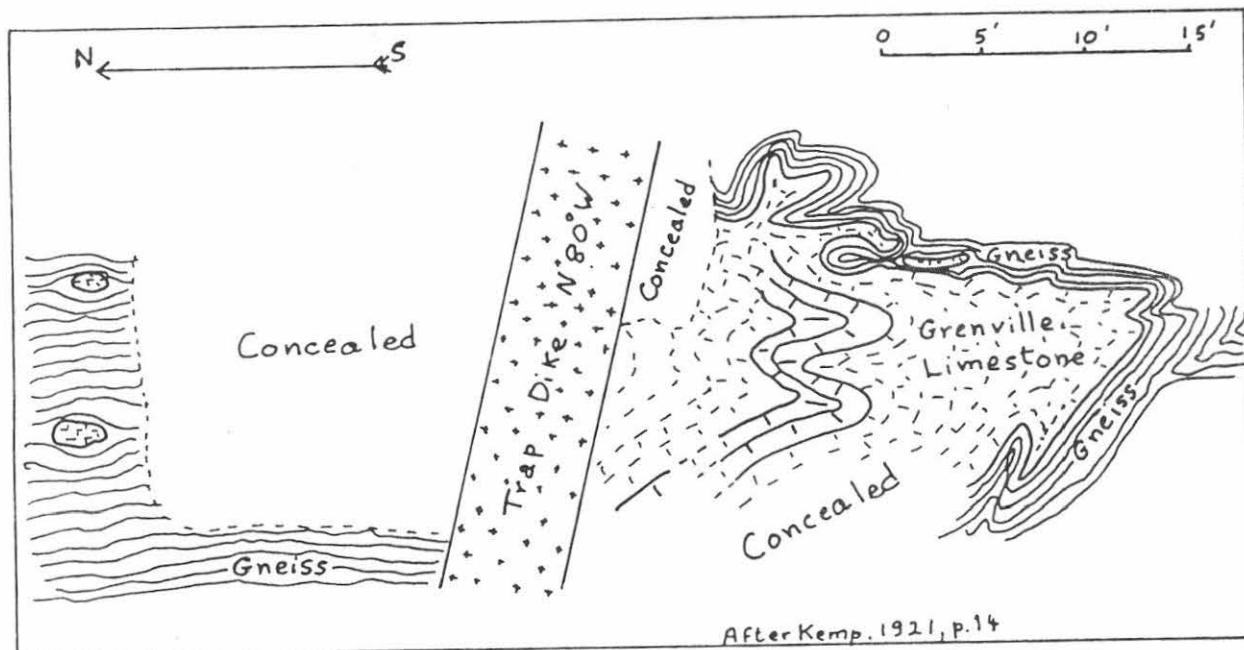


Figure 5. Contorted folding in diopside-calcite-pargasite-calcite marble, quartz leucosyenite gneiss, and anorthosite gneiss in the West Branch of the Ausable River south of Keene, N.Y. A camptonite dike cuts the marble-gneiss section. After Kemp, 1921. Mt. Marcy quadrangle.

At the northernmost end of the outcrop, the diopsidic marble and the quartz syenite are transected by a 4' (1.2 m) wide N80W90 trending lamprophyre dike (Fig. 5) which displays good chilled margins. It is a classic lamprophyre: a dark, dense, porphyritic dike rock in which the ferromagnesian minerals occur in two generations and in which only the dark minerals form the phenocrysts. It consists of 1-5 mm diameter phenocrysts of partially serpentinized magnesian olivine, and zoned clinopyroxene with augite cores and titanaugite rims, which display spectacular zoning, intense anomalous interference colors and dispersion, and hourglass structure. The groundmass contains a second generation of

microphenocrysts of titanite, kaersutite, titanian biotite and abundant very thin needles of apatite in a quasi-isotropic base that has too high an index of refraction to be analcime or leucite; it has a mean index of refraction = 1.525 and is either untwinned anorthoclase or a zeolite. The dike may be classified as either a camptonite or a monchiquite, but exactly conforms to neither.

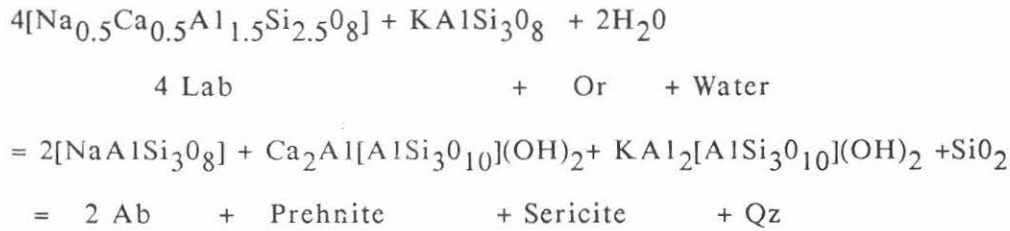
Notes:

Stop 6 THE 1063 MYLONITE

On the west side of Route 73, 1.3 miles (2.1 km) south of the village of Keene Valley at BM 1063 and opposite the Beer Bridge across the Ausable River, the anorthosite is cut by a well-developed mylonitic zone about 2' (0.6 m) wide which trends N55E35NW. Park on the west shoulder of the road south of the outcrop and walk back. The anorthosite here appears to be the normal gabbroic type; however, the mafic minerals occur in clots and aggregates of augite+apatite, many of which are bent into mini- and microfolds. These clots and the sparse megacrysts of labradorite form a foliation which trends N70W70SW. The coarse grained contaminated felsic anorthosite and the mafic clots of partially assimilated augite+apatite represent either remnants of a Grenville phosphate-rich calc-silicate rock, or a mafic cumulate segregated from a gabbroic anorthosite melt. The iron content of the augite, $100\text{Fe}/(\text{Fe}+\text{Mg}) = 47$, while too high for felsic anorthosite, is representative for anorthositic gabbro. Further, the profusion of "100" and "001" metamorphic pigeonite exsolution lamellae in the host augite (Jaffe et al., 1975) suggest that the clots may derive from anorthositic gabbro, where such are common, rather than from a Grenville calc-silicate lithology, where they are rare. Labradorite megacrysts in this rock are nevertheless higher in anorthite than felsic anorthosites of the Marcy region, and show $\text{An}_{50.5-54.5}$ rather than the typical An_{46-48} , suggesting a probable assimilation of calcium from the augite-apatite-rich clots of xenoliths. For this reason we classify such rocks as a percalcic subfacies of the gabbroic anorthosite facies.

Just north of a small waterfall, the outcrop changes dramatically: the rough foliation gives way to fine layering along which the dark minerals occur as streaks and schlieren, though occasional megacrysts have escaped granulation and appear as flaser. The mylonite is focused in a 2' (0.6 m) zone which dies out gradually to the north after about 20' (6 m) giving way again to percalcic anorthosite. Just beyond a covered interval, the north end of the outcrop contains a mafic rock, in rudely vertical attitude, but somewhat bent about a sub-horizontal axis, perhaps earlier than the mylonitization. It has been named "aproxite" by one of the authors, in allusion to its bimineralic apatite + pyroxene composition, which is identical with that comprising the mafic clots in anorthosite host rock at the south end of the outcrop. The mineralogy thus suggests that the "aproxite" is a folded layer in anorthosite rather than a mafic dike.

The mylonitic zone does not retain any of its primary magmatic or high grade metamorphic mineralogy but is totally retrograded to a fine-grained mixture of albite, prehnite, sericite, quartz, chlorite, pumpellyite, epidote, and calcite. Labradorite is altered by the following probable retrograde reaction:



Augites have been drawn out into elongate lenses, spindles, and schlieren, and totally retrograded to a mixture of fibrous, isotropic chlorite and pumpellyite with a little calcite. Apatite, alone, remains unaltered, appearing as microflaser in the mylonitized base (Fig. 6).

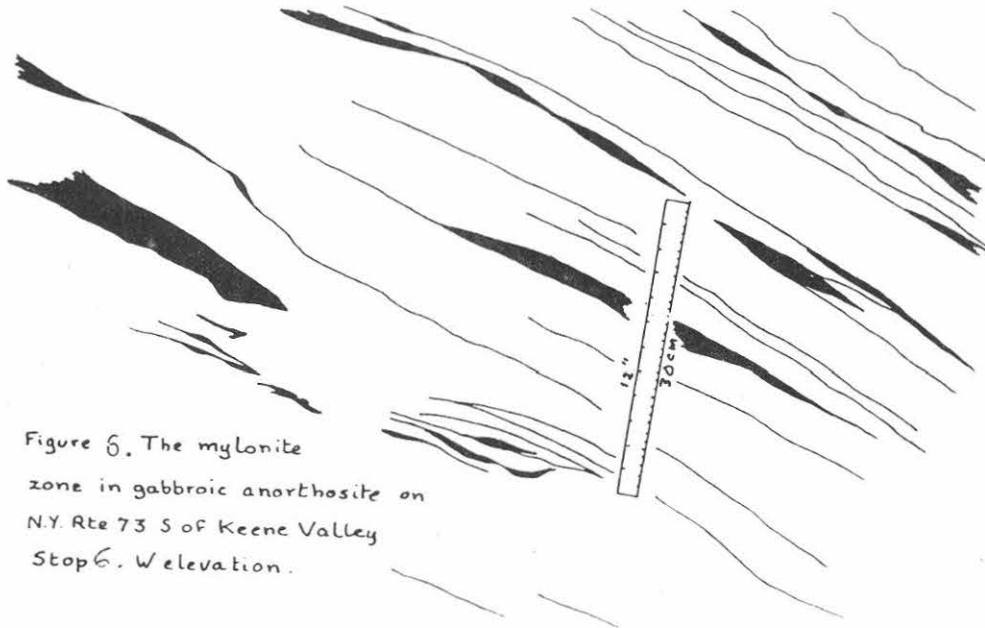


Figure 6. The mylonite zone in gabbroic anorthosite on N.Y. Rte 73 S of Keene Valley Stop 6. W elevation.

This wet assemblage is inconsistent with deep, ductile shear and suggests that the mylonitized zone originated by brittle shear or cataclasis in a wet, relatively shallow crustal setting.

That the shear zone was initially a deep, ductile mylonite, later retrograded, remains a possibility.

Stop 7. CHAPEL POND ANORTHOSITE, EAST CENTRAL MARGIN OF 15' MT. MARCY QUADRANGLE

Outcrops on the E side of Rte. 73 consist of andesine anorthosite containing shear zones of scapolite gneiss and a garnetiferous aplite dike (Fig. 7). For a detailed description of these outcrops, see Kelly (1974).

Most of the rock here is Marcy facies andesine anorthosite.

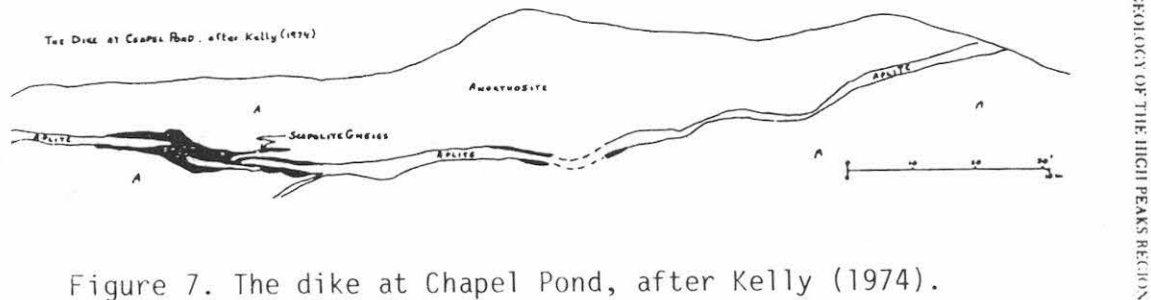


Figure 7. The dike at Chapel Pond, after Kelly (1974).

It consists of 30-40% dark blue-gray megacrysts of calcic andesine, An45-49, set in a matrix of white andesine, hypersthene, augite, and a little hornblende. Plagioclase makes up about 90% of the rock. A fine-grained aplite dike, up to 1 m thick, trends roughly parallel to the road where it may be seen to crosscut the foliation marked by aligned megacrysts of plagioclase in the anorthosite. The aplite contains about 60% micropertthite, 25% quartz, 10% altered plagioclase, 3% magnetite, and 1% each of garnet and altered ferromagnesian silicates.

Along anorthosite-dike contacts, fracture zones in the anorthosite contain clear andesine, An44-47, abundant scapolite, Me36-47, dark olive hornblende, and a little hypersthene. Fluids carrying Cl and CO₂ apparently migrated into fractures in the anorthosite to convert plagioclase into scapolite.

The abundance of the plagioclase megacrysts here and the overall texture of the rock is typical of the anorthosite that forms the core of the Adirondack high peaks to the west.

Stop 8. GABBROIC ANORTHOSITE PROTOMYLONITIC GNEISS, SOUTH CENTRAL ELIZABETHTOWN QUADRANGLE

The prominent outcrop on the W side of Rte. 9 is a gabbroic anorthosite protomylonite or straight gneiss located in one of the prominent northeast-trending fault zones that abound in the NE Adirondacks. Note that the size reduction and mylonitization of this gabbroic anorthosite are not so intense as that seen at Stop 6, the 1063 mylonite.

The rock consists of very fine crenulations and streaks of hornblende, garnet, ilmenite, and augite in a fine matrix of white andesine, An₃₂, and anorthoclase. Recrystallization took place under dry conditions, and all minerals are fresh.

The high strain nature of the gabbroic anorthosite gneiss is evident, and is illustrated by the total granulation and virtual absence of plagioclase megacrysts. An occasional block or xenolith of felsic anorthosite is present. Punky grey veins of finely altered rock occur in fracture zones.

Notes:

Stop 9. MULTIPLY DEFORMED LAYERED GABBROIC ANORTHOSITE
GNEISS, RTE. 9, 2 KM S OF ELIZABETHTOWN

The prominent cliff on the W side of Rte. 9 is a hydrothermally altered layered gabbroic anorthosite or leucogabbro located in one of the prominent northeast-trending fault zones that abound in the NE Adirondacks.



Figure 8. Refolded layered gabbroic anorthosite neiss.

The rock contains kaolinitized andesine, titanian brown hornblende, augite, and garnet, with a little ilmenite and apatite. Compositional layering is marked, with more mafic layers rich in augite and garnet, and more felsic layers richer in altered andesine and hornblende and without garnet. Many thin veinlets of white prehnite, calcite, and chlorite crosscut the gneiss. The layered gneiss was subsequently intruded by one or more aplite dikes, composed of altered albitic plagioclase, potassium feldspar, and quartz, along with garnet, and small amounts of apatite. Garnet is altered to chlorite. The rock is sliced on a mm scale, and slickensided, fracture surfaces often being coated with bright green pistacite.

The gneiss was recumbently folded under a high strain rate and then subjected to open folding (Fig. 8). Do the conspicuous open folds delineated by the pink aplite represent:

- 1) refolding of the recumbently folded gneiss?
- 2) a sheath fold squeezed or squirted up inside the gneiss?
- 3) are there one or two aplite dikes, and does the aplite layer close into a fold hinge beneath the road?

Just across Rte. 9 on the E side, the rock has a completely different texture. About half the rock consists of 0.5-5cm green, euhedral kaolinite pseudomorphs after plagioclase phenocrysts lying in a foliated matrix of brown hornblende, quartz, anorthoclase, augite, magnetite, and apatite. The fine black matrix is unaltered, in contrast to the large plagioclase phenocrysts. The green kaolinite pseudomorphs show good albite and Carlsbad twinning, but under the microscope only trace amounts of unaltered plagioclase remain. Compositionally, the rock is a quartz gabbro or quartz diorite. However, it may represent a porphyritic gabbro with its groundmass recrystallized to a metamorphic assemblage.

Stop 10. THE WOOLEN MILL GABBRO AND ANORTHOSITE, RTE. 9N, 15' ELIZABETHTOWN QUADRANGLE

On Rte. 9N about 1.6 km W of the intersection of Rtes. 9 and 9N at the golf course on the southern edge of Elizabethtown are outcrops of gabbro and anorthosite at the site of an old, long disused broken dam. Recent reconstruction of the dam and installation of a penstock along the Branch River just N of the road may limit our examination of a fine exposure of anorthosite block structure along the river.

On the S side of the road, a prominent cliff exposes the very irregular contact of a garnet- and magnetite-rich gabbro with a white gabbroic anorthosite in which almost all of the plagioclase megacrysts have been granulated. A rude foliation may be observed in both rocks. Modes of the gabbro and optically determined compositions of plagioclase, augite and hypersthene from the gabbro and anorthosite are given in Table 6. The contrast in Fs content of coexisting clinopyroxene and orthopyroxene in gabbro and anorthosite is marked. Note that the iron-rich gabbro has abundant garnet, while the relatively iron-poor anorthosite has none. The presence in the gabbro of isolated blue-gray, well-twinned (Carlsbad and albite) labradorite xenocrysts and occasional xenoliths, as well as contact relations, suggests that the gabbro has intruded the anorthosite before regional deformation. Toward the center of the roadcut, a pink aplite dike has intruded both the anorthosite and the gabbro.

The complexity of the contact relations here has led different geologists to different interpretations. Kemp and Ruedemann (1910) and Kemp (1921) reported that river outcrops showed "anorthosite tonguing in to the dark supposed gabbro"

Table 6. MODES AND MINERAL COMPOSITION OF GABBRO AND ANORTHOSITE FROM THE WOOLEN MILL LOCALITY, RTE 9N, 1.6 KM W OF ELIZABETHTOWN

<u>Mineral</u>	<u>metamorphosed gabbro</u> % by volume		<u>anorthosite</u>	
orthoclase	0.5-----0.5			tr
andesine	43.0-----50.1	An ^{1/}	andesine An ^{2/}	
		33,5		44.5
augite	12.9-----16.4	Fs ^{3/}	augite Fs ^{4/}	
		48		29
hypersthene	4.5-----4.1	Fs ^{5/}	hypersthene Fs ^{6/}	
		60		40.5
almandine	9.9-----10.2			none
ilmenite	8.2-----2.7			tr
magnetite	15.0-----10.0			none
apatite	6.0-----6.0			none

	100.0	100.0		

^{1/} mol % An from optical meas., $\alpha = 1.546$

^{2/} " " " " " " " $\alpha = 1.5520$

^{3/} mol % Fs, Fe/(Fe+Mg) from meas. of $\gamma = 1.730$

^{4/} " " " " " " " " $\gamma = 1.717$

^{5/} " " " " " " " " $\gamma = 1.740$

^{6/} " " " " " " " " $\gamma = 1.715$

A plagioclase xenocryst in gabbro has $\alpha = 1.555$, An

50.5

For optical composition curves, see Jaffe, Robinson, Tracy and Ross (1975). *Amer. Mineral.* 60, 9-28.

and suggested that the gabbros might represent "surviving inclusions of Grenville sedimentary gneisses impregnated with matter from the anorthosites." They suggested that the Woolen Mill gabbro was thus an old Grenville rock hybridized by later intrusion of anorthosite. Commenting on this interpretation, Miller (1919) assigned these plagioclase-megacryst-bearing gabbros to the Keene gneiss, which he believed to be a syenitic magma containing assimilated anorthosite! Buddington (1962) described the Woolen Mill gabbro as a typical olivine gabbro intrusive into anorthosite, in which olivine was extensively converted to garnet during regional metamorphic recrystallization. No evidence of relict olivine could be found under the microscope.

How would you interpret the outcrop relations?

REFERENCES

- Ashwal, L.D. and Wooden, J.L. (1983), Sr. and Nd isotope geochronology, geologic history, and origin of Adirondack anorthosite, Geoch. Cosmochim. Acta.
- Bohlen, S.R. and Boettcher, A.L. (1981) Reinvestigation and application of olivine quartz-orthopyroxene barometry. Earth and Planetary Sci. Letters, 47, 1-10.
- Buddington, A.F. (1969) Adirondack anorthosite series, in Y.W. Isachsen, ed., Origin of anorthosite and related rocks, N.Y. State Mus. and Sci. Serv. Mem. 18, 215-231. Albany, N.Y.
- _____ and Leonard, B.F. (1962) Regional geology of the St. Lawrence County magnetite district, northwest Adirondacks, New York, U.S. Geol. Surv. Prof. Pap. 376.
- Jaffe, H.W., Jaffe, E.B., Ollila, P.W. & Hall, L.M. (1983): Bedrock geology of the High Peaks Region, Marcy Massif, Adirondack, New York. Friends of the Grenville Guide 1983 Field Excursion, Dep. Geol. Geogr., Univ. Massachusetts, Contr. 46.
- _____, Robinson, P. and Tracy, R.J. (1978) Orthoferrosilite and other iron-rich pyroxenes in microperthite gneiss of the Mount Marcy area, Adirondack Mountains. Amer. Mineral. 63, 1116-1136.
- _____, Robinson, P., Tracy, R.J. and Ross, M. (1975) Orientation of exsolution lamellae in metamorphic augite: correlation with composition and calculated optimal phase boundaries. Amer. Mineral. 60, 9-28.
- Jaffe, E.B. & Jaffe, H.W. (1987): Geology of the Adirondack High Peaks Region. A Hiker's Guide. Adirondack Mountain Club, Glens Falls, N.Y.
- Kelly, W.A. (1974) Occurrence of scapolite in the vicinity of Chapel Pond and Keene Valley, Central Adirondacks, New York, M.S. Thesis, Department of Geology and Geography, Univ. of Massachusetts, Amherst.
- Kemp, J.F. (1921) Geology of the Mount Marcy Quadrangle, Essex County, New York, N.Y. State Mus. Bull. 229-230.
- _____ and Alling, H.L. (1925) Geology of the Ausable Quadrangle, New York, N.Y. State Mus. Bull. 261, 126 pp.
- _____ and Ruedemann, R. (1910) Geology of the Elizabethtown and Port Henry Quadrangles, N.Y. State Mus. Bull. 138.
- Lindsley, D.H. (1983) Pyroxene thermometry. Amer. Mineral. 68, 477-493.
- Ollila, P.W., Jaffe, H.W. and Jaffe, E.B. (1988) Pyroxene exsolution: an indicator of high pressure igneous crystallization of pyroxene-quartz syenite gneiss from the High Peaks region of the Adirondack Mountains. Amer. Mineral. 73, 261-73.

Silver, L.T. (1969) A geochronologic investigation of the Adirondack complex, Adirondack Mountains, New York, in Y.W. Isachsen, ed., Origin of anorthosite and related rocks, N.Y. State Mus. and Sci. Serv. Mem. 18, 232-251.

Simmons, G. (1964) Gravity survey and geological interpretation, northern New York, Geol. Soc. Amer. Bull. 75, 81-98.

ROADLOG AND TIMETABLE--H.W. & E.B. Jaffe Adirondack High Peaks Trip.

MILES	CUMUL		TIME
0.00	0.0	STOP 0. Arby parking lot, Plattsburgh,R	8:30
0.3		on Rt.3W to 187S,turn L	
14.25	14.55	to Ex.34,Ausable Forks	8:45
		turn L on Rt.9N	
10.6	25.15	STOP 1. Rt.9N 1.3 miles E of Ausable Fks.	9:05-9:35
1.3	26.45	Turn L at blinker in Ausable Fks.	
		with Rte.9N	
6.1	32.55	Turn L off Rte.9N in Jay, cross	
		covered bridge, park R	
0.2	33.15	STOP 2. Outcrop in river,on bank.	9:50-10:20
0.2	33.25	Continue W on 9N through Jay to Upper	
6.6	39.85	Jay, where we turn L(S) with 9N	
3.9	43.75	STOP 3. Rock cut S of Upper Jay	10:35-11:05
		Go S on Rt.9N to Rt.73 in Keene,turn R	
2.3	46.05	(W) on Rte.73	
4.5	50.55	STOP 4. Park on L at Cascade Lks., cross	11:20-12:05
		Rt.73 cautiously, follow path up to cliff	
4.4	54.95	Turn E on Rte.73, return to Keene	
		Turn R(S) on small road before bridge	
0.75	55.70	STOP 5. Park,E side of road, scramble	12:15-12:55
		down to river,see outcrop, lunch	
1.8	57.50	Proceed S on small road to Rte 73,	
4.0	61.50	go S through Keene Valley.	
		STOP 6. Roadside,Rte.73	13:07-13:37
3.0	64.50	Continue S on Rte 73 to Chapel Pond.	
		STOP 7. Walk N to E side outcrop.	13:43-14:13
		Continue S to Rte.9 intersection.	
4.1	68.60	turn L on Rte 9	
2.3	70.90	STOP 8. Park R, cross to outcrop	13:26-14:56
		Continue N on 9 through New Russia	
6.4	77.30	STOP 9. Park on right	15:26-15:56
1.3	78.60	At Rt. 9N, turn L	
1.0	79.60	STOP 10. Park on right,Rte.9N	16:00-16:20
1.0	80.60	Return E on Rt 9N to Rt 9, turn L	
		Return via I-87 to Plattsburgh by either 9N to	
		exit 31(5 mi),or 9 to exits 32(6mi),33(10mi) or	
		34(20 mi). Exit 37 in Plattsburgh returns you	
		to the Arby parking lot where you started, in about an hour.	

APPENDIX I.

JAFFE ET AL. IRON-RICH PYROXENES (1978)

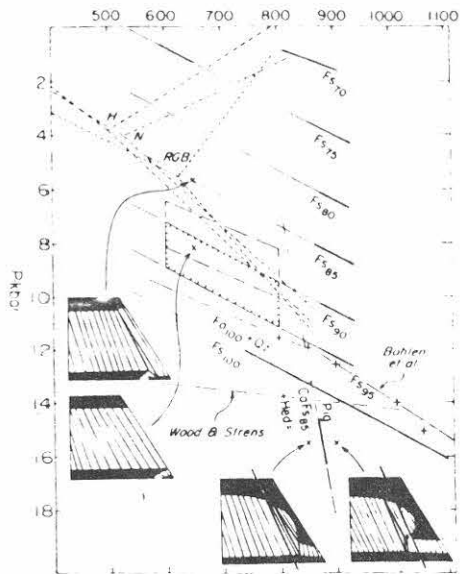


Fig. 9. P-T diagram with isopleths showing the compositions of orthopyroxene in equilibrium with olivine and quartz, based on experimental work of Lindsley (1965) and Smith (1971b) in the system MgSiO₃-FeSiO₃. Determination of Fs₁₀₀ isopleth by Bohlen *et al.* (1978) and a calculation of its position by Wood and Strens (1971) are also shown, the former with an inflection consistent with the high-low quartz inversion. Also shown are the low temperature stability of pigeonite on the join hedenbergite₁₀₀-ferrosilite₁₀₀ as determined by Smith (1972) and the stabilities of the Al₂SiO₅ polymorphs based on Richardson *et al.* (1969), Newton (1966), and Holdaway (1971). Outlined areas indicate brackets for minimum pressure estimates for metamorphism of Mt. Marcy orthoferrosilite according to data of Smith (hachures) or of Bohlen *et al.* (long dashed). See text for detailed interpretation.

In order to estimate pressures for the Adirondacks, the calculated ferrosilite contents of orthopyroxenes have been applied to the isopleths of Smith (1971b) on Figure 9. The Smith calibration was used rather than the Wood and Strens calibration because the Fs₁₀₀ curve of Smith is in reasonable agreement with the Fs₁₀₀ curve of Bohlen *et al.* (1978), especially considering Smith's suggestion that his pressures are probably slightly high due to the mechanical behavior of the solid-media apparatus.

The ferrosilite content of the most iron-rich orthopyroxene of this study, Po-17, is calculated to be Fs 95 and Fs 90 respectively, using the two extreme calculation methods. If equilibration occurred at 800°C, then *minimum* pressure was 9 kbar and could

have been as high as 11 kbar. Equilibration at 600°C implies *minimum* pressure of 7 kbar to 9 kbar (Table 9). These limiting minimum pressure values based on experimental data of Smith (1971b) are outlined on Figure 9, together with adjusted values estimated from the Fs₁₀₀ experiments of Bohlen *et al.* (1978). Similar reasoning based on optical data for the eulite-bearing (Fs 88) specimen FFG-2 from near Wana-kena, Cranberry Lake quadrangle, yields the minimum pressure estimates given in Table 9.

On the other hand, composition of olivine in the

Table 7. Estimates of pressure of metamorphism of selected Adirondack rocks*

Estimates of <u>minimum pressure</u> (kbar) based on orthopyroxene composition in olivine-free assemblage.			
	"Fs"	600°C	800°C
Po-17, Mt. Marcy quad., probe analyses			
Fe/(Fe + Mg)	.95	9	11
Fe ²⁺ /2.00	.90	7	9
FFG-2, Cranberry Lake quad., optical estimates			
Fe/(Fe + Mg)	.88	6.5	9
Fe ²⁺ /2.00	.84	4.5	7
Estimates of <u>maximum pressure</u> (kbar) based on olivine-augite assemblage where "hypothetical orthopyroxene" composition has been estimated.			
	"Fs"	600°C	800°C
FFG-6, Cranberry Lake quad., probe analyses			
Fe/(Fe + Mg)	.97	9.5	12
Fe ²⁺ /2.00	.91	7.5	10
AF-1A, Ausable Forks quad., optical estimates			
Fe/(Fe + Mg)	.97	9.5	12
Fe ²⁺ /2.00	.91	7.5	10

*To accord with the experiments of Bohlen *et al.* (1978) these values should be adjusted approximately -0.8 kbar at 600°C and -1.7 kbar at 800°C.

METASEDIMENTARY AND METAVOLCANIC ROCKS OF THE AUSABLE SYNCLINE,
NORTHEASTERN ADIRONDACKS

PHILIP R. WHITNEY
Geological Survey, New York State Museum

JAMES F. OLMSTED
Center for Earth and Environmental Sciences
State University of New York College at Plattsburgh

INTRODUCTION

On this trip we will examine two sections of granulite facies metamorphic rocks, exposed in stream cuts in the southern and central Ausable Forks 15' quadrangle (Figs. 1,2). The first section is dominated by calc-silicate rocks, marbles, and quartzites, typical of metasedimentary rocks in the northeastern Adirondacks. The second includes both metasedimentary rocks and the Lyon Mountain Gneiss, an unusual lithologic unit comprising a diverse suite of rocks which we believe are chiefly metavolcanic. Points for discussion on the trip include possible protoliths, the tectonic and sedimentary environment at the time of deposition, the metamorphic environment(s), and contact relationships with olivine metagabbros and anorthositic gneisses. Both stops on this trip involve moderately long hikes along scenic Adirondack brooks. While the hikes are not particularly arduous, we recommend sturdy boots and the exercise of caution; some of the stream banks are quite steep, and frequent crossings of streams on slippery rocks will be necessary.

Geological Setting

The Ausable Forks quadrangle (Figs. 1,2) in the northeastern Adirondack Mountains, near the border of the Marcy anorthosite massif, contains four major rock units (Fig. 2). Several large bodies of metanorthosite and gabbroic anorthosite gneiss, roughly domical in shape, are the lowermost exposed rocks. Overlying the domical metanorthosites is a complex of layered metamorphic rocks several kilometers thick. These layered rocks dip away from the metanorthosite domes; foliation and layering in them are parallel or subparallel to foliation in the outermost parts of the domes. Individual lithic units within these supracrustal rocks are locally well defined, but exhibit large variations in thickness along strike, and ordinarily cannot be traced for more than a few kilometers. The layered complex includes the metasedimentary rocks which will be described in detail below, as well as diopside-bearing quartzofeldspathic gneisses, granitic gneisses, jotunites (monzodiorite gneisses), and anorthosite and gabbroic anorthosite gneisses.

The third major unit in the quadrangle is a heterogeneous quartzofeldspathic gneiss that crops out over an area of nearly 1000 km² in the northeastern Adirondacks. This has been named the Lyon Mountain Granitic Gneiss by Postel (1952); we have shortened this to Lyon Mountain Gneiss (LMG) because it contains substantial amounts of rock that are not of granitic composition. This unit underlies much of

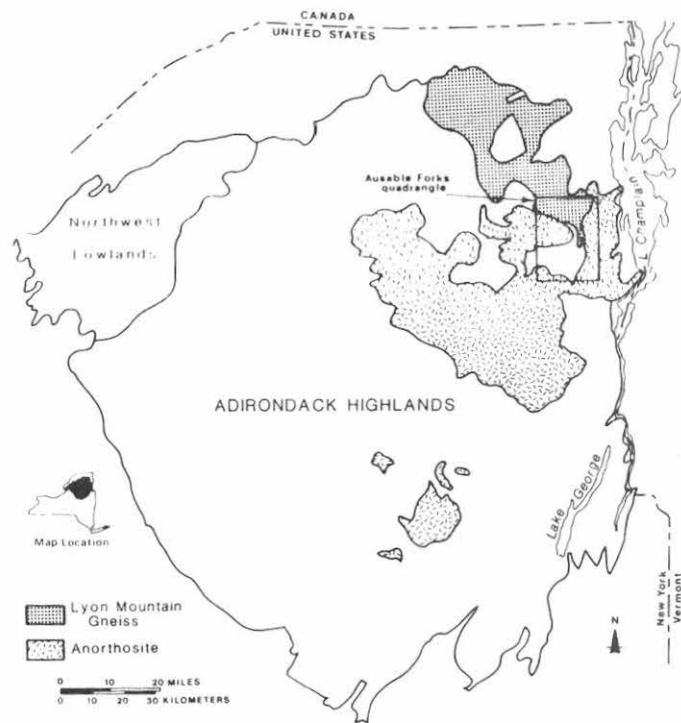


Figure 1 Index map showing location of the Ausable Forks Quadrangle.

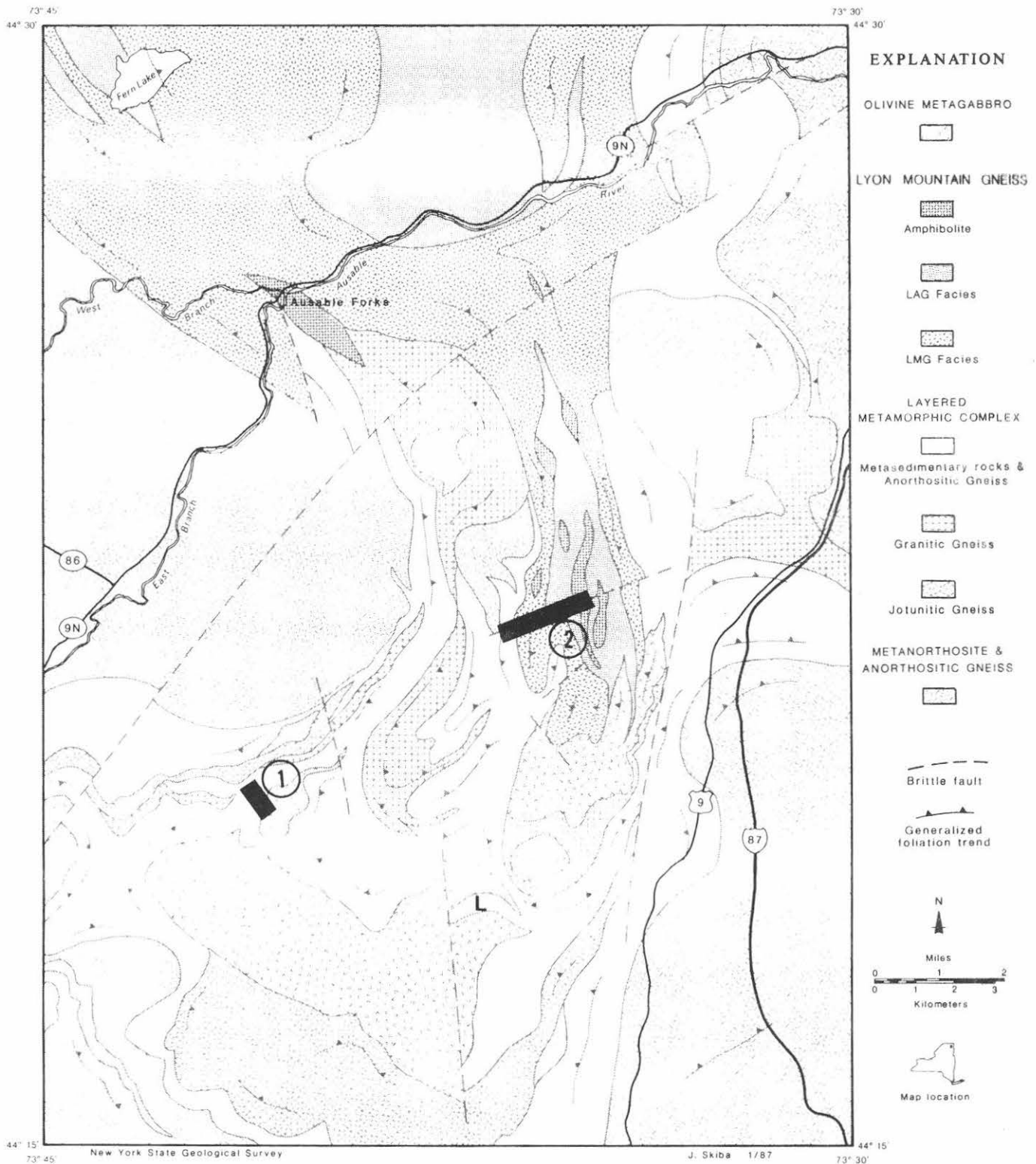


Figure 2 Map showing the general geology of the Ausable Forks Quadrangle, after Whitney and Olmsted, 1988. "1" and "2" show approximate locations of the two traverses. "L" is the Lewis wollastonite mine. "IMG" on the map is the GG facies of the Lyon Mountain Gneiss. After Whitney and Olmsted (1988).

TABLE 1. Partial list of mineral assemblages in metasedimentary rocks of the Ausable Forks quadrangle.

<u>Carbonate-free assemblages</u>	<u>Assemblages with carbonates</u>
Cpx	Cc
Cpx-kf	Cc-cpx
Cpx-kf-qz	Cc-cpx-gt
Cpx-pf	Cc-cpx-sc
Cpx-pf-qz	Cc-cpx-sc-kf
Cpx-pf-tn	Cc-cpx-sn-gt
Cpx-pf-gt	Cc-sn
Cpx-sc	Cc-sn-ph
Cpx-sc-tn	Cc-wo
Cpx-wo	Cc-wo-cpx
Cpx-wo-qz	Cc-wo-gt
Cpx-wo-gt	Cc-cpx-wo-gt
Cpx-ph	Cc-ch-sp
Qz-ph	Cc-cpx-wo-gt-id
Qz-ph-opx	Do
Qz-tr	
Qz-opx-cpx	-----
Qz-opx-cpx-tr	cpx clinopyroxene (Di-Hd ss)
Qz-opx-cpx-tr-ph	opx orthopyroxene
Pf-cpx-wo-gt-qz	qz quartz
Pf-cpx-opx-ph	kf microcline or mesoperthite
Gt	pf plagioclase
Gt-wo	gt garnet (Gr-And ss)
Gt-cpx	wo wollastonite
	tr tremolite
	bi biotite
	ph phlogopite
	cc calcite
	sc scapolite
	tn titanite (sphene)
	sn serpentine (after forsterite)
	sp spinel
	ch chondrodite
	id idocrase
	do dolomite

Graphite and pyrite are commonly present in minor amounts. Low-T alteration products include prehnite, chlorite, and sericite.

the northern third of the Ausable Forks Quadrangle, and forms the core of a tight, upright, north-plunging synform (the Ausable Forks Syncline of Balk, 1931) in the central third (Fig. 2). North of the Ausable River, the LMG is host to numerous small, and a few rather large, bodies of low-Ti magnetite iron ore that were worked throughout much of the nineteenth century and the first half of the twentieth (Gallagher, 1937; Postel, 1952). The first three units are intruded by a fourth, coronitic olivine metagabbro, which occurs as several large bodies in the southern half of the quadrangle, and as smaller pods and lenses in the layered rocks throughout the area. The metagabbro ordinarily retains primary igneous textures in the interiors of all but the smallest bodies, and is metamorphosed to garnet amphibolite or mafic granulite near the contacts. All four units display mineral assemblages consistent with granulite facies metamorphism, except for local retrograde assemblages in the vicinity of late, brittle faults.

Locations of the field trip stops are shown on a generalized geologic map (Fig. 2). The first stop is a traverse along a stream that drains a cirque on the north flank of Jay Mountain, crossing a section of metasedimentary rocks of the layered complex. The second, along Doyle Brook in the central part of the quadrangle, begins in the core of the Ausable Forks Syncline where several variants of the Lyon Mountain Gneiss are exposed, and continues into some of the underlying metasedimentary rocks.

Metasedimentary Rocks

The metasedimentary rocks in the layered complex consist principally of diopside-rich calcsilicate granulites, together with impure quartzites and calcite marbles. Phlogopite and biotite schists are less common, and there is one occurrence of dolomite marble. At the top of the layered complex, directly underlying the Lyon Mountain Gneiss, is a thin, graphitic, sillimanite-garnet-quartz-microcline metapelite. Substantial amounts of quartzofeldspathic gneiss of granitic composition, and lesser amounts of amphibolite and biotite-rich mafic granulite are interlayered with the metasedimentary rocks; these rocks probably are the metamorphic equivalents of felsic and mafic volcanics, respectively.

Most individual layers within the metasedimentary sequence are relatively thin (less than a few tens of meters). Accurate measurement of thicknesses is prohibited by scarcity of outcrop. Layers are commonly discontinuous along strike, possibly due in part to tectonic disruption. Because of these factors, and the common presence of interlayered gabbroic and anorthositic rocks, it has not been possible to recognize a coherent stratigraphy. It is conceivable that there is repetition due to folding or faulting.

Table 1 lists observed mineral assemblages in the calcsilicate granulites, quartzites, and marbles. The dominant mineral in most of the calcsilicate rocks is diopsidic clinopyroxene, ranging from nearly colorless to dark green. The color, which depends largely on ferrous iron content, may vary widely within a few cm. With the clinopyroxene are variable amounts of alkali feldspar, quartz, plagioclase, calcite, scapolite, phlogopite, wollastonite, and titanite. Rocks with over 90% diopside ("diopsidites") are common, as are diopside-microcline rocks. Wollastonite-rich rocks occur locally in economic quantities. At the Lewis wollastonite mine (Fig. 2), the ore is a wollastonite-diopside-

TABLE 2. MODES OF LYON MOUNTAIN GNEISS

	A			B			C		
	LMG FACIES (12)			LAG FACIES (6)			MAG FACIES (11) #		
	Mean	Min	Max	Mean	Min	Max	Mean	Min	Max
PLAGIOCLASE (includes Antiperthite)	11.7	0	46	64.1	51	74	65.6	33	83
K FELDSPAR	53.5	11	78	0.7	0	2.6	0.6	*	*
QUARTZ	27.5	10	38	27.2	18	43	8.9	0	45
CLINOPYROXENE	1.5	0	6.1	2.7	0	13	16.7	0.3	34
AMBHIBOLE	1.6	0	8.3	1.0	0	3.2	3.8	0	17
OXIDES	1.9	0.3	4.7	2.9	0.7	4.4	1.2	0	4.6
TITANITE	0.2	0	1.3	0.5	0	1.3	1.7	0	2.7
OTHER+	2.0	0	6.7	0.8	0	2.9	1.5	0	13

All modes based on at least 1000 points counted.

* Present in one sample only.

Excludes one sample with 30% scapolite.

+ Includes biotite, zircon, apatite, garnet (in two samples), fayalite (in one sample), fluorite, chlorite and low-temperature alteration products.

garnet rock, with numerous nearly monomineralic zones. The high-variance mineral assemblages, as well as the common absence of either quartz or calcite with the wollastonite, suggest that this ore, like that at Willsboro in the next quadrangle east, is partly metasomatic in origin (Buddington, 1939; DeRudder, 1962).

With the addition of quartz, the calcsilicate rocks grade into impure quartzites that are commonly tremolite-bearing. The magnesium-rich assemblage tremolite-enstatite-diopside-(phlogopite)-quartz is locally present. Calcite marbles, usually with abundant calcsilicate minerals, tend to occur in lenses and irregular layers. In the central part of the quadrangle west of Black Mountain, prominent marble "dikes" crosscut a stratiform metanorthosite body, illustrating the ductile behavior of the marble relative to that of anorthosite during deformation. Graphite and pyrite are common accessory minerals in all assemblages, with the exception of wollastonite- and garnet-rich rocks, which tend to be relatively oxidized.

Several features of these metasedimentary rocks suggest the former presence of evaporites. The preponderance of diopside-rich calcsilicate rocks, the metamorphic equivalent of silicious dolostones, is significant in that dolomite is commonly a product of hypersaline depositional environments (Friedman, 1980). The diopside-rich rocks locally contain major amounts of microcline, possibly the metamorphic equivalent of low temperature, authigenic or diagenetic microcline. The latter, in part pseudomorphous after evaporite minerals, has been reported from late Proterozoic, evaporite-bearing dolomitic rocks in South Australia (Rowlands and others, 1980) and in the Damara Orogen of Namibia (Behr and others, 1983). Magnesium-rich metasedimentary rocks, in particular phlogopite schists and enstatite-diopside-tremolite-phlogopite-quartz rocks, are likely granulite facies equivalents of evaporite-related talc-tremolite-quartz schists, such as those found near Balmat in the northwest Adirondacks (Brown and Engel, 1956), in stratigraphic association with diopside-rich rocks and bedded anhydrite. Magnesite-dolomite-chlorite-quartz rocks are a possible sedimentary protolith. The common presence of scapolite in both marbles and calcsilicate rocks is another possible indicator of former evaporites (Serdyuchenko, 1975). Granulite facies metasedimentary rocks similar to those of the Ausable Forks quadrangle occur in the Caraiba mining district of Brazil (Leake and others, 1979), and in the Oaxacan Complex of southern Mexico (Ortega-Gutierrez, 1984); in both localities anhydrite is present in the subsurface.

Lyon Mountain Gneiss

The Lyon Mountain Gneiss (LMG) comprises three distinct facies. Granitic (sensu lato) gneisses (GG facies) consist chiefly of quartz and mesoperthite with minor amounts of biotite, hornblende, clinopyroxene, or garnet and up to 5 percent magnetite. Locally present is a potassium-rich variety with microcline as the principal feldspar. Modal compositions are widely variable, both with respect to proportions of quartz and feldspar present, but also with respect to the amount and identity of the mafic minerals (Table 2). These heterogeneous rocks are common throughout the outcrop area of the LMG. A second facies, leucocratic albite gneiss (LAG), is composed of quartz and albitic plagioclase (Ab₉₅-Ab₉₈), minor clinopyroxene with up to 40 percent acmite component, and as much as 4 percent magnetite. Both the

TABLE 3. CHEMICAL ANALYSES OF LYON MOUNTAIN GNEISS

Element	<u>LAG FACIES (6)</u>			<u>MAG FACIES (9)</u>				
	Mean		Maximum	Minimum	Mean	Maximum	Minimum	
SiO ₂	71.63	+ 2.63	75.07	68.45	64.39	+ 5.78	78.24	59.24
TiO ₂	.48	+ .08	.62	.38	.94	+ .16	1.16	.63
Al ₂ O ₃	12.71	+ .81	13.49	11.47	13.17	+ 2.22	16.46	8.01
Fe ₂ O ₃	4.13	+ .85	5.48	2.91	2.85	+ 1.18	4.72	1.36
FeO	2.11	+ .46	2.86	1.65	2.15	+ .58	3.09	1.25
MnO	.02	+ .01	.03	.01	.04	+ .02	.08	.02
MgO	.31	+ .11	.45	.17	3.05	+ .69	3.79	1.71
CaO	1.28	+ .71	2.57	.43	5.21	+ 1.92	7.66	2.69
Na ₂ O	6.81	+ .91	7.76	5.54	6.98	+ 1.92	8.69	3.24
K ₂ O	.48	+ .29	.99	.11	.68	+ .95	2.99	.15
P ₂ O ₅	.07	+ .04	.13	.02	.16	+ .07	.22	.01
Rb	7	+ 4	12	2	19	+ 31	80	2
Sr	31	+ 9	42	18	61	+ 43	153	25
Ba	55	+ 28	101	27	121	+ 174	501	10
Zr	1015	+ 228	1320	653	290	+ 54	385	195
Y	137	+ 50	210	75	55	+ 19	85	34
Nb	40	+ 11	48	18	18	+ 5	23	10
Ce	223	+ 106	342	75	68	+ 19	103	47
Ga	29	+ 4	33	24	18	+ 5	25	10

TABLE 3. (CONTINUED)

Element	<u>GG FACIES (9)</u>			<u>MICROCLINE GG (3)</u>				
	Mean		Maximum	Minimum	Mean	Maximum	Minimum	
SiO ₂	70.04	+ 3.98	74.41	62.75	69.49	+ 1.04	70.66	68.67
TiO ₂	.56	+ .26	1.04	.33	.52	+ .09	.59	.42
Al ₂ O ₃	12.96	+ 1.16	15.44	11.88	12.89	+ .81	13.66	12.04
Fe ₂ O ₃	2.61	+ 1.49	5.06	.17	3.69	+ .76	4.51	3.03
FeO	2.92	+ 1.02	4.45	1.24	1.98	+ .25	2.22	1.72
MnO	.08	+ .04	.13	.04	.01	+ .01	.02	.01
MgO	.22	+ .24	.77	.01	.24	+ .11	.37	.16
CaO	1.41	+ .35	2.02	.95	.45	+ .26	.71	.19
Na ₂ O	4.27	+ .87	5.36	2.46	1.34	+ .56	1.98	.97
K ₂ O	4.44	+ 1.25	5.73	2.23	8.79	+ .98	9.71	7.75
P ₂ O ₅	.11	+ .09	.27	.03	.11	+ .06	.17	.06
Rb	114	+ 50	215	61	237	+ 31	272	212
Sr	64	+ 36	138	28	42	+ 22	65	21
Ba	441	+ 285	866	88	1188	+ 550	1822	837
Zr	844	+ 351	1229	388	532	+ 164	641	343
Y	120	+ 66	228	58	59	+ 6	64	53
Nb	35	+ 16	59	17	19	+ 1	20	18
Ce	183	+ 84	375	108	113	+ 10	120	101
Ga	29	+ 6	38	22	18	+ 1	19	17

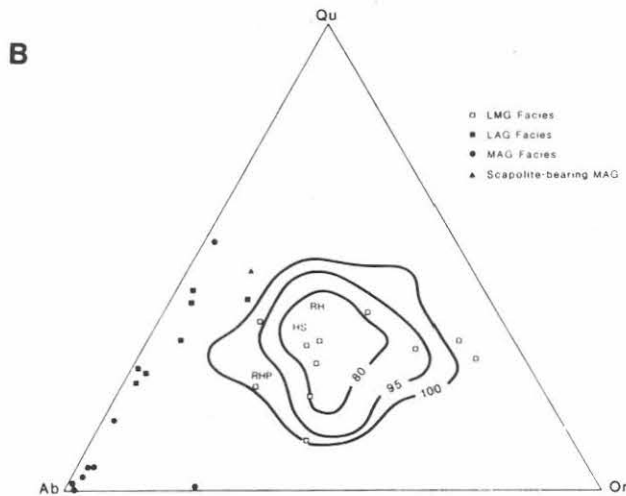
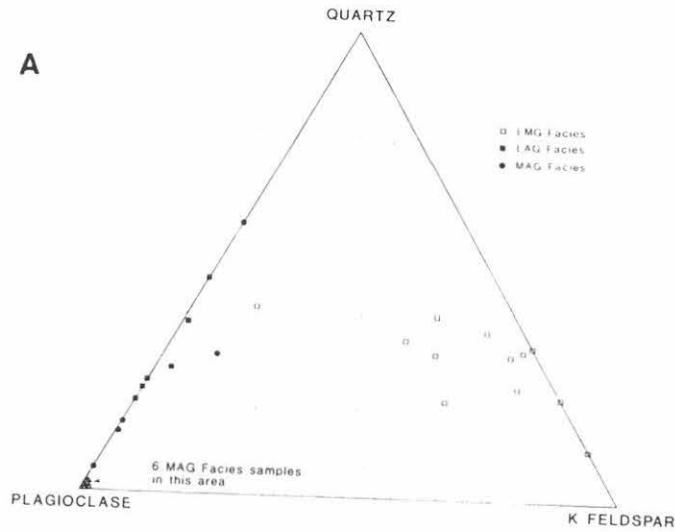


Figure 3 A. Modal quartz, plagioclase, and K feldspar (microcline or perthite) in rocks of the Lyon Mountain Gneiss.

B. Normative quartz, albite and orthoclase in the Lyon Mountain Gneiss. Contours show percentages of 137 analyses of Adirondack granitic rocks. After Whitney and Olmsted (1988).

GG and LAG facies commonly appear as fine- to medium- grained granoblastic rocks, massive to weakly foliated but with locally strong compositional layering. Colors range from white to pink or buff; mafic varieties are locally gray. Table 2 shows modal data for these rocks, and figures 3A and 3B illustrate the variability of both modal and normative quartz and feldspar.

These quartzofeldspathic gneisses are interlayered with lesser amounts of a third facies, mafic albite gneiss (MAG). The latter is a distinctive albite-pyroxene rock, with varying amounts of quartz and a blue-gray sodic amphibole, plus minor titanite. The pyroxenes are dark green and acmite-rich (up to 35%). Oxide minerals are uncommon; where they do occur they consist of laminar intergrowths of hematite and ilmenite or rutile, in contrast to the ubiquitous magnetite of the GG and LAG facies. These MAG rocks are commonly pink to gray, fine-grained, with a sugary granoblastic texture. In some outcrops, they display a prominent pinstripe layering, with alternating mm-scale pyroxene-rich and albite-rich layers. More commonly the MAG facies is massive. Both banded and massive varieties locally contain pink megacrysts of nearly pure albite, up to 5 cm across. Quartz content is commonly under 5 percent, but one sample contains 45 percent, suggesting admixture of a quartz-rich sedimentary component. Scapolite is locally present.

Table 3 shows the average chemical composition of several facies of the Lyon Mountain Gneiss. Notice in particular the high Na₂O, low K₂O nature of the LAG and MAG facies. In contrast, the microcline-bearing variant of the GG facies (not exposed on Doyle Brook) is K₂O-rich. Whitney and Olmsted (1988) attribute the heterogeneity of these rocks and the extreme alkali metal ratios to diagenetic alteration of felsic volcanoclastics in a hypersaline environment such as a playa lake. Possible unmetamorphosed analogs of these rocks are found in several areas in the southwestern United States, where rhyolitic tuffs of Pliocene to recent age have been altered in a playa setting to produce rocks with diagenetic analcite (Na-rich), zeolites, or K feldspar (Surdam, 1981). A weakly metamorphosed analog of the MAG facies is present in the Damara orogen of Namibia, in the form of albite-dolomite-quartz rocks, locally with albite porphyroblasts. These late Proterozoic metasedimentary rocks also originated in a playa environment (Behr and others, 1983).

In the section we will see, in the southernmost, tightly folded part of the Ausable Forks Syncline, all three facies of the LMG are interlayered with amphibolite, at least some of which has been derived from intrusive olivine metagabbro.

<u>ROAD LOG</u>		
<u>Mileage</u>	<u>Cumulative</u>	<u>Remarks</u>
0	0	This trip will assemble in the parking lot at the west end of Hudson Hall. As you leave, turn R (west) into Broad Street and continue west about two miles to the entrance to I-87 south.
1.8	1.8	Turn L into entrance to I-87. Keep right after you make this turn so as to elect I-87 south.

- 14.6 16.4 Take exit 34 to NY 9N.
- 0.2 16.6 Turn L onto NY 9N south toward Whiteface Mountain.
- 4.5 21.1 Clintonville. This hamlet is a former iron mining town said to have had a population of over 10,000.
- 4.7 25.8 Outcrops in roadcut on right are an unusual ferrohedenbergite-fayalite granite, first described by Buddington (1939). This may be a reduced facies of the Lyon Mountain Gneiss, or a subsequent intrusive rock.
- 0.4 26.2 Village of Ausable Forks.
- 1.0 27.2 Turn L at red blinker onto Main St.
- 0.2 27.4 Route 9N turns R at bridge. We will leave 9N briefly to examine a spectacular exposure of metasedimentary rocks in a roadside outcrop.
- 0.1 27.5 Turn R at other end of bridge onto Sheldrake Road.
- 1.3 28.8 Stop at several small outcrops in a bank on the L (east) side of the road, directly downslope from a house. Cameras are a must at this stop, but no hammers, please. This informal stop illustrates the differing mechanical properties of various rock types, including marble, diopsidite, amphibolite, and granitic gneiss. This exposure has been called "The Snake", for obvious reasons.
- 1.3 30.1 Turn R on Stickney Bridge Road.
- 1.1 31.2 Cross bridge and turn L on 9N.
- 3.1 34.3 Village of Jay.
- 0.8 35.1 Turn L at intersection with route 86, toward the "Old Covered Bridge".
- 0.2 35.3 Covered bridge. Drive across bridge and bear R up hill. Exposures on R in the bed of the Ausable River are metanorthosite of the Jay Dome, cut by several unmetamorphosed mafic dikes.
- 0.7 36.0 Y intersection; continue on L fork.
- 0.7 36.7 Bear R at yellowish house.

0.1 36.8 Turn L on Nugent Road (unpaved).

1.75 38.55 STOP 1. Gelina Basin.

The road forks at this point, with the R fork leading steeply uphill. There may be a gate across the L fork. This is private property, owned by Ward Lumber Co. in Jay. If you come here on your own, get permission. We will park here and proceed on foot up the R fork. If you have an altimeter, set it for 1280 feet. After about a half mile, the road ends at a hunting cabin in a clearing. Walk to the R of the cabin past the john, where you will find a trail that follows the top of a steep bank. Follow the trail S to about 1800 feet altitude, and work your way down the bank to the stream at the bottom. This unnamed, north-flowing stream drains a cirque (Gelina Basin on the 15' quadrangle map) on the north flank of Jay Mountain. We will attempt to hit the stream at about 1700 feet and traverse upstream over a well-exposed section of NNE-striking metasedimentary rocks.

1730-1750' (altitudes approximate) Calcsilicate rocks with diopside and wollastonite, locally rusty weathered, with quartzite layers.

1750-1760' Strongly foliated amphibolite, overlain by coarse, rusty calcite-diopside-phlogopite-graphite marble.

1780-1820' First of three waterfalls. At the base of this falls, layered diopside-wollastonite calcsilicates (WoDi) and quartzite are exposed. The caprock is tremolite-bearing quartzite; just above this is Mg-rich enstatite-diopside-tremolite-quartz rock.

1830' 5' cascade over diopsidite and diopsidic marble with thin quartzite layers.

1840-1870' Interlayered metasedimentary rocks (diopsidites and WoDi) and thin amphibolites.

1880-1900' Amphibolite, overlain by metasedimentary rocks, including a calcite-diopside-wollastonite-grossular-idocrase marble at the base of a second waterfall. The cap of this falls is a dark, feldspathic diopsidite with locally abundant sphene. The amphibolite here may be a sill or dike of olivine metagabbro satellitic to the larger body exposed just upstream.

1910-1960' Third falls. The lower part of the falls is a cascade over banded WoDi rock; the upper part is olivine metagabbro locally mixed with granitic gneiss. The gabbro contact here appears to have a steep easterly dip, truncating the more gently dipping metasedimentary layers. Thin sections of the WoDi rock here show thin rims of grossularitic garnet around wollastonite, possibly a result of the reaction wollastonite + plagioclase = grossular + quartz.

0.0 38.55 Turn around and retrace route on Nugent Road.

1.75 40.3 Turn R on The Glen Road.

- 0.1 40.4 Fork in road, bear L toward Village of Jay.
- 1.3 41.7 Turn R just before covered bridge.
- 0.5 42.2 Turn L on North Jay Road.
- 4.2 46.4 Turn R on Green Street.
- 5.4 51.8 Turn R on Trout Pond Road.
- 5.0 56.8 Stop 2. Clear Pond Park and Doyle Brook Gorge.

Park on R side of road. To reach the traverse up Doyle Brook we will walk along a private logging road (permission needed) that runs SW from Trout Pond Road. [Note: the 1953 USGS topographic map (1:62,500) is accurate in this area; the 1980 1:25,000 version is not]. Proceeding SW along the logging road, we will pass Copper Pond, which occupies a small basin in albite gneisses of the IAG and MAG facies. Just S of Nesbitt Pond, a short trail leads S to Doyle Brook. From here, we will traverse upstream. The stream gradient is small, so altitudes are not listed. The first rocks encountered in the streambed are amphibolites. A short distance upstream, Doyle Brook emerges from a slot formed at an ENE-trending fault here occupied by an unmetamorphosed mafic dike of indeterminate age that shows evidence of multiple episodes of intrusion. The walls of the gorge are MAG facies albite gneisses, with massive, banded, and megacrystic variants all present. Notice the complex folding in the banded gneisses.

After leaving this first slot, continue upstream along a flat stretch with occasional outcrops of the GG and LAG facies, some quite magnetite-rich. Then enter a second gorge, walled by heterogeneous, intensely fractured LMG, mostly of the GG facies. Shortly beyond the SW end of this gorge, the stream crosses a concealed contact between the LMG and the underlying metasedimentary rocks. The first outcrop of the latter is a rusty-weathered, graphitic, sillimanite-garnet metapelite. Continuing upstream, the course of the stream swings around to a nearly NS direction, with outcrops of garnetiferous granitic gneiss. At the S (upstream) end of this segment are several marble outcrops, including a coarse white calcite marble with serpentine and graphite, and a nearly pure, gray, tan-weathering dolomite marble. A large spring marks the underground outlet of Lawson Pond, located just to the south and about 80' higher in elevation. The surface outlet shown on the map does not exist. The rocks here strike NNE and dip east; the marble overlies the granitic gneiss seen in the previous outcrop. Another bend in the stream leads first SW and then W (downsection) over outcrops of amphibolite and rusty calcsilicate rocks, back into garnetiferous granitic gneiss, followed by gabbroic anorthosite gneiss. The latter is part of a large, irregular lens of metanorthosite within the layered metamorphic rocks. At this point we will leave the stream and walk back to the access road, following the N rim of Doyle Brook gorge.

To return to Plattsburgh, follow the Trout Pond Road south about three and one half miles to Route 9. A left turn here will take you north toward Plattsburgh. You may get on I87 (north) at exit 33, located at the intersection of routes 9 and 22 about one mile north of Poko-Moonshine Park.

REFERENCES

- Balk, R., 1931, Structural geology of the Adirondack anorthosite: *Min. Pet. Mitt.*, v. 41, p. 308-434.
- Behr, H.-J., Arendt, H., Martin, H., Porada, H., Rohrs, J., and Weber, K., 1983, Sedimentology and mineralogy of upper Proterozoic playalake deposits in the Damara orogen, In Martin, H., and Eder, F.W., eds., *Intracontinental fold belts*. New York, Springer Verlag, p. 577-610.
- Brown, J.S., and Engel, A.E.J., 1956, Revision of Grenville stratigraphy and structure in the Balmat-Edwards district, northwest Adirondacks, New York: *Geol. Soc. Amer. Bull.*, v. 67, p. 1599-1622.
- Buddington, A.F., 1939, Adirondack igneous rocks and their metamorphism: *Geol. Soc. Amer. Memoir* 7, 354 p.
- DeRudder, R.D., 1962, Petrology and genesis of the Willsboro wollastonite deposit, Willsboro, New York. PhD thesis, Indiana University, 156 p.
- Friedman, G.M., 1980, Dolomite is an evaporite mineral: evidence from the rock record and sea-marginal ponds of the Red Sea. In Zenger, D.H., Dunham, J.B., and Etherington, R.L., eds., *Concepts and models of dolomitization: SEPM Special Publication* 28, p. 69-80.
- Gallagher, D., 1937, Origin of the magnetite deposits at Lyon Mountain, New York. *New York State Museum Bull.* 311, 85 p.
- Leake, B.E., Farrow, C.M., and Townend, R., 1979, A pre-2000 myr-old granulite facies metamorphic evaporite from Caraiba, Brazil?: *Nature* v. 277, p. 49-51.
- Ortega-Gutierrez, F., 1984, Evidence of Precambrian evaporites in the Oaxacan granulite complex of southern Mexico: *Precambrian Research*, v. 23, p. 377-393.
- Postel, A.W., 1952, Geology of the Clinton County magnetite district, New York. *U.S. Geol. Surv. Prof. Paper* 237, 88 p.
- Rowlands, N.J., Blight, P.G., Jarvis, D.M., and von der Borch, C.C., 1980, Sabkha and playa environments in late Proterozoic grabens, Willouran, South Australia: *J. Geol. Soc. Australia*, v. 27, p. 55-68.
- Serdyuchenko, D.P., 1975, Some Precambrian scapolite-bearing rocks evolved from evaporites: *Lithos*, v. 8, p. 1-7.
- Surdam, R.C., 1981, Zeolites in closed hydrologic systems: In Mumpton, F.A., ed., *Mineralogy and geology of natural zeolites*. *Mineral. Soc. Amer. Reviews in Mineralogy*, v. 4, p. 65-91.
- Whitney, P.R. and Olmsted, J.F., 1988, Geochemistry and origin of albite gneisses, northeastern Adirondack Mountains, New York: *Contrib. Mineral. Petrol.*, in press.

IRON INDUSTRY OF THE EASTERN ADIRONDACK REGION

JAMES C. DAWSON

Center for Earth and Environmental Science
State University of New York
Plattsburgh, NY 12901

JOHN R. MORAVEK

Center for Earth and Environmental Science
State University of New York
Plattsburgh, NY 12901

MORRIS F. GLENN

Mapping and Charting Department
Defense Mapping Agency
U.S. Department of Defense
Washington, DC 20310

GORDON C. POLLARD

Department of Anthropology
State University of New York
Plattsburgh, NY 12901

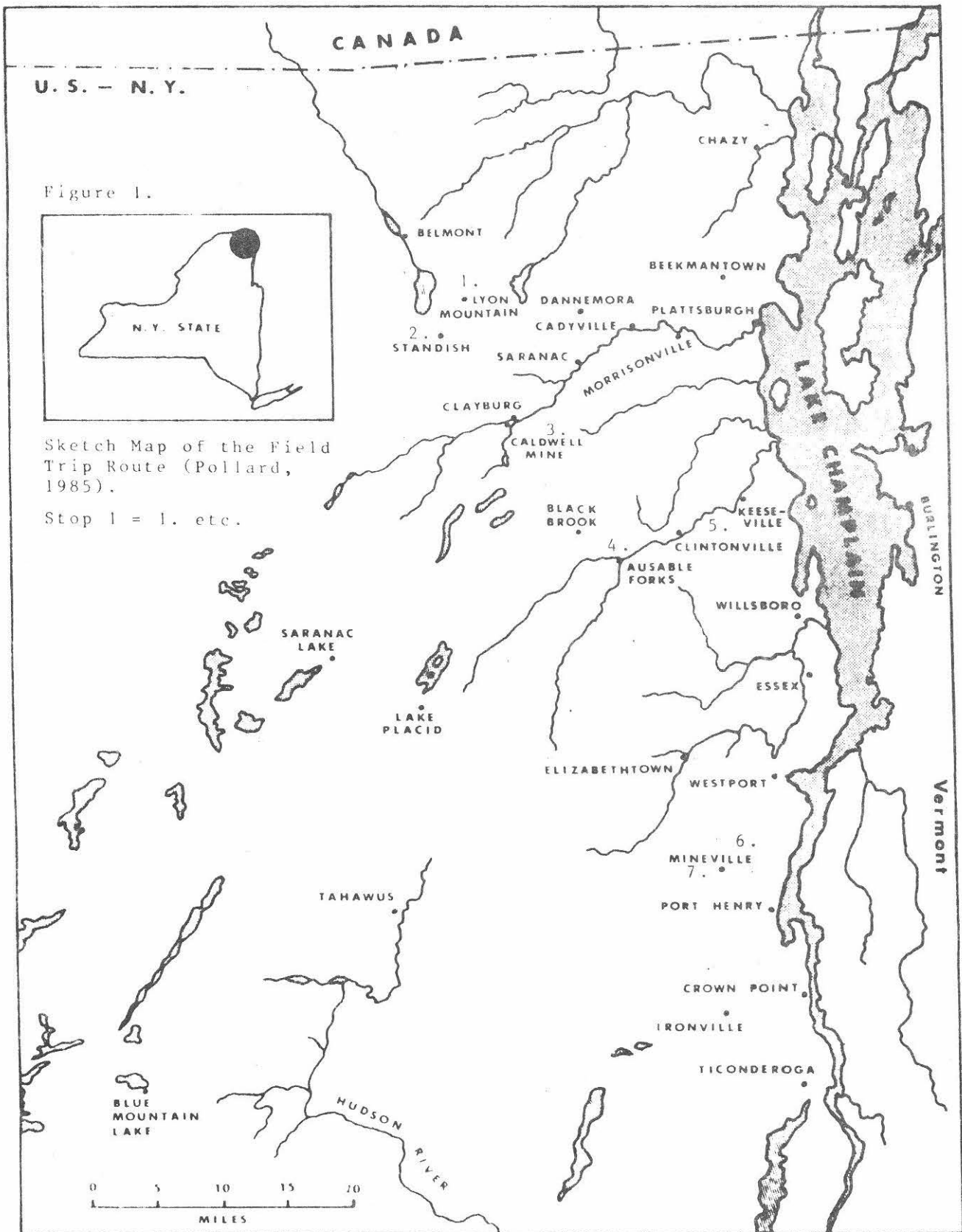
Introduction

Developments in mining and iron smelting in the Adirondack-Champlain region (Figure 1) commenced with effective American settlement after the 1812-1814 war, and in some instances preceded it. Iron ore had been observed on the lakeshore near Crown Point as early as 1749 by Swedish naturalist Peter Kalm (1770).

The crude ironworks on the manor of British military officer, Philip Skene, at Skenesborough (Whitehall, NY) at the head of Lake Champlain smelted ore from the vicinity of what later became the Cheever Mine a few miles north of Port Henry, NY (Morton, 1959). At the mouth of the Saranac River on Lake Champlain, Zephaniah Platt and associates operated a Catalan forge or bloomery in 1798 using ore from Vermont. In 1801, an ironworks was erected at Willsboro Falls on the Boquet River.

Catalan Forge

Adirondack and Champlain iron makers employed two methods for smelting iron, each with centuries-old European



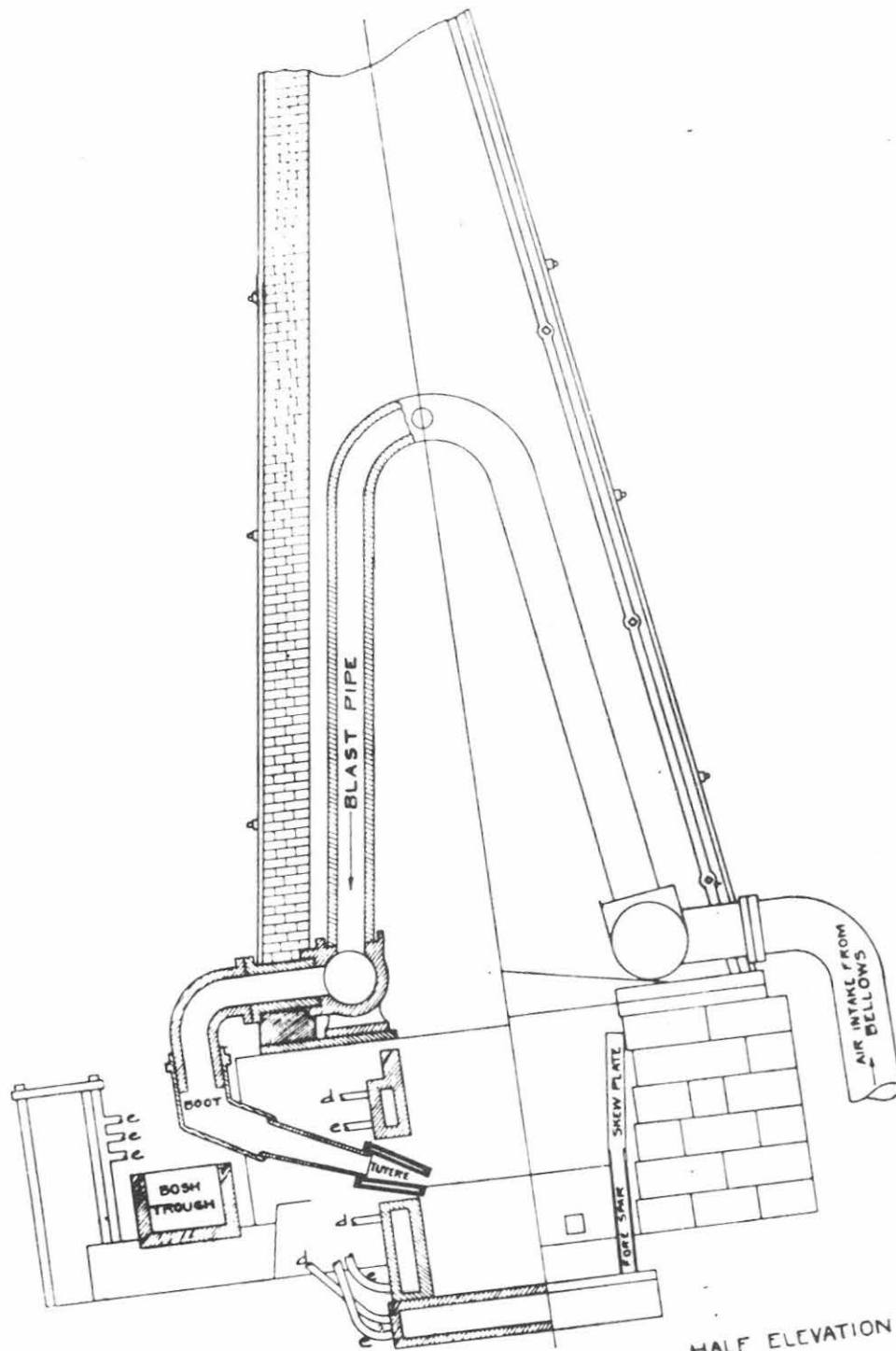
antecedents. The Catalan forge or bloomery, the older and simpler apparatus, resembled a blacksmith's hearth (Hunt, 1870). The raw materials of finely crushed and calcinated or roasted ore, crushed limestone or marble, and charcoal were shoveled into a heavy cast iron firebox that was surrounded by fire brick and provided with a chimney (Glenn, 1987). An activated bellows forced an updraft that intensified the heat while a bloomer stirred the charge with a long-handled rod. The ore was heated to a semi-molten state as the smelting process separated impurities from metal. The metal was gradually worked into a pasty, ball-like mass that was repeatedly hammered on an anvil to expel impurities. Heavy trip hammers, driven mechanically by water-driven wheels, were used for this. Following successive reheatings and hammerings, the loupe or iron mass was shaped into a bloom or billet, a nearly pure, malleable form of wrought iron (Chahoon, 1880). These blooms were in great demand among regional blacksmiths and nail factories (Chahoon, 1875 and Egleston, 1880).

Blast Furnace

The alternate technique employed a blast furnace (Figure 2), a hollow inner chamber or tunnel open on both ends, lined with fire-brick, and supported by a stack of heavy cut stone. The stack, square at the base and top, tapered upward in the shape of a truncated pyramid. All raw materials were fed through the tunnel head or top from a "charging bridge". As the alternating layers of iron ore, limestone, and charcoal (later coke) descended through the furnace, they encountered the forced ascent of heat and gases liberated by the burning of charcoal/coke lower down in the tunnel (Richards, et. al., 1895). The rising gases (including carbon monoxide) readily united with oxygen in the ore, thus leaving a spongy mass of iron. The hot gases formed by that process were expelled from the top of the stack into the atmosphere in the early years, but were later captured and conducted through downcomer pipes to be used as fuel in heating ovens.

The metallic iron and the limestone melted along with the various impurities it absorbed. This molten matter then trickled into a catchment basin or hearth at the base of the furnace. The more dense iron settled on the bottom while the liquid lime-rich impurities floated on top as scum. A clay plug in the hearth wall was removed periodically, allowing molten iron to pour forth to cool in molding troughs. The scum was drained through a separate taphole and allowed to solidify as slag. The solid metal, pig iron, a carbon-rich and relatively brittle product, required subsequent reworking in a puddling furnace or refining forge to remove excess carbon and render the metal strong and malleable.

Although the blast furnace technique entailed a two-step process, it was more efficient for smelting large quantities



HALF SECTION
 THREE-PIPE BLOOMERY FORGE AT BELMONT, N. Y.
 Figure 2. TYPICAL OF FORGES USED IN EARLY PART OF NINETEENTH CENTURY
 (Linney, 1934)

of ore. Both processes were employed in the Adirondack-Champlain region. The bloomery was widely favored, and during the second half of the 19th century this region became the greatest and last stronghold of the bloomery smelting process in the United States. The reasons for this included: (1) initial investment and operating costs were low; (2) it produced the quality of iron sought by regional blacksmiths and nail-makers; (3) many smelting operations were of necessity small in scale because it was impractical to haul the large quantities of charcoal required for blast furnaces long distances; (4) it was subject to practical operation on an intermittent and seasonal basis and thus could be successfully synchronized with seasonal farming, lumbering and charcoal making; (5) given the abundance of local ore, efficiency with respect to raw-material consumption was not an overriding priority; and (6) advances such as the introduction of the hot-air blast improved the efficiency of the process and extended its useful life in the Adirondack-Champlain region.

Raw Materials

The iron industry spread westward from the shores of Lake Champlain as settlement advanced up the river valleys. In many instances, iron accounted for initial settlement, spurred population growth, and promoted overall economic development in these remote areas. Although this region offered relatively little in the way of agricultural assets, it was well endowed with the resources needed for an iron enterprise. First, numerous deposits of magnetite were discovered in the granitic gneisses of the Adirondack foothills. These deposits were variously described as occurring in bodies, shoots, masses, pods, beds, veins, sheets, and lenses. They were readily detected by the behavior of a simple surveyor's compass and later by magnetic dipmeters. Secondly, the high-gradient rivers that emanate from the hundreds of lakes and ponds in the mountains and flow to Lake Champlain and the Hudson River offered excellent water-power to drive bellows, air compressors, trip-hammers, and other machinery. The great mantle of virgin forest formed the third ingredient as it offered an ample supply of wood for making charcoal. Charcoal was the primary smelting fuel used throughout most of the 19th century in this region. Finally, an availability of Grenville marble in the Adirondack region and Ordovician limestone in the Champlain Lowland provided the necessary fluxing material for the smelting process (Kemp and Ruedeman, 1919).

Primitive transportation methods made it difficult to import iron products from outside of the region. Thus, ironmongers seized the opportunity to supply local markets. The Adirondack-Champlain region eventually grew to attain a national ranking in the iron business, however, it was not unusual in its possession of all prerequisites for iron making; many regions throughout the eastern United States

maintained iron-working enterprises of varying magnitudes in the late 18th and early 19th centuries.

Early Years

Thus, with a superb resource base at hand and settlers arriving in the early 1800s, the growth of the iron industry was inevitable. The early ironworks were concentrated along the Saranac, Ausable, Bouquet, and Schroon Rivers. Later the Chazy Valley in northern Clinton County and the Towns of Moriah and Crown Point in Essex County emerged as important centers of iron making.

By 1820, significant mining operations were being carried on at Arnold Hill, which opened in 1806, in south-central Clinton County (Hardy, 1985) and in Essex County's Town of Moriah at Cheever north of Port Henry (Warner and Hall, 1931) and in the Town of Newcomb (at Tahawus near the headwaters of the Hudson River (Masters, 1923). Small surface pits had yielded modest quantities of ore in a number of widely scattered localities elsewhere.

Major regional development was inaugurated in the 1820s by the imposition of a tariff on imported iron and by the opening of the Champlain Barge Canal at Whitehall in 1823. The latter provided an all-water transport connection between the Champlain Valley and the Hudson River. Direct access to the burgeoning industrial city of Troy, New York provided a major market for Adirondack-Champlain ores and smelted iron. Additional markets were also secured further south in the Hudson Valley, throughout southern New England and in Pennsylvania and Ohio.

Middle Years

By the mid-19th century, the iron industry was a multi-million dollar enterprise. It attained a position of dominance in parts of the Adirondack-Champlain region and ranked among the leading iron regions of the country. The basic geographic pattern was an elaboration of that established earlier. The primary mining operations were mostly subsurface drifts such as those at Arnold Hill and nearby Palmer Hill in the Ausable River Valley, the Cheever Mines, and the Mineville-Witherbee developments. Numerous secondary and relatively small enterprises were active in and near the Saranac River Valley and at points scattered across northern, eastern, and southern Essex County (Glenn, 1977).

The Ausable Valley stood out as the prominent corridor of iron-making, rolling mills, foundries, and fabricating industries. Horse-shoe nails were the chief finished product. Ausable Chasm, Keeseville, Clintonville, Ausable Forks, Black Brook, and Lower Jay were all thriving centers of iron making and/or fabricating. To the north, the Saranac Valley formed

another primary subregion (Hurd, 1880). South of the Ausable Valley, Port Henry stood out as the dominate node of smelting, with smaller works located inland in the Town of Moriah; at Ticonderoga; and in the Schroon Valley of south-central Essex County (Watson, 1869 and Smith, 1885).

The Peak Period - Mining

The peak period of the Adirondack-Champlain iron enterprise was ushered in by and during the Civil War. Iron markets continued to remain strong after the Civil War in response to the rapid urban-industrial growth of the Northeastern United States and the birth of the Steel Age which significantly increased the demand for iron. Continued expansion of the nation's rail network and the replacement of iron trackage with steel rails created huge new markets. These factors sustained favorable conditions for the Adirondack-Champlain iron industry until the early 1880s.

In 1880, when the United States Bureau of the Census officially recognized the region as one of the ten leading iron regions of the country (Pumpelly, 1886), Clinton and Essex counties together produced 724,000 tons of iron ore (slightly over nine per cent of the national total). This represented 30% of the Nation's magnetite production. In 1870 and 1880, New York was the third most productive iron ore producing state, surpassed only by Pennsylvania and Michigan (Moravek, 1976).

Essex County's output of 631,800 tons of iron ore exceeded Clinton County's 92,200 tons, but even Clinton County ranked 13th among iron-ore producing counties in the country. Essex County was only surpassed by Marquette County, Michigan, whose output of 1,346,400 tons represented 16.9% of nation's iron ore. Three of the most productive mines in the United States were located in Essex County in 1880. The Mineville-Witherbee complex, centered in the Town of Moriah, constituted the most significant mining district in the Adirondack-Champlain Region, as its production of 465,740 tons of ore accounted for nearly two-thirds of the total. The Cheever and Lee mines also in the Town of Moriah produced 51,000 tons of ore in 1880, and a new group of mines opened at Hammondville in the west-central portion of the Town of Crown Point in 1872, yielded 112,000 tons of ore in 1880 (Kemp, 1908).

In Clinton County, the Palmer Hill mines continued to produce with an output of 36,670 tons of ore in 1880. The Williamsburgh-Petersburgh (Tremblay) mines near the junction of the north and south branches of the Saranac River produced 8,850 tons of ore. Arnold Hill, long an important mining center, was only active for a small part of the census year, yielding a mere 1,845 tons.

Those sites had been joined by a major new enterprise at Lyon Mountain (Miller, 1926) in the west-central portion of the county. There in the Town of Dannemora, 30 miles west of Lake Champlain, plans for a substantial enterprise were laid in the late 1860s and implemented in the next decade (Linney, 1934). Lyon Mountain emerged as a leading mining center after rail connections were secured in 1879 and the operation became the object of vigorous promotion by the Chateaugay Ore and Iron Company. In 1880, Lyon Mountain yielded nearly 45,000 tons of ore. A more representative picture of the status of the Lyon Mountain enterprise can be seen by examining the production figures for the years following the 1880 census. In 1882, the first full year of operation by the Chateaugay Ore and Iron Company, production soared to more than 240,000 tons. Production for the three years from 1882-84 inclusively averaged 216,500 tons per year. In addition to the above, a number of small pits, scattered throughout the two-county region, were worked, but their aggregate yield was inconsequential in the overall industry (Pumpelly, 1886).

The Peak Period - Smelting

The iron content of the ore approached 70% iron in a few cases in the Mineville-Witherbee area, not far below the 72.4% iron in pure magnetite. It averaged 55% region-wide. In some areas it dropped to as low as 25-30%. Regardless of its iron content, all Adirondack non-titaniferous ores were considered exceptional in the sense that even the leanest could be beneficiated by magnetic separation and concentration processes to 65%-70% iron content.

The zenith of iron-smelting and associated enterprises also occurred in the 1860-1885 period. No fewer than 50 blast furnace and bloomeries operated in 1880. The region's relative position in iron-smelting was far less impressive than it was in mining. Although Clinton County accounted for nearly 85% of the nation's bloomery iron in 1880, the vast bulk of American iron was being made in blast furnaces by that date. By 1890 Clinton was the only county in the country still producing wrought iron by means of the antiquated Catalan forge. The U.S. Census noted that its charcoal blooms and billets were highly esteemed in outside markets for use in the manufacture of plate, sheet iron and fine grades of steel. Clinton County's production of pig iron in 1880 was minimal, but Essex County produced 66,725-ton of iron. While it was important locally, this represented slightly less than one percent of the national total of 7,265,140 tons.

The heart of iron smelting and associated fabricating industries during the 1860-1885 peak period was still found in the Ausable Valley. To the south the primary centers of pig-iron making included the long-established blast furnace operations at Port Henry and two modern, coke-fired works producing Bessemer pig iron near the shores of Lake Champlain

in the Town of Crown Point that opened in the early 1870s. Those blast furnaces were operated by the Crown Point Iron Co. in conjunction with its major mining activities at Hammondville. The established smelting and secondary works north of the Ausable Valley continued unchanged from that of mid-century with a number of new enterprises. The principal new enterprises were established in the Chazy Valley at Altona and vicinity, at Standish (Figure 3) a few miles south of Lyon Mountain, and at Popeville, on the outlet of Lower Chateaugay Lake 12 miles northwest of Lyon Mountain. Popeville's 22-fire bloomery operation, reportedly the largest of its kind in the world, converted the low-phosphorus Chateaugay magnetite from Lyon Mountain into superior quality blooms and billets (Pope, 1968).

Throughout this peak period, significant quantities of regionally produced bloom iron were rolled, slit, and converted into horse-shoe nails at Saranac and Plattsburgh on the Saranac River and at Ausable Chasm, Keeseville, Clintonville, and AuSable Forks on the Ausable River (Moravek, 1976). The region's pig iron was shipped to markets throughout the Northeast.

If we consider all the phases of the iron industry together, including mining, ore processing, charcoal-making, smelting and product fabrication, the industry dominated the region during the peak period. A labor force of 8,000-10,000 was engaged in one or more phases of the iron industry which formed the lifeblood of some 50 villages and hamlets. The enterprise dominated life in whole corridors and subregions as levels of prosperity paralleled the ebb and flow of economic tides in the iron industry. In some townships, up to 85% of the labor force was engaged in iron, and the products of that endeavor constituted nearly 95% of the value of all manufactured goods. At its zenith, the iron industry stood unrivaled as the economic cornerstone of the region. In numerous iron townships, the 1880 levels of population and relative prosperity remain all-time highs to this day (Moravek, 1976).

The Industry in Decline

The momentum gained by the iron industry during the Civil War was sustained into the early 1880's by the brisk markets generated by railroad construction and by great urban-industrial developments of the northeast. It declined rapidly thereafter. Many Adirondack-Champlain ironmongers blamed the collapse of the industry after 1885 on detrimental tariff policies. A nation-wide financial panic in 1893 was a mortal blow to many struggling enterprises. Nationally, the iron and steel industry was undergoing revolutionary change. Sweeping changes made the Adirondack-Champlain region an industrial dinosaur wholly ill-adapted to the new industry. Bigness emerged as the hallmark of the new era. The scale of both

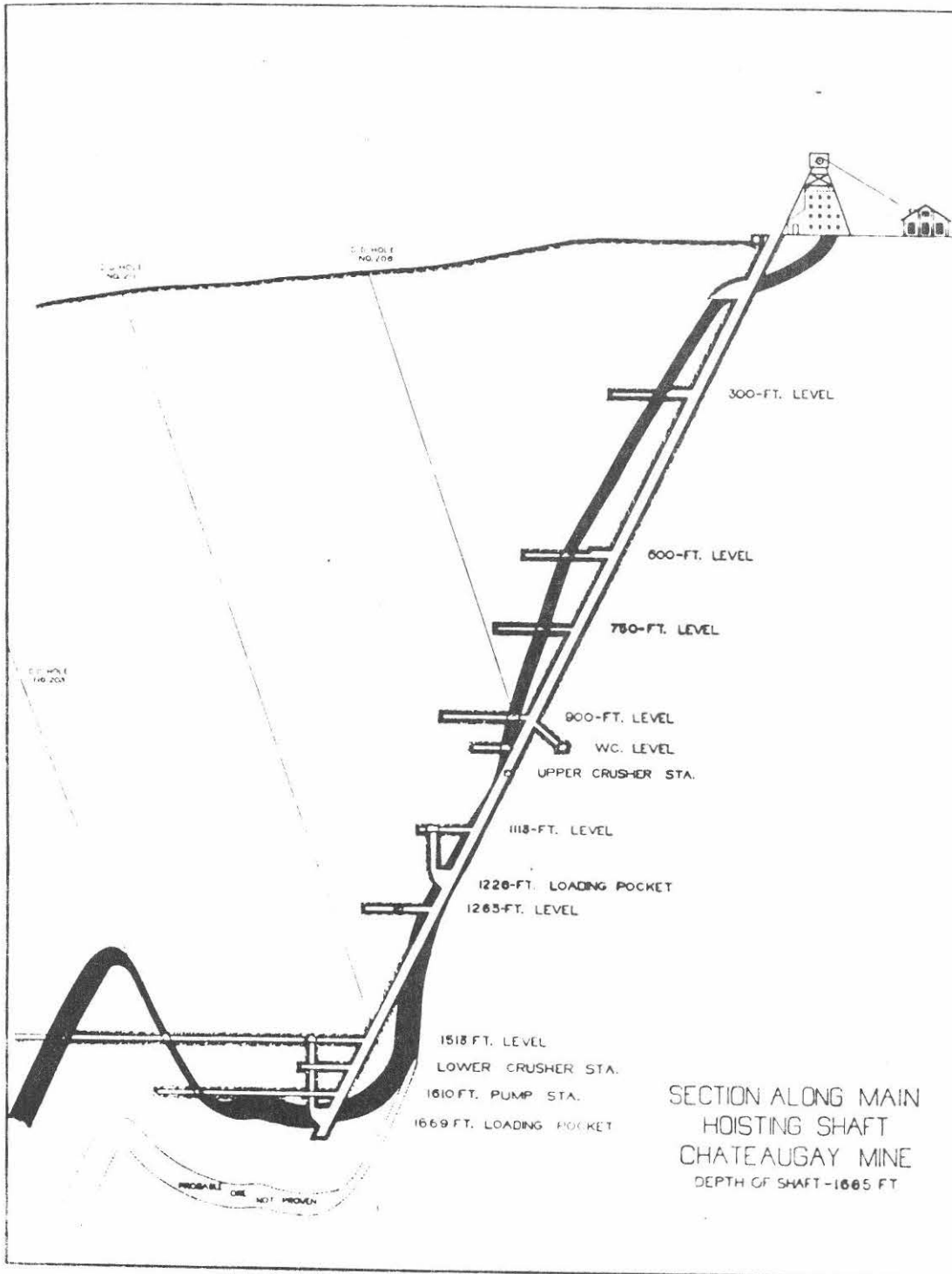


Figure 3. SECTION ALONG MAIN HOISTING SHAFT, CHATEAUGAY MINE (Linney, 1934).

mining and smelting in new iron regions created economies of scale that were unattainable in the Adirondack-Champlain region.

In the mining phase, production shifted to the Lake Superior Region with the opening of the Mesabi, Vermillion, Cuyuna, Gogebic, Marquette and Menominee iron ranges of northeastern Minnesota in the 1890's (Walker, 1979). Immense quantities of rich, untapped ores could be surface-mined, handled in bulk by modern power machinery, and shipped via Great Lakes freighters. Mining and delivery costs per unit were a small fraction of those incurred in the small-scale underground mines of the Adirondack-Champlain region. Moreover, in numerous cases ore deposits once viewed as "inexhaustible" in the Adirondack-Champlain region had in fact become largely depleted.

The westward migration of mining was accompanied by a geographic shift in the smelting phase. The Steel Age was the result of the development of the modern Bessemer process in the mid-19th century (McHugh, 1980). By the late 19th century steel production was highly concentrated in a few districts on the shores of the Great Lakes and in the Upper Ohio Valley. These areas had marked advantages with the Great Lakes providing access to ore, coal for fuel as coke and markets. The smelting process itself had assumed a gigantic scale that resulted in major economies. These revolutionary developments spelled the permanent doom of local, small-scale, geographically dispersed, antiquated iron-making ventures such as those largely characteristic of the Adirondack-Champlain region and gave rise to modern, integrated, heavily capitalized industrial-corporate behemoths as symbolized, by the United States Steel Corporation, formed in Pittsburgh in 1901, as the nation's first billion-dollar corporation.

The Final Years

By 1900, with two exceptions, the smelting phase was nearly over. Blast furnace operations were continued at Standish and Port Henry until the mid-1930's, but only a few bloomeries remained active after the turn of the century. The last bloomery of record in this region and in the United States survived until 1907 at Standish. Twentieth-century mining was restricted to the Mineville-Witherbee-Fisher Hill area in Essex County and Lyon Mountain in Clinton County. The early nineteenth century mining venture at Tahawus was reactivated, after lying abandoned for a century, during World War II to produce ilmenite (TiO_2) for strategic purposes. The titaniferous iron ore associated with ilmenite was a byproduct and during the 1940's over 100,000 tons per year of this byproduct was shipped to blast furnaces. Greater amounts of concentrated iron ore were sold for use in making high-density concrete and for various other purposes (Stephenson, 1945).

Production levels at Mineville and Lyon Mountain fluctuated in accordance with national economic conditions and the relative competitiveness of other mining regions. The impact of the Great Depression was especially severe. The Witherbee-Sherman Co., long the controlling force in the Town of Moriah, made a decision in 1937 to lease its properties and facilities to the Republic Steel Corporation. Republic was the first national firm to operate in the eastern Adirondack region and it was to control the destiny of the eastern Adirondack iron industry during its final three decades of activity. After purchasing the Mineville-Witherbee-Fisher Hill physical plant and ore properties, Republic modernized and expanded the scale of mining, but shut down the blast furnace at Port Henry. Republic shipped sinter and lump ore directly to its sprawling, modern iron and steel works in Cleveland and to Buffalo and Troy. In 1939, Republic followed the same pattern when it leased and, in 1943, purchased the Chateaugay mines at Lyon Mountain and the blast furnace at Standish (Figure 4). This division was administered separately until the 1950's. Port Henry and Chateaugay were subsequently consolidated into the Adirondack Division of Republic Steel Corp.

The advent of World War II confirmed the wisdom and timing of Republic's Adirondack ventures and full-scale operations continued. By the late 1940s the Adirondack share of the national iron ore output had risen to nearly three percent, up from an estimated 0.6% for the decade from 1918-28. Production of concentrates and sintered ore averaged approximately a million and a half tons per year during the 1940's to 1957 in the Port Henry District alone. While levels of activity fluctuated considerable from year to year, they remained quite stable over the long run until the late 1950's. Production fell to a half million tons in 1958 from an all-time high of nearly two million tons in 1953. It rebounded to some 800,000 tons in 1954 but varied greatly from year to year thereafter. Only in 1965 and 1966 did output ever return to one million tons per year. Comparable data for the Chateaugay enterprise are not available, but the level of activity at Lyon Mountain, while typically well below that of the Town of Moriah, paralleled the trends of the latter. The production gyrations of the late 1950s and 1960s were symptomatic of increasingly troubled times and the weakening competitive position of the Adirondack Division within Republic's international iron-ore mining framework. In the face of declining profitability, Republic decided to phase out its Adirondack operations altogether and permanently. The final shutdowns occurred at Lyon Mountain in 1967 and four years later at Mineville. Substantial reserves of ore remain (Postel, 1952) at both sites and some estimate that the reserves exceed the total extracted. However, mining costs are considered prohibitive under current market conditions and there is little likelihood that either mining center will be reactivated in the foreseeable future.

References Cited

- Allen, Richard S., 1975, Fletcherville Furnace: Unpublished manuscript at The Adirondack Museum, Blue Mountain Lake, NY. 15 pages.
- Chahoon, George, 1875, Iron Making in Northern New York: Catalan Forges: Bulletin of the American Iron and Steel Association, 9:250, August 20, 1875.
- Chahoon, George, 1880, Report on the Iron Deposits in the North Eastern Division (with Industrial Memoranda): Appendix pp. 413-428 in Verplanck Colvin, 1880, 7th Annual Report on the Progress of the Topographical Survey of the Adirondack Region of New York, to the Year 1879: Weed, Parsons and Co., Albany, NY, 536 pp.
- Egleston, T., 1880, The American Bloomery Process for Making Iron Direct from the Ore: Transactions, American Institute of Mining Engineers, 8:515-550+ plates.
- Glenn, Morris F., 1977, The Story of Three Towns: Westport, Essex and Willsboro, New York: Distributed by Morris F. Glenn, Alexandria, VA, 354 pp.
- Glenn, Morris F., 1987, Glenn's History of the Adirondacks (Essex Co., New York), Volume 10: The Adirondack-American Bloomery Process for Making Iron: Distributed by Morris F. Glenn, Alexandria, VA, ix + 4 pages + five additional parts.
- Hardy, Philip J., 1985, The Iron Age Community of the J & J Rogers Iron Company, Au Sable Valley, New York: 1825-1900: Ph.D. Dissertation. Bowling Green State University. University Microfilms International, Ann Arbor, MI. Order No. 85-18, 421. 315 pp.
- Hunt, T. Sterry, 1870, Iron and Iron Ores: Geological Survey of Canada Report of Progress 1866 to 1869.
- Hurd, Duane H., 1880, History of Clinton and Franklin Counties, New York: J. W. Lewis and Co., Philadelphia, PA. 1978 Reprint Edition by the Clinton County American Revolution Bicentennial Commission, 556 pp.
- Kalm, Peter, 1770, Travels into North America: Translated into English by John Reingold Forster. 1972 Reprint Edition by The Imprint Society Inc., Barre, MA, 514 pp.
- Kemp, James F., 1908, The Mineville-Port Henry Mine Group: pp. 57-88 in New York State Museum Bulletin 119, 182 pp.

- Kemp, James F. and Rudolf Ruedemann, 1910, Geology of the Elizabethtown and Port Henry Quadrangles: New York State Museum Bulletin 138, 173 pp.
- Lincoln, Frederic, 1909, A Concrete Industrial Village: Cement Age, 9:158-165, September, 1909.
- Linney, Joseph R., 1934, A History of the Chateaugay Ore and Iron Company: The Delaware and Hudson Railroad, 176 pp.
- Masten, Arthur H., 1923, The Story of Adirondac: Privately Printed. 199 pp.
- McHugh, Jeanne, 1980, Alexander Holley and the Makers of Steel: The Johns Hopkins University Press, Baltimore, MD, 402 pp.
- Miller, William J., 1926, Geology of the Lyon Mountain Quadrangle: New York State Museum Bulletin 271, 101 pp.
- Moravek, John R., 1976, The Iron Industry as a Geographic Force in the Adirondack-Champlain Region of New York State, 1800-1971: Ph.D. Dissertation. University of Tennessee. University Microfilms International, Ann Arbor, MI. Order No. 76-24,847. 304 pp.
- Morton, Doris, 1959, Philip Skene of Skenesborough: Bicentennial Issue. Grastorf Press, Granville, NY, 84 pp.
- Pollard, Gordon C., 1985, Historical Archaeology of a 19th Century Iron Mine Community in the Northern Adirondacks of New York State: Northeastern Anthropological Association Annual Meeting Symposium. Includes five student papers: Daniel Bancroft, 19th Century Catalan Forges in the Adirondacks: A Comparison with the Caldwell Mine Site; Mark C. Beauharnois, Classified Archaeological Information Management Systems (CLAIMS): A Computer Application for the Caldwell Site; Lisa Brothers, The Sociology and Physical Structure of 19th Century Adirondack Iron Communities: Implications for the Caldwell Site; Kimberly Holtyn, Ore Extraction and the Physical Configuration of 19th Century Iron Ore Mines: The Caldwell Site in Contemporary Perspective; Marjorie Brown Weinberg, The Caldwell Mine Site in Historical-Archaeological Perspective: The First Field Season, 1984: Department of Anthropology, State University of New York, Plattsburgh, NY. Unpublished.
- Pope, Connie C., 1968, Popeville, Franklin County's Ghost Town: York State Tradition, 22:38-49.

- Postel, A. Williams, 1952, Geology of Clinton County Magnetite District, New York: United States Geological Survey Professional Paper 237, 88 pp.
- Pumpelly, Raphael, 1886, Report on the Mining Industries of the United States (Exclusive of the Precious Metals) with Special Investigations into the Iron Resources of the Republic and Into the Cretaceous Coals of the Northwest: Department of the Interior Census Office, Washington, DC.
- Richards, Robert H., editor, J.W. Cabot, R.H. Sweetser and W.A. Tucker, 1895, Notes on the Metallurgy of Iron: Prepared for the Use of the Students of the Massachusetts Institute of Technology, Boston, MA, 148 pp.
- Smith, Henry P., 1885, History of Essex County: D. Mason and Co. Publishers, Syracuse, NY, 754 pp.
- Stephenson, Robert C., 1945, Titaniferous Magnetite Deposits of the Lake Sanford Area, New York: New York State Museum Bulletin 340, 95 pp.
- Walker, David A., 1979, Iron Frontier: The Discovery and Early Development of Minnesota's Three Ranges: Minnesota Historical Society Press, St. Paul, MN, 315 pp.
- Warner, Charles B. and C. Eleanor Hall, 1931, History of Port Henry, N.Y.: The Tuttle Company, Rutland, VT, 182 pp.
- Watson, Winslow C., 1869, The Military and Civil History of the County of Essex, New York: J. Munsell, Albany, NY, 504 pp.
- Wetherbee, T. F., 1874, The Manufacture of Bessemer Pig-Metal at the Fletcherville Charcoal Furnace, near Mineville, Essex County, New York: Transactions, American Institute of Mining Engineers, 2:5:65-78.

ROAD LOG FOR THE IRON INDUSTRY
OF THE EASTERN ADIRONDACK REGION

CUMULATIVE MILEAGE	MILES FROM LAST POINT	ROUTE DESCRIPTION
0	0	Begin the trip at the corner of Broad Street and Draper Avenue, Plattsburgh, NY just west of the Hudson Hall Parking Lot, SUNY-Plattsburgh campus. Head west on Broad Street, which runs into Cornelia Street (Route 3) and continue west.
1.0	1.0	Cross under I-87 on Route 3.
3.1	2.1	Intersection of Route 3 and 22B. Turn right and continue west on Route 3.
8.0	4.9	Intersection of Route 3 and 374. Cross the intersection and turn left to head west on Route 374 toward Dannemora, New York.

CUMULATIVE MILEAGE	MILES FROM LAST POINT	ROUTE DESCRIPTION
13.6	5.6	Pass Main Gate of the Clinton Correctional Facility in Dannemora, New York.
25.8	12.2	Enter Lyon Mountain, New York on Route 374.
26.1	0.3	Turn left at Belmont Street when Route 374 turns north. Belmont Street becomes Standish Road.
26.3	0.2	Turn left at Depot Street.
26.6	0.3	Follow Depot Street uphill with Separator Brook on your right to the gate that marks the entrance to the mine property and park.

STOP 1. LYON MOUNTAIN MINES

Lyon Mountain was the site of the Chateaugay ore beds. During its century-long life as a mining center, it produced more ore in aggregate than any other area in the Adirondack-Champlain Region, except for the Mineville-Witherbee complex

of Essex County. The Prall Vein or Mine 81, an open pit situated two and a half miles to the southwest, was the probable source of ore that supplied a bloomery operating on the Chateaugay River to the north as early as 1803, but the Chateaugay deposits at Lyon Mountain were not discovered until 1822-1823. Development lagged for a full half century due to the remoteness of the area.

In 1868, a group of four Saranac Valley speculators purchased the ore beds and devised plans for an extensive enterprise. In 1873, this interest was transferred to the newly organized Chateaugay Iron Ore Company. Substantial quantities of ore were shipped to the large bloomery erected in 1872 at Popeville. The Chateaugay Railroad Company was formed to construct a railroad from Lyon Mountain east to the rail terminus from Plattsburgh at Clinton Prison in Dannemora. This was completed in 1879. The railroad, mining, and smelting interests were consolidated into a powerful new firm, the Chateaugay Ore and Iron Co. in 1881. This creation launched development on a great scale (Figure 3).

Our excursion will walk by the head frames of the later works and a former employee of Republic Steel who is familiar with the structures will describe their purpose at the time that operations were closed in 1967.

In Lyon Mountain, New York century-old residential structures border the mines, together with the 1920s-vintage standard "company" houses that line Route 374 (Belmont Street). Today's inhabitants, descendants primarily of Lithuanian, Polish, Russian, Italian, Spanish, Irish, and French-Canadian immigrants who labored in the mines and mills, are either retired or, if employed, commute to jobs on the outside, or since 1984, have found jobs on Belmont Street itself at the former public school house, now converted to a minimum-security state prison.

CUMULATIVE MILEAGE	MILES FROM LAST POINT	ROUTE DESCRIPTION
26.6	0	From Stop 1 follow Depot Street downhill.
26.9	0.3	Turn left at the Standish Road and immediately cross Separator Brook.
30.9	4.0	Turn right on Ross Street in Standish.
31.1	0.2	Park at the end of Ross Street in front of the only house on the left.

STOP 2. SITE OF CATALAN FORGE AT STANDISH

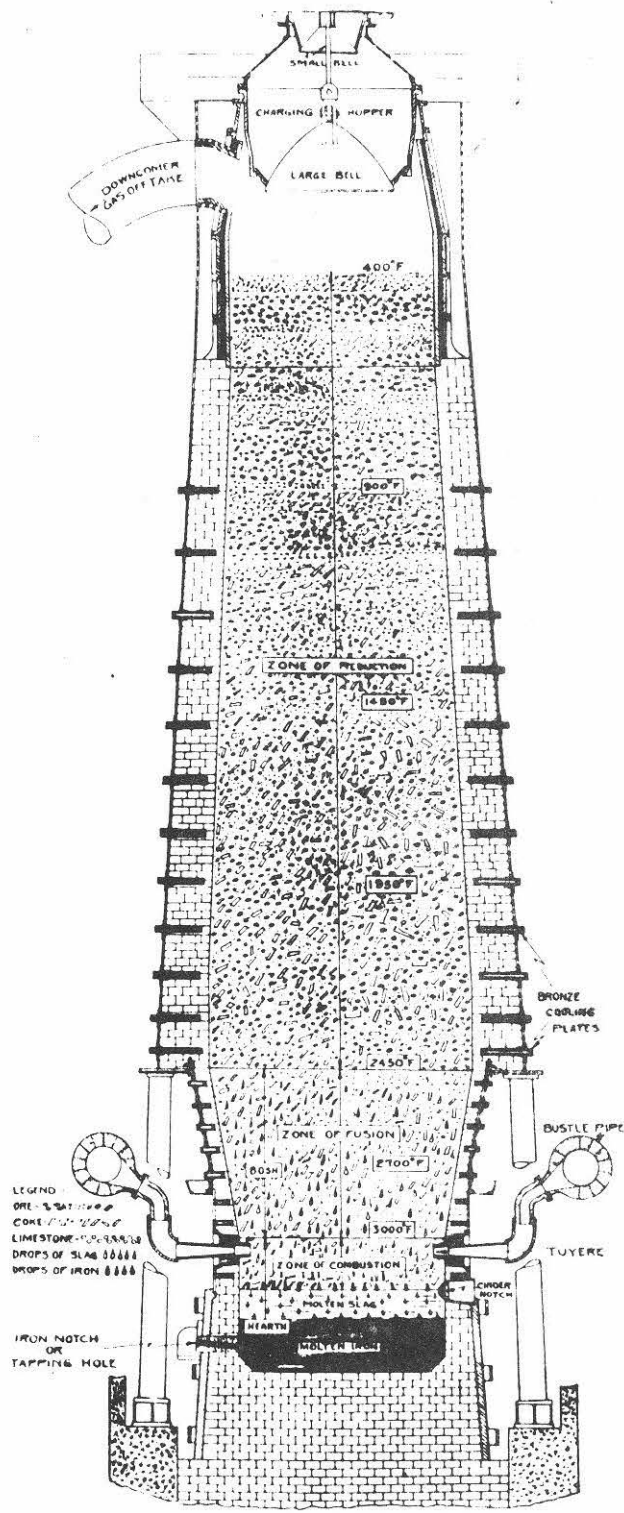
The Chateaugay Ore and Iron Company had an 8-fire bloomery at Standish by 1883. This was enlarged several times until it was shut down in 1907. In 1885 the company constructed a blast furnace (Figure 4) at Standish to produce pig iron in addition to bloom iron (Linney, 1934). The trade name "Chateaugay" quickly gained a highly favorable reputation for excellence. Blooms, pigs, and the celebrated low-phosphorus magnetite were widely sought after, and commanded premium prices everywhere. The crude ore was/is rather lean, averaging only 26%-28% iron content, but was practically free from phosphorus, sulfur, and other chemical impurities, and could be readily beneficiated to 65-70% iron content. Iron and high-grade alloy steels made from Chateaugay ore were renowned for toughness and strength and widely used for the fabrication of wire rope, munitions, ordnance, and other specialties. For such purposes, it was considered unsurpassed in all the world, and steel cables made of Lyon Mountain's ore can be found today in such mighty and notable structures as the Brooklyn bridge, the Golden Gate Bridge in San Francisco, and the George Washington Bridge in New York City.

CUMULATIVE MILEAGE	MILES FROM LAST POINT	ROUTE DESCRIPTION
31.1	0	From Stop 2 retrace your route on Ross Street.
31.3	0.2	At the corner of the Standish Road continue east and then south toward Clayburg.
41.6	10.3	Route 3, Clayburg. Turn left.
41.7	0.1	Turn right onto the Silver Lake Road and immediately cross the Saranac River North Branch.
42.0	0.3	Turn left into the NYS Department of Environmental Conservation fishing access parking area and park.

STOP 3. CALDWELL MINE SITE

Ore was discovered at the Caldwell site in 1840 and mining began in 1841. This was the first iron ore discovery in the Saranac River valley and it resulted in the establishment of a settlement named after the original property owner Leander Cadwell. Early newspapers and subsequent histories managed to misspell his name.

Leander Cadwell and Lawrence Myers erected four forges and a separator at the site in 1844. By 1846 this was expanded to



STANDISH BLAST FURNACE
YEAR-1934

Figure 4. Blast Furnace at Standish, NY (Linney, 1934).

six forges, two separators, two trip hammers and a finishing hammer. About 100 men were employed. Myers became the sole owner in 1855 and by 1860 the mine was yielding 1500 tons of iron ore per year. The property changed ownership in 1863 and again in 1873 and the mine was considered "mined out" and closed in 1881.

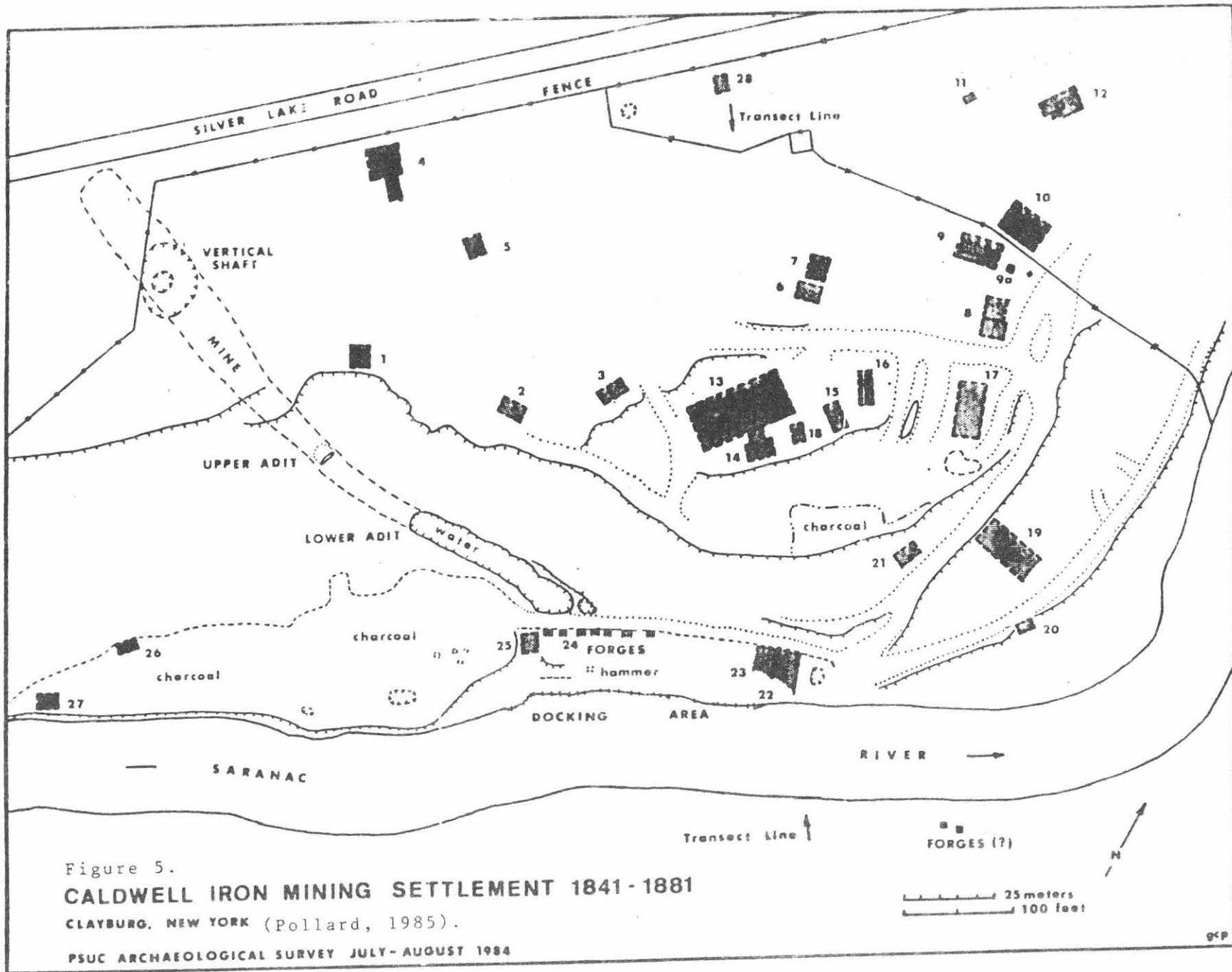
Historical archaeological research has been conducted by Gordon C. Pollard (Pollard, 1985). The research has produced a map of the eleven-acre site (Figure 5) and has documented the mine, ore processing site, charcoal production and storage, residences and company store. Dr. Pollard will be on hand to guide this portion of the field trip.

CUMULATIVE MILEAGE	MILES FROM LAST POINT	ROUTE DESCRIPTION
42.0	0	From Stop 3 turn left out of the fishing access parking area and head south on the Silver Lake Road.
45.7	3.7	Cross the Saranac River.
47.6	1.9	Stop sign at Hawkeye, corner of the Union Falls Road and Silver Lake Road. Turn left and stay on the Silver Lake Road.
55.3	7.7	Cross Black Brook in the hamlet of Black Brook.
58.5	3.2	Turn left on the Palmer Hill Road.
59.1	0.6	Turn left on the Palmer Hill Tower Road.
59.8	0.7	Park at the gate.

STOP 4. PALMER HILL MINE SITE.

Iron ore was discovered at Palmer Hill, in the Town of Black Brook, in 1824-1825 by Zephaniah Palmer. In 1829 he sold a three-eighths interest, the eastern extension of ore, to the Peru Steel and Iron Company. Later he sold the western five-eighths interest to the J. and J. Rogers Iron Company of Au Sable Forks, NY.

Mining commenced about 1830 and continued to 1892-1893. The Palmer Hill Mines were initially excavated as open pits but as time passed increasing depth rendered impractical the removal of overburden, and drifts were developed as the companies followed bands of ore ranging in thickness from 10 feet to 20 feet. The deepest set of workings bottomed at a



depth of 2,200 feet, down a dip slope that began at 60° and flattened to a nearly horizontal position at the bottom. Other pits extended to a depth of 1,000 to 1,200 feet down dips of roughly 30°. In some cases workings followed shoots of ore across the dip. The texture of Palmer Hill ore was rather fine, and in appearance and mode of occurrence resembled the Chateaugay ores at Lyon Mountain.

Our stop will briefly explore the honeycombed southern brow of Palmer Hill, with its numerous irregular openings and chambers and piles of rock and mine rubble. This site continues to hold a certain fascination, and remains potentially dangerous, to local explorers and students. In places the surface workings have caved in and are inaccessible, but numerous pits do allow access and invite cautious investigation. Deep water fills the lower parts of these "caves," and in some pits ice can be found at any time of the year.

CUMULATIVE MILEAGE	MILES FROM LAST POINT	ROUTE DESCRIPTION
59.8	0	From Stop 4 retrace your route down the Palmer Hill Tower Road.
60.5	0.7	Turn left at the Palmer Hill Road.
61.1	0.6	Continue straight at the intersection of the Palmer Hill Road and the Golf Course Road.
65.7	4.6	Turn very sharply to the right at the road to Clintonville.
66.9	1.2	Turn left on Route 9N in Clintonville.

STOP 5. DRIVING TOUR OF CLINTONVILLE.

The Peru Steel and Iron Company was heavily engaged in smelting and iron fabrication in Clintonville, New York and reached its peak prosperity in the 1850s and 1860s when 900 men were employed (Moravek, 1976). The bloomeries, separator and rolling mill occupied more than a mile of the north bank of the Ausable River.

The national decline of the iron industry in 1873 was hard on Clintonville and by 1880 the activities of the Peru Steel and Iron Company at Palmer Hill and at Clintonville were over.

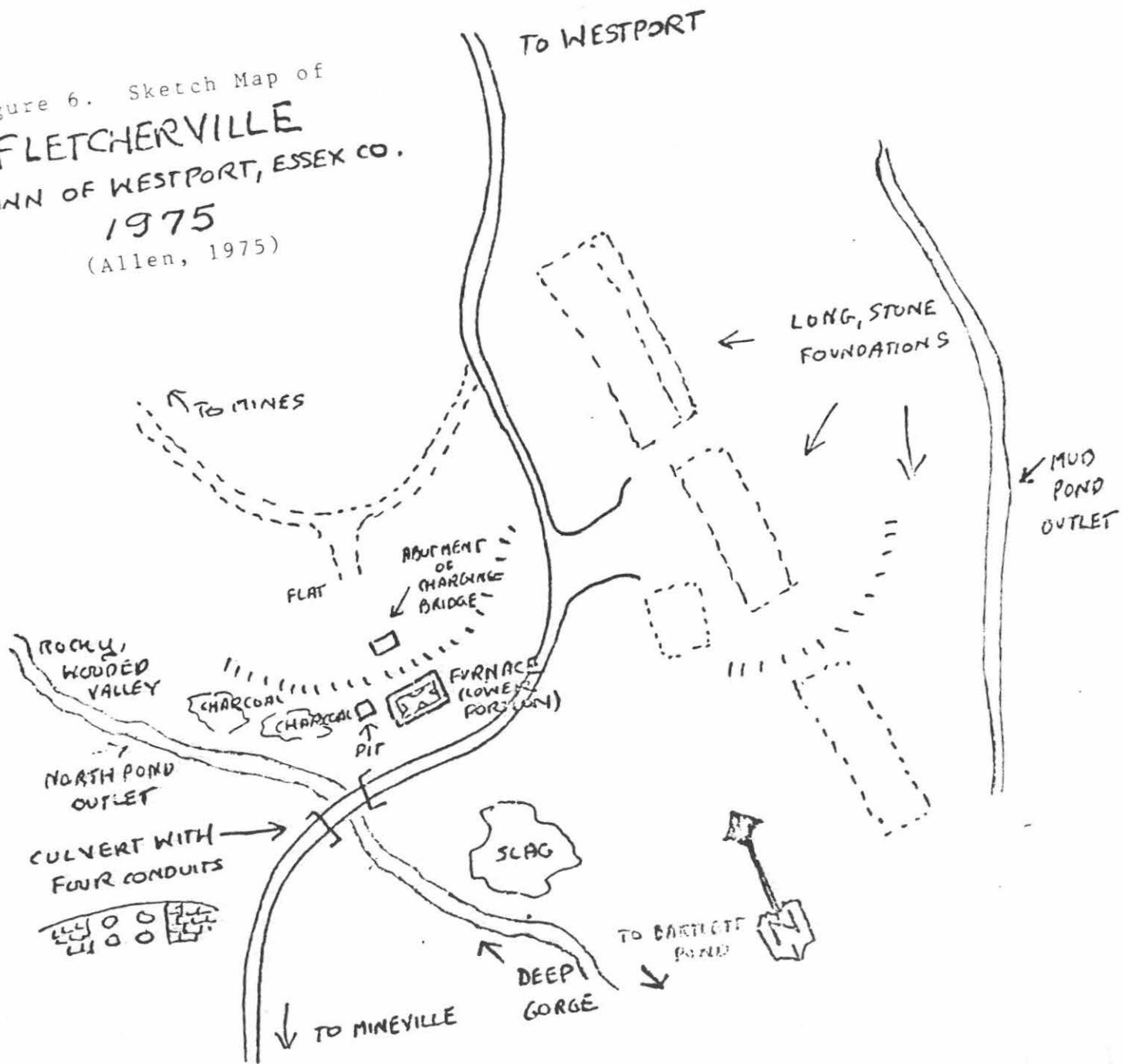
CUMULATIVE MILEAGE	MILES FROM LAST POINT	ROUTE DESCRIPTION
72.4	5.5	At intersection of Route 9N and I-87 (Exit 34) turn right and head south on I-87.
94.1	21.7	Leave I-87 at Exit 31 and turn right on Route 9N to head toward Elizabethtown.
97.6	3.5	As you enter Elizabethtown, at the foot of the hill, turn left on the Lincoln Pond-Moriah Road.
101.1	3.5	Cross I-87 on a bridge.
106.4	5.3	Bear left toward Mineville at the Witherbee-Mineville intersection.
108.3	1.9	Enter Mineville.
108.6	0.3	Turn left on the Bartlett Pond Road.
108.9	0.3	Turn left on the Cook Shaft/Mountain Spring/Nichols Pond Road.
110.2	1.3	Just after the road crosses a culvert over a small stream, flowing from left to right, pull over and park. The old Fletcherville furnace is the overgrown mound on the left side of the road.

STOP 6. FLETCHERVILLE BLAST FURNACE AND SHERMAN MINE.

Friend P. Fletcher joined with Silas H. Witherbee and Jonathon G. Witherbee to manufacture iron in a furnace on Fletcher's 4000 acres of land. Jerome B. Bailey of Plattsburgh, New York built the blast furnace in 1864-1865. It was a stone stack 42 feet high, later increased to 61 feet, on a 42 foot square base. Nearby ten enclosed rectangular brick charcoal kilns were constructed, each capable of charring 65 cords at a time (Allen, 1975).

The town (Figure 6) that sprang up was known locally as Fletcherville, but people in Westport referred to it as Seventy Five because it was thought to be in Lot 75 in the Town of Elizabethtown. A survey showed that it was really in Lot 48 of Westport which then received the taxes.

Figure 6. Sketch Map of
FLETCHERVILLE
TOWN OF WESTPORT, ESSEX CO.
1975
(Allen, 1975)



In the early 1870s much of Fletcher's pig iron was shipped from Port Henry to Troy, New York where it was used in the experimental Bessemer steel process for railroad track (Witherbee, 1874). The early success began to fade in the 1870s and after Fletcher's death in 1874 the works closed down.

The Sherman Mine and other small mines on the Fletcher property were occasionally revisited with activity at the Sherman continuing as late as 1921.

Our visit will examine the remains of the blast furnace, charcoal beds, ore roasting kilns, various out buildings and perhaps the Sherman Mine.

CUMULATIVE MILEAGE	MILES FROM LAST POINT	ROUTE DESCRIPTION
110.2	0	From Stop 6 retrace your route.
111.5	1.3	Turn right at the Bartlett Pond Road.
111.8	0.3	Turn left at the Lincoln Pond Road and enter Mineville.
112.2	0.4	Turn right at the Rexall Drugstore onto the road to Witherbee.
113.3	1.1	Intersection of Powerhouse Road and Dalton Hill Road.

STOP 7. DRIVING TOUR OF WITHERBEE

The mines of the Mineville-Witherbee-Fisher Hill area in the Town of Moriah have been the most productive iron ore producers in the eastern Adirondacks. Our drive will circle through the sites of the "Old Bed," "21," "Barton Hill," "Harmony," and "Joker" mines of the extensive Mineville Group (Kemp, 1908). These mines were greatly expanded in the 1860s by the Port Henry Iron Ore Company after their initial discovery about 1825 (Warner and Hall, 1931). A variety of interests including the Witherbee, Sherman and Company operated in the area until Republic Steel Corporation took control from 1937 to 1971. Be sure to note the concrete block buildings that incorporate tailings material (Lincoln, 1909).

CUMULATIVE MILEAGE	MILES FROM LAST POINT	ROUTE DESCRIPTION
113.3	0	After tour of Witherbee turn right off the Powerhouse Road from Mineville onto the Dalton Hill Road and immediately turn left onto the Tracy Road. The Tracy Road is marked with signs for I-87 and North Hudson.
120.9	7.6	Turn right onto Route 9 and immediately turn right onto I-87 northbound at Exit 30.
169.2	48.3	Leave I-87 at Exit 37 and follow the off ramp to Route 3.
170.2	1.0	Turn right onto Route 3.
171.6	1.4	Bear right at the Y intersection of Route 3/Cornelia Street and Broad Street onto Broad Street.
172.0	0.4	Trip ends at Broad Street and Draper Avenue where it began.

LATE WISCONSINAN LACUSTRINE AND MARINE ENVIRONMENTS IN THE CHAMPLAIN LOWLAND, NEW YORK AND VERMONT

by

David A. Franzi
Center for Earth and Environmental Science
State University of New York
Plattsburgh, New York 12901

Thomas M. Cronin
United States Geological Survey
M.S. 970 National Center
Reston, Virginia 22092

INTRODUCTION

The Champlain Sea was a Late Wisconsinan marine incursion into the isostatically depressed St. Lawrence and Champlain Lowlands following ice recession from the eastern St. Lawrence Lowland (ca. 12.5 to 10.0 ka (kilo anno)). The marine episode followed a freshwater proglacial lacustrine interval in the Champlain and western St. Lawrence Lowlands (Fulton and others, 1987; Chapman, 1937). Sedimentary sequences containing till, ice-contact gravel, subaqueous outwash, and sparsely fossiliferous lacustrine sediment overlain by fossiliferous marine sediment record the transition from glacial to lacustrine to marine conditions in the basin.

This trip will examine the nature of the transition from freshwater to marine conditions and the paleoenvironments of the Champlain Sea as shown by the lithostratigraphic and biostratigraphic records in the Champlain Lowland. Faunal assemblages are used to reconstruct the areal and temporal distribution of water temperature and salinity within the basin. Emphasis is placed on the microfauna, particularly the ostracodes, and how changing microfaunal assemblages record environmental changes in this part of the Champlain Sea. The data summarized here are taken primarily from detailed faunal studies of foraminifers (Cronin, 1979) and ostracodes (Cronin, 1981) which concentrated in the southern arm of the sea in the Champlain Lowland of northwestern Vermont, northeastern New York, and southern Quebec. It should be stressed, however, that the sequence of faunas found in this region are not necessarily the same as those in other parts of the Champlain Sea where different hydrologic conditions caused a distinctly different sequence of paleoenvironments (Rodrigues and Richard, 1986; Rodrigues, 1987).

PHYSIOGRAPHIC AND GEOLOGIC SETTING

Late glacial ice flow and deglacial sedimentary environments in the northern Champlain Lowland were influenced by the regional physiography. The St. Lawrence and Champlain lowlands form a broad, contiguous lowland underlain by Cambrian and Ordovician sedimentary rocks (Fig. 1). The lowlands are bounded on the north and southwest by the Precambrian metamorphic rocks of the Laurentian Highlands and the Adirondack Upland, respectively, and on the

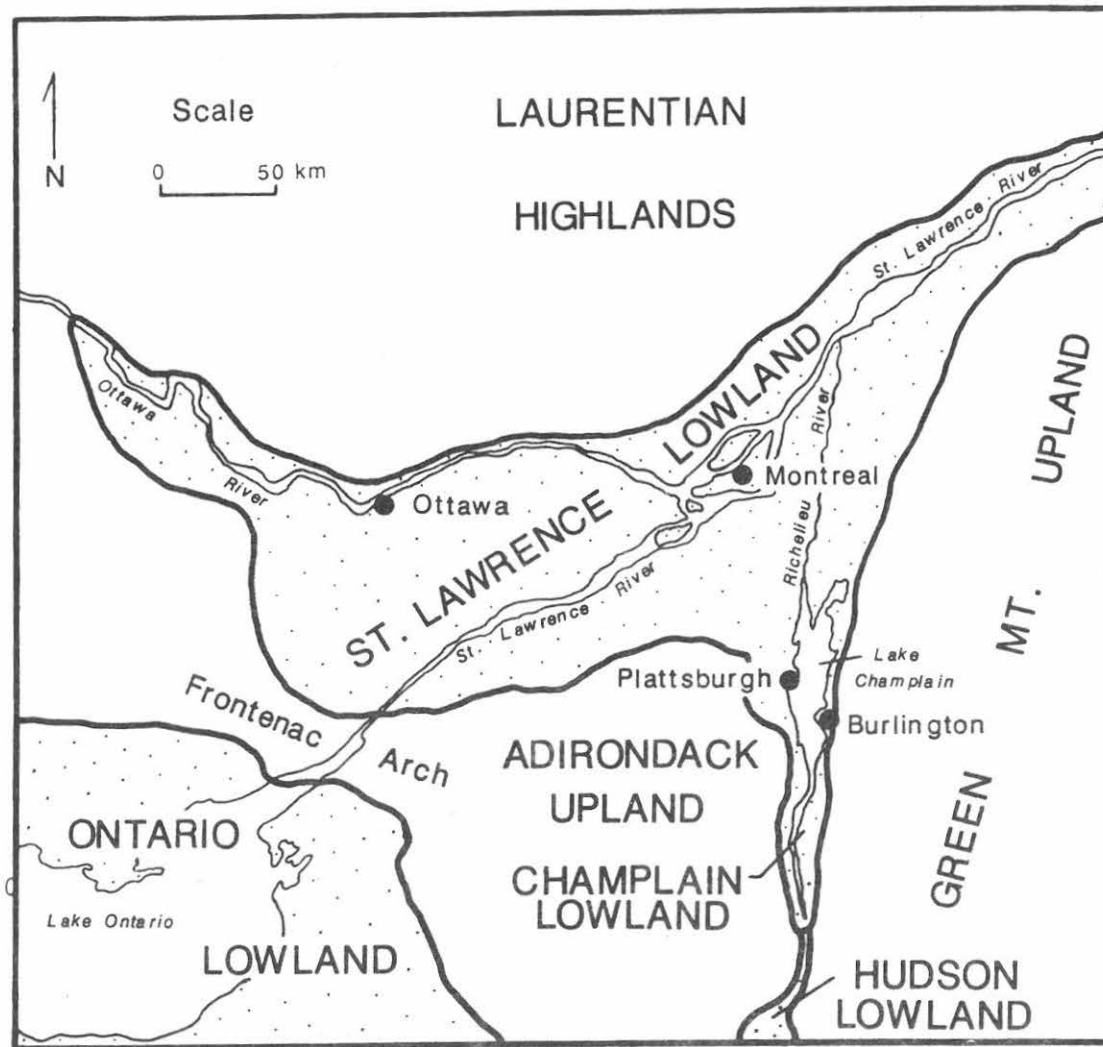


Figure 1. Physiographic map of the Champlain and St. Lawrence lowlands region.

southeast by the Precambrian and Lower Paleozoic metamorphic rocks of the Green Mountain Uplands. The Champlain Lowland narrows to the south where it merges with the Hudson-Mohawk Lowland.

Late Wisconsinan ice flow was concentrated in the lowland regions creating terrestrial ice streams (Hughes and others, 1985). One ice stream flowed southward through the Champlain and Hudson lowlands, while a larger ice stream flowed southwestward through the St. Lawrence and Ontario lowlands. Deglacial drawdown of ice into lowland ice streams caused thinning of ice in uplands and lobation of the ice front. Analyses of striae, drumlins, grooved drift, and dispersal trains in the Champlain Lowland and adjacent uplands generally conform to a model of southward flow at the Late Wisconsinan glacial maximum and more complex localized flow patterns during deglaciation (Denny, 1974; Ackerly and Larsen, 1987). The local flow patterns are associated with the formation of the Hudson-Champlain Lobe during deglaciation.

Digitate secondary lobes along the margin of the Hudson-Champlain Lobe penetrated tributary valleys and created local upland proglacial lakes. The drainage chronologies of these impoundments are complex and incompletely understood. Documentation of upland proglacial lakes in the northeastern Adirondack region includes work by Alling (1916), Denny (1974), Clark and Karrow (1984), Diemer, Olmsted, and Sunderland (1984), and Diemer and Franz (this volume). Upland-lake studies in northwestern Vermont include Stewart and MacClintock (1969), Connally (1972), and Larsen (1972, 1987).

DEGLACIATION OF THE CHAMPLAIN LOWLAND

Recent investigations in the Champlain lowlands (Connally and Sirkin, 1971, 1973; Parrott and Stone, 1972; Denny, 1974; Connally, 1982; DeSimone and LaFleur, 1986) favor a deglacial model that involves a single Late Wisconsinan glaciation followed by stagnation-zone retreat that may have been interrupted by minor ice-front oscillations. The terminus of the Hudson-Champlain Lobe lay in deep, proglacial lakes that expanded northward with ice recession. Backwasting of the ice front was probably enhanced by calving. Deposits of till, subaqueous outwash, and ice-contact stratified drift record the passing of the ice front during its northward retreat (Denny, 1974; DeSimone and LaFleur, 1986).

Minor readvances of the ice front in the Champlain Lowland have been proposed based upon morphologic relationships of glacial and lacustrine landforms and stratigraphic sequences containing intercalated glacial, lacustrine, and marine sediments (Table 1). The Luzerne (ca. 13.2 ka) and Bridport (ca. 12.8 ka) readvances were documented by Connally and Sirkin (1971, 1973). DeSimone and LaFleur (1986) have questioned the validity of the Luzerne readvance based upon their reconstructed ice margins in the northern Hudson Lowland. Wagner (1972) presented evidence for a minor readvance in the northern Champlain Lowland that may have temporarily reestablished freshwater conditions following the initial formation of the Champlain Sea. Denny (1974) proposed that several ice-front oscillations near Covey Hill alternately opened and closed drainage from proglacial lakes in the St. Lawrence basin to the Champlain Lowland. The discharge events removed previously deposited sediment and produced large areas of bare rock such as Flat Rock, near Altona.

Table 1. Comparison of lacustrine and marine water levels and biostratigraphy in the St. Lawrence and Champlain lowlands.

Lacustrine & Marine Water Levels		Biostratigraphy
St. Lawrence Lowland ¹	Champlain Lowland ²	Champlain Lowland ³
	Lake Champlain	
Level V	Port Henry Plattsburgh Burlington Port Kent Beekmantown Upper Marine Limit	<u>Mya</u> Phase <u>Hiatella arctica</u> Phase Transitional Phase
Level IV		
Level III		
Level II	Lake Fort Ann (multiple levels proposed)	Nonmarine
Level I		
	Lake Coveville	

1. Clark and Karrow (1984)

2. Chapman (1937); Wagner (1972); Denny (1974)

3. Elson (1969); Cronin (1977)

PROGLACIAL WATER BODIES

Chapman (1937) proposed a generalized chronostratigraphic framework of proglacial lake stages in the Hudson and Champlain lowlands. Chapman recognized two principal stages of Lake Vermont in the Champlain Lowland, the Coveville and Fort Ann stages, named for their presumed outlet channels (Fig. 2). An earlier stage, the Quaker Springs Stage, proposed by Woodworth (1905), was reintroduced by later authors (e.g. LaFleur, 1965; Stewart and MacClintock, 1969; Wagner, 1972; Connally and Sirkin, 1973). LaFleur (1965) demonstrated that the Quaker Springs, Coveville, and Fort Ann lake stages in the Champlain Lowland were contiguous with impoundments in the Hudson Lowland. Connally and Sirkin (1973) recommended that use of the name Lake Vermont be discontinued and that the previously defined stages be considered as independent lake levels. Other modifications to Chapman's deglacial lake sequence have been proposed (e.g. Wagner, 1972; Connally, 1982; DeSimone and LaFleur, 1986) and these are summarized in Table 1. Denny (1974) and Clark and Karrow (1984) discussed drainage relationships between lakes in the St. Lawrence and Champlain lowlands (Table 1).

The freshwater proglacial lakes persisted until continued northward ice recession allowed marine water to inundate the isostatically depressed St. Lawrence and Champlain lowlands (Fig. 3). Stratified sediment containing marine fossils documents the marine episode, which is referred to as the Champlain Sea. The oldest radiocarbon dates from shell material within the Champlain Valley include 11.7 ka (Parrott and Stone, 1972), 11.8 ka (GSC 2338) and 11.9 ka (GSC 2366) (Cronin, 1979). The Champlain Sea episode has been subdivided based upon the regional distribution of shoreline deposits (Chapman, 1937) and the temporal distribution of faunal assemblages (Elson, 1969; Cronin, 1977; Rodrigues and Richard, 1986). Regression of marine water from the region was caused by isostatic uplift and ended with the establishment of Lake Champlain, ca. 10.0 ka.

Stratified sediments of variable thickness and composition were deposited into the proglacial lake and marine water bodies in the Champlain Valley during deglaciation. Littoral zone sedimentation is characterized by extensive fluviodeltaic sandplains, cobbly to bouldery beach deposits, wave-cut and wave-built terraces, and spits (Chapman, 1937; Denny, 1974). Fine-grained sediment was deposited in deeper water and in quiet-water embayments. Bathymetric lows served as sediment sinks and accumulated thick sequences of bottom sediment, ice-rafted debris, and sediment-flow deposits.

PALEOZOOGEOGRAPHY OF THE CHAMPLAIN SEA

The faunal assemblages of the Champlain Sea have been the subject of studies for over 150 years and continue to receive attention today. Among the most notable paleontologic studies are those of the dwarfed or stunted molluscan fauna by Goldring (1922), the marine mammals by Harington (1977), the macroinvertebrates by Wagner (1970), and the benthic microfaunas, especially the

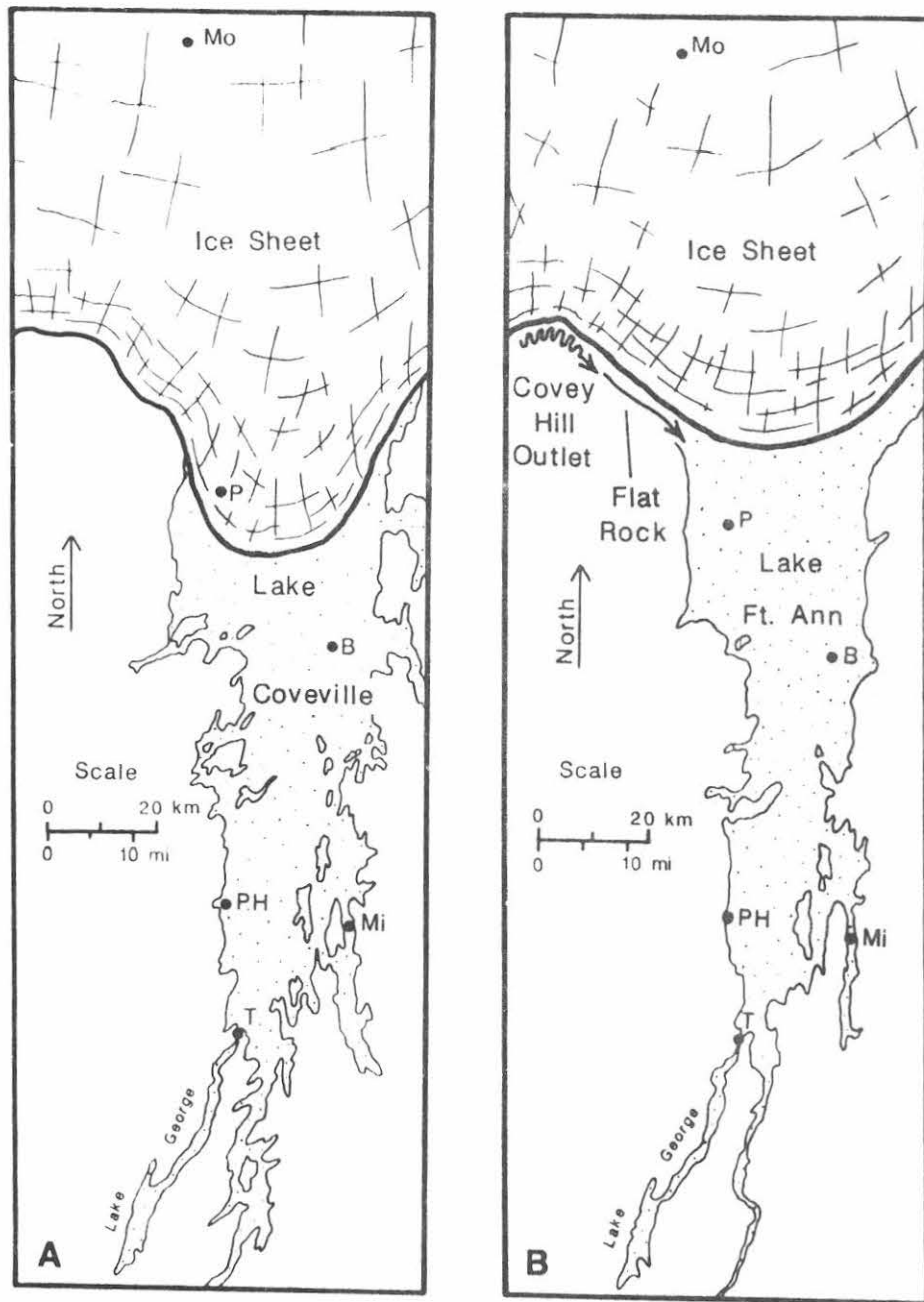


Figure 2. Proglacial lakes in the Champlain Lowland. A) Lake Coveville at its maximum extent. B) Lake Fort Ann showing eastward drainage from Lake Iroquois through the Covey Hill spillway. (After Chapman, 1937; Connally and Sirkin, 1973; and Denny, 1974). Mo- Montreal, P- Plattsburgh, B- Burlington, PH- Port Henry, Mi- Middlebury, T- Ticonderoga.

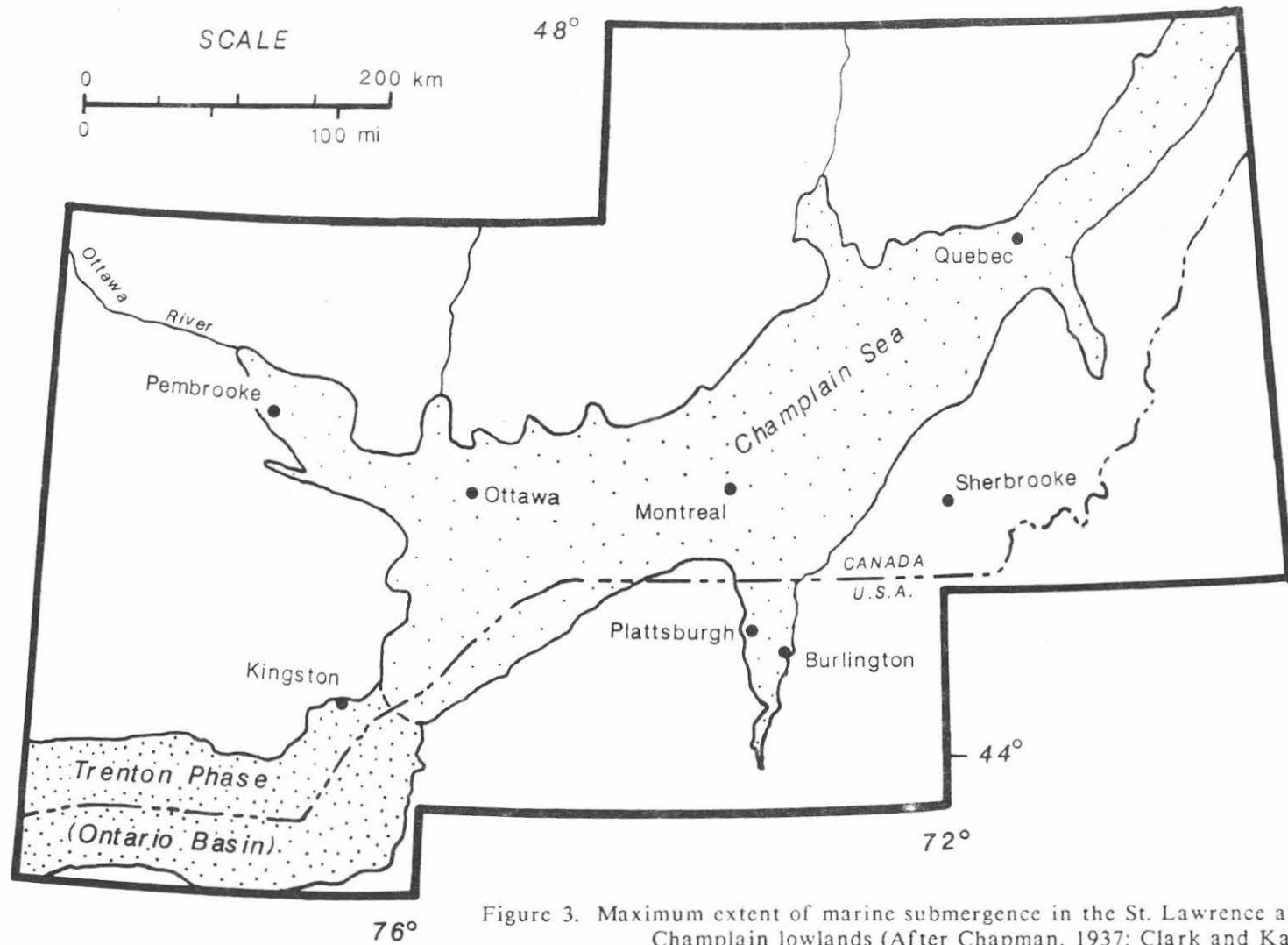


Figure 3. Maximum extent of marine submergence in the St. Lawrence and Champlain lowlands (After Chapman, 1937; Clark and Karrow, 1984; Fulton and others, 1987).

foraminifers and ostracodes (Cronin, 1979, 1981; Guilbault, 1980; Rodrigues and Richard, 1986; Rodrigues, 1987). Wagner (1967) listed published references to the Champlain Sea faunas from 1837 to 1966, while Cronin (1981) and Rodrigues and Richard (1986) provide references to more recent work.

Postglacial faunas from northeastern North America

Ostracodes from the eastern Goldthwait Sea of western Newfoundland, the western Goldthwait Sea of Quebec, the Presumpscot Formation of Maine, and the Boston "blue clay" of Massachusetts have been studied and compared to ostracodes from three regions of the Champlain Sea; the southern region in the Champlain Lowland, the western region in eastern Ontario, and the eastern region between Montreal and Quebec City (Cronin, in press). Intraregional and extraregional comparisons of the ostracode assemblages were made using the binary Otsuka coefficient of faunal similarity. The results showed that three of the four highest similarities were among the three Champlain Sea regions. Within the Champlain Sea regions, the highest similarity between the western and southern regions was highest and that between the eastern and western regions was next highest. The third highest similarity was found between the faunas from the eastern Champlain Sea and the western Goldthwait Sea.

The results indicate that the Champlain Sea faunas are distinct from other postglacial faunas because of the predominance of eurytopic species and the presence of non-marine taxa. Atlantic coast postglacial ostracode assemblages are distinct and reflect their location adjacent to open North Atlantic water. The results also indicate that the constriction in the St. Lawrence Lowland near Quebec City did not serve as a barrier for marine invertebrates since the assemblages from the eastern Champlain and Goldthwait seas are similar.

Extraregional Comparisons

The combined postglacial ostracode fauna of northeastern North America, including the Champlain Sea, was compared to other high latitude faunas (Cronin, in press) to provide a large-scale zoogeographical perspective. The northeastern North American faunas display the highest similarity to the modern fauna at Novaya Zemlya, with 29 species in common. A relatively low but still significant similarity was observed between the North American postglacial faunas and the Late Pliocene fauna of the Daishaka Formation of northern Honshu, Japan recently studied by Tabuki (1986). The Daishaka Formation contains a cold water marine fauna, the Omma-Manganji fauna, that represents an interval of cool climate during which high latitude species migrated southward as they did in the western North Atlantic during glacial periods. Cronin and Ikeya (1987) recently studied the Omma-Manganji fauna from other formations in Japan and found at least 26 circumpolar ostracode species common to both the western North Pacific and North Atlantic oceans. At least 11 ostracode species occurring in the Omma-Manganji fauna also occur in the Champlain Sea deposits and another 10 species occur in the Goldthwait Sea deposits and the Presumpscot Formation.

In summary, the microfaunal record of the Champlain Sea has not only provided important insight into local and regional paleoenvironments during the final withdrawal of continental ice from the Champlain Lowland region it also contains important information concerning the evolution and paleogeography of circumpolar species.

DESCRIPTION OF FIELD TRIP LOCALITIES

STOP #1: Town Gravel Pit, Isle LaMotte, Vermont

The predominant lithofacies consists of thinly bedded, molluscan-rich sand with minor gravelly sand and sandy to silty mud interbeds. The sands are generally medium to coarse grained and are cross bedded or horizontally laminated. Individual beds range from a few centimeters to about 20 cm thick and can be traced laterally for several meters. The sandy facies contains two biofacies, a Macoma balthica facies and a Mytilus edulus facies. The faunal assemblages were previously described by Cronin (1977 (loc. 11), 1979, 1981 (loc. 33)). Articulated valves of both species are commonly found in living position. Occurrences of Mytilus in living position in Champlain Sea deposits are rare since this mollusc usually lives attached to the substrate by a byssus and its two valves have an adont hinge that disarticulates easily.

Ostracodes and benthic foraminifers are rare in these sands. The following species occur;

Cyprideis sp.

Cythere lutea (Mueller, 1785)

Cytheromorpha macchesneyi (Brady and Crosskey, 1871)

Cytheropteron latissimum (Brady, Crosskey, and Robertson, 1874)

Cytherura gibba (Mueller, 1875)

Eucythere declivis (Norman, 1865)

Finmarchinella logani (Brady and Crosskey, 1871)

Heterocyprideis sorbyana (Jones, 1857)

Ilyocypris gibba (Rahmdohr, 1808)

Leptocythere quebecensis (Cronin, 1981)

Palmenella limicola (Norman, 1865)

Sarsicytheridea bradii (Norman, 1865)

Sarsicytheridea macrolaminata (Elofson, 1939)

Sarsicytheridea punctillata (Brady, 1865)

Semicytherura cf. similis (Sars, 1865)

These deposits probably represent the latest phase of the Champlain Sea in this region known as the Mya arenaria Phase (Elson, 1969; Cronin, 1977). Mya arenaria is absent at this locality because it is usually found in clay substrates in low-lying areas west of Lake Champlain. Based on modern temperature tolerances of the ostracode species, the annual temperature range is estimated to have been about 0° to 20°C. Salinities during the Mya Phase were oligohaline to mesohaline (1 to 18 ppt) and all the ostracode species occurring at the Isle LaMotte locality tolerate, and often thrive in brackish water environments.

A coarse gravel facies that contains decimeter-scale foreset beds that range from poorly sorted coarse pebbly sand to open-work cobble gravel was recently exposed in a small excavation at the south end of the pit. The facies contains marine fossils that are commonly disarticulated and fragmented. The gravel facies underlies the fossiliferous sand facies described above and may be related to coarse gravel in an excavation 0.5 km to the west. Gravel foresets at both localities indicate a southward to southeastward paleocurrent. It is difficult to reconstruct the sedimentary environment that existed at the time the gravel facies was deposited because of the limited extent of the exposure at this locality. The gravel facies may be related to a high-energy littoral marine environment during the late regressive phase of the Champlain Sea. Alternatively, it may represent ice-proximal subaqueous outwash that was deposited during ice recession or possibly an ice readvance. A readvance of this nature had been previously proposed by Wagner (1972) based upon stratigraphic evidence from northwestern Vermont.

STOP #2: Beach Ridges of the Champlain Sea, Sciota, New York

The ridges consist of coarse, flaggy gravel that is derived from the underlying Potsdam Sandstone. Outcrops of sandstone can be observed in drainage ditches nearby and presumably bedrock underlies the ridges at a shallow depth. These ridges were mapped and described by Denny (1970, 1974) who traced them over a distance of 0.3 km. They trend roughly north-south but curve westward at their northern ends along the margin of a former headland. The elevations of the ridge crests lie between 91 and 98 m.

STOP #3: Ingraham Esker, Ingraham, New York

The sedimentology and stratigraphy of the Ingraham Esker was summarized by Denny (1972, 1974) and more recently by Diemer (in press). The esker consists predominantly of upwardly fining subaqueous outwash that was deposited in a series of esker fans at the terminus of the northward retreating ice front. The ridge is overlain by fresh water rhythmites which are in turn conformably overlain by a massive mud facies. Diemer (in press) attributes the massive mud facies to an early, transitional phase between fresh (Lake Fort Ann) and marine conditions (Champlain Sea). The section is unconformably overlain by coarse, fossiliferous gravel that probably represents wave-reworking of the previously deposited sediment during the marine regression. Denny (1972, 1974) attributed the low relief of the ridge to extensive wave erosion, however, Diemer (in press) suggests that the morphology of the ridge is a consequence of its origin as subaqueous outwash.

The faunal assemblages at this locality were described by Cronin (1977, loc. 18; 1979, 1981, loc. 4). Hazel studied ostracodes from several localities in the esker and found a total of nine species (in Denny, 1972). The esker's faunas represent the Hiatella artica Phase of the Champlain Sea (Elson, 1969; Cronin, 1977) which occurred between 11.6 to 10.6 ka. The following ostracodes were found at this locality in the shelly marine gravels that cap the rhythmite facies.

Candona sp.
Cythere lutea (Mueller, 1785)
Cytheromorpha macchesneyi (Brady and Crosskey, 1871)
Cytheropteron champlainum (Cronin, 1981)
Cytheropteron latissimum (Norman, 1865)
Finmarchinella logani (Brady and Crosskey, 1871)
Heterocyprideis sorbyana (Jones, 1857)
Sarsicytheridea bradii (Norman, 1865)
Sarsicytheridea punctillata (Brady, 1865)

The annual range of bottom-water paleotemperature was probably 0^o to 12^oC and salinities were polyhaline, between 18 and 30 ppt, as indicated by the faunal assemblages. This salinity was the closest to normal marine conditions that was reached in this part of the Champlain Sea, at least for shallow-water environments.

STOP #4: Korths Farm Section, East Beekmantown, New York

This stop will involve two sections along the east bank of Ray Brook. Cronin (1977, loc. 34; 1979, 1981, loc. 84) described the faunal assemblages from the northern section approximately 100 m upstream from the Korths Farm road. Marine clays (formerly known as the Leda clay) overlie rhythmites and contain the mollusc Portlandia arctica and the following ostracodes;

Cytheromorpha macchesneyi (Brady and Crosskey, 1871)
Cytheropteron latissimum (Brady, Crosskey, and Robertson, 1874)
Heterocyprideis sorbyana (Jones, 1857)
Sarsicytheridea bradii (Norman, 1865)
Sarsicytheridea macrolaminata (Elofson, 1939)
Sarsicytheridea punctillata (Brady, 1865)

The faunas at this locality represent the Transitional Phase of the Champlain Sea (Cronin, 1977), which has been dated between 11.6 and 12.0 ka, however, the age for the earliest marine inundation in the region is not yet certain. The bottom-water temperatures ranged annually from about -2^o to 10^oC. Normal marine and polyhaline ostracodes are absent from the Transitional Phase and salinities fluctuated between 0 and 18 ppt. The term "Transitional Phase" was given to this interval because the faunas indicate a lacustrine to marine transition during which there was mixing of pre-Champlain Sea freshwater with the earliest influx of marine water that entered the region via the St. Lawrence estuary.

The southern section, 50 m downstream from the Korths Farm road, resulted from recent cutbank erosion. Approximately 3 m of flow-slide colluvium, derived primarily from the marine clay unit described above, overlie intact marine clay. The base of the colluvium is marked by an erosional unconformity that includes buried logs. The freshwater rhythmites were not observed at this section but may occur on or below the stream bed. Geomorphological evidence for other flow-slides exists throughout this part of the Ray Brook valley.

STOP #5: Slump-earthflow, Whallonsburg, New York

The Whallonsburg slump-earthflow (Fig. 4) occurred during the night of 28 July, 1987, following localized, light to moderate thunderstorm activity. The slump involved the eastward displacement of 0.9 ha of Pleistocene lacustrine sediment on a cutbank of the Bouquet River. This portion of the Bouquet Valley has a history of landslide activity (Newland, 1938; Whitcomb, 1938; Buddington and Whitcomb, 1941). The 1987 Whallonsburg slump was described by Franzi, Bogucki, and Allen (1988).

The slump is roughly rectangular in plan with an average length of 85 m and an average width of 110 m. The crown is 16 m above stream level. A 0.2 ha toe bulge, composed of highly plastic clay and alluvial sediment, was raised to a height of 4.5 m in the stream channel. The slump consists of a primary mass that was involved in the initial slump and two smaller retrogressive slumps (Fig. 4).

The slump exposed 0.5 to 1 m of coarse sand and gravel over 4 m of nonfossiliferous lacustrine clay and silt at the headscarp. The lacustrine section is estimated to be 23 m thick based upon seismic refraction data from the crown. The clays are characterized by high plasticity and natural water content with low bulk density and shear strength (Fig. 5). The lacustrine unit grades upward from soft, blue-gray, thinly laminated, clay and clayey silt rhythmites to stiff, brown, thinly bedded silt and clay. The textural variation probably reflects the effects of shoaling or infilling during the waning stages of the lake's history. The overlying gravel is part of a large terrace that may be graded to Late Pleistocene marine deltas near Willsboro.

Hillslope reconstructions based on slide-deposit morphometry and laboratory analysis of the long-term shear strength of undisturbed clay samples were used to determine the geological controls on slope stability (Franzi, Bogucki, and Allen, 1988). The factor of safety (FS = resisting forces/driving forces) of the reconstructed preslide slope was calculated using the slope stability model STABR (Duncan and Wong, 1985) under a range of "likely" pore pressure conditions. The results indicate that the preslide factor of safety was close to the threshold value of 1.0 (range 1.0 to 1.2). Although the slump may have been triggered by the rainstorm activity, the actual cause is probably related to pore pressure conditions at the clay-bedrock contact and long-term processes such as cutbank erosion at the toe of the slope and fissure development in the upper, overconsolidated clay.

ACKNOWLEDGEMENTS

The authors would like to thank Fred Larsen (Norwich University), Robert LaFleur (Rensselaer Polytechnic Institute) and Donald Bogucki (S.U.N.Y., Plattsburgh) for critically reviewing the manuscript and providing many useful suggestions. John Diemer (Franklin and Marshall College) provided a prepublication copy of his Ingraham esker paper and his insights concerning the complex sedimentology of the esker deposits are greatly appreciated. Special thanks are extended to Samuel Clemence (Syracuse University) for his help with the geotechnical aspects of the Whallonsburg slump-earthflow.

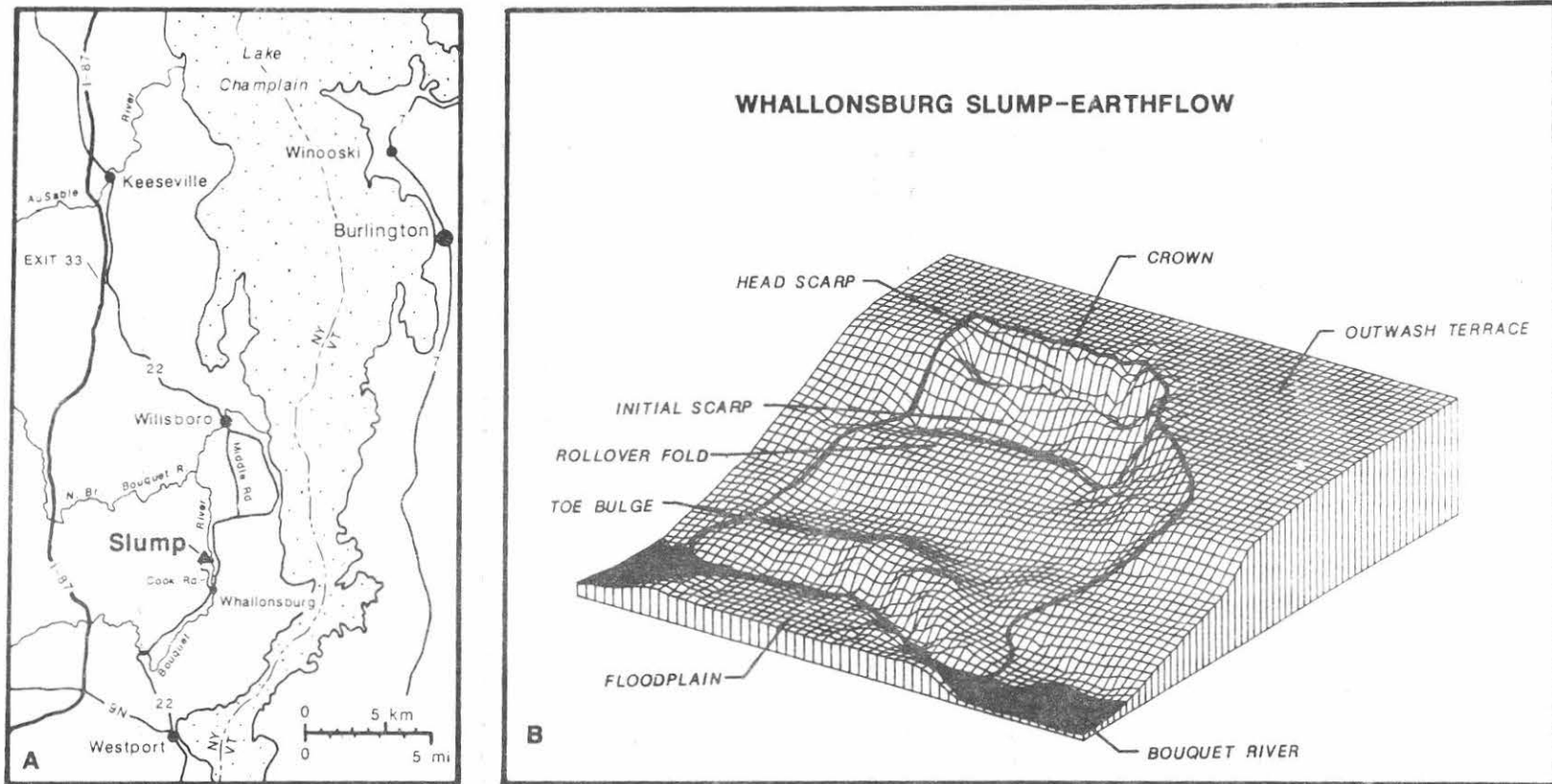


Figure 4. The Whallonsburg slump-earthflow. A) Location map. B) Block diagram showing the major morphological features (From Franzi, Bogucki, and Allen, 1988).

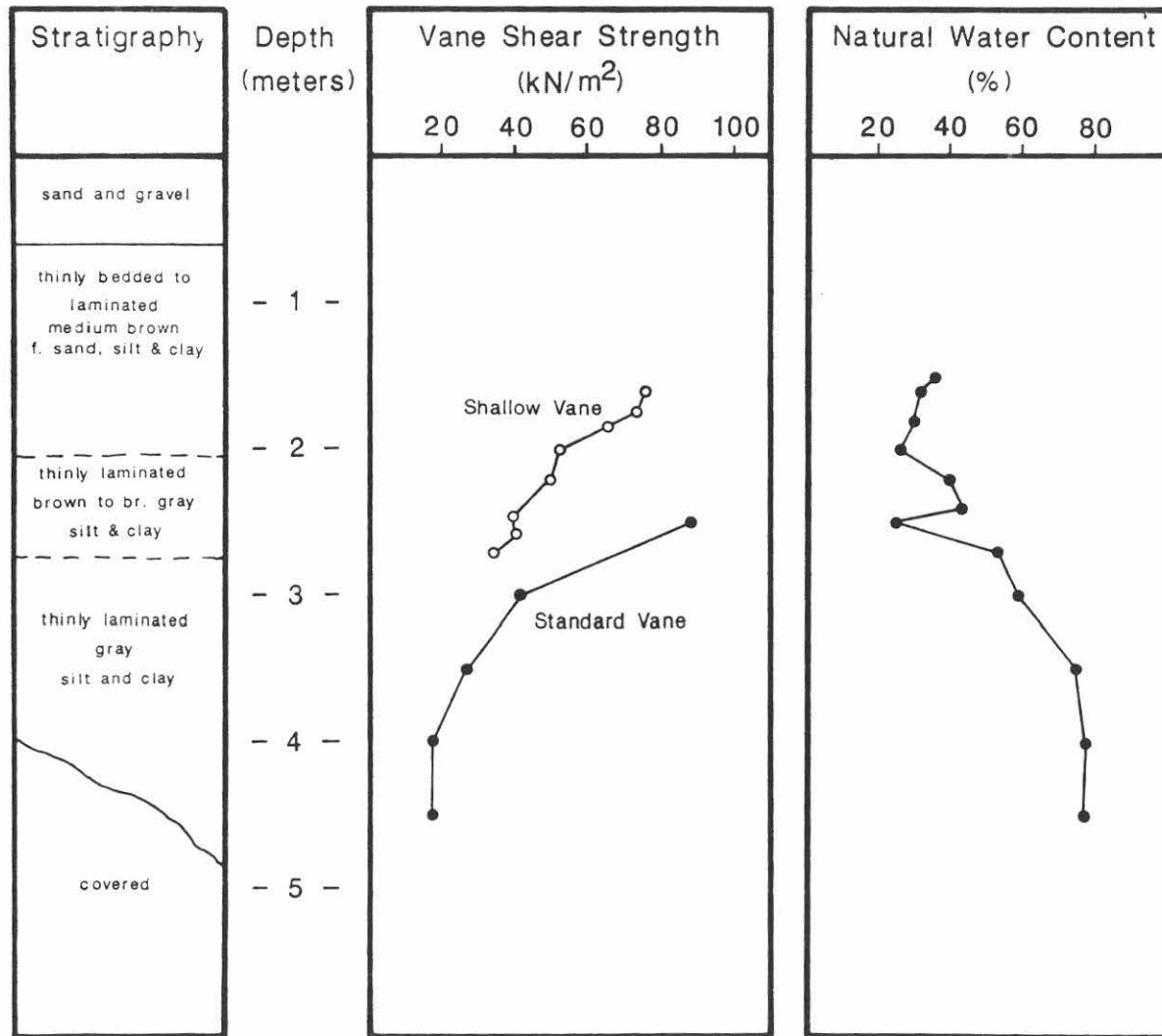


Figure 5. Vane shear strength and natural water content of lacustrine sediment exposed at the headscarp of the slump-earthflow near Whallonsburg (Franzi, unpub. data).

REFERENCES CITED

- Ackerly, S.C., and Larsen, F.D., 1987, Ice flow patterns in the Green Mountains, central Vermont: in Westerman, D.S. (ed.), Guidebook for field trips in Vermont, Volume 2: New England Intercoll. Geol. Conf., Montpelier, Vermont, p.369-382.
- Alling, H.L., 1916, Glacial lakes and other glacial features of the central Adirondacks: Geol. Soc. Amer. Bull., V.27, p.645-672.
- Buddington, A.F., and Whitcomb, L., 1941, Geology of the Willsboro Quadrangle: New York State Mus. Bull., No.325, 137p.
- Chapman, D.H., 1937, Late-glacial and postglacial history of the Champlain Valley: Amer. Jour. Sci., V.34 (5th Ser.), p.84-124.
- Clark, P., and Karrow, P.F., 1984, Late Pleistocene water bodies in the St. Lawrence Lowland, New York, and regional correlations: Geol. Soc. Amer. Bull., V.95, p.805-813.
- Connally, G.G., 1972, Proglacial lakes in the Lamoille Valley, Vermont: in Doolan, B.L. and Stanley, R.S. (eds.), Guidebook for field trips in Vermont: New England Intercoll. Field Conf., p.343-358.
- , 1982, Deglacial history of western Vermont: in Larson, G.J. and Stone, B.D. (eds.), Late Wisconsinan glaciation in New England: Kendall/Hunt, Dubuque, Iowa, p.47-69.
- Connally, G.G., and Calkin, P.E., 1972, Woodfordian glacial history of the Champlain Lowland, Burlington to Brandon, Vermont: in Doolan, B.L. and Stanley, R.S. (eds.), Guidebook for field trips in Vermont: New England Intercoll. Field Conf., p.389-397.
- Connally, G.G., and Sirkin, L.A., 1970, The Luzerne Readvance near Glens Falls, New York: Geol. Soc. Amer., V.82, p.989-1008.
- , 1973, Wisconsinan history of the Hudson-Champlain Lobe: in Black, R.F., Goldthwait, R.P., and Willman, H.B. (eds.), The Wisconsinan Stage: Geol. Soc. Amer. Mem. 136, p.47-69.
- Cronin, T.M., 1977, Late-Wisconsinan marine environments of the Champlain Valley (New York, Vermont): Quaternary Research, V.7, p.238-253.
- , 1979, Late Pleistocene benthic foraminifers from the St. Lawrence Lowlands: Jour. Paleo., V.53, p.781-814.
- , 1981, Paleoclimatic implications of Late Pleistocene marine ostracodes from the St. Lawrence Lowlands: Micropalaeontology, V.27, p.384-418.

- , in press, Paleozoogeography of post-glacial Ostracoda from northeastern North America: in Gadd, N. (ed.), Late Quaternary development of the Champlain Sea basin: Geological Assoc. Canada Spec. Paper
- Cronin, T.M., and Ikeya, Noriyuki, 1987, The Omma-Manganji ostracode fauna (Plio-Pleistocene) of Japan and the zoogeography of circumpolar species: *Micropaleontology*, V.6, p.65-88.
- Denny, C.S., 1972, The Ingraham Esker, Chazy, New York: U.S. Geol. Survey Prof. Paper 800-B, p.B35-B41.
- , 1974, Pleistocene geology of the northeast Adirondack region, New York: U.S. Geol. Surv. Prof. Paper, No.786, 50p.
- DeSimone, D.J., and LaFleur, R.G., 1986, Glaciolacustrine phases in the northern Hudson Lowland and correlatives in western Vermont: *Northeastern Geology*, V.8, No.4, p.218-229.
- Diemer, J.A., in press, Subaqueous outwash deposits in the Ingraham ridge, Chazy, New York: *Sedimentology*.
- Diemer, J.A., Olmsted, J.F., and Sunderland, L., 1984, The evolution of a high-altitude glacial lake, Keene Valley, New York: *Geol. Soc. Amer. Bull. Abstr. with Prog.*, V.16, No.1, p.12.
- Diemer, J.A., and Franzi, D.A., this volume, Aspects of the glacial geology of the Keene and lower Ausable valleys, northeastern Adirondacks.
- Duncan, J.M., and Wong, K.S., 1985, STABR: A computer program for slope stability analysis with circular slip surfaces, microcomputer version: Dept. Civil Eng., Virginia Polytechnic Institute, Blacksburg, Virginia, 20p.
- Elson, J.A., 1969, Radiocarbon dates, Mya arenaria phase of the Champlain Sea: *Canadian Jour. Earth Sci.*, V.6, p.367-372.
- Franzi, D.A., Bogucki, D.J., and Allen, E.B., 1988, Recent slump-earthflow near Whallonsburg, Essex County, New York: *Geol. Soc. Amer. Abstr. with Prog.*, V.20, No.1, p.19.
- Fulton, R.J., Anderson, T.W., Gadd, N.R., Harington, C.R., Kettles, I.M., Richard, S.H., Rodrigues, C.G., Rust, B.R., and Shilts, W.W., 1987, Summary of the Quaternary of the Ottawa region: in Fulton, R.J. (ed.), Quaternary of the Ottawa region and guides for day excursions: XIIth INQUA International Congress, Ottawa, Canada, p.7-20.
- Goldring, W., 1922, The Champlain Sea, evidence of its decreasing salinity southward as shown by the character of the fauna: *New York State Mus. Bull.*, 232-240, p.53-194.
- Guilbault, J.-P., 1980, Stratigraphic approach to the study of the late-glacial Champlain Sea deposits with the use of foraminifera: unpublished doctoral dissertation, Aarhus University, Denmark.

- Harrington, C.F., 1977, Marine mammals in the Champlain Sea and the Great Lakes: *Annals of the New York Academy of Science*, V.288, p.508-537.
- Hughes, T., Borns, H.W., Jr., Fastook, J.L., Hyland, M.R., Kite, J.S., and Lowell, T.V., 1985, Models of glacial reconstruction and deglaciation applied to maritime Canada and New England: *in* Borns, H.W., Jr., LaSalle, P., and Thompson, W.B. (eds.), *Late Pleistocene history of northern New England and adjacent Quebec*: *Geol. Soc. Amer. Spec. Paper* 197, p.139-150.
- LaFleur, R.G., 1965, *Glacial geology of the Troy, New York quadrangle*: *New York State Mus. and Sci. Serv., Map and Chart Ser., No.9*, 23p.
- Larsen, F.D., 1972, *Glacial history of central Vermont*: *in* Doolan, B.L. and Stanley, R.S. (eds.), *Guidebook for field trips in Vermont: New England Intercoll. Field Conf.*, p.296-316.
- , 1987, *History of glacial lakes in the Dog River Valley of central Vermont*: *in* Westerman, D.S. (ed.) *Guidebook for field trips in Vermont, Volume 2: New England Intercoll. Geol. Conf., Montpelier, Vermont*, p.213-236.
- Newland, D.H., 1938, *The landslide on the Bouquet River near Willsboro, New York*: *New York State Museum Circular*, No.20, 7p.
- Parrott, W.R. and Stone, B.D., 1972, *Strandline features and Late Pleistocene chronology of northwest Vermont*: *in* Doolan, B.L. and Stanley, R.S. (eds.), *Guidebook for field trips in Vermont: New England Intercoll. Geol. Field Conf.*, p.359-376.
- Rodrigues, C.G. and Richard, S.H., 1986, *An ecostratigraphic study of Late Pleistocene sediments of the western Champlain Sea basin, Ontario and Quebec*: *Geol. Surv. Canada Spec. Paper*, No.85-22, p.1-33.
- Rodrigues, C.G., 1987, *Late Pleistocene invertebrate macrofossils, microfossils, and depositional environments of the western basin of the Champlain Sea*: *in* Fulton, R.J. (ed.), *Quaternary geology of the Ottawa region, Ontario and Quebec*: *Geol. Surv. Canada Paper*, No.86-23, p.16-23.
- Stewart, D.P. and MacClintock, P., 1969, *The surficial geology and Pleistocene history of Vermont*: *Vermont Geol. Survey Bull.*, No.31, 251p.
- Tabuki, R., 1986, *Plio-Pleistocene Ostracoda from the Tsugaru Basin, North Honshu, Japan*: *Bulletin College of Education, University of the Ryukyus*, V.29, No.2, p.27-160.
- Wagner, F.J.E., 1967, *Published references to the Champlain Sea faunas 1837-1966 and list of fossils*: *Geol. Surv. Canada Paper*, No.67-16, p.1-87.
- , 1970, *Faunas of the Pleistocene Champlain Sea*: *Geol. Surv. Canada Bull.*, V.181, p.1-104.

Wagner, W.P., 1972, Ice margins and water levels in northeastern Vermont: in
Doolan, B.L. and Stanley, R.S. (eds.), Guidebook for field trips in Vermont:
New England Intercoll. Geol. Field Conf., p.297-316.

Whitcomb, L., 1938, Possible landslip scars on the Bouquet River at Willsboro, New
York: Science, V.87, No. 2267, p.530-531.

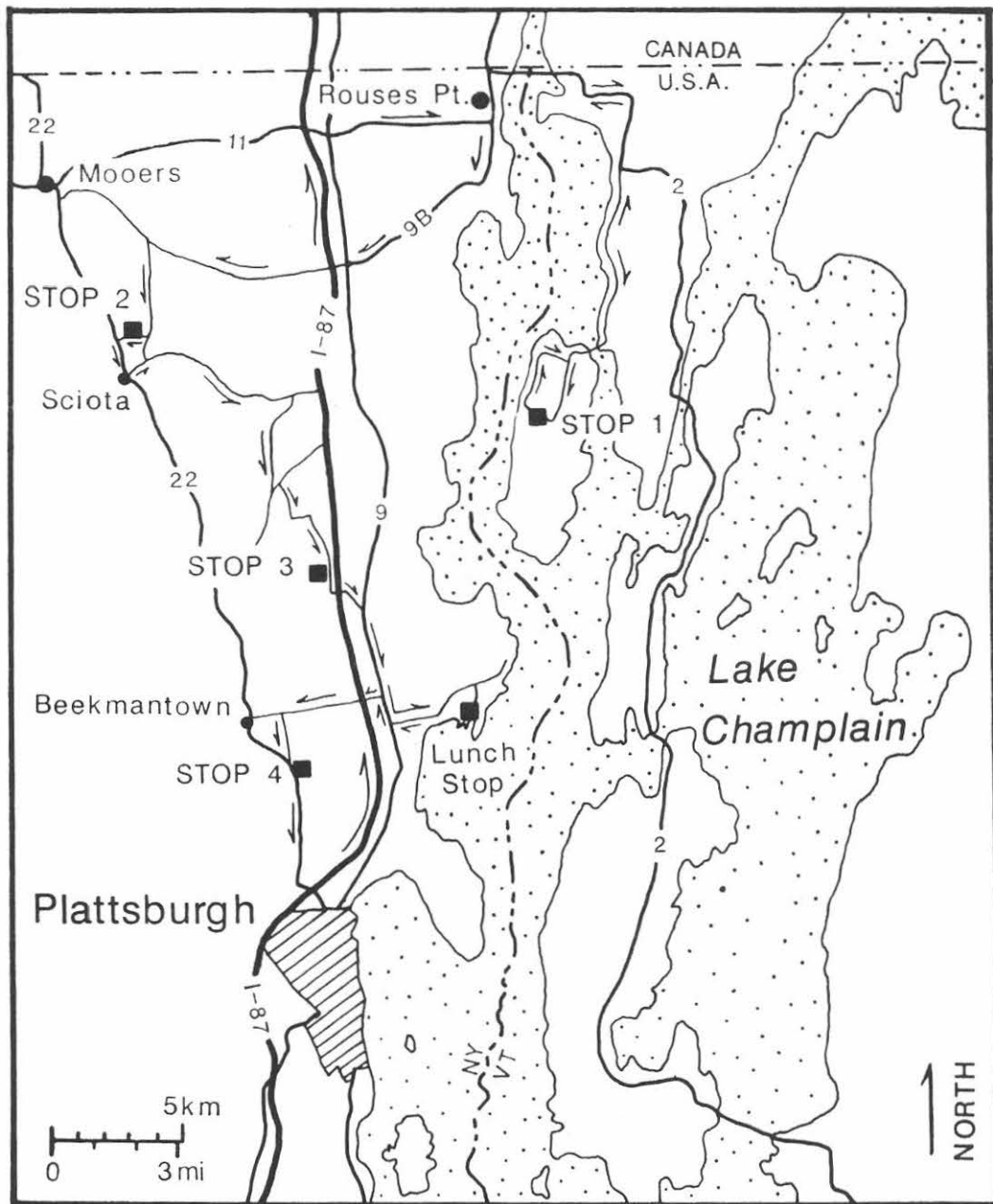
Woodworth, J.B., 1905, Ancient water levels of the Champlain and Hudson valleys:
New York State Mus. Bull., No.84, 265p.

ROAD LOG

CUM. MILES	MILES F.L.P.*	DESCRIPTION**
0.0	0.0	Assemble in the west parking lot of Hudson Hall on the P.S.U.C. campus. Leave parking area, turn right at entrance, and proceed northwestward on Broad St.
0.1	0.1	Traffic light, continue northwestward on Broad St.
0.2	0.1	Traffic light, continue northwestward on Broad St.
0.4	0.2	Traffic light at intersection of Broad and Cornelia streets. Bear left onto Cornelia and proceed westward. Continue westward on Cornelia St. through two traffic lights.
1.1	0.7	Junction I-87 North; Turn right onto entrance ramp and proceed northward to Exit 42 in Champlain.
6.3	5.2	Outcrop of the Cumberland Head argillite.
14.4	8.1	Outcrop of the Chazy Gp.
21.8	7.4	Exit 42, Champlain, N.Y.; Exit I-87 and proceed to the Route 11 intersection.
21.9	0.1	Turn right onto Route 11 and proceed eastward to Rouses Point.
23.1	1.2	Bridge over Great Chazy River.
26.6	3.5	Intersection of Routes 11 and 9B. Turn left at stop sign and proceed northward through the village of Rouses Point.
27.7	1.1	Intersection of Routes 11, 9B and 2. Turn right and proceed eastward toward the Korean Veterans Memorial Bridge.
28.3	0.6	Korean Veterans Memorial Bridge (formerly Rouses Point Bridge). The ruins of Fort Blunder (Ft. Montgomery), an American fort that was originally built on Canadian soil, can be seen on your left. The "blunder" was corrected by moving the border northward.

* From last point

** Refer to Fig. 6 for stops 1-4 and Fig. 4A for stop 5.



↗ Trip Route

Figure 6. Location map for field-trip localities 1-4.

CUM. MILES	MILES F.L.P.	DESCRIPTION
28.6	0.3	Vermont state line. Continue eastward on Route 2 to the village of Alburg.
32.2	3.6	Alburg, Vermont.
33.3	1.1	Route 2 bears to the left; turn sharply right onto unmarked road and proceed southward along lake shore.
37.5	4.2	Outcrop of Stony Point argillite.
37.7	0.2	Intersection of unmarked road and Vermont Route 129. Turn right at stop sign and proceed southward across causeway to Isle LaMotte.
40.3	2.6	Route 129 ends in the village of Isle LaMotte at a crossroad. Turn right adjacent to a large, gray limestone building onto unmarked road and proceed westward.
40.7	0.4	STOP #1. Isle LaMotte Landfill.
41.1	0.4	Gravel pit. Coarse gravel foresets indicating a southerly paleocurrent are exposed in the working face of the pit.
41.2	0.1	Stop sign at a "T" intersection. Turn right and proceed northward along the lake shore.
42.3	1.1	St. Anne's Shrine. The road takes a 90 ⁰ turn to the right (east) immediately north of the shrine entrance.
43.3	1.0	Intersection of unmarked road and Vermont Route 129. Turn left at stop sign and proceed northward on Route 129.
44.3	1.0	Isle LaMotte causeway. Continue northward across causeway on Route 129.
44.4	0.1	Intersection with unmarked road. Turn left onto unmarked road and proceed northward along the lake shore to Alburg.
48.7	4.3	Intersection of unmarked road and Route 2 in Alburg. Turn left onto Route 2 and proceed northward through town.
53.7	5.0	Korean Veterans Memorial Bridge. Continue eastward across bridge to Rouses Point, New York.

CUM. MILES	MILES F.L.P.	DESCRIPTION
54.2	0.5	Intersection of Routes 2, 11, and 9B. Turn left and proceed southward on Routes 11 and 9B through Rouses Point.
55.4	1.2	Route 11 turns westward, turn right and continue on Route 11.
58.9	3.5	Bridge over Great Chazy River. Continue westward on Route 11.
59.5	0.6	Intersection of Routes 9 and 11. Turn left onto Route 9 and proceed southward.
62.7	3.2	Intersection of Routes 9 and 9B and LaValley Road. Turn right and proceed westward on LaValley Road.
67.0	4.3	Cross Great Chazy River and continue westward on LaValley Road.
67.7	0.7	Intersection of LaValley and McBride roads. Turn left and proceed southward on McBride Road.
68.0	0.3	Cross Great Chazy River and continue southward on McBride Road.
69.1	1.1	McBride Road bears sharply eastward. Turn right onto George Duprey Road and proceed southward.
69.7	0.6	Intersection of George Duprey and Blair roads. Turn right onto Blair Road and proceed westward.
70.0	0.3	STOP #2. Champlain Sea beach ridges. Continue westward following the discussion at this stop.
70.3	0.3	Intersection of Blair Road and Route 22. Turn left onto Route 22 and proceed southward to Scioto.
71.7	1.4	Intersection of Routes 22 and 191 in Scioto. Turn left onto Route 191 and proceed eastward.
76.2	4.5	Intersection of Route 191 and Sand Ridge Road at the W.H. Miner Agricultural Institute. The Miner Institute is affiliated with the Center for Earth and Environmental Science at P.S.U.C.
		Turn right onto Ridge Road and proceed southward. The road follows the crest of the Ingraham Esker. Note that in places gravel operations have removed nearly all the esker material except for that under the road.

CUM. MILES	MILES E.L.P.	DESCRIPTION
77.4	1.2	Lake Alice, named for Alice Miner. Continue southward on Ridge Road.
78.9	1.5	Intersection of Ridge and Clark roads. Turn left onto Clark and proceed eastward to Old Route 348.
79.0	0.1	Intersection of Clark Road and Old Route 348. Turn left onto Old Route 348 and proceed northeastward.
79.3	0.3	Intersection of Old Route 348 and Ashley Road. Turn right onto Ashley Road and proceed southward along the crest of the esker.
80.2	0.9	Cross the Little Chazy River and continue southward to the Slosson Road intersection.
80.3	0.1	Intersection of Ashley and Slosson roads. Turn left onto Slosson road and proceed eastward.
80.6	0.3	Cross the Little Chazy River and continue eastward to the Esker Road intersection.
80.7	0.1	Intersection of Slosson and Esker (Ridge Road on some maps) roads. Turn right and proceed southward on Esker Road. The road follows the crest of the esker.
80.8	0.1	Cross the Little Chazy River and continue southward.
82.2	1.4	STOP #3. Ingraham Esker. Continue southward to the Stratton Hill Road intersection following the discussions at this stop. The next stop will be at Point Au Roche State Park for lunch.
82.7	0.5	Intersection of Esker and Stratton Hill roads. Turn left and proceed eastward across I-87 overpass on Stratton Hill Road.
82.9	0.2	Intersection of Stratton Hill Road and an unmarked road. Turn right at the stop sign and proceed southward on Stratton Hill Road to the hamlet of Ingraham.
83.9	1.0	Intersection Stratton Hill Road and Route 9. Turn right and proceed southward on Route 9. The esker crosses the highway 0.3 mi south of this intersection.
86.0	2.1	Intersection of Route 9 and Point Au Roche Road. Turn left and proceed eastward on Point Au Roche Road.
87.6	1.6	Entrance to Point Au Roche State Park (beach and picnic area). Turn right into park for lunch.

CUM. MILES	MILES F.L.P.	DESCRIPTION
		After lunch proceed to entrance and turn left onto Point Au Roche Road.
89.2	1.6	Intersection of Point Au Roche Road and Route 9. Turn right onto Route 9 and proceed northward to blinking light at the Spellman Road intersection.
89.6	0.4	Intersection of Route 9 and Spellman Road. Turn right and proceed westward on Spellman Road.
90.1	0.5	Continue westward on Spellman Road across the I-87 overpass.
91.8	1.7	Continue westward across railroad crossing.
92.0	0.2	Intersection of Spellman and Ashley roads. Turn left and proceed southward on Ashley Road.
93.1	1.1	Cross Ray Brook and continue southward to Route 22 intersection.
93.3	0.2	STOP #4, Korths Farm Sections. Park along the side of the road near the cemetery at the intersection of Ashley Road and Route 22.
		Proceed southward on Route 22 following the discussions at this stop. For those who do not wish to continue to Stop 5 (Whallonsburg Slump-earthflow) follow the road log to the I-87 interchange in Plattsburgh.
96.1	2.8	Intersection of Routes 9 and 348. Turn left and proceed eastward to the I-87 interchange.
96.3	0.2	Entrance ramp for I-87 southbound. For those who wish to continue to Stop 5, turn right onto I-87 and proceed southward to Exit 33 south of Keeseville.
115.6	19.3	Exit 33. Turn right onto exit ramp.
115.9	0.3	Intersection of exit ramp and I-87 overpass. Turn left and proceed eastward across overpass.
116.0	0.1	Intersection of Routes 9 and 22 at traffic light. Proceed straight through the intersection and proceed southeastward on Route 22 to Willsboro.
124.2	8.2	Cross the Bouquet River at Willsboro and continue southward on Route 22 through town.

CUM. MILES	MILES F.L.P.	DESCRIPTION
124.6	0.4	Intersection of Route 22 and Middle Road. Turn sharply right onto Middle Road and proceed southward.
128.2	3.6	Intersection of Middle Road and Route 22. Turn right onto Route 22 and proceed westward on Route 22.
129.3	1.1	Route 22 curves sharply southward. Continue on Route 22 to Whallonsburg.
131.9	2.6	Cross Bouquet River and proceed to intersection of Cook Road (0.1 mi)
132.0	0.1	Intersection of Route 22 and Cook Road. Turn sharply onto Cook Road and proceed northward. The roadbed is composed of wollastonite tailings from nearby mines in Willsboro.
132.9	0.9	STOP #5, Whallonsburg slump-earthflow. Leave cars and follow the trail northward to the slump. Proceed southward on Cook Road to the intersection with Route 22 following the discussions at this stop.
133.8	0.9	Intersection of Cook Road and Route 22. For those with southbound destinations turn right and follow Route 22 southward to Route 9N in Westport. From this point follow the signs to I-87. For those with northbound destinations turn left and follow Route 22 northward through Willsboro to its intersection with I-87 near Keeseville.
		END LOG

LATE QUATERNARY GLACIAL TO MARINE SUCCESSIONS
IN THE CENTRAL ST. LAWRENCE LOWLAND

Cyril G. Rodrigues
Department of Geology
University of Windsor
Windsor, Ontario N9B 3P4

INTRODUCTION

The Central St. Lawrence Lowland includes the area between the Ottawa and St. Lawrence Rivers, straddles the St. Lawrence as far as Quebec City, and extends a short distance beyond the north shore only (Bostock, 1970). Marine water from the Atlantic Ocean inundated the Central St. Lawrence Lowland and Champlain Valley during the final retreat of the Laurentide Ice Sheet from eastern North America, forming the Champlain Sea (Fig. 1). The purpose of this paper is to describe the lithologic and invertebrate faunal successions at two sites in the lowland and to discuss the significance of the successions.

SPARROWHAWK POINT SITE

A ten-metre section of glacial and marine sediments is exposed in the shore cliffs on the south side of the St. Lawrence River between Ogdensburg and Waddington (Fig. 1). The sediments are divided into the following units, (1) massive stony till, (2) rhythmically laminated silt and clay ("varves"), (3) massive mud, and (4) sand (Fig. 2). Unit 1 is equivalent to the Fort Covington Till of MacClintock and Stewart (1965) and is overlain disconformably by Unit 2. The contact between Units 2 and 3 is gradational and the contact between Units 3 and 4 is abrupt. The succession from till to massive mud was also reported by MacClintock and Stewart (1965) and Terasmae (1965) from sections exposed near Cornwall during the St. Lawrence Seaway Project.

Unit 1 is unfossiliferous. Ostracodes are present in Units 2, 3, and 4. Foraminifers are absent in Unit 2 and are present in Units 3 and 4. Invertebrate macrofossils are common in Unit 3 and in the lower part of Unit 4. Portlandia arctica (Gray) is the most abundant macrofossil in Unit 3 and is accompanied by Cylichna alba Brown, Macoma calcarea (Gmelin), and Hiatella arctica (Linné). Macoma balthica (Linné) is present in the lower part of Unit 4.

Radiocarbon dates, $11\ 900 \pm 100$ years BP (GSC-3767) and $11\ 300 \pm 100$ years BP (GSC-3788), were obtained for shells of Portlandia arctica from the lower part of Unit 3 and for shells of Macoma balthica from the lower part of Unit 4 respectively (Rodrigues and Richard, 1985). At one spot along the shore the laminated sediments are truncated and underlain by massive mud which in turn is underlain by laminated sediments. Rodrigues (1987) proposed that the presence of massive mud below laminated sediments is related to post depositional slumping. Radiocarbon dates of $11\ 900 \pm 100$ years BP (GSC-3767) for

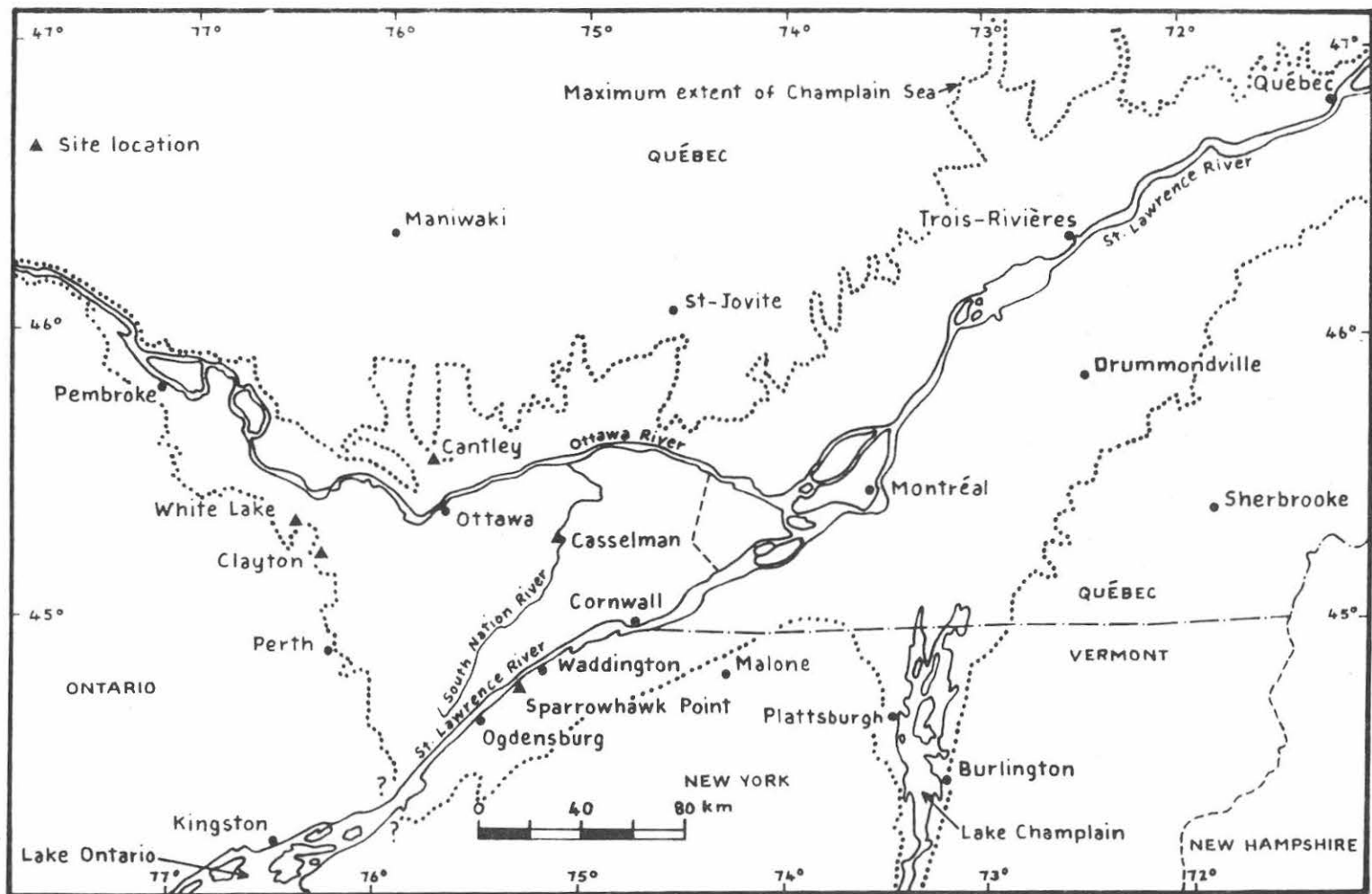


Figure 1. Map showing maximum extent of Champlain Sea and locations of site discussed in text.

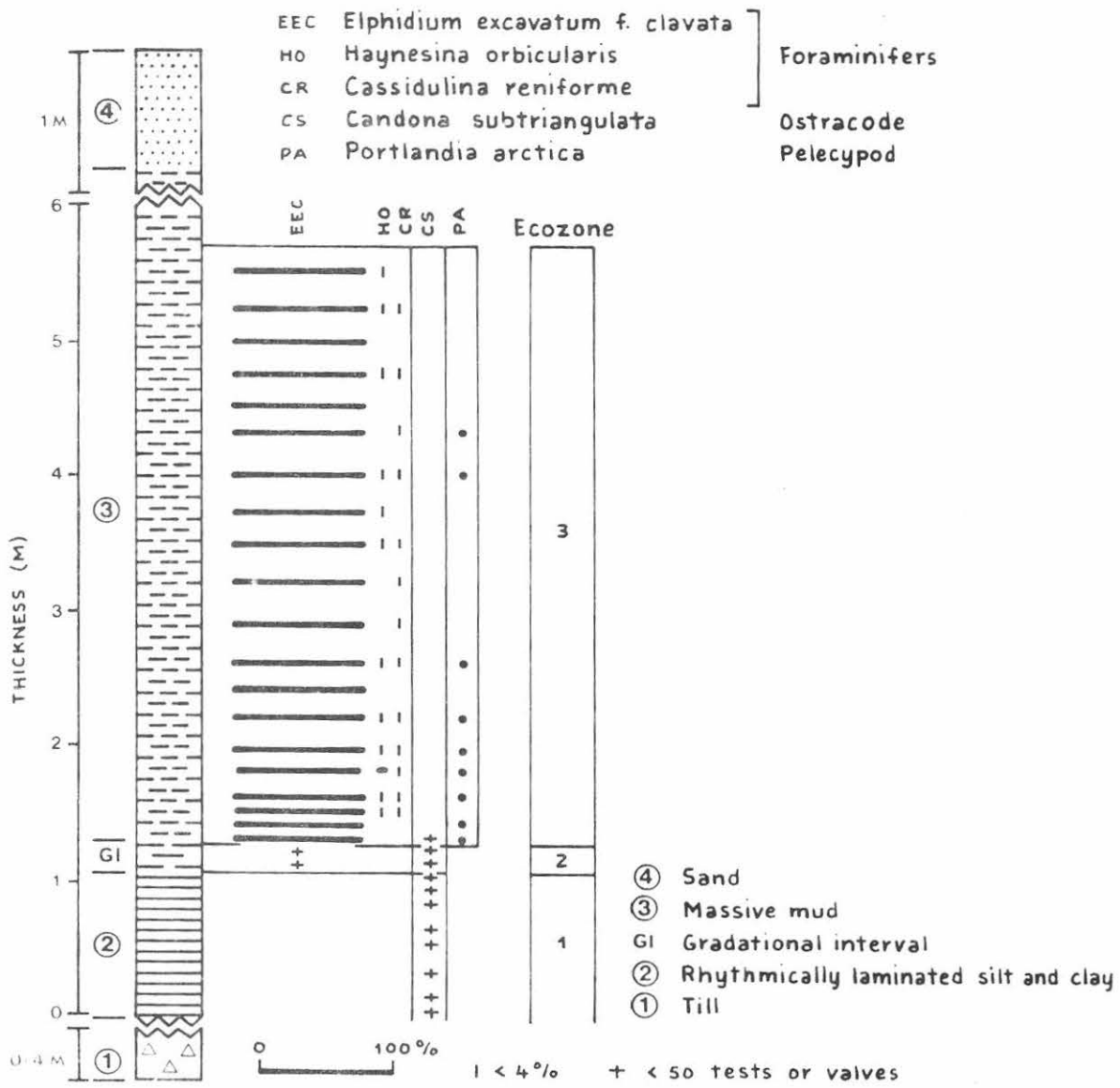


Figure 2. Distribution of selected invertebrate fossils at Sparrowhawk Point site. Foraminiferal abundance data based on samples containing >110 tests.

Portlandia arctica from the lower part of the massive mud overlying the laminated sediments and 11 900 ± 140 years BP (GSC-4044) for the same pelecypod species from the massive mud below the laminated sediments, are consistent with the slumping hypothesis.

Three ecozones are recognized on the basis of foraminiferal and ostracode assemblages from 30 samples which were collected from 6 m of section (Fig. 2). Ecozone 1 is characterized by the ostracode Candona subtriangulata Benson and MacDonald and is restricted to the rhythmically laminated silt and clay (Unit 2). Ecozone 2 contains low numbers of the foraminifer Elphidium excavatum (Terquem) forma clavata Cushman and Candona subtriangulata; it is associated with the gradational interval between Unit 2 and the massive mud (Unit 3). Elphidium excavatum forma clavata-dominant foraminiferal assemblages characterize Ecozone 3. The foraminifers Cassidulina reniforme Nørvang, Haynesina orbicularis (Brady) and Polymorphinids (species of the Family Polymorphinidae) are also present in Ecozone 3. The ostracodes Cytheromorpha macchesneyi (Brady and Crosskey) and Cytheropteron pseudomontrosiense Whatley and Masson are present throughout Ecozone 3, whereas Cytheropteron paralatissimum Swain occurs in the lower part and Roundstonia globulifera (Brady) occurs in the middle and upper parts of Ecozone 3. Portlandia arctica is the most common invertebrate macrofossil in Ecozone 3.

The laminated sediments (Unit 2) characterized by Candona subtriangulata (Ecozone 1) were deposited in a glacial lake which occupied the area during early stages of ice retreat (Fig. 3). The interval between Unit 2 and the massive mud (Unit 3) containing the Elphidium excavatum forma clavata - Candona subtriangulata assemblages (Ecozone 2) were deposited in low salinity bottom-water during the early part of the marine episode. The salinity of the bottom-water was highest (<250/oo) during deposition of Unit 3 which is characterized by Elphidium excavatum forma clavata - dominant foraminiferal assemblages and the pelecypod Portlandia arctica (Ecozone 3).

The inferred freshwater environment for the rhythmically laminated silt and clay ("varves") is based on the modern and fossil occurrences of Candona subtriangulata. Congeners of Candona live in freshwater environments, i.e. lakes and rivers (Delorme, 1970). Identical Candona subtriangulata assemblages were reported from the Late Pleistocene Sheboygan Member of the Lake Michigan Formation (Burke, 1987). The presence of Canadona subtriangulata and Elphidium excavatum forma clavata in Ecozone B (Fig. 2) indicates that C. subtriangulata can survive in marine environments characterized by low salinity. This does not imply that the varve-like rhythmites containing Candona subtriangulata were deposited in a marine environment. The distinction between freshwater and marine environments is based on the total fossil assemblage, rather than the presence of a single species in the assemblage. Thus, assemblages containing only Candona subtriangulata are related to freshwater conditions, whereas assemblages containing C. subtriangulata plus marine ostracodes and/or foraminifers are related to low salinity conditions during the early part of the Champlain Sea episode in the Central St. Lawrence Lowland.

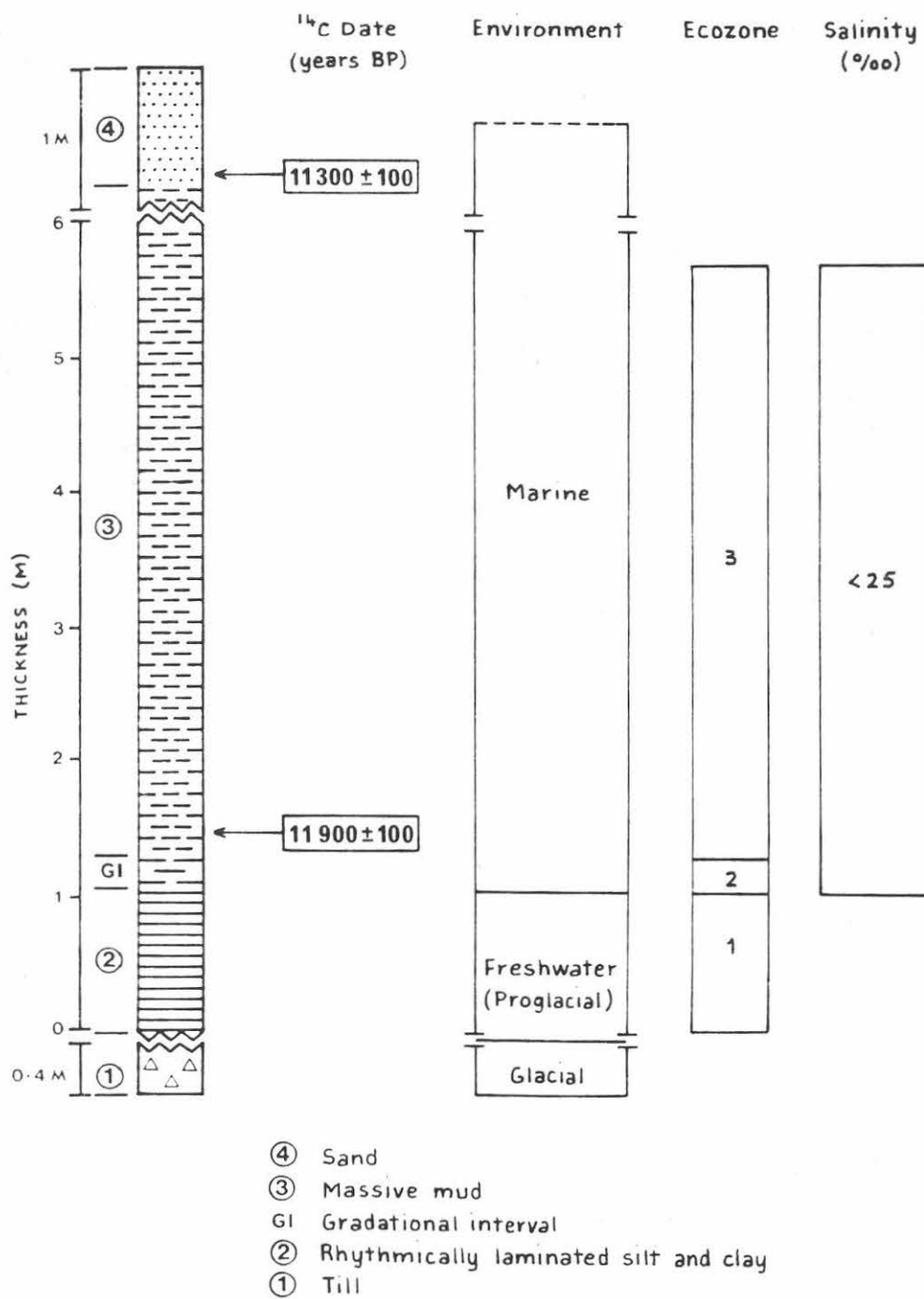


Figure 3. Chronology and paleoenvironmental interpretation for section at Sparrowhawk Point site. Top of section is about 84 m a.s.l.

Cronin (1977) described assemblages containing Candona subtriangulata, marine ostracodes, and foraminifers from deposits near the maximum extent of the Champlain Sea in the Champlain Valley. He also concluded that the assemblages are related to low salinity conditions during the early part of the marine episode.

CASSELMAN SITE

About 17 m of glacial and post-glacial sediments are exposed along the west bank of the South Nation River, northwest of the town of Casselman (Fig. 1). The sediments rest unconformably on Ordovician carbonate rocks. The glacial and post-glacial sediments are divided into the following units, (1) till, (2) rhythmically laminated silt and clay ("varves"), (3) massive mud, and (4) red- and grey-banded mud (Fig. 4). The contacts between Units 2 and 3 and Units 3 and 4 are gradational. The succession from Unit 2 to Unit 4 was described by Fransham and Gadd (1977) and Gadd (1977, 1986) from boreholes in the deeper parts of the lower Ottawa Valley.

Unit 1 is unfossiliferous. Foraminifers are absent in Unit 2 and are present in Units 3 and 4. Ostracodes occur in Units 2, 3 and 4. The pelecypods Macoma calcarea, Mytilus edulis Linné, Portlandia arctica and Yoldiella sp., and the sponge Tethya logani Dawson are present in Unit 3. Invertebrate macrofossils were not observed in Units 2 and 4.

Six ecozones are recognized on the basis of foraminiferal and ostracode assemblages from 22 samples which were collected from Unit 2 and Unit 3 and the gradational interval between the units (Fig. 4). The varve-like rhythmites (Unit 2) and the lower part of the gradational interval between Unit 2 and the massive mud (Unit 3) are assigned to Ecozone A which is characterized by the ostracode Candona subtriangulata. Foraminifers and ostracodes are present in low numbers in Ecozone B which is restricted to the upper part of the gradational interval between Unit 2 and Unit 3. Ecozones C to F are associated with Unit 3. Cassidulina reniforme and Islandiella helenae Feyling-Hanssen and Buzas are the characteristic species of foraminiferal assemblages from Ecozone C. Cassidulina reniforme, Elphidium excavatum forma clavata and Haynesina orbicularis are the most abundant species in Ecozones D and E. The abundance of Cassidulina reniforme is lower and that of Elphidium excavatum forma clavata is higher in Ecozone E by comparison with their abundances in Ecozone D. Cassidulina reniforme is absent and Haynesina orbicularis is the most abundant species in Ecozone F. Portlandia arctica is the most common invertebrate macrofossil and ostracodes are rare in Ecozones C to F. Foraminifers and ostracodes are present in low numbers in the upper part of Unit 3 and in the lower part of the colour-banded mud (Unit 4).

The Candona subtriangulata assemblages of Ecozone A are related to freshwater conditions (Fig. 5). Marine conditions are inferred for Ecozones B to F which are characterized by foraminifers. Ecozone B represents a transition from freshwater to maximum salinity conditions.

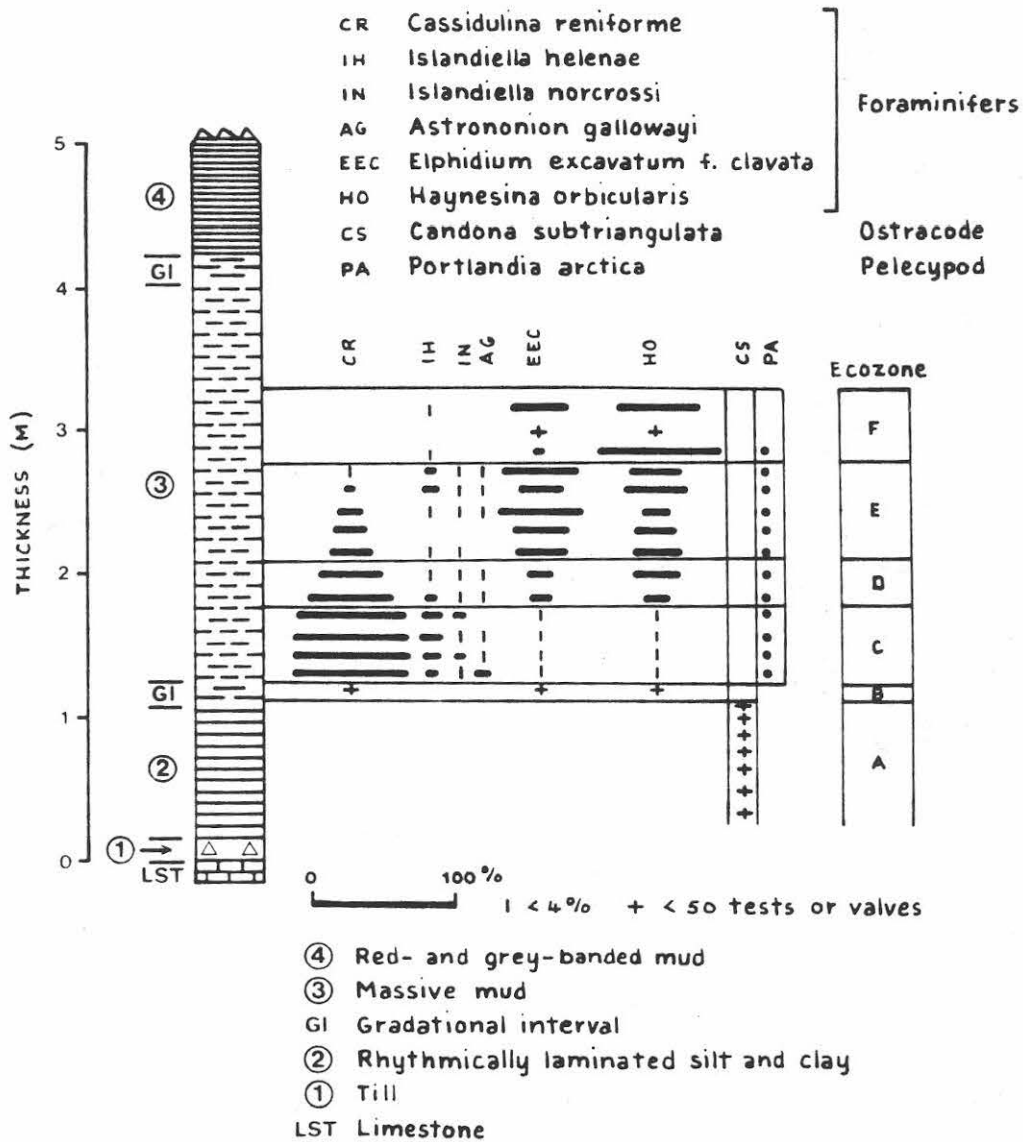


Figure 4. Distribution of selected invertebrate fossils at Casselman site. Foraminiferal abundance data based on samples containing >170 tests.

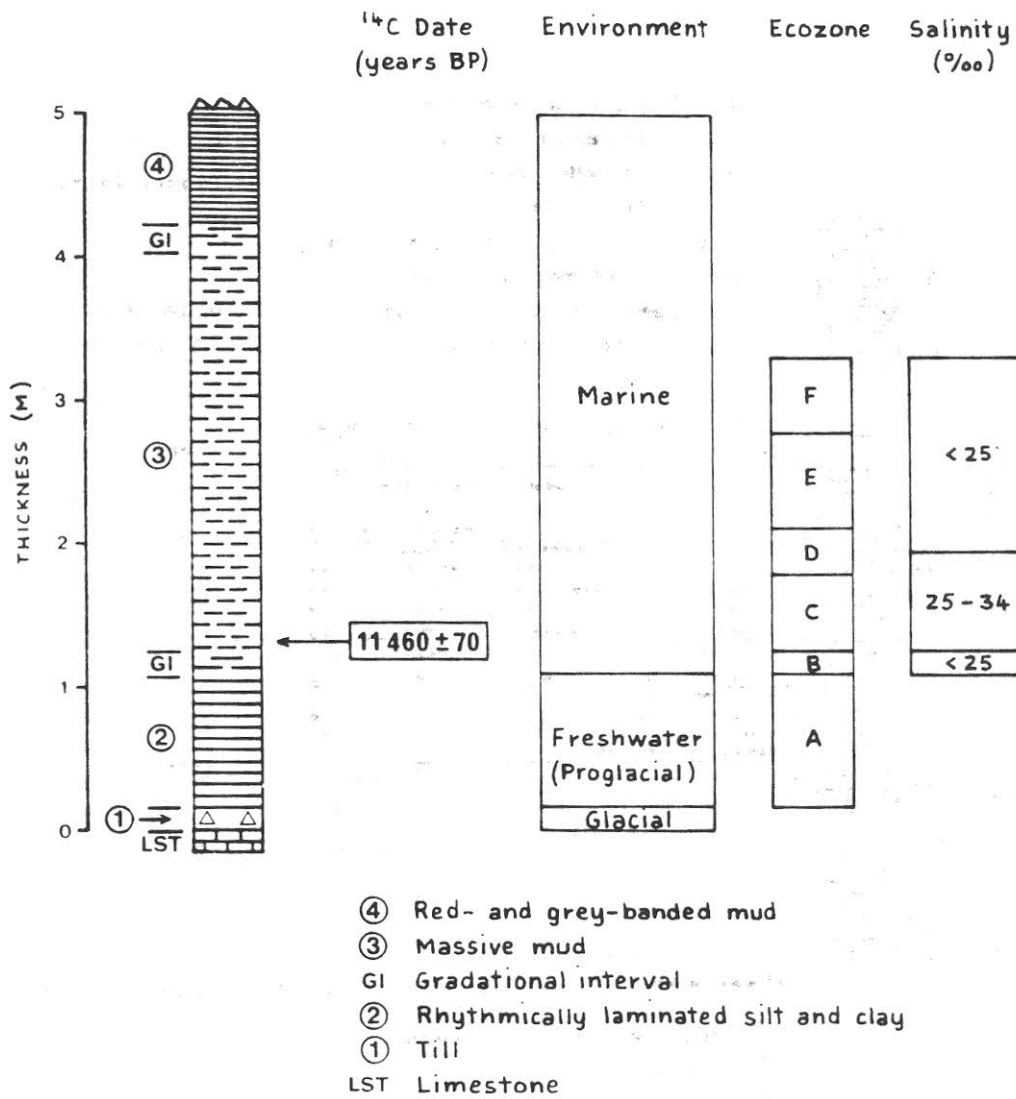


Figure 5. Chronology and paleoenvironmental interpretation for section at Casselman site. Top of section is about 51 m a.s.l.

Salinity was $<25^0/00$ in Ecozone B and from the upper part of Ecozone D to Ecozone F. Maximum salinity conditions ($25-34^0/00$) existed from Ecozone C to the lower part of Ecozone D.

The rhythmically laminated silt and clay (Unit 2) was deposited in a glacial lake which occupied the area during the early stages of deglaciation. The massive mud (Unit 3) and the upper part of the gradational interval between Unit 2 and Unit 3 were deposited during the Champlain Sea episode. Low salinity water replaced freshwater during the deposition of the gradational interval between Unit 2 and Unit 3. Maximum salinity conditions were followed by decreasing salinity during deposition of Unit 3. The lower part of colour-banded mud (Unit 4) was deposited under relatively low salinity conditions during regression of the Champlain Sea.

A radiocarbon date of $11\ 460 \pm 70$ years BP (T0-702) was obtained for foraminifers from the base of Unit 3, i.e. the base of the maximum salinity Ecozone C (Fig. 5). The date indicates that maximum salinity water arrived at the Casselman site ca. 11 500 to 11 400 years BP. T0-702 is younger than the date of $11\ 900 \pm 100$ years BP (GSC-3767) for *Portlandia arctica* from the lower part of the massive mud (Unit 3, Fig. 3) which overlies varve-like rhythmites at the Sparrowhawk Point Site.

COMPARISON OF FAUNAL ASSEMBLAGES

The invertebrate faunal assemblages indicate a succession from glacial to glaciolacustrine to marine conditions at the Sparrowhawk Point site in the upper St. Lawrence Valley and at the Casselman site in the lower Ottawa Valley. The glacial deposits consist of unfossiliferous, massive, stony till. The glaciolacustrine environment is characterized by rhythmically laminated silt and clay ("varves") containing *Candona subtriangulata*. Foraminifers are absent in the varve-like rhythmites. *Portlandia arctica* is the most abundant pelecypod in the massive, fine-grained, marine sediments overlying the laminated sediments. However, the foraminiferal assemblages from the marine sediments at the sites are significantly different (Figs. 2 and 4). The differences in the foraminiferal assemblages are related to the salinity of the water which covered the sites during the Champlain Sea episode. Salinity was $<25^0/00$ at the Sparrowhawk Point site (Fig. 3). Low salinity conditions ($<25^0/00$) were followed by maximum salinity conditions ($25-34^0/00$) and then decreasing salinity conditions ($<25^0/00$) at the Casselman site (Fig. 5).

The highest salinity water ($25-34^0/00$) was present in the deep parts of the Champlain Sea, e.g. Casselman site, and lower salinity water occupied the shallow parts of the sea, e.g. Sparrowhawk Point site. The maximum salinity water reached its upper depth limit (UDL) during the early stages of the marine transgression and retreated from the Central St. Lawrence Lowland during regression of the sea. Maximum salinity foraminiferal assemblages are not present at the Sparrowhawk

Point site because it was above the UDL of the maximum salinity layer. The absence of maximum salinity foraminiferal assemblages at the site may be related to outflow of freshwater from the Lake Ontario basin into the upper St. Lawrence Valley.

DEGLACIATION OF CENTRAL ST. LAWRENCE LOWLAND

Some workers, e.g. Antevs (1925), Prest (1970), Goldthwait (1971), LaSalle (1981), and Clark and Karrow (1984), concluded that a glacial lake occupied part of the Central St. Lawrence Lowland before the Champlain Sea. Thomas (1977) proposed that the area was deglaciated by calving of the Laurentide Ice Sheet and that a calving bay extended up the St. Lawrence Valley from Quebec City to Lake Ontario (Fig. 1). Gadd (1980) agreed with the concept of a calving bay in the Central St. Lawrence Lowland, however he proposed that the calving bay extended into the deeper Ottawa Valley west of Montreal. The succession from rhythmically laminated silt and clay to marine sediments at the Sparrowhawk Point and Casselman sites and the Candona subtriangulata assemblages in the varve-like rhythmites, are evidence for a glacial lake in the Central St. Lawrence Lowland before the Champlain Sea. Anderson et al. (1985), Naldrett (1987), Parent (1987), and Rodrigues (in press) have also reported Candona subtriangulata assemblages from varve-like rhythmites which are overlain conformably by marine sediments at other sites in the lowland.

Glacial Lake Iroquois and glacial Lake Vermont occupied the Lake Ontario basin and Champlain Valley respectively, before deglaciation of the western part of the Central St. Lawrence Lowland. The glacial lake in the Lake Ontario basin expanded into the lowland as ice retreated from the upper St. Lawrence Valley into the lower Ottawa Valley and merged with the glacial lake in the Champlain Valley. Candona subtriangulata migrated into the Central St. Lawrence Lowland from the Lake Ontario basin and reached the Champlain Valley after the glacial lakes in the lowland and Champlain Valley were confluent. Water levels fell in the Lake Ontario basin, Champlain Valley, and along the northwest slope of the Adirondack Mountains as the body of freshwater in the Central St. Lawrence Lowland increased in size. Marine waters of the Champlain Sea replaced the freshwater in the lowland and Champlain Valley after ice retreated from the Quebec City area.

The names Lake Frontenac (Antevs, 1925), Lake St. Lawrence (Goldthwait, 1971), Lake Chambly (LaSalle, 1981), and Lake Candona (Parent and Occhietti, in press *fide* Parent, 1987) were used for the glacial lake which was present in the Central St. Lawrence Lowland before the Champlain Sea. The name Lake St. Lawrence has priority over the other names. Glacial Lake St. Lawrence correlates with the Belleville or Trenton phase of glacial Lake Iroquois and with the Fort Ann phase of glacial Lake Vermont.

AGE OF CHAMPLAIN SEA

The oldest radiocarbon dates in the western part of the Central St. Lawrence Lowland are on the pelecypod Macoma balthica from the Clayton, White Lake and Cantley sites (Fig. 1). Richard (1974) reported a radiocarbon date of $12\ 800 \pm 220$ years BP (GSC-1859) for shells from the Clayton site. Radiocarbon age determinations on a second collection of shells from the same unit at the Clayton site were done at the Radiocarbon Dating Laboratory of the Geological Survey of Canada (GSC) and at Isotracer Laboratory, University of Toronto (TO). The GSC dates for the second collection are $12\ 800 \pm 100$ years BP outer fraction and $12\ 700 \pm 100$ years BP inner fraction (GSC-2151; Richard, 1978). The TO date for the same collection is $12\ 180 \pm 90$ years BP (TO-245; Fulton and Richard, 1987). The discrepancy between GSC-2151 and TO-245 is puzzling. Radiocarbon dates for shells from the White Lake site are $12\ 100 \pm 100$ years BP outer fraction, $12\ 200 \pm 100$ years BP middle fraction, and $12\ 100 \pm 100$ years BP inner fraction (GSC-3110; Rodrigues and Richard, 1983). Romanelli (1975) reported a date of $12\ 200 \pm 160$ years BP (GSC-1646) for shells from the Cantley site.

The Clayton, White Lake and Cantley sites are at or near the maximum extent of the Champlain Sea. The radiocarbon dates for Macoma balthica from the sites are significantly older than the date of $11\ 460 \pm 70$ years BP (TO-702) for foraminifers from the base of the maximum salinity Ecozone C at the Casselman site (Fig. 5). If the radiocarbon dates are taken at face value then marine water arrived in the Ottawa region by at least $12\ 200$ to $12\ 000$ years BP and maximum salinity water migrated into the region at least 600 radiocarbon years after the beginning of the Champlain Sea in the western part of the Central St. Lawrence Lowland. However, the transition from freshwater to maximum salinity conditions (Ecozone B, Fig. 5) appears to have been rapid at the Casselman site. Thus, the radiocarbon dates for Macoma balthica may be "too old" (see Hillaire-Marcel, 1981 and Karrow, 1981).

Anderson (1987, in press) and Rodrigues (in press) concluded that marine water entered the lower Ottawa and upper St. Lawrence Valleys ca. $11\ 500$ to $11\ 000$ years BP. The radiocarbon date ($11\ 460 \pm 70$ years BP) for foraminifers from the base of the maximum salinity Ecozone C at the Casselman site is compatible with the younger age proposed for the Champlain Sea in the western part of the Central St. Lawrence Lowland.

CONCLUSIONS

There is considerable controversy concerning the Late Quaternary deglaciation of the Central St. Lawrence Lowland and age of the Champlain Sea. Invertebrate faunal data from rhythmically laminated silt and clay ("varves") which are overlain conformably by marine sediments indicate that a glacial lake occupied part of the lowland during early stages of ice retreat. Some workers accept the oldest radiocarbon dates (mean values $> 12\ 000$ years BP) at face value and other workers consider the dates to be "too old".

REFERENCES

- Anderson, T.W., 1987, Terrestrial environments and age of Champlain Sea based on pollen stratigraphy of the Ottawa-Lake Ontario region, in Fulton, R.J., ed., Quaternary of the Ottawa region: Geological Survey of Canada Paper 86-23, p. 31-42.
- _____, in press, Late Quaternary pollen stratigraphy of the Ottawa Valley-Lake Ontario region and its application in dating the Champlain Sea, in Gadd, N.R., ed., The Late Quaternary development of Champlain Sea basin: Geological Association of Canada Special Paper 35.
- Anderson, T.W., Mott, R.J., and Delorme, L.D., 1985, Evidence for a pre-Champlain Sea glacial Lake phase in Ottawa Valley, Ontario, and its implications, in Current Research, Part A: Geological Survey of Canada Paper 85-1A, p. 239-245.
- Antevs, E., 1925, Retreat of the last ice-sheet in eastern Canada: Geological Survey of Canada, Memoir 146, 142 p.
- Bostock, H.S., 1970, Physiographic subdivisions of Canada, in Douglas, R.J.W., ed., Geology and Economic Minerals of Canada: Geological Survey of Canada, Economic Geology Report No. 1, Chapter II, p. 9-30.
- Burke, C.D., 1987, The effect of Late Quaternary climatic changes and glacioisostatic rebound on lake level fluctuations and benthos of Lake Michigan: Palaios, v. 2, p. 514-522.
- Clark, P., and Karrow, P.F., 1984, Late Pleistocene water bodies in the St. Lawrence Lowland, New York, and regional correlations: Geological Society of America Bulletin, v. 95, p. 805-813.
- Cronin, T.M., 1977, Late-Wisconsin marine environments of the Champlain Valley (New York, Quebec): Quaternary Research, v. 7, p. 238-253.
- Delorme, L.D., 1970, Freshwater ostracodes of Canada. Part III. Family Candonidae: Canadian Journal of Zoology, v. 48, p. 1099-1127.
- Fransham, P.B., and Gadd, N.R., 1977, Geological and geomorphological controls on landslides in Ottawa Valley, Ontario: Canadian Geotechnical Journal, v. 14, p. 531-539.
- Fulton, R.J., and Richard, S.H., 1987, Chronology of Late Quaternary events in the Ottawa region, in Fulton, R.J., ed., Quaternary of the Ottawa region: Geological Survey of Canada Paper 86-23, p. 26-30.
- Gadd, N.R., 1977, Offlap sedimentary sequences in Champlain Sea, Ontario and Quebec, in Report of Activities, Part A: Geological Survey of Canada Paper 77-1A, p. 379-380.

- _____, 1980, Late-glacial regional ice-flow patterns in eastern Ontario: Canadian Journal of Earth Sciences, v. 17, p. 1439-1453.
- _____, 1986, Lithofacies of Leda clay in the Ottawa basin of the Champlain Sea: Geological Survey of Canada Paper 85-21, 44 p.
- Goldthwait, J.W., 1971, The St. Lawrence Lowland, in Gadd, N.R., Geology of the Central St. Lawrence Lowland (with selected passages by J.W. Goldthwait): Geological Survey of Canada, Memoir 359, p. 118-149.
- Hillaire-Marcel, C., 1981, Late-glacial regional ice-flow patterns in eastern Ontario: Discussion: Canadian Journal of Earth Sciences, v. 18, p. 1385-1386.
- Karrow, P.F., 1981, Late-glacial regional ice-flow patterns in eastern Ontario: Discussion: Canadian Journal of Earth Sciences, v. 18, p. 1386-1390.
- LaSalle, P., 1981, Géologie des dépôts meubles de la région de Saint-Jean-Lachine: Ministère de l'Énergie et des Ressources, Rapport Préliminaire, DPV-780, 13 p.
- MacClintock, P., and Stewart, D.P., 1965, Pleistocene geology of the St. Lawrence Lowland: New York State Museum and Science Service, Bulletin No. 394, 152 p.
- Naldrett, D.L., 1987, Pre-Champlain Sea glacial lake sedimentation in the Ottawa Valley, Ontario, Canada: International Union for Quaternary Research XIIth International Congress, Programme with Abstracts, p. 231.
- Parent, M., 1987, The Asbestos-Valcourt and Sherbrooke area, in Lamothe, M., ed., Pleistocene stratigraphy in the St. Lawrence Lowland and the Appalachians of southern Québec: A field guide: Université de Montréal, Collection Environnement et Géologie, v. 4, p. 102-139.
- Parent, M., and Occhietti, S., in press, Late Wisconsinan deglaciation and Champlain Sea invasion in the middle St. Lawrence Valley, Québec, in Gadd, N.R., ed., The Late Quaternary development of Champlain Sea basin: Geological Association of Canada Special Paper 35.
- Prest, V.K., 1970, Quaternary geology of Canada, in Douglas, R.J.W., ed., Geology and Economic Minerals of Canada: Geological Survey of Canada, Economic Geology Report No. 1, Chapter XII, p. 676-764.
- Richard, S.H., 1974, Surficial geology mapping: Ottawa-Hull area (Parts of 31 F, G), in Report of Activities, Part B: Geological Survey of Canada Paper 74-1B, p. 218-219.

- _____, 1978, Age of Champlain Sea and "Lampsilis Lake" episode in the Ottawa-St. Lawrence Lowlands, in Current Research, Part C: Geological Survey of Canada Paper 78-1C, p. 121-128.
- Rodrigues, C.G., 1987, Late Pleistocene invertebrate macrofossils, microfossils and depositional environments of the western basin of the Champlain Sea, in Fulton, R.J., ed., Quaternary of the Ottawa region: Geological Survey of Canada Paper 86-23, p. 16-23.
- _____, in press, Late Quaternary invertebrate faunal associations and chronology of the western Champlain Sea basin, in Gadd, N.R., ed., The Late Quaternary development of Champlain Sea basin: Geological Association of Canada Special Paper 35.
- Rodrigues, C.G., and Richard, S.H., 1983, Late glacial and postglacial macrofossils from the Ottawa-St. Lawrence Lowlands, Ontario and Quebec, in Current Research, Part A: Geological Survey of Canada Paper 83-1A, p. 37-379.
- _____, 1985, Temporal distribution and significance of Late Pleistocene fossils in the western Champlain Sea basin, Ontario and Quebec, in Current Research, Part B: Geological Survey of Canada Paper 85-1B, p. 401-411.
- Romanelli, R., 1975, The Champlain Sea episode in the Gatineau River Valley and Ottawa area: Canadian Field-Naturalist, v. 89, p. 356-360.
- Terasmae, J., 1965, Surficial geology of the Cornwall and St. Lawrence Seaway Project area, Ontario: Geological Survey of Canada, Bulletin 121, 54 p.
- Thomas, R.H., 1977, Calving bay dynamics and ice sheet retreat up the St. Lawrence Valley system: Géographie Physique et Quaternaire, v. XXXI, p. 347-356.

DIKES OF THE NORTHEAST ADIRONDACK REGION -
INTRODUCTION TO THEIR DISTRIBUTION, ORIENTATION,
MINERALOGY, CHRONOLOGY, MAGNETISM, CHEMISTRY, AND MYSTERY

Y.W. ISACHSEN and W.M. KELLY
New York State Geological Survey

C. SINTON and R.A. COISH
Middlebury College

M. T. HEIZLER
SUNY Albany

INTRODUCTION AND SCOPE

More than 1300 dikes in the Adirondack region have been compiled on a map at 1:250,000 (Isachsen and Wright, in press). Figure 1 is a severe reduction of this map. While 1300 may seem a large number of dikes, the sparsity of rock exposures in the region suggests that it represents at most a few percent of the total number actually present. Most dikes are exposed over a length of only a few meters or less, and are a meter or so thick. Several, however, are exposed intermittently for distances up to 15 km, and are as much as 10 m thick. Twenty-four types are represented, five of which are metamorphic. Mafic dikes clearly predominate. Their prominence, in decreasing order, using the names given in the literature, are as follows: diabase, "mafic dike", basalt, gabbro, metagabbro, metadiabase, hyperthene metadiabase, and garnet metadiabase. Next most prominent are lamprophyres and granite pegmatite dikes. Rose diagrams of dike orientations (Isachsen and Wright, in press) show these dominant strike directions: 1) NNE-NE for the basalt, diabase, gabbro and "mafic" dikes, 2) WNW to EW for the lamprophyres, and 3) NS to NNW for the metamorphic dikes. The northeasterly strikes of most of the unmetamorphosed mafic dikes corresponds to the predominant trend of faults and zero-displacement crackle zones that account for the great number of linear valleys in the southeastern half of the Adirondacks (Isachsen and McKendree, 1977; Isachsen and others, 1983). The easterly-westerly trends of the lamprophyre dikes correspond to the trends of similar dikes in Vermont (McHone and Corneille, 1980, McHone, 1984). Their radiometric dates are similar as well.

This trip will include two stops to see lamprophyre dikes and one to see the most impressive concentration of dikes in the Adirondacks - the Rand Hill dike swarm. Here, more than 100 dikes, up to 180 m in exposure length, are exposed in three cross-cutting orientations. Diabase, olivine diabase, and trachyte porphyry dikes intrude gabbroic anorthosite gneiss.

Subjects for discussion will include: dike orientations vs regional fracture patterns, magnitude of extensional strain, dike propagation mechanisms, relative and radiometric ages (and problems), paleomagnetism and apparent polar wander path, geochemical

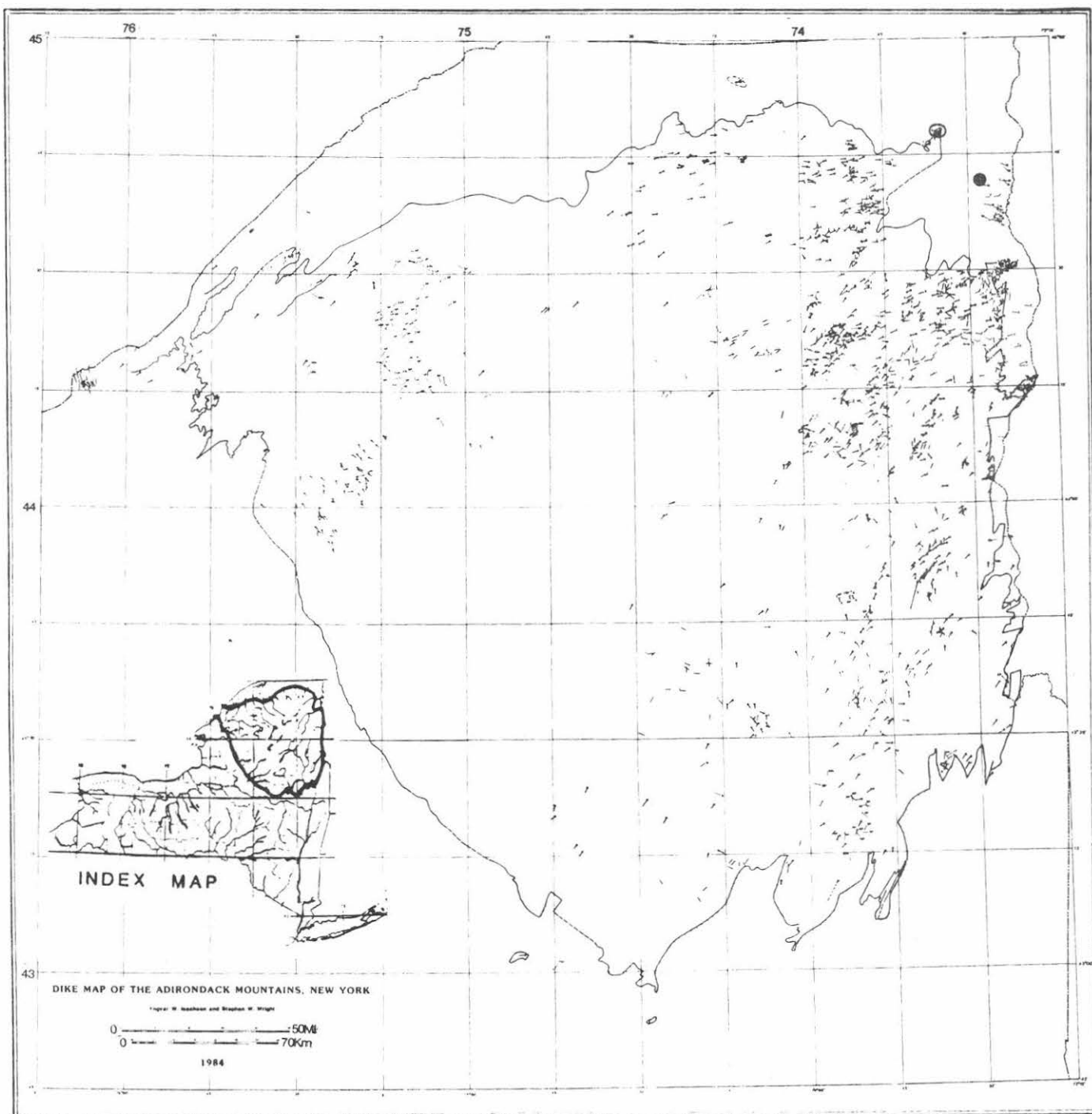


Figure 1. Dike map of the Adirondacks showing the distribution and attitudes of dikes in the region (reduced from Isachsen and Wright, in press, 1:250,000). Twenty-four types, five of them metamorphic, are differentiated on the original large scale map. Multiple dikes with similar orientations at many sites increase the number beyond those shown here. Dikes are concentrated in the eastern Adirondacks and the Thousand Islands region, the general paucity of dikes in between is probably real (Isachsen & Wright, in press). Plattsburgh is shown by solid circle, Rand Hill by open circle.

characterization, and plate tectonic inferences.

Authorship contributions are as follows: Geochronology, M.T.H. and Y.W.I.; petrography, W.M.K., Y.W.I., C.W.S.; paleomagnetism, W.M.K.; geochemistry, C.W.S., R.A.C.; stop descriptions, Y.W.I., C.W.S. We are very grateful to David Seidemann for K/Ar dating, James Olmsted for helpful conversations, Shirley Pytlak for petrographic information on the Rand Hill dikes, Robert Barry for Figure 11, and to Mr. McKinney and Dr. John Mazur for their cordial cooperation in allowing field studies on their respective properties. We are most grateful for helpful reviews by J.G. McHone, J.F. Olmsted, W.B. Rogers, and P.R. Whitney.

GEOCHRONOLOGY

A major goal of compiling a map of Adirondack dikes (Isachsen and Wright, in press) was to determine the history of paleostress in the region through K-Ar dating of dikes of known orientation. Making the simplest assumptions, dikes will intrude perpendicular to the axis of least principal horizontal stress, and parallel to the axis of maximum principal stress. A successful study would show the changes in stress orientation through whatever time interval was represented by the dikes, and thus elucidate the regional tectonic history of the northeastern part of North America (Isachsen and Seidemann, 1983). Conventional K-Ar analyses were made by Seidemann on 24 whole rock samples from unmetamorphosed dikes including diabase, olivine diabase, trachyte, and lamprophyres. Five lamprophyre dates ranged from 146 to 123 Ma and one trachyte porphyry intruded into Paleozoic strata gave a date of 113 Ma (Isachsen and Wright, in press). Spanning the Late Jurassic to Middle Cretaceous period, these ages indicate an easterly-westerly maximum principal stress at that time. This agrees with trends and dates reported by McHone and Corneille (1980) and McHone (1984) for trachyte dikes cutting Ordovician strata along the Vermont shores of Lake Champlain. They obtained an Rb/Sr isochron for several dikes of 125 ± 5 Ma.

The K/Ar dates for diabase and olivine diabase in the eastern Adirondacks show a wide range (Geraghty and Isachsen, 1979; Isachsen and Wright, in press). Seven dates at Rand Hill cluster in the comparatively narrow range 588-542 Ma. Progressing southward, however, ages become younger, reaching 261 Ma at Pottersville which is located 140 km south of Rand Hill. This is consistent with the younging of K-feldspars along this same trend (Heizler and Harrison, 1987). With respect to the Rand Hill dikes, it is interesting to note that diabase dikes with the same ENE trend and "Iapetan age" occur in the Ottawa graben, where Bourne and Hogarth (1978) report K/Ar dates of 564-570 Ma.

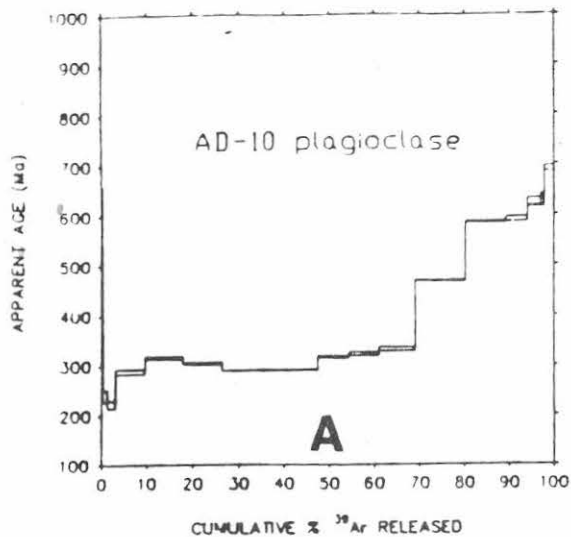
The younger diabase dikes in the south central and southern Adirondacks, however, are surprising because no diabase dikes have yet been found that cut rocks younger than the Middle Proterozoic basement. Kemp and Marsters (1893) and Cushing (1898) early noted that diabase dikes did not cut the basal Paleozoic Potsdam Sandstone of Middle Cambrian age. The pre-Potsdam age of such dikes is further confirmed

by Cushing's discovery of glacial boulders of Potsdam sandstone containing pebbles of diabase. Cushing also found trachyte porphyry fragments in such boulders. This demonstrates the existence of a pre-Potsdam intrusive episode of trachyte in addition to that of Mesozoic age referred to above. Also, there is field evidence that the diabase and trachyte porphyry dikes at Rand Hill are coeval: Cushing (1901) describes a diabase dike that cuts a trachyte porphyry dike, while at another site (about 300 m southwest of the map area in Fig. 11), Geraghty and others (1979) document the reverse intrusive relationships. This suggests that if these trachytes are of the same generation, the Rand Hill dike swarm is a bimodal comagmatic suite. This conclusion receives support in the section on Geochemistry, although more dikes in the Rand Hill swarm should be dated and analyzed to test this possibility.

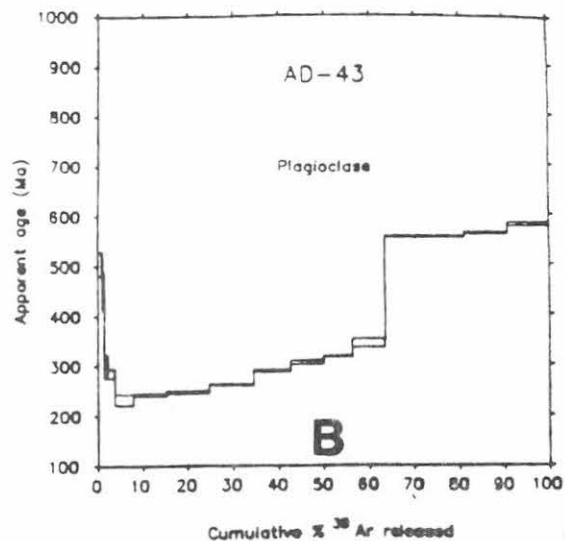
The ambiguity between the relative and K/Ar ages of diabase dikes in the southeastern Adirondacks inspired the use of the $^{40}\text{Ar}/^{39}\text{Ar}$ method to some of the K-Ar dated dikes. Before discussing the results, it is desirable to give a brief review of the $^{40}\text{Ar}/^{39}\text{Ar}$ method because of its bearing on the interpretation of the data obtained.

True crystallization age can be determined only if there has been neither a gain nor loss of ^{40}Ar , either during or after emplacement. Such an assumption, however, can be hazardous. Argon, being an inert gas, can diffuse into dike minerals from K-rich country rock or incorporated xenoliths during intrusion. Alternatively, it can readily diffuse out of minerals during even relatively small temperature perturbations if they are persistent on geological time scales (i.e. millions of years). Thus, for example, argon will diffuse out of plagioclase at temperatures between 100-200°C and cause an anomalously young K-Ar age. An additional problem is that plagioclase generally contains ^{40}Ar in excess of that produced from in situ decay of ^{40}K . Such argon contamination will result in a K-Ar date older than the crystallization age. Nevertheless, conventional K-Ar dates can only be based on the assumption that all the non-atmospheric ^{40}Ar was produced by in situ decay of ^{40}K .

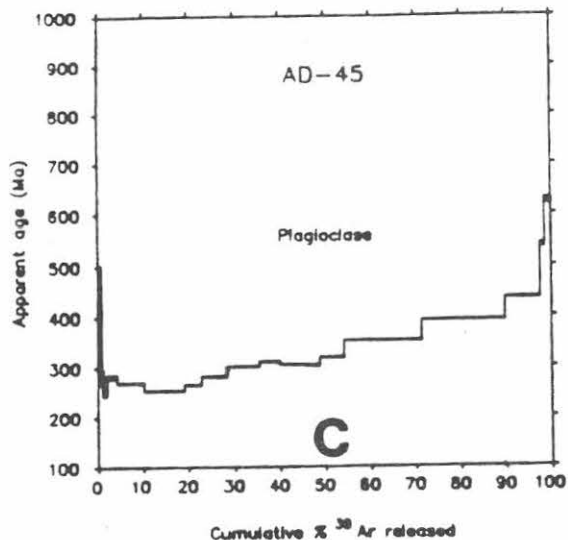
To test this assumption, an $^{40}\text{Ar}/^{39}\text{Ar}$ incremental heating technique can be used. Briefly, this requires irradiation of the sample whereby ^{39}K is transmuted to ^{39}Ar through a neutron-proton reaction. Inasmuch as ^{39}Ar is proportional to ^{40}K , and is thus a measure of the parent concentration in the material, the $^{40}\text{Ar}/^{39}\text{Ar}$ ratio (essentially the daughter-to-parent ratio) will be proportional to age. Heating the sample in a series of increasing temperature steps and plotting the percentage of ^{39}Ar evolved at each step versus its calculated age creates an age spectrum (Fig. 2). If the sample has undergone neither argon loss nor gain, each incremental release of gas should yield the same age, resulting in a flat spectrum or "plateau". Deviations from a plateau will generally indicate a gain, loss, or both of ^{40}Ar during the geological history of a sample. Such release spectra can provide dates that are far more geologically significant than those obtained through conventional K-Ar dating. For a complete description of the $^{40}\text{Ar}/^{39}\text{Ar}$ method and the interpretation of release spectra see McDougall and Harrison (1988).



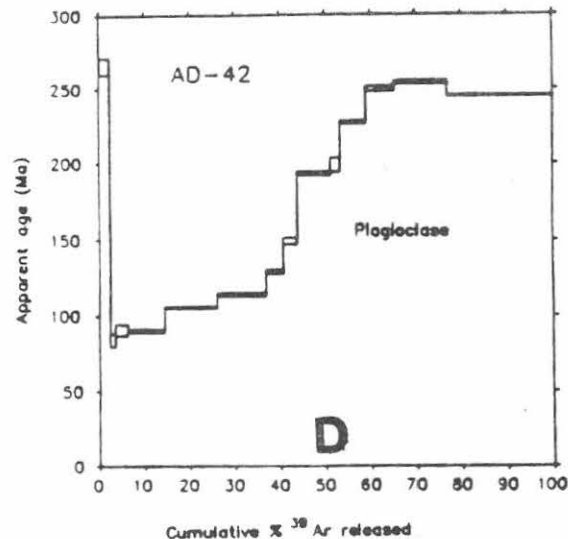
Fort Ann dike, north of Fort Ann on Rt. 22.



Pottersville dike, Pottersville entrance ramp to I-87.



The Glen dike, quarry -2 km south of The Glen.



Big Nose dike, Rt. 5, -12 km west of Fonda.

Figure 2. $^{40}\text{Ar}/^{39}\text{Ar}$ release spectra for plagioclase separates from three diabase dikes located within a 40 km radius in the southeastern Adirondacks, 140 km south of Rand Hill, and one (Big Nose) from the southernmost Adirondacks. The age gradients suggest post-crystallization argon loss. **A.** Sample yields a plateau from 3 percent to 70 percent of the ^{39}Ar released, with an age of -300 Ma. This may be a cooling age following Paleozoic burial. The last 35 percent released may reflect the -600 Ma crystallization age of the dike, excess ^{40}Ar , or a combination of the two. **B.** Age spectrum shows excess ^{40}Ar over the first -5 percent of gas released, with a minimum at -233 Ma. The age gradient for the first -63 percent of gas released is indicative of argon loss. The unusual dramatic age increase at -63 percent may reflect a relatively retentive siting for the argon then being released. The final 580 Ma age may be a minimum date of intrusion. A conventional K/Ar whole rock analysis gave a date of 261 ± 5 Ma (Isachsen and Wright, in press). **C.** Age spectrum shows an overall increase in age from early release until -97 percent release. The age gradient probably reflects the ^{40}Ar concentration distribution that resulted from later reheating following emplacement prior to 450 Ma. The final gas release appears to be excess ^{40}Ar . A conventional K/Ar determination gave a date of 370 ± 7 Ma (Isachsen and Wright, in press). **D.** The young apparent ages of -80 Ma reflect cooling below 100°C of this relatively low-retentive plagioclase. The very steep gradient probably results from excess ^{40}Ar , an interpretation strengthened by the age decrease for final gas release. If not caused by excess argon, the release spectra may indicate a minimum crystallization age of 250 Ma. A K/Ar determination gave a date of 377 ± 8 (Isachsen and Wright, in press).

Figure 2 shows release spectra for plagioclase from three dikes that are located from 120 to 140 km south of Rand Hill (Fig. 1). The apparent ages are variable, with all spectra displaying apparent age gradients rather than true-age plateaus. These age gradients reflect ^{40}Ar concentration gradients within the plagioclase crystals that result from both excess argon and argon loss, and thus probably do not yield dike crystallization ages.

The age spectra for plagioclase samples from the diabase dikes shown in Fig. 2 lack broad plateaus, and, aside from the Pottersville dike, even the oldest ages are younger than the age bracketed by field relationships. Conventional K-Ar ages on these samples would therefore be meaningless geologically.

The timing and cause of the apparent argon loss is a question of interest. Dalrymple and Lamphere (1969) have reviewed seven geological factors that can potentially cause argon loss in minerals: 1) the inability of the mineral lattice to retain argon, 2) melting, 3) metamorphism, 4) weathering and alteration, 5) recrystallization, 6) reheating, and 7) physical damage. In this connection, all thin sections of Adirondack dikes examined thus far show moderate to extensive alteration. Whether this alteration is deuteric or a later hydrothermal effect is not known, but the absence of hydrothermal alteration in associated country rocks suggests the former. Regardless of this question, a number of studies other than $^{40}\text{Ar}/^{39}\text{Ar}$ bear on the cause of argon loss.

As reviewed by Johnson (1986) and Friedman (1987), seven independent indicators have shown that temperatures approaching $175^{\circ}\text{--}200^{\circ}\text{C}$ are recorded in the Middle and Upper Devonian strata of New York -- strata that Rickard's (1988) isopach maps suggest originally extended across the Adirondack region. The thermometers used are vitrinite reflectance, conodont coloration, distinctive authigenic minerals, reset fission track ages in apatites and zircons, fluid inclusion homogenization, stable isotopes of oxygen, and stable isotopes of carbon. Assuming that these elevated temperatures resulted from burial rather than igneous activity, 4 km of post-Upper Devonian sediments must have once covered the area (e.g. Johnson, 1986), burying the basement to 8-9 km. This implies that the Carboniferous strata of Pennsylvania once extended northward across New York State. Reheating to 200°C by burial would cause argon loss in the plagioclase of diabase dikes and explain the Phanerozoic K/Ar ages.

$^{40}\text{Ar}/^{39}\text{Ar}$ studies by Heizler and Harrison (1987) suggest that the time of this reheating and subsequent uplift and cooling to below 150°C was about 180 Ma ago (Early to Middle Jurassic). They proposed another cause of reheating, namely, burial during the Devonian coupled with influx of heat from an inferred failed rift to the east related to the opening of the Proto-Atlantic, (Iapetus).

PETROGRAPHY OF THE RAND HILL DIKES

Introduction

The petrography of dikes at Rand Hill is treated in some detail in this separate section because of its application to the next section, Paleomagnetism. The petrography of the other dikes is discussed under the appropriate field trip stop descriptions.

Three types of dikes occur at Rand Hill: diabase, olivine diabase, and trachyte porphyry. These will be examined at STOP 2 in both fresh roadcuts and an extensive area of natural exposures. Although some of the dike rocks are very fine-grained, they are classified as diabase rather than basalt, following the convention for hypabyssal versus extrusive rocks.

Diabases

As applies to basaltic rocks in general (e.g. Hatch and others, 1973) both diabase varieties at Rand Hill contain plagioclase and clinopyroxene as essential minerals, as well as abundant oxides of iron and titanium oxides. In addition to clinopyroxene, a calcium-poor pyroxene, either pigeonite or orthopyroxene, may also be present depending on temperature of crystallization. Plagioclase commonly appears in two sizes and generations: as early-formed phenocrysts and as more sodic microlites in the groundmass. Similarly pyroxene may be present in two generations. Hornblende is rare, but small amounts of biotite are not uncommon. Apatite, in small acicular crystals, is plentiful. As to the presence or absence of olivine, Hatch and others (1973) note that it occurs in most, though not all basalts and diabases, and is present either because (1) the magma is undersaturated in silica or (2) if slightly oversaturated, because early-formed olivine is prevented from converting to orthopyroxene by rapid chilling of the magma. In Adirondack olivine basalts and diabases, the olivine may be found in all stages of alteration to serpentine, talc, iddingsite, chlorite, magnetite, limonite, rhombohedral carbonate. Pyroxene may be replaced by chlorite, calcite, epidote.

In conjunction with a paleomagnetic study of the dike rocks at Rand Hill, a number of thin and polished sections were examined in transmitted and reflected light. The observations are given below.

Diabase. The samples examined were taken from sites RH-17 and RH-24 of Geraghty and others (1979), which correspond to samples collected by W. Kelly and L. Brown for a paleomagnetic study reported on by Brown (1982). Plagioclase, which makes up about 60 percent of the rock, forms laths and anhedral crystals that range up to 1.5 mm in length and average 0.1-0.5 mm. The laths are fairly strongly zoned and flow-aligned, and show 10-20 percent alteration. Biotite, generally in anhedral crystals, appears to be primary, and makes up 10-15 percent of the rock. It ranges from extremely fine-grained to 0.1 mm in diameter, and is abundant in the 0.01 mm size range. Intergrown with it is a secondary fine-grained greenish phase, possibly chlorite. Apatite

needles, 0.05 mm in length, are abundant. Epidote, defined in the broad sense, occurs in amounts up to 10 percent and is probably a replacement of plagioclase. It is anhedral and averages 0.1 mm in size. Secondary calcite forms in rhombohedral grains 0.1 mm in diameter.

Opaque minerals make up approximately 15 percent of the rock. These, as in all the Rand Hill dikes, are dominantly iron-titanium oxides. Titanomagnetite has a bimodal grain size distribution. Subhedral grains, 0.02-0.04 mm with an observed maximum of 0.1 mm, display subsolidus oxidation exsolution textures as shown by the presence of ilmenite lamellae on the {111} planes of the magnetite (Haggerty, 1976). Homogeneous anhedral magnetite, 0.01-0.001 mm, is ubiquitous. An oxide dust, <0.001mm, is present in the silicates. It is probably magnetite but is too fine for definite identification with an optical microscope. Traces of pyrite, 0.025-0.05 mm, are present, and some contain minor patches oxidized to magnetite.

It is noteworthy, and will be referred to in the section on Geochronology, that both silicates and oxides are altered in the dikes, although silicates are the more altered.

Olivine diabase (porphyritic). This rock displays a range of textures that are related to the degree of alteration of the rock and the presence or absence of olivine or pyroxene phenocrysts -- minerals that weather to form pits. The mafic phenocrysts are concentrated in the central part of the dikes by flow differentiation. In contrast, the less dense plagioclase phenocrysts are more abundant near the margins. The samples examined were collected from sites RH-16, RH-20, RH-22 and RH-23 of Geraghty and others (1979). The following summarizes the characteristics of this entire suite of samples.

Plagioclase laths are present as phenocrysts, 1-5 mm long, in a groundmass of finer-grained laths 0.01-0.05 mm in length. The plagioclase phenocrysts commonly occur in rafts as though they stuck together during flow. The core of the plagioclase is tan, probably due to submicroscopic inclusions, and fades towards the rim. All the plagioclase is fairly strongly zoned. It constitutes 40-65 percent of the rock, and is 5-10 percent altered to sericite. Clinopyroxene occurs between the plagioclase laths in typical ophitic fashion, with a grain size of about 0.05 mm. A few highly-altered phenocrysts measuring 0.1-0.2 mm were observed. Clinopyroxene now forms only 1-3 percent of the rock whereas before its alteration to epidote, serpentine and clinozoisite, it made up about 40 percent in some samples.

Moderately to severely altered grains of olivine, 0.1-0.2mm in size are present in most samples. Where olivine is absent, its ghosts remain as clots of alteration products. These comprise oxides plus serpentine, with or without a brown alteration phase which is probably iddingsite. Only trace amounts of olivine remain, although originally it formed several percent of the rock. The relict alteration clots are rimmed, corona-like structures. Their core is a cloud of magnetite, hematite and pyrite which appears massive in thin section, but in

polished section is revealed to be composed of many very small grains. The core is generally surrounded by a thin (<0.1 mm) discontinuous rim of a very fine grained colorless phase. This is rimmed by a green phase, probably serpentine, which is itself rimmed by or mixed with a fine-grained brown alteration product that contains small biotite crystals. The brown phase probably is iddingsite that overgrew biotite in the matrix as the alteration rim formed. It is the selective weathering of these alteration clots that accounts for the pitted surface of these dikes.

Biotite, in 0.25-1.0 mm anhedral to subhedral grains, is disseminated throughout the groundmass. It occurs both as primary grains and as secondary grains in alteration rims on FeMg silicates, and in aggregates of grains that seem to be derived from totally altered FeMg silicates. It forms up to 10% of the rock. Apatite needles have the same size range as in the diabase dikes, but are less abundant.

Epidote and serpentine are very common alteration minerals in these rocks. Epidote, in anhedral to subhedral 0.01 mm crystals, is disseminated in the matrix and also occurs in aggregates 0.3 mm across. These clots of epidote contain no relict mineral core but may be altered clinopyroxene. Epidote also occurs in the alteration rims of the silicates that form the weathered pits. The serpentine generally has a fibrous habit, radial to the edges of the altered FeMg silicate. Serpentine also occurs as veinlets. Epidote and serpentine together form as much as 30 percent of the rock. Opaque minerals make up 10-20 percent of the rock. These are distributed evenly through the matrix and are concentrated in the cores of the coronal structures. Although the most common opaque mineral is FeTi oxide, there is a wide variation in the degree of alteration of the oxides. Magnetite occurs both as a homogeneous phase and with included lamellae of ilmenite. Some grains are considerably altered to maghemite or hematite. In samples with altered oxides, completely altered grains may coexist in close proximity to unaltered grains.

Magnetite occurs as skeletal to subhedral 0.001-0.2 grains, both homogeneous and with exsolved ilmenite on {111} of the magnetite. Maghemite, formed as a late, patchy alteration product, may replace 50-100 percent of some grains. A very fine grained (<<0.001 mm) dusting of an oxide mineral, possibly magnetite, occurs in what appears in reflected light to be plagioclase.

Anhedral homogeneous magnetite occurs as clusters or clouds of 0.01 mm grains in the core of the rimmed aggregates that represent altered phenocrysts of olivine or pyroxene. These oxides are obviously secondary, formed from the breakdown of the silicate phase. A lesser amount of secondary acicular hematite is commonly associated with the magnetite in these clusters.

Late pyrite occurs as anhedral and locally euhedral grains 0.01-0.1 mm, both in the matrix of the rock and in the cores of the coronal structures that contain FeTi oxides. Pyrite makes up less than 1 percent of the opaques. A trace of chalcopyrite was also observed in the oxide clusters.

Trachyte. A general description of the Rand Hill trachytes by Cushing (1901) is summarized under STOP 2A. The following details are from specific samples of Rand Hill trachyte collected at station RH-21 of Geraghty and others (1979).

Plagioclase, which occurs as 0.1-0.2 mm laths with abundant very fine alteration products, constitutes approximately 25 percent of the rock. Potassium feldspar forms laths and anhedral crystals in the same size range, and was distinguished from plagioclase by staining. It makes up about 35 percent of the rock.

Fresh biotite, in subhedral, 0.01-0.1 mm grains, constitutes roughly 25 percent of the rock, and highly-altered clinopyroxene comprises about one percent. Apatite occurs as abundant needles, 0.05 mm and finer in size.

Opaque minerals make up about 15 percent of the trachyte. Anhedral magnetite is the most common, occurring with a bimodal grain size distribution. The larger grains, averaging 0.05 mm, are either homogeneous or display ilmenite lamellae on the {111} planes. These grains show up to 25 percent alteration to hematite, and perhaps 10 percent alteration to maghemite. The smaller grains, 0.01 mm and finer, are homogeneous, with only a minor amount of hematite alteration. Overall, the primary magnetite is 10-20 percent replaced by later minerals.

Minor discrete hematite grains, 0.05 mm and finer, appear anhedral and homogeneous. These lack any internal relict structure and so are probably secondary. In thin section, bright red hematite flakes were noted. Very minor pyrite forms 0.05-0.001 mm anhedral grains.

PALEOMAGNETISM OF THE RAND HILL DIKES

One hundred two oriented samples were collected from 20 sites among the Rand Hill dikes to establish paleomagnetic poles to accompany the K/Ar dates (Late Proterozoic, Lower and Middle Cambrian and Lower and Middle Devonian) published by Geraghty and others (1979). Natural remanent magnetization direction shows a strong preference for the earth's present magnetic field (Fig. 3). There is a fairly strong viscous component to the magnetization which may be due to secondary mineralization or to alteration of the primary magnetic phases. This component decreases in intensity fairly rapidly upon thermal demagnetization, reaching 20-30 percent of original intensity at 500°C. After alternating-field demagnetization up to 50 mT, the direction moved to a more easterly declination, although the inclination remained steep. The mean direction for 17 dikes is $I = 64.4^\circ$ and $D = 63.4^\circ$ ($\alpha-95 = 7.5^\circ$) (Fig. 4). This corresponds to a geomagnetic pole at 46.8° N latitude and 351.2° E longitude, which is far removed from Paleozoic poles for North America and is not similar to any younger poles for the continent (Fig. 5). Instead, the Rand Hill pole corresponds fairly well to some Precambrian poles (Brown, 1982).

The apparent polar wander (APW) path for Proterozoic rocks is not firmly established but paths have been suggested which share many

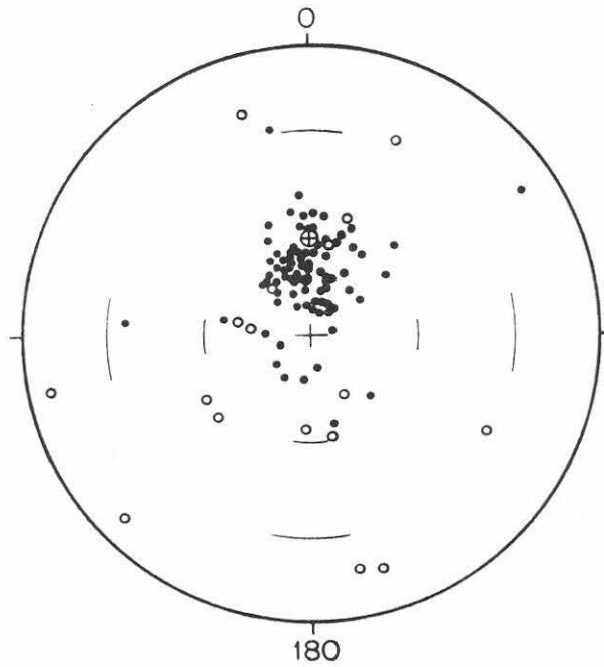


Figure 3. Natural remanent magnetization directions for all Rand Hill samples (n=102). Present earth field is indicated by cross in circle. Solid circle indicates positive inclination, open circle negative inclination.

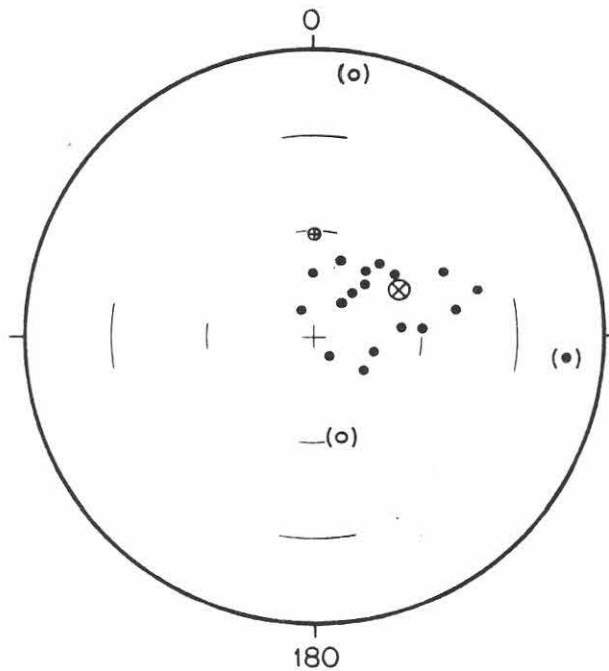


Figure 4. Inclination and declination of all Rand Hill sites. The mean is indicated by circled "x". Sites in parentheses are not included in the mean. The present earth field is shown by circled cross.

features. Figure 6 shows the position of the Rand Hill pole in relation to Grenville poles for North America. The correspondence is not exact but does suggest that the dikes may be older than the Paleozoic dates would indicate. Grenville paleopoles and part of the North American polar wander path of Buchan et al. (1983) are shown in Figure 7. The Rand Hill pole falls at a point on this APW path which is pre-980 Ma in age. Given that the dikes are not metamorphosed, their maximum age is constrained by the Grenville event which affected the Adirondack rocks 1.0-1.1 by ago.

Another APW path, (Roy and Robertson, 1978) is shown in Figure 8. The Late Proterozoic (Hadrynian) track in this figure is uncalibrated except for age limits between 950 Ma and 650 Ma from equator to equator. The Rand Hill pole falls on this track near the younger end but clearly before the 650 Ma position.

As was discussed under Geochronology, the K/Ar dates are now considered minimum dates of crystallization. Inasmuch as the dikes are relatively fine-grained and in places have glassy chill borders, they are interpreted to be Late Late Proterozoic or earliest Paleozoic, although this would be younger than the age suggested by the APW path proposed by Roy and Robertson above. In any case, the $^{40}\text{Ar}/^{39}\text{Ar}$ release spectra and the fact that the oxide phases, as well as the silicates, are altered, leaves further refinement of the diabase dike ages to the future.

GEOCHEMISTRY

Analytical methods

Four major and trace element analyses of dike rocks from Stop 1, and 15 from Stop 2, were made using an argon-plasma spectrometer at Middlebury College (Table 1). Neutron activation analysis of one sample was made for rare earth elements (REE) by Nuclear Activation Services, Ltd. in Ontario.

Results

The results show that although some of the major elements may have been mobile during alteration, all of the rocks have SiO_2 contents within the range of basalts.

Major and trace elements. All of the samples contain relatively high amounts of TiO_2 (2.32-2.65 percent). The differences among the three older dike types can be seen by plotting P_2O_5 vs. TiO_2 , Sc vs TiO_2 , and Ni vs FeO/MgO (Figs. 9a, 9b, 9c). In figures 9d and 9e, geochemical properties are plotted on tectonic diagrams. The Ti-Zr-Y diagram (Fig 9d) of Pearce and Cann (1973), shows that the diabase-olivine diabase dikes all fall in the center of the continental (within plate) basalt field, and the coarse-grained diabase (fine-grained gabbro) lies along its border. This classification fits the regional setting of these dikes. In the $\text{FeO}-\text{MgO}-\text{Al}_2\text{O}_3$ tectonic diagram (Fig. 9e) of Pearce and others (1977), the coarse-grained diabase again plots along the border of the continental basalt field. However, the diabase-olivine diabase

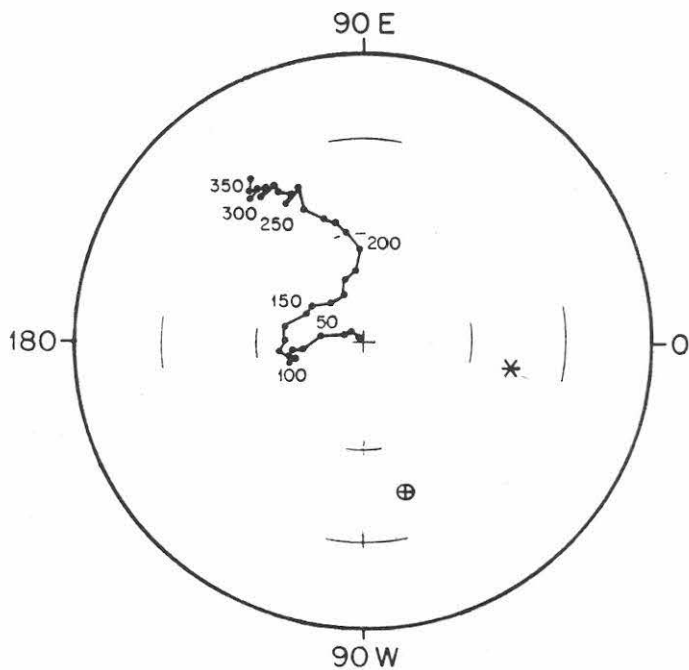


Figure 5. Apparent geomagnetic paleopole positions for the period 350 Ma to present. Center of diagram = north geographic pole. Star = pole position indicated by mean inclination and declination for Rand Hill. Circled cross = present position (latitude - longitude) of Rand Hill.

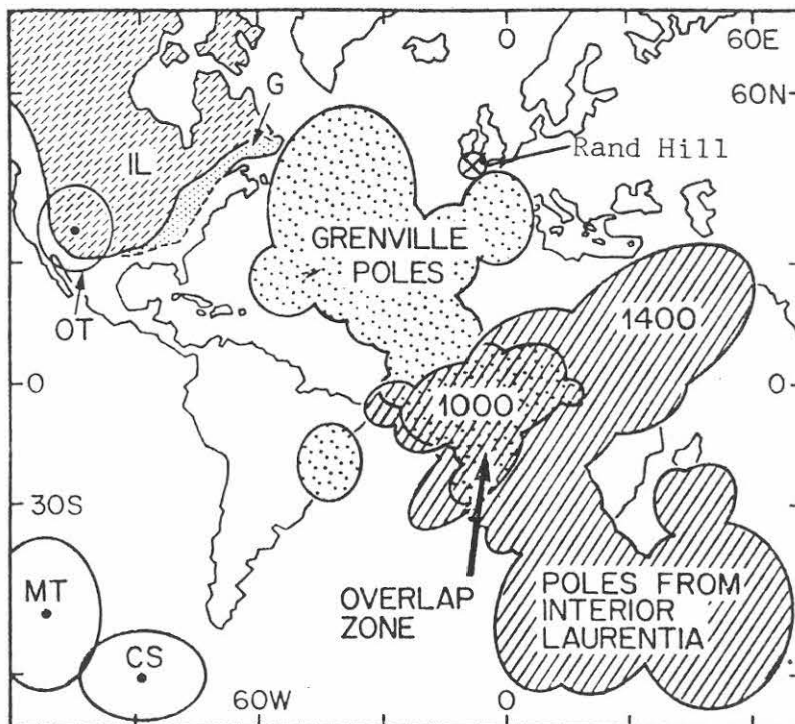


Figure 6. Rand Hill paleopole shown relative to Grenville paleopoles and others of the Grenville Structural Province. Modified from Irving and McGlynn (1976).

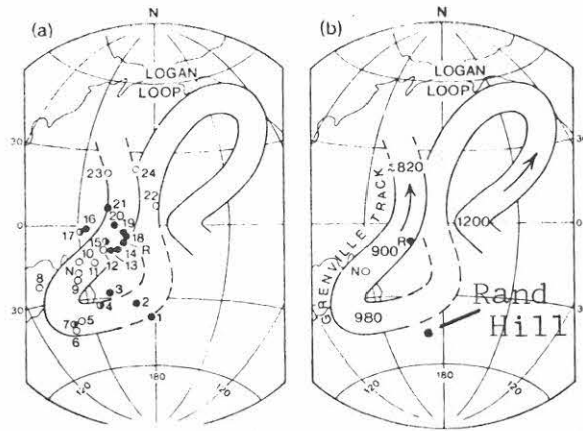


Figure 7. Grenville paleopoles and part of the APW path for North America (Buchan and others, 1983).

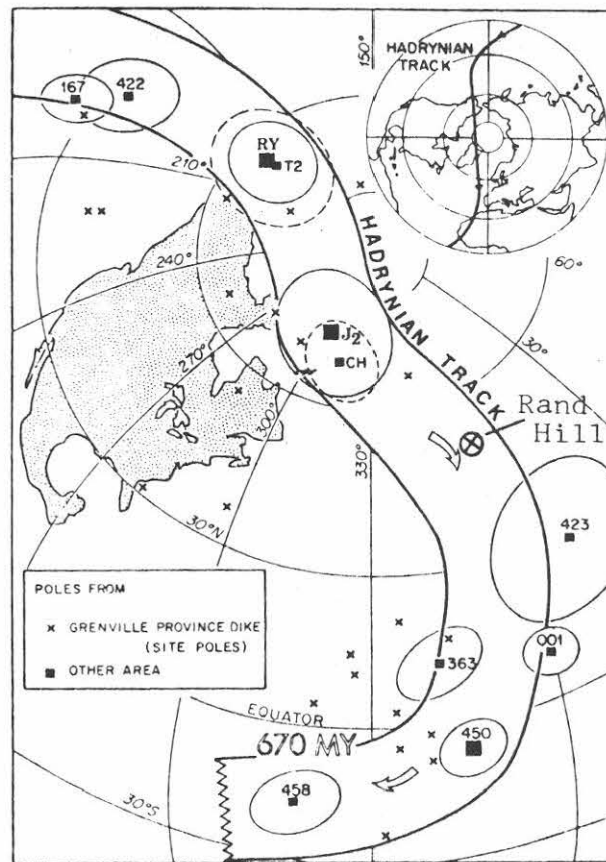


Figure 8. Part of the APW path for the Late Proterozoic, from Roy and Robertson (1978). Rand Hill paleopole is shown by circled "x".

Table 1

	Lamprophyres				Diabase + Olivine								Coarse Diabase		Trachyte Porphyry				
Sample	6257	6258	6282	6283	6189	6190	6191	6193	6196	6198	6200	6201	6194	6197	6183	6184	6185	6186	6187
SiO ₂	49.36	44.07	42.67	42.48	47.33	49.84	49.76	51.07	52.19	50.16	49.48	50.06	48.79	48.71	51.33	49.29	50.78	52.63	51.75
TiO ₂	2.17	2.42	2.73	2.74	2.66	2.49	2.58	2.46	2.35	2.64	2.65	2.52	2.36	2.32	2.60	2.64	2.48	2.45	2.49
Al ₂ O ₃	11.25	13.26	12.99	12.91	15.05	14.70	15.09	13.48	13.67	13.75	12.21	15.26	14.23	14.01	15.76	15.72	16.08	16.18	15.79
FeO	13.07	13.12	12.64	12.85	13.87	12.39	12.52	11.82	11.73	11.75	11.63	11.83	12.87	13.89	12.60	12.06	11.70	11.53	11.76
MnO	0.19	0.17	0.18	0.16	0.11	0.19	0.22	0.20	0.19	0.15	0.15	0.15	0.19	0.19	0.15	0.14	0.13	0.13	0.13
MgO	9.55	8.60	9.31	9.34	9.83	6.95	7.00	9.01	6.89	7.67	7.89	5.81	6.09	5.97	4.12	4.08	3.82	3.65	3.74
CaO	11.32	12.44	12.82	13.22	3.46	5.85	6.22	7.89	6.67	7.87	8.43	7.78	7.72	8.33	4.64	4.85	4.79	4.67	4.50
Na ₂ O	1.79	2.74	2.23	2.63	3.20	3.65	3.66	3.07	3.24	3.43	3.20	3.96	2.70	2.36	4.66	4.59	4.81	4.81	4.84
K ₂ O	2.15	1.97	2.28	2.28	1.78	1.65	1.86	1.43	1.44	1.55	1.45	1.69	1.52	1.79	2.84	3.06	3.40	3.45	3.31
P ₂ O ₅	0.85	1.01	1.10	1.14	0.84	0.89	0.91	0.54	0.47	0.61	0.62	0.88	0.45	0.42	1.36	1.35	1.27	1.27	1.28
Total	101.70	99.80	98.95	99.75	98.13	98.60	99.82	100.97	98.84	99.58	97.71	99.94	96.92	97.99	100.06	97.78	99.26	100.77	99.59
LOI	9.10	5.80	4.67	4.64	4.94	2.36	2.33	2.33	2.99	2.16	1.85	1.84	2.00	1.67	2.11	1.70	1.52	1.54	1.68
Trace Elements (ppm)																			
Sc	23	23	25	24	21	18	17	22	23	21	22	18	33	32	12	12	13	11	12
V	202	229	270	266	211	179	179	197	189	206	186	179	275	276	96	102	93	88	87
Cr	191	191	169	158	220	148	141	335	217	233	304	141	168	129	23	10	29	7	19
Cb	75	89	101	112	100	89	95	94	82	89	88	83	100	92	72	73	72	75	91
Ni	184	157	169	176	173	121	114	234	144	173	193	112	90	82	39	32	25	39	31
Sr	879	1121	2016	1630	390	570	537	422	334	488	526	706	238	226	620	652	647	658	593
Y	26	29	35	35	25	29	29	26	28	27	28	29	37	40	34	37	41	39	39
Zr	168	195	203	207	213	222	230	161	160	188	234	230	190	188	47	44	44	63	56
Ba	800	943	1393	1631	455	497	496	373	329	429	419	477	319	294	769	762	793	850	789

samples span the continental and adjacent ocean island fields. This is probably because any samples collected near the center of these flow-differentiated dikes would contain an above-average concentration of olivine and this would move the plots towards the MgFe side of the triangle. The trachyte porphyry samples fall outside of the tectonic fields of Pearce and Cann (1973) in Fig. 9d, but lie on the boundary of the continental basalt field in Fig. 9e. As discussed under Geochronology, field relationships suggest that the diabase and trachyte dikes are a coeval. Their geochemistry supports the interpretation that they are derived from a common magma source.

Rare-earth elements. The one sample of olivine diabase (sample no. 1968) that was analyzed for rare earth elements shows strong enrichment in the light rare-earth elements (LREE) relative to the heavy rare-earth elements (HREE) (Fig. 9f). This is similar to patterns found in early rift basalts in the Green Mountains (Coish and others, 1986) and in the Hudson Highlands (Ratcliffe, 1987). Modern alkali basalt from the African Rift system and oceanic islands have similar patterns.

The plots of Fig. 9e suggest that the olivine diabase and trachyte porphyry are geochemically similar to within-plate intrusions. This supports the interpretation that they are part of the rift-related volcanism along the eastern coast of North America that preceded the opening of the Proto-Atlantic (Iapetan) basin (e.g. Rankin, 1976). The diabases are similar to other basaltic rocks found along the Appalachians that are rich in Ti, Zr, Y, and P, and enriched in LREE.

The olivine diabases are chemically similar to the metadiabase dikes of the Hudson Highlands (Ratcliffe, 1987) and the Bakersville dikes of North Carolina (Goldberg and others, 1986) which cut Grenville-age basement along the western edge of the Appalachians and have been subjected to Taconian metamorphism. The chemically-similar dikes in the eastern Adirondacks are probably of the same vintage, but because the Adirondacks are part of the craton rather than the foldbelt, they are unmetamorphosed. The above metadiabase dikes have been interpreted as being associated with extension accompanying Iapetan rifting of North America, and the same interpretation fits the Adirondack diabases based on their relative age, geochemistry, and paleomagnetism.

Greenstones of the Tibbet Hill Formation in Vermont were interpreted by Coish and others (1986) as transitional to alkalic basaltic rocks that have high TiO₂, P₂O₅, Zr, and Y contents and are strongly enriched in the LREE relative HREE. Although the olivine diabases of Rand Hill have slightly lower Ti content and higher LREE. This may be because the Rand Hill dikes intruded the crust during earlier stages of Iapetan rifting (Coish and Sinton, 1988).

The geochemistry of lamprophyre dikes is described under Stop 1.

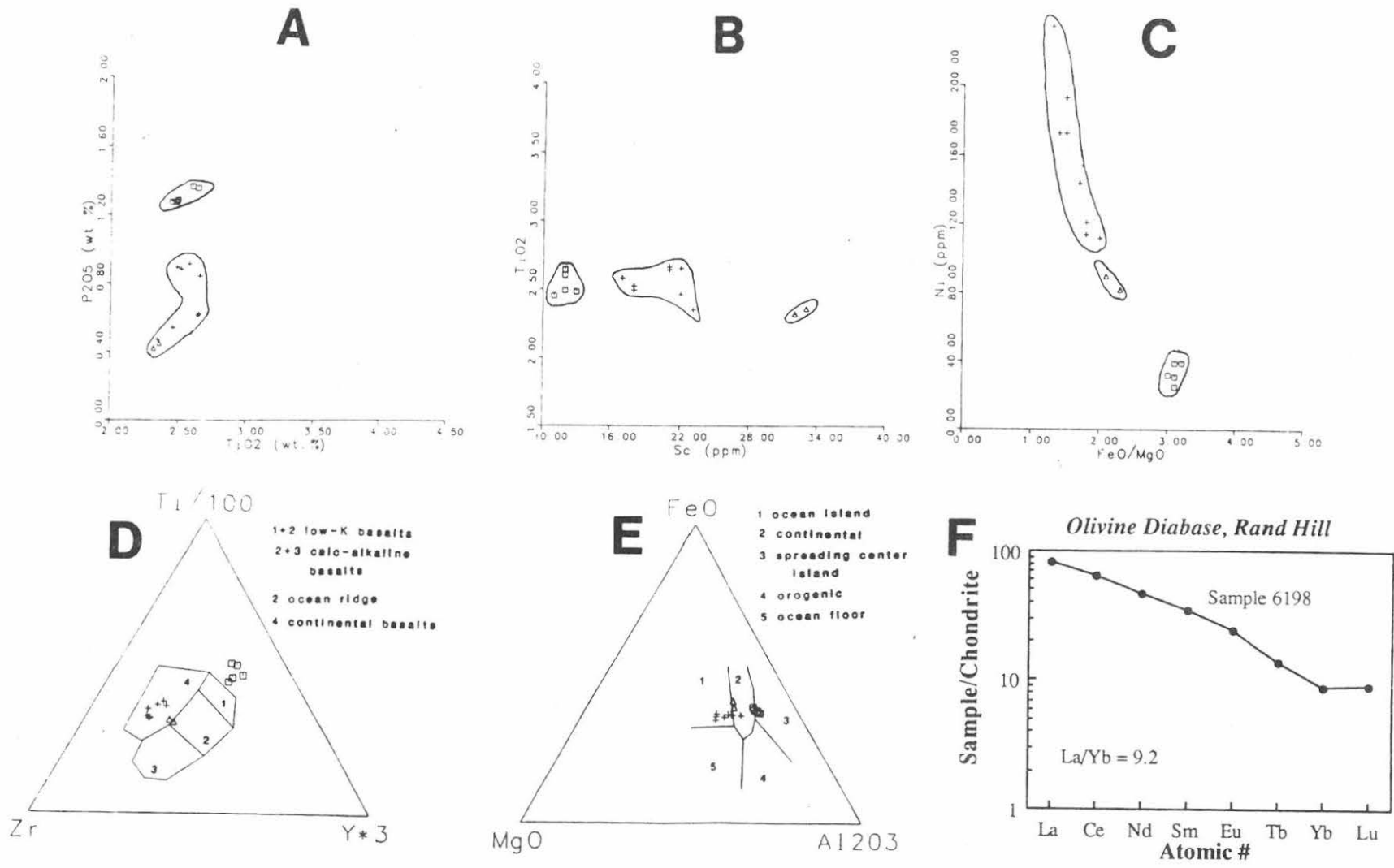


Figure 9. Geochemical plots showing the separate compositional fields of the three dike types: diabase-olivine diabase (plus sign), coarse-grained diabase (triangle), and trachyte porphyry (square). Triangular diagrams show tectonic fields proposed in the literature, as discussed in the text, and 9f shows rare earth element plot for olivine diabase sample 6198.

ROAD LOG

"For the structural geologist, eroded dykes may be viewed as the remnants of full-scale tests of the fracture strength of the Earth's crust. If field observations are properly interpreted, they will provide important constraints on the process of dyke emplacement."

David Pollard, 1987

MILEAGE		ROUTE DESCRIPTION
BETWEEN POINTS	CUMU- LATIVE	
0	0	From parking lot at west end of Hudson Hall at SUNY-Plattsburgh, turn right onto Broad St. and head west.
0.3	0.3	Turn right (north) onto N. Prospect St.
0.7	1.0	Tom Miller Rd. Turn left (west) cross overpass over I-87.
0.3	1.3	Quarry Rd. Turn right (north). Pass Plattsburgh Quarries on left.
0.9	2.2	Intersection with NYS Rts. 374 and 22. Turn left (west) onto 374, get into right lane, and park.
0.2	2.4	STOP 1. LAMPROPHYRE DIKES

Two lamprophyre dikes cutting a tilted fault block of Crown Point Limestone (Middle Ordovician) of the Chazy Group. The dikes strike N65-73W and dip 83-85 NE, parallel to the prominent joint set here. They are about 50 cm thick and display chilled margins. They contain calcite amygdules, clinopyroxene phenocrysts and local xenoliths of gabbroic metanorthosite. The subject of lamprophyres has recently been reviewed by Rock (1987). The name covers a number of alkalic rock types that form dikes or sills, and rarely lavas. They are defined by their content of abundant euhedral to subhedral phenocrysts of mafic minerals such as olivine, amphibole, biotite, clinopyroxene, apatite or oxides, but not felsic phenocrysts; the groundmass may be mafic, felsic or glassy. Silica content and Na/K ratio vary widely.

In the field, lamprophyres may be difficult to distinguish from diabase dikes, but a careful examination of textures shows lamprophyres to lack the familiar ophitic or diabasic texture with its visible laths of plagioclase. Instead, lamprophyres have a pronounced panidiomorphic-granular (sugary) texture with mafic phenocrysts of various sizes in a fine-grained alkali groundmass. Spherical, calcite-bearing

amygdules are common. They, and mafic phenocrysts, may weather preferentially to produce a pitted weathering surface. Although similar weathering also characterizes olivine diabase and olivine basalt, these show the lath-shaped crystals of plagioclase, commonly of phenocryst size.

The dikes at this locality are rich in amygdules filled with calcite. One dike shows an equigranular texture of biotite, plagioclase laths, subhedral and skeletal opaques, and olivine micro-phenocrysts, with some apatite and amphibole. Two samples taken from the southern side of the road show a characteristic porphyritic, texture, with large euhedral to subhedral phenocrysts of zoned clinopyroxene. The groundmass consists of essential biotite, plagioclase, subhedral opaques, apatite, and possibly amphibole. Alteration of the rock is minimal, but some of the mafic phenocrysts have been altered to chlorite and calcite. The presence of rounded anorthosite xenoliths suggests possible contamination of the magma.

From the whole rock chemistry (Table 1) these rocks can be classified as alkaline lamprophyres, according to Rock (1987). Note the high concentration of alkalis, particularly K_2O . The SiO_2 contents of the dikes are similar to those of the camptonites of the Champlain Valley studied by McHone and Corneille (1980). Rock (1987) notes that lamprophyres have distinctly higher concentrations of Ba and Sr relative to other silicate igneous rocks, and this is shown here. The lamprophyres have Sr values ranging from 879 to 2016 ppm and Ba values of 800 to 1631 ppm (Table 1), as compared to the diabase dikes at Stop 2 (Rand Hill) which have Sr values of 334 to 706 ppm and Ba values of 373 to 496 ppm (Table 1).

These dikes are probably related to other lamprophyres of Mesozoic age found within the Champlain Valley which have been associated with the alkalic syenite gabbro intrusions of the Monteregian Hills of Quebec (e.g. McHone and Corneille, 1980; deBoer and others, 1988).
Continue west on Rt. 374.

- | | | |
|-----|------|---|
| 3.2 | 5.6 | Turn right (north) onto Rt. 190 (Old Military Turnpike) |
| 6.4 | 12.0 | STOP 2A. RAND HILL DIKE SWARM |

Road cuts along Rt. 190 immediately south of Murtaugh Hill Road. Examination will be made first of the roadcuts here which provide fresh 3D exposures of the

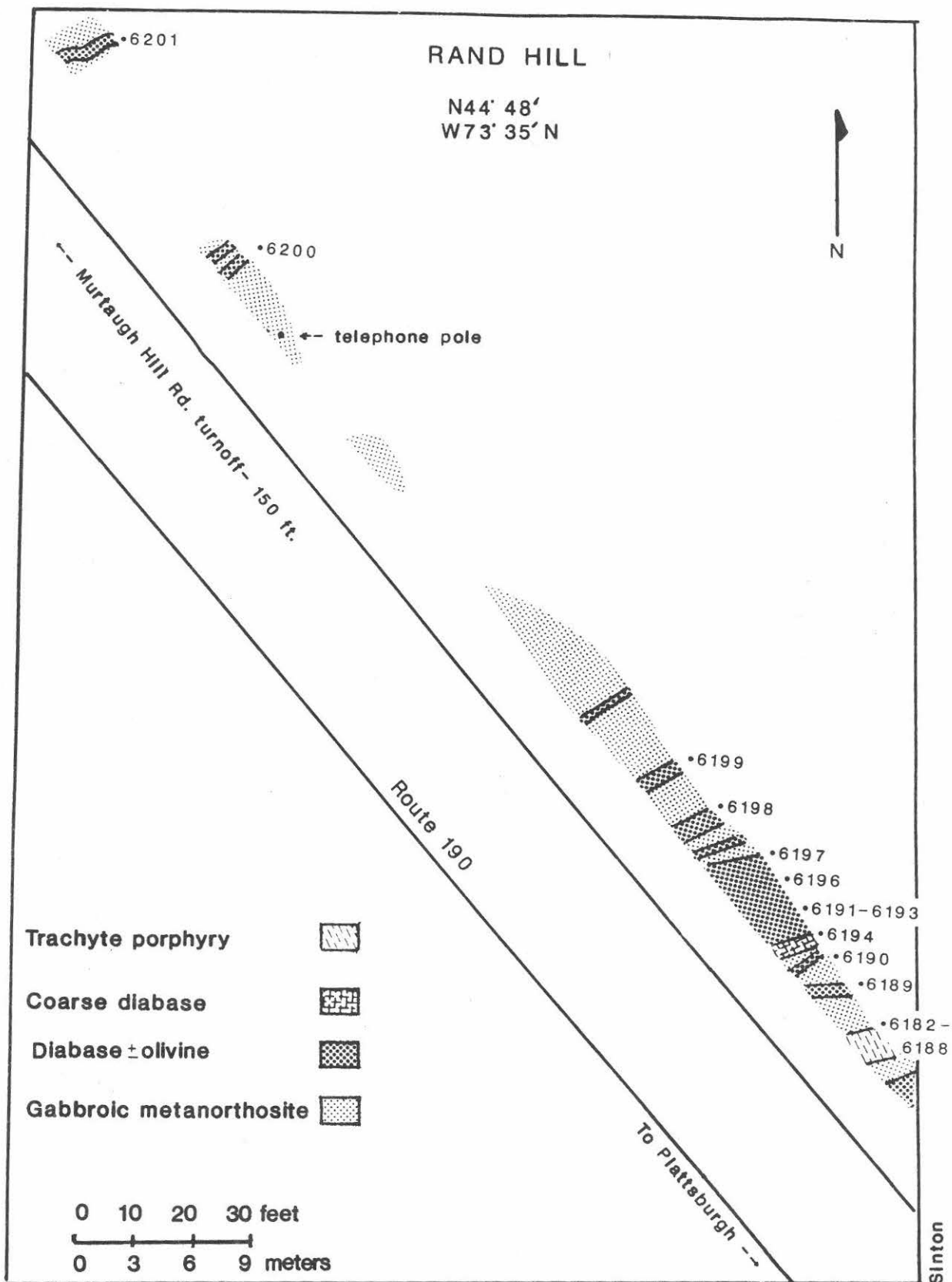


Figure 10. Pace and compass map of dike exposures on Rt. 190 at eastern flank of Rand Hill. Only dikes wider than 40 cm are shown. Sample site numbers are keyed to the chemical analyses of Table 1.

several dike types that make up the Rand Hill dike swarm. Very extensive exposures will then be examined in the largely open area that extends half a kilometer to the west, STOP 2B. The intruded country rock is gabbroic anorthosite gneiss.

The Rand Hill swarm is located at the eastern foot of Rand Hill. It was first described by H.P. Cushing (1898) who called attention to three localities in the northeastern Adirondacks with "exceedingly numerous dikes": Rand Hill, Dannemora Mountain, and the shores of Upper Chateaugay Lake. The Rand Hill dikes are nearly all vertical or sub-vertical, and consist of three types: diabase, olivine diabase, and trachyte porphyry (the "red syenite porphyry" of Cushing). Cushing noted that the thinner diabasic dikes are almost without exception porphyritic, and that the same applies to the borders of the wider dikes. In thin section, he found two generations of plagioclase and augite but only one of olivine. Biotite was observed in about 25 percent of the dikes.

Nineteen dikes are intruded into gabbroic meta-anorthosite in these road cuts. Their thicknesses range from 1 cm to 7 m. Some contain xenoliths and blocky plagioclase xenocrysts derived from incorporated host rock. The dikes are chilled at both their margins and along their contacts with xenoliths.

The distribution, dimensions, orientations, and classification of all dikes thicker than 40 cm is shown in Fig. 10. Dike identifications are based on field examination, including staining for K-feldspar, and then corroborated by thin section study. Numerous geochemical analyses were made in order to evaluate possible plate tectonic settings of the intrusions, as was discussed under Geochemistry.

The dominant dike type at Rand Hill is olivine diabase. Typically, altered olivine phenocrysts are concentrated in the central part of the dike by flow differentiation. The phenocrysts are altered to blackish serpentine clots (check hardness). The selective weathering of these clots accounts for the characteristic pitted surface. Although the olivines, with a specific gravity of 3.3 are concentrated in the centers of the dike by flow differentiation, the less dense plagioclase phenocrysts with a specific gravity of 2.7 are not; in fact they are generally concentrated in the finer grained border zones.

A 2.4 m wide trachyte porphyry dike with flow-aligned laths of Carlsbad-twinned plagioclase and K-feldspar is exposed near the southern end of the

roadcut (sample numbers 6182-6188). It is typical of this group, although the color of these dikes vary: they may be either red, greenish, or gray to black. Cushing (1901) identified 19 trachyte porphyry dikes at Rand Hill and summarized their petrography. The essential minerals are microperthite and biotite, and accessory minerals are magnetite or specular hematite, hornblende, quartz, albite, orthoclase, microcline, apatite, and sphene; secondary minerals are chlorite, calcite, sericite, epidote, and hematite. Microperthite and biotite or chlorite are the only two minerals found in all dikes examined. Staining here shows that both K-feldspar and plagioclase laths are up to 1 cm long but vary in size and abundance. Total feldspar makes up about 55 percent of the rock, chlorite-altered biotite about 40 percent, and opaque minerals plus apatite needles the remainder. Note small blocky xenocrysts(?) of gray plagioclase and incorporated angular fragments of mafic dike rock. As discussed under Geochronology and Geochemistry, the diabase and trachyte dikes at Rand Hill are coeval, and presumably derived from a common magma source.

The northern contact of this dike is faulted, as indicated by shearing of the dike (probably cataclasis) and the introduction of anastomosing, hematite-stained calcite veins.

A small xenolith(?) of coarse-grained diabase or fine-grained gabbro (sample site 6194) adjoins the 7 m-wide olivine diabase dike at its southern margin (Fig. 10). The xenolith(?) is crosscut by a thin diabase dike that is chilled against it.

Relict ophitic texture is visible in the xenolith(?) although the rock is pervasively stained by oxides. It contains about 50 percent subhedral plagioclase and 20 percent relict orthopyroxene, most of it altered to serpentine and chlorite. Its similar composition (Table 1) suggests that it may be a cognate inclusion (autolith) brought up from a deeper level in the same magma system.

0.1 12.1 **STOP 2B. RAND HILL DIKE SWARM**

Turn left (west onto Murtaugh Hill Rd. and park. Walk across the road onto open hillocks that expose at least 100 mafic dikes in gabbroic anorthosite gneiss (Fig. 11). This locality, at the eastern foot of Rand Hill, is by far the best exposed mafic dike swarm in the Adirondacks. Dikes are intermittently exposed for lengths in excess of 150 m. Their thicknesses range up to at least 5 m. Ramble westward, in a zig-zag course across the dike swarm to the end of the

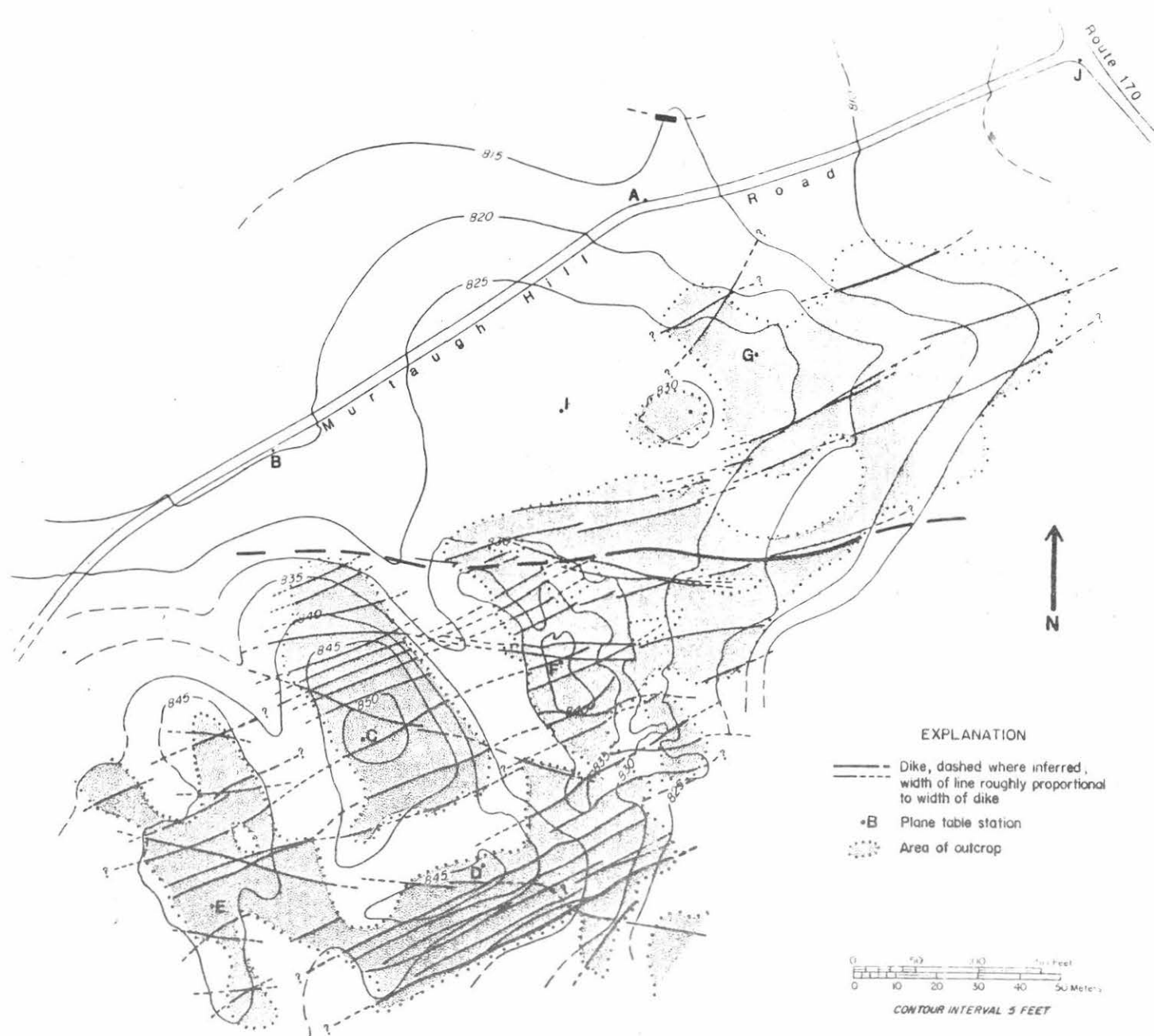


Figure 11. Plane table map of dike swarm on eastern flank of Rand Hill adjacent to Rt. 190. A few of the dikes shown are composites of two sheeted dikes, and some others are too closely spaced to be shown as separate dikes. More than 100 dikes are present here, representing three types: diabase, pitted olivine diabase, and trachyte porphyry. Modified after R. Barry, unpublished map. For location see Fig. 1.

exposure area about 350 m to the west. Exposures extend beyond the map area to the south and west.

Dikes here have three trends (Fig. 11), all cross-cutting the N30E strike of foliation in the host rock. The large irregular EW dikes bear alkali feldspar as shown by Kf staining. They are the "syenite porphyry dikes" of Cushing (1898). The N60-70E dikes are prophyritic olivine diabase dikes that show clear evidence of flow differentiation. Olivine phenocrysts that formed at depth have been concentrated in the centers of the rising magma by flow. The olivines are generally highly to completely altered, and weather out to produce the characteristic pitted surface. A N40E set is sparsely represented.

Note these interesting features of dikes during your ramble, and recall that basaltic dikes are emplaced almost instantaneously, the average velocity of propagation being 0.4-0.5 m/sec (Delaney and Pollard, 1982):

- 1) Chill borders against host rock.
- 2) Dikes may be straight, stepped, segmented.
- 3) Joints within the dikes do not penetrate the host rock: cooling cracks? compression features?
- 4) Dike walls may be even, irregular, cusped, and may have horn-like extensions or irregular apophyses.
- 5) Dike terminations may be tapered, blunt, rounded or irregular, and may have narrow extensions or "squirts".
- 6) Some dikes are composites of two sheeted dikes. The boundary between such dike pairs is a thin line of preferential erosion between the two adjacent chill borders. In at least one locality southwest of the mapped area, a sheeted dike pair bifurcates along strike around a slabbed inclusion of wall rock.
- 7) Relative age and direction of opening can be determined by analysis of dike intersections. These and en echelon configurations can also permit reconstruction of stress axes during emplacement. En echelon dikes indicate a reorientation of principal stress trajectories at the fingered propagation front of intrusive sheets (e.g. Delaney and Pollard, 1981).
- 8) Dike-parallel joints generally are absent in the host rock. This suggests that emplacement was not along pre-existing fractures but along an opening created and propagated by magma pressure in advance of the dike tip, in a plane perpendicular to the least compressive stress axis.
- 9) Concentration of olivine phenocrysts toward the center by flow differentiation.
- 10) Concentration of plagioclase phenocrysts near the margins rather than in the center.

11) Flow-aligned plagioclase laths indicate direction of magma propagation.

12) The amount of extensional strain produced by intrusion was significant in this swarm, reaching a magnitude of 18.8 percent north of Station C. A number of the dikes measured in this section could not be shown on the map of Fig. 11 because of its small scale.

Return southward on Rt. 190 to Rt. 374.

- | | | |
|------|-------|--|
| 6.5 | 18.6 | Turn left (east) on Rt. 374. |
| 3.4 | 22.0 | Intersection with NY Rt. 22 and Quarry Road; continue through intersection towards I-87. |
| 0.5 | 22.5 | Enter northbound entrance of (I-87), second right. |
| 1.8 | 24.3 | Turn right on NY 314 and continue straight through traffic light at NY Rt. 9 intersection. |
| 1.45 | 25.75 | Turn left at intersection between store on left and firehouse on right. |
| 0.85 | 26.6 | Turn left into private road. |

STOP 3. CAMPTONITE DIKE

NO HAMMERS; cameras instead. Xenolith-filled augite camptonite dike, Martin Bay. Private property; permission required of landowner.

The dike makes a low garden wall that strikes N80W. It is 0.5 m thick, and exposed over a length of 7m.

The place to concentrate on, however, is along the shore, where an isolated block of dike rock, 70 cm thick, has weathered out of its host rock, the Cumberland Head Argillite (Middle Ordovician). Note the parallel dike walls bordering the 10 cm-thick fine-grained chill margins. Note also the striking number of xenoliths concentrated in the 50 cm-thick central part of the dike by flow differentiation. These subangular to round xenoliths constitute about 50 percent of the dike, and appear megascopically to have sharp boundaries with the dike material. They range in diameter from 1 mm to 9 cm, most exceeding 2 cm. Lithologies include pyroxene syenite gneiss, gabbroic metanorthosite, metagabbro, and trachyte, as well as one ultramafic xenolith and a round xenocryst of hornblende. Note the slight flow alignment of elongate xenoliths.

In crushed grains and thin sections D.H. Newland (in

Hudson and Cushing, 1931) found that the syenitic inclusions contain microcline, microperthite, much-altered greenish pyroxene, and iron-stained grains that may be hornblende, biotite or both, along with small amounts of quartz, and occasional garnet crystals. The dike material is a fine-grained holocrystalline lamprophyre with phenocrysts of clinopyroxene and olivine in a felted groundmass of plagioclase, augite and opaque oxides. Staining indicates about 20% K-feldspar in the groundmass.

The xenoliths are typical of Adirondack rock types, so their source along the path of intrusion is easy to visualize. What is unusual is the fact that 1) among the 250 lamprophyre and trachyte dikes in the Lake Champlain area of New York and Vermont (McHone and Corneille, 1980) such xenoliths are extremely rare, and 2) the xenoliths are so remarkably rounded. Does the abundance in this one dike suggest that the magma advanced through a brecciated and fragmented fault zone? through a basal Paleozoic conglomerate? If the latter, the xenoliths are considerably larger than the pebbles in the rare exposures of basal Potsdam in the eastern Adirondack region. If the former, was the rounding produced by mechanical abrasion of incorporated breccia? by melt abrasion or partial resorption?

This particular dike gives a K/Ar date of 131 ± 5 Ma (Greg McHone, written comm., 2-19-85) which falls in the age range of the NY-Vt. lamprophyres and corresponds to the oldest ages of the Montereian Hills intrusions of Quebec (McHone and Corneille, 1980).

A similar xenolith-laden dike is well exposed farther south, in Indian Bay, Willsboro Point. It is an augite camptonite dike, more than 2 m thick, intruding Canajoharie Shale (Middle Ordovician). It is pictured and described by Buddington and Whitcomb (1941). McHone (written comm., 2-19-85) reports a K/Ar age of 119 ± 5 for this dike.

The narrow range of strike of the lamprophyre and trachyte dikes, in the Lake Champlain valley, as well as the consistency of Cretaceous ages, suggest that they are a cogenetic suite, perhaps a mafic-felsic pair formed by an immiscible liquid mechanism from mantle-derived camptonitic magma (McHone and Corneille, 1980).

Return to Rt. 9. Turn left to Plattsburgh, or straight ahead to enter the Northway (I-87).

REFERENCES CITED

- Bourne, J. and Hogarth, D.D., 1978, The Grenville Supergroup and younger rocks of the Gatineau-Lieore region: Ottawa, Ontario, Grenville Club Annual Meeting Fieldtrip Pamphlet.
- Brown, L.L., 1982, Anomalous paleomagnetic directions from Paleozoic(?) dikes, northeast Adirondacks: Geol. Soc. America, Abstracts with Programs, v. 14, p.8.
- Buchan, K.L., Farig, W.F., Freda, G.N., and Frith, R.A., 1983, Paleomagnetism of the Lac St-Jean anorthosite and related rocks, Grenville Province, Quebec: Can. J. Earth Sci., v. 20, pp. 246-258.
- Buddington, A.F., and Whitcomb, L., 1941, Geology of the Willsboro quadrangle, New York: New York State Museum Bulletin 325, 137p.
- Coish, R.A., Fleming, F.S., Larsen, M., Poyner, R., and Seibert, J., 1985, Early rift history of the proto-Atlantic ocean: geochemical evidence from metavolcanic rocks in Vermont: Am. J. Sci., v. 285, p. 351-378.
- _____ and Sinton, C.W., 1988, Opening of Iapetus: Rift & Ridge volcanics in Vermont. Ann. Meeting Geological Association of Canada, abstr. with programs, v. 13, p. A23.
- Cushing, H.P., 1898, Syenite porphyry dikes in the northern Adirondacks: Geol. Soc. America Bull., v. 9, p. 239-256.
- _____, 1901, Geology of Rand Hill and vicinity, Clinton County: New York State Mus., 53rd Ann. Rept. of the Regents for the year 1899, p. r37-r82.
- Dalrymple, G.B. and Lamphere, M.A., 1969, Potassium-argon dating, principles, techniques and applications to geochronology: W.H. Freeman and Company, San Francisco, 258p.
- deBoer, J.Z., McHone, J.G., Puffer, J.H., Ragland, P.C., and Whittington, D., 1988, Mesozoic and Cenozoic magmatism: in The geology of North America, v. 12, The atlantic continental margin: U.S. The Geol. Soc. Amer., p. 217-241.
- Delaney, P.T., 1982, Solidification of basaltic magma during flow in a dike: Amer. Jour. Sci., v. 282, p. 856-885.
- _____, and Pollard, D.D., 1981, Deformation of host rocks and flow of magma during growth of minette dikes and breccia-bearing intrusions near Ship Rock, New Mexico: U.S. Geol. Survey Prof. Paper 1202, 61p.

- Friedman, G.M., 1987, Deep-burial diagenesis: its implications for vertical movements of the crust, uplift of the lithosphere, and isostatic unroofing - a review: *Sedimentary Geology*, v. 50, p. 67-94.
- Geraghty, E.P., Isachsen, Y.W., and Wright, S.F., 1979, Dikes of Rand Hill, northeast Adirondacks, as paleostrain indicators: U.S. Nuclear Regulatory Commission Report NUREG/CR-0889, 13p.
- Goldberg, S.A., Butler, J.R., and Fullagar, P.D., 1986, The Bakersville dike swarm: geochronology and petrogenesis of late Proterozoic basaltic magmatism in the Southern Appalachian Blue Ridge: *Am. Jour. Sci.* v. 286, p. 403-430.
- Haggerty, S.E., 1976, Oxidation of opaque mineral oxides in basalts: in *Oxide Minerals*, Min. Soc. of America Short Course notes, v. 3, pp. hg-1 - hg-98.
- Hatch, F.H., Wells, A.K., and Wells, M.K., 1973, *Petrology of the igneous rocks*: Hafner Press, 551p.
- Heizler, M.T. and Harrison, T.M., 1987, The ups and downs of the Northeastern U.S. from the Proterozoic to the Jurassic: *Geol. Soc. America Abstracts with Programs*, v. 19, No. 7, p. 698.
- Hudson, G.H. and Cushing, H.P., 1931, *The dike invasions of the Champlain Valley*, New York: New York State Mus. Bull. 286, p. 81-112.
- Irving, E., and McGlynn, J.C., 1976, Proterozoic magnetostratigraphy and tectonic evolution of Laurentia: *Phil. Trans. Roy. Soc. of London, Series A*, p. 433-468.
- Isachsen, Y.W., and McKendree, W.G., 1977, Preliminary brittle structures map of New York: New York State Museum Map and Chart Series No. 31.
- _____, and Seidemann, D., 1983, Dike orientations in basement rocks of the Adirondack dome, New York, and regional paleostrain history as deduced using their K/Ar ages: 5th International Conference on Basement Tectonics, Cairo, 1983, *Abstracts of Papers*, p. 30.
- _____, Geraghty, E.P., and Wiener, R.W., 1984, Fracture domains associated with a Neotectonic, basement-cored dome-The Adirondack Mountains, New York: in Gabrielsen and others, eds., *Proceedings of the Fourth International Conference on Basement Tectonics*, Basement Tectonics Association, p. 287-305.
- _____, and Wright, S.F., in press, *Dike Map of the Adirondack Mountains*, New York: New York State Museum Map and Chart Series.

- Johnsson, M.J., 1986, Distribution of maximum burial temperatures across northern Appalachian Basin and implications for Carboniferous sedimentation patterns: *Geology*, v. 14, p. 384-387.
- Kemp, J.F., and Marsters, V.M., 1893, Trap dikes of the Lake Champlain region: *U.S. Geol. Survey Bull.* 261, 126 p.
- McDougall, I., and Harrison, T.M., 1988, Geochronology and Thermochronology by the $^{40}\text{Ar}/^{39}\text{Ar}$ Method: Oxford Univ. Press, New York (in press).
- McHone, J.G., 1984, Mesozoic igneous rocks of northern New England and adjacent Quebec: *Geol. Soc. Amer. Map and Chart Series MCH-049*.
- _____, and Corneille, E.S., 1980, Alkalic dikes of the Champlain Valley: *Vermont Geology*, v. 1, p. 16-21.
- Pearce, J.A., and Cann, J.R., 1973, Tectonic setting of basic volcanic rocks determined by using trace element analysis: *Earth and Planet. Sci. Lett.*, v. 19, p. 290-300.
- _____, Gorman, B., and Birkett, T., 1977, The relationship between major element chemistry and tectonic environment of deposition of basic and intermediate rocks: *Earth Planet. Sci. Lett.*, v. 36, p. 121-132.
- Pollard, D.D., 1987, Elementary fracture mechanics applied to the structural interpretation of dykes: in Halls, H.C. and Fahrig, W.F., eds *Mafic dyke swarms: Geol. Assn. Canada Sp. Paper 34*, p. 5-24.
- Rankin, D.W., 1976, Appalachian salients and recesses: Late Precambrian continental breakup and the opening of the Iapetus Ocean: *Jour. Geophys. Research*, v. 81, p. 5605-5619.
- Ratcliffe, N.M., 1987, High TiO_2 metadiabase dikes of the Hudson Highlands, New York and New Jersey: possible late Proterozoic rift rocks in the New York recess: *Am. Jour. Sci.*, v. 287, p. 817-850.
- Rickard, L.V., 1988, Stratigraphy of the subsurface Lower and Middle Devonian of New York, Pennsylvania, Ohio and Ontario: *New York State Mus. Map and Chart Series No. 39*.
- Rock, N.M.S., 1977, The nature and origin of lamprophyres: some definitions, distinctions, and derivations: *Earth Science Reviews*, v. 13, p. 123-169.
- Roy, J.L., and Robertson, W.A., 1978, Paleomagnetism of the Jacobsville Formation and the apparent polar path for the interval -1100 to -670 m.y. for North America: *J. Geophys. Res.*, v. 83, pp. 1289-1304.

"MIDDLE ORDOVICIAN STRATIGRAPHY AND SEDIMENTOLOGY -
SOUTHERN LAKE CHAMPLAIN VALLEY"

Bruce W. Selleck
Colgate University

David MacLean
Con-Test, Inc.

Introduction:

The Middle Ordovician strata (Chazy, Black River and Trenton Groups) of the Champlain Valley record the latter stages of passive margin deposition on the early Paleozoic continental margin of eastern North America. The onset of foredeep development, in response to loading of this portion of the continental margin during the late Middle Ordovician Taconic orogeny, is also recorded in this section by development of generally deepening-upward facies patterns in the Black River and Trenton Groups. The goals of this trip are to examine these units in the Southern Champlain Valley, interpret the depositional environments represented, and to assess the importance of tectonic controls upon regional facies patterns.

Regional Stratigraphic Framework:

The bedrock geology of the Lake Champlain Valley is dominated by Cambrian and Ordovician platform strata. The abundance of exposure in the area, the relative ease of access and early settlement account for the long history of geological study in the region. Early workers recognized that the Paleozoic rock units in northern and eastern New York consisted of basal sandstones (Potsdam Sandstone of Emmons, 1842) overlying highly deformed metamorphic basement (Grenvillian metamorphic terrain). Basal sandstones are succeeded by mixed quartz sandstones and dolostones (Calcareous Sandrock of Emmons, 1842 and Mather, 1843; later included in the Beekmantown Group by Clarke and Schuchert, 1899). The Beekmantown Group is overlain by younger calcite limestones (Chazy of Emmons, 1842; Black River of Vanuxem, 1842 and Trenton Group of Conrad, 1837). The stratigraphy of the Cambrian and Ordovician of New York has been recently reviewed by Fisher, 1977, whose nomenclature we generally follow in this paper.

In the past two decades, the evolution of the Cambrian and Ordovician platform sequence has been interpreted within the context of the plate tectonic history of the northern Appalachians. In general, basal non-marine clastics of the Potsdam Sandstone (Ausable Member) are thought to represent deposition in fault-bounded basins that formed during late Proterozoic-medial Cambrian rifting of the continental margin as the Proto-Atlantic opened (Fisher, 1977). Marine sandstones and carbonates of the Beekmantown Group document the development of the passive margin phase. Chazy Group strata indicate continued carbonate platform deposition, although regional stratigraphic and facies patterns suggest that the platform underwent localized faulting and minor uplift prior to, and during, Chazy Group deposition. Black River and Trenton Group strata are interpreted as an overall deepening upward sequence, documenting the onset of platform subsidence and foredeep development during the initial stages of the Taconic Orogeny. Calcareous argillites and deepwater limestones of the Cumberland Head Formation represent the "last gasp" of carbonate deposition prior to black shale and flysch facies of the late Ordovician foreland basin (Mehrtens, 1984). Latest Ordovician and Early Silurian units in central New York record the infill of the foreland basin. These units are not present in the Champlain Valley.

Chazy Group: Stratigraphy and Sedimentology

The regional stratigraphy of the Chazy Group has been most recently investigated by Oxley and Kay (1959) and Hoffman (1963) and is presently under study by one of us (BWS). Fisher (1968) provides descriptions of the Chazy Group in the northern Champlain Valley.

In the northern Champlain Valley, the Chazy Group is subdivided into three formations, the Day Point, Crown Point and Valcour. In the southern Champlain Valley, these subdivisions are difficult to apply. Oxley and Kay (1959) assigned the entire sequence at Crown Point, New York to the Crown Point Formation, whereas Raring (1973) recognized both Crown Point and Valcour Formations.

The Chazy Group overlies upper Beekmantown Group strata throughout the Champlain Valley. At Westport, New York, the contact is an angular unconformity, with tilted and truncated Bridport Formation dolostones overlapped by basal shales and sandstones. Elsewhere in the outcrop belt, the basal contact is apparently disconformable, although Speyer (1982) has suggested that the contact exposed on Isle La Motte (northern Champlain Valley) is conformable. The maximum thickness of the Chazy is estimated at 235 meters in the Valcour-Valcour Island sections (Oxley and Kay, 1959), however this section is characterized by numerous normal faults and incomplete exposure. Recent work by one of us (BWS) suggests that the thickness is less than 200 meters in the Valcour section. The Chazy Group generally thins to the south in the Champlain Valley, with 95 meters present at Crown Point, and less than 25 meters at Ticonderoga, New York. Chazy Group strata are absent from the platform stratigraphy

Stratographic Nomenclature of Ordovician
 Strata - Southern Lake Champlain Valley

MEDIAL ORDOVICIAN	MOHAWKIAN	TRENTON	GLENS FALLS
		BLACK RIVER	ISLE LA MOTTE
L. ORD.	CHAMPL.	CHAZY	VALCOUR CROWN POINT DAY POINT
	CANAD.	BEEKMAN-TOWN	BRIDPORT FORT CASSIN WHITEHALL

south of Whitehall, New York. Chazy rocks are present beneath the Taconic thrust sheets south and east of the Whitehall area, based upon the occurrence of Crown Point strata in fault slivers at the base of the Taconic Frontal Thrust near Granville, N.Y. (Selleck and Bosworth, 1985).

Rapid facies changes occur along the Champlain Valley outcrop belt, apparently in response to irregular topography on the underlying Beekmantown erosional surface and perhaps, syndepositional faulting. Tidal flat, shelf lagoon, shoal sand, reef and reef flank facies are exposed in the Champlain Valley. Terrigenous clastics are present at the base of the Chazy, and are thickest in the Ottawa Valley, where non-marine (braided stream) facies occur (Hoffman, 1963).

In the southern Lake Champlain Valley, reef facies are not present in the Chazy Group, but faunal diversity is generally high. Brachiopods, calcareous algae, bryozoans, gastropods, nautiloids, trilobites and pelmatozoans are abundant in subtidal shelf facies. Tidal flat and sand shoal facies bear a restricted fauna, dominated by the large gastropod Maclurites magnus.

A disconformity caps the Chazy Group in the southern Champlain Valley, suggesting slight emergence of the shelf prior to deposition of the overlying Black River Group. At Crown Point, this interval is marked by a thin arkosic sandstone which contains Adirondack-derived quartz and feldspar. These sands indicate that Proterozoic basement was exposed nearby at the end of Chazy deposition, perhaps in response to uplift along normal faults to the west.

Black River Group:

In the type area of the Black River Group in northwestern New York State, four formations are recognized in the Black River Group; in ascending order, the Pamela, Lowville, Chaumont and Watertown. Although facies resembling portions of these formations are recognizable in the southern Champlain Valley, the Black River Group is considerably thinner than in the type area, and a single formation name, the Orwell, is generally applied to the entire Black River. Fisher (1984) has suggested two formations, the Isle La Motte and Amsterdam, can be recognized in the Glens Falls region.

In the southern Champlain Valley, the Orwell consists of basal sandy dolostone overlain by poorly fossiliferous lime mudstones. These facies are rapidly succeeded by fossiliferous packstones and wackstones which characterize the Orwell in most exposures. The faunal diversity of typical Orwell is high, with gastropods, nautiloids, rugose and tabulate corals, crinoids, stromatoporoids, bryozoans, brachiopods and trilobites common. This faunal assemblage indicates deposition on a shallow, but relatively quiet subtidal shelf. The sequence is punctuated by bioclastic and intraclastic current-stratified grainstones, suggesting sporadic storm events.

Exposures of the Black River Group in the Champlain Valley are rarely complete, and geographically scattered, limiting correlation from south to north. This unit has received very little detailed study, and we encourage interested workers to pursue study of this unit.

Trenton Group:

In the southern Champlain Valley, the contact between the Black River and Trenton Groups is relatively abrupt and is characterized by increased terrigenous mud content and change in bedding style. The entire Trenton Group in the region is assigned to the Glens Falls Formation, which typically consists of interbedded calcareous shales and limestones. The fauna of the Trenton is diverse, although it lacks the large stromatoporoids, corals and bryozoans of the Black River. Brachiopods, trilobites and smaller bryozoans are particularly abundant. Overall, the Trenton was deposited at depths below normal wave base or on a low gradient ramp-type shelf. The interbedding of limestone and shale is interpreted as resulting from storm deposition, with intervening periods of mud accumulation. Turbidite bedding features are recognized in some exposures.

The Trenton Group in the Champlain Valley becomes progressively shallier up-section, and is overlain by calcareous argillites of the Cumberland Head Formation. This unit gives way to black shales and siltstones of the Canajoharie Shale. This trend resulted from the deepening; of the Trenton shelf to depths sufficient; to reduce biogenic carbonate production, coupled with increasing terrigenous sediment input. This facies transition to deepwater dark muds marks the development of the Taconian foreland basin in New York. Progressive east-to-west deepening was accomplished by normal faulting of the shelf, and was linked to the onset of the Taconic Orogeny. Wedging of the continental margin into an east-dipping subduction zone, followed by loading of the margin by west-direct thrusting of the Taconic accretionary prism accounts for the development of this basin. Cisne, et al (1982) have suggested that the convergent tectonic regime of the Taconic Orogeny and related history of the Ordovician foreland basin of the northern Appalachians is analogous to the modern Timor-Timor Trough-north Australia shelf collisional system. In the Timor analogue, the attempted underthrusting of the northern Australian plate margin has led to progressive deepening and syndepositional normal faulting of the previously shallow water north Australia platform, producing a deep-over-shallow facies pattern that is very similar to the Canajoharie-over-Trenton sequence of the middle Ordovician of New York State.

Following the deposition of the black muds atop the foundered carbonate platform, synorogenic sands and muds were shed from the rising Taconic accretionary prism. In some areas, these deposits are deformed by later thrusting. Molasse deposition is recorded in deltaic and marine shelf facies of the upper Ordovician Lorraine group and Oswego Sandstones in west-central New York. These units are not exposed in the Champlain Valley.

FIELD TRIP STOP DESCRIPTIONS

Since this trip consists of two major stops, we have not included a detailed trip log. From Plattsburg, we will proceed south on I87 to the Westport exit, continue south on Rt. 9N through the village of Westport. Our first stop is located approximately 3 miles south of Westport on Rts. 9N and 22 at roadcuts immediately south of the railroad overpass. Please exercise extreme caution - traffic is heavy and visibility poor!

Stop #1: Westport, New York

These roadcuts expose approximately 24 meters of the Glens Falls Formation of the Trenton Group. Stratigraphically, we are located in the middle and upper portion of the Glens Falls, within the zone of Cryptolithus tessellatus. The Glens Falls at this exposure consists of two major facies. The lowermost three meters, and the uppermost ten meters of the section are characterized muddy packstone beds, often capped by Chondrites burrows. The limestone beds are separated by thin calcareous shale interbeds. Each limestone bed consists of a couplet, with the basal portion of the bed characterized by whole-shell and fine bioclastic grainstones, and the upper portion consisting of slightly fossiliferous mudstones. This facies is interpreted as a storm surge ebb current deposit, resulting from the turbidity current-like flows generated as storm wave surge resuspended mud and shell debris on shallower portions of the shelf. Fossils are relatively abundant in this facies, and include the typical Trenton brachiopods, bryozoans and rare trilobites.

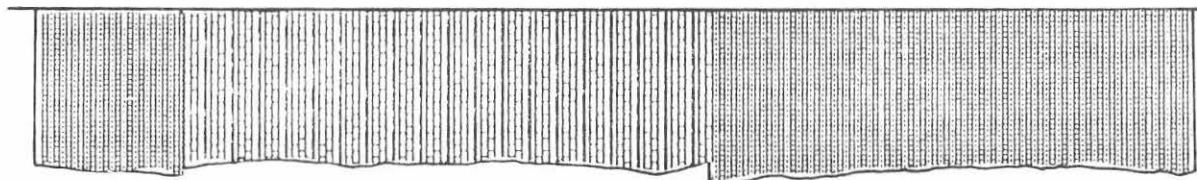
The middle ten meters of the exposure consists of somewhat more regularly bedded argillaceous micrites, with relatively thick (2-20 cm.) shale interbeds. The argillaceous mudstone beds show limited size grading, and are often highly bioturbated. Fossils are scarce in the limestone beds, but interbedded shales may contain bryozoans and other bioclasts. This facies is interpreted as a hemipelagite, resulting from deposition of suspended lime and terrigenous mud in a setting unaffected by wave and storm driven currents. The abundant shales in this facies indicate a sudden increase in the influx of terrigenous sediment to the shelf at this time. Insoluble residues from the limestone beds often contain abundant silt-size euhedral quartz, plagioclase and sanidine crystals, suggesting that volcanic ash was supplied, perhaps from the Taconian island arc system to the east. This facies is traceable to the east in sections on the Vermont side of Lake Champlain.

Route to Stop #2: Continue south on Rts. 9N and 22, through the village of Port Henry. Turn left (east) approximately 4 miles south of Port Henry, following signs for Bridge to Vermont. Continue northeast toward Crown Point Bridge, turning left onto entrance road for Crown Point Historic site. Continue on entrance road and park at Picnic Pavilion. Note: NO COLLECTING OR HAMMERING ALLOWED AT THIS SITE!!!

10 METERS



GLENS FALLS FORMATION

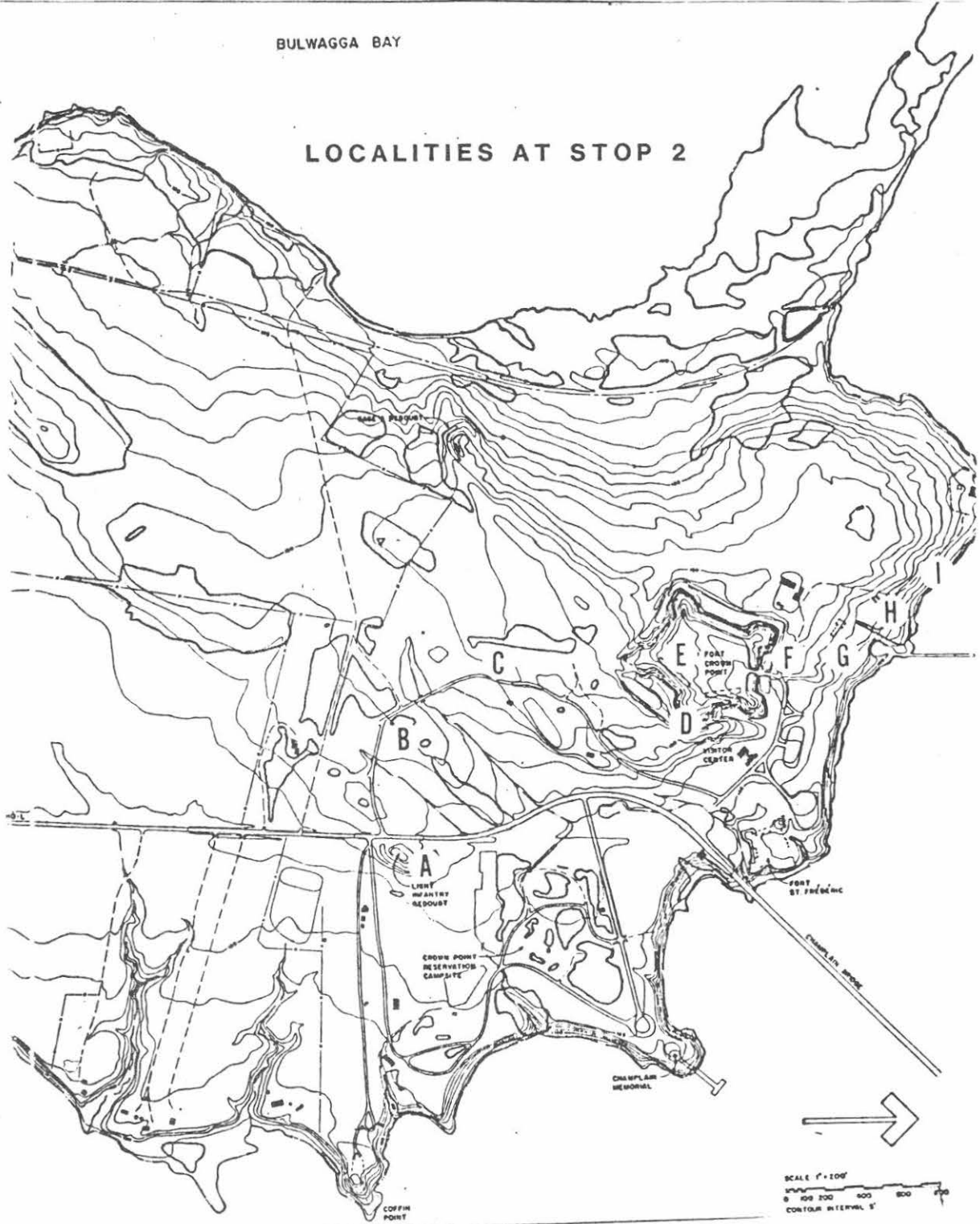


ARGILLACEOUS MICRITES
W/THICK SHALE INTERBEDS

MUDDY PACKSTONE
W/THIN SHALE INTERBEDS

SECTION AT WESTPORT (STOP 1)

LOCALITIES AT STOP 2



Crown Point Section:

The Crown Point section provides one of the most complete middle Ordovician sequences available in the Champlain Valley. The strata here dip gently (approx. 8 degrees) to the northwest, such that as we walk to the north, we travel continuously up-section. The main exposures are within a single fault block, however, north-northeast trending normal faults are present on the west and east sides of the peninsula. The contact between the Chazy Group and underlying lower Ordovician Bridport Formation is exposed on the east side of the point, on the shoreline of Bullwagga Bay. This section will not be visited on this trip, but can be accessed from the main road just south of the Historic Site entrance. Those who wish to examine this contact may do so after the last stop.

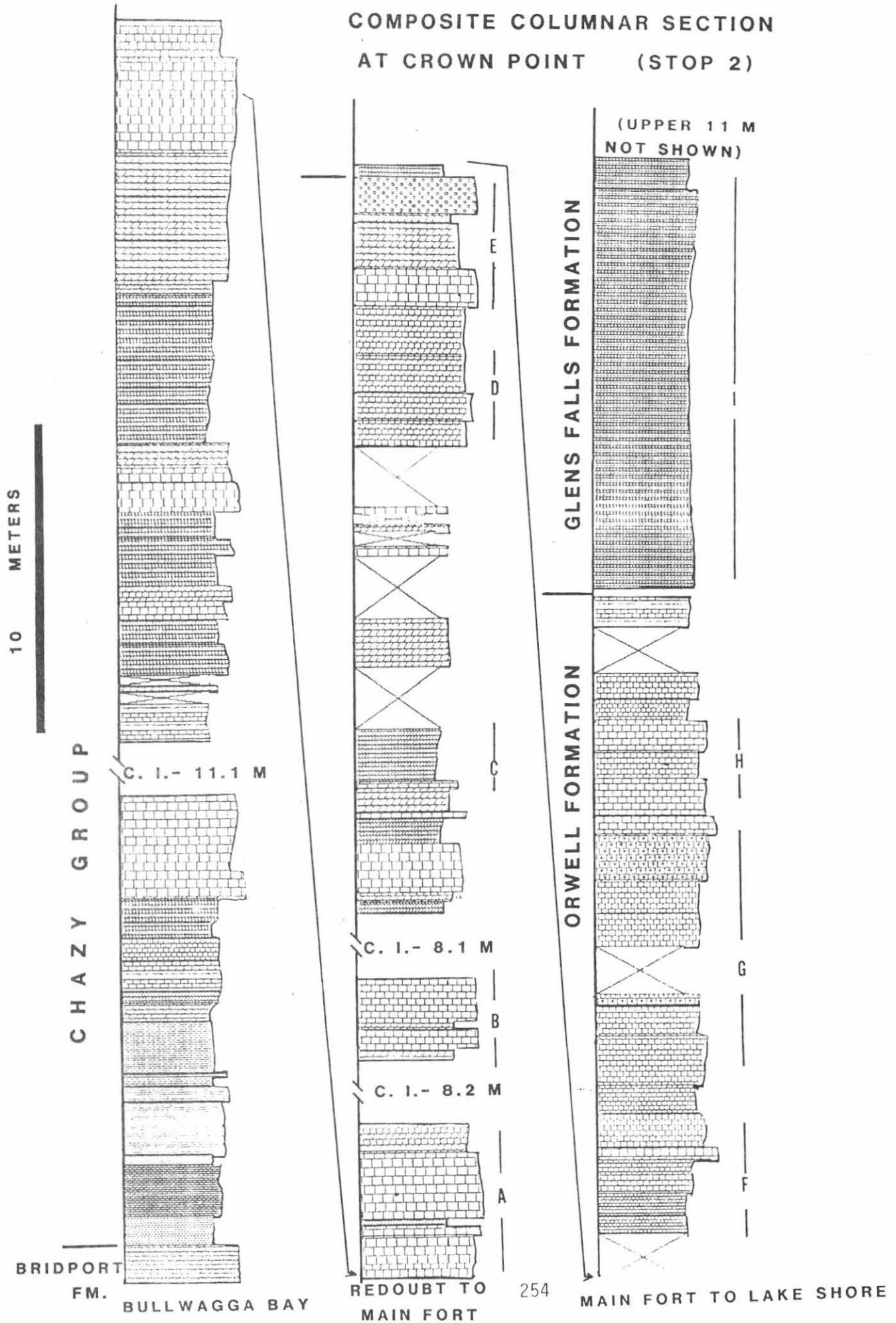
The Chazy Group at Crown Point comprises approximately 95 meters, the Black River Group approximately 24 meters, and the Trenton, 25 meters with the summit not exposed. The uniform strike and dip of the section allow for straightforward calculation of the thickness of covered intervals, making this an excellent site for introductory field course mapping exercises.

To reach stop 2A from the Picnic Pavilion, we will walk back along the entrance road and cross the main highway to the Redoubt Fort excavations immediately southeast of the entrance road.

Stop #2A: Redoubt Fort east of N.Y. 8

Approximately 6 meters of variously burrowed, slightly dolomitic, thin to medium bedded bioclastic packstones are exposed in this section. The dolomite occurs in shaly weathering wisps and laminae and in burrow fills. Abundant "Girvanella" algal oncolites (algal accretionary grains) are present in the beds approximately 4 meters from the base of the section. Rounded dark calcite grains (abraded gastropod fragments) form the cores of the oncolites, and are scattered in other beds. Fossils are relatively abundant and best seen on bedding surfaces. Trilobite fragments, brachiopods, byozoans, pelmatozoan plates, nautiloids and large Maclurites magnus are present. The relatively high faunal diversity, abundant lime mud and burrowing argue for a normal marine, low energy shallow subtidal carbonate environment. A possible modern analogue is found in the mixed mud and sand shelf to the west of the emergent Andros Island tidal flats, as described by Bathurst (1971) and Purdy (1963). The 5-10 cm thick beds of "oncolite conglomerate" and other more well-sorted grainstone beds may represent periods of storm winnowing of the bottom, with transportation of abraded sand from adjacent sand shoal environments (e.g. Locality 2B). The wavy, irregular dolomite laminae appear to result from post-depositional dolomitization of lime mud, followed by compaction and local pressure solution of calcite, producing irregular, clay- and dolomite-rich stylocumulate seams. Preferential dolomitization of burrows may be due to contrasts in porosity or permeability of burrow-fill versus burrow-matrix sediment. The burrow-fill sediment may have retained

COMPOSITE COLUMNAR SECTION
AT CROWN POINT (STOP 2)



permeability longer during diagenesis, permitting pervasive dolomitization. This sort of fabric selective dolomitization is common throughout the Chazy and Black River Groups in the southern Lake Champlain Valley.

Stop #2B: Ledge immediately NE of gate to Historic Site

Cross-stratified coarse lime grainstones with bipolar crossbed dip directions are well-exposed near the entrance road. Siliciclastic sand grains (angular quartz and feldspar up to 2 mm in diameter) are locally concentrated along prominent stylolite seams. The carbonate particles are dominantly subrounded, abraded pelmatozoan plates, plus gastropod and brachiopod fragments. Large Maclurites fragments and grainstone intraclasts are present on the upper bedding plane surfaces of the ledge.

We envision the environment of deposition of this facies as shallow subtidal wave and/or current reworked sand bars. Active transport of abraded grains may have been accomplished by tidal currents as suggested by the bipolar cross-beds. The lack of burrows and well-preserved fossils may be due to the inhospitable shifting sand substrate. This environment may have been rather like the unstable sand shoal environments described from the Bahamas Platform by Bathurst (1971) and Ball (1967). The scale and style of cross-stratification present here are similar to that predicted by Ball from his studies of the bedforms and primary structures of the Bahamian sand bodies. Similar Chazyan facies in the northern Champlain Valley contain abundant oolites (Oxley and Kay, 1959).

Stop #2C: Low ledges on entrance road approx. 50 meters north of 2B

Brown weathering, slightly shaley dolostone exposed here contains small lenses and stringers of fossiliferous lime packstone. Trilobites, small brachiopods and Maclurites fragments are common. This exposure resembles the shelf lagoon facies of Stop 2A, although dolomitization is more pervasive.

Stop #2D: East point of British Fort, by horizontal water tank and adjacent south moat

Approximately 3 meters of thickly laminated limestone and dolostone is exposed in the southeast "moat" of the British Fort. The dominant facies here consists of alternating 0.5-2 cm thick laminae of limestone and dolostone - often termed a "ribbon rock". The limestone ribbons are mudstones and appear blue-grey on slightly weathered surfaces. The more resistant dolostone weathers tan to brown. An erosional surface with 10-20 cm of relief is exposed near the base of the south wall. Abundant Maclurites occur in a shell bed on this surface. Trough cross-strata consisting of gently dipping ribbon rock are present above the erosional surface. Dolomitized burrows transect the limestone ribbons in the lower 1 meter of the section. On the less-weathered prominence on the SE corner of the

moat, shallow scours containing a shell hash of brachiopods and gastropod debris are present, along with intraclasts of lime mudstone in dolostone and "Mexican Hat" structures (rolled intraclasts or pseudoclasts with a dolomitized burrow center).

We interpret this sequence as a tidal flat facies. The rhythmic limestone/dolostone "ribbon" fabric is interpreted as representing alternating slightly finer (lime mudstone) and coarser (dolostone) "tidal bedding" similar to that described by Reineck and Singh (1980) from the clastic mud/sand tidal flats of the North Sea. The Maclurites shall bed may mark the basal erosional level of a tidal channel, with the cross-stratified ribbon laminites forming by draping on the channelled surface. Variations in degree of burrowing record subtle differences in degree of subaerial exposure of the flat and/or reworking by tidal currents. Limited in situ faunal diversity is also expected in the stressed tidal environments. The absence of mudcracks and any indication of evaporite minerals suggests that we are seeing only the lower portion of a wet intertidal flat system preserved here.

Stop #2E:

Enter Parade Grounds by barracks. Around 1916, gunite was sprayed on the interior walls to protect the mortar from deteriorating. Starting in 1976, the N.Y. State Division for Historic Preservation began extensive maintenance, removing loose gunite, replacing rotted stones and repainting the stone walls.

In the outer wall of the first barracks, note at about eye level the stones that are nearly white-weathering. These are lime mudstones from the "Lowville" facies of the Orwell Limestone, exposed at Stop 2F.

The broad limestone outcrop west of the barracks is a cross-stratified limestone with scattered subrounded quartz and feldspar sand grains. Trough cross-strata and "herringbone" co-sets of planar-tabular cross-strata are visible on the low vertical face. Large angular clasts of slightly dolomitic lime grainstones and Maclurites magnus shells are present on the uppermost bedding surfaces.

We interpret this facies as a current-dominated sand shoal environment rather similar to the exposures at Stop 2B.

Westward across the parade grounds there is a massive, bioturbated, brown weathering dolostone unit (similar to Stop 2C), overlain by 0.5 meters of very coarse-grained bioturbated, lightly dolomitic feldspathic quartz sandstone. This sandstone forms the summit of the Chazy Group (Crown Point Formation). The abundant angular quartz and feldspar granules in the sandstone suggest derivation from a relatively close granitic (Adirondack?) source terrane. These sands were apparently transported from the west

during an interval of relative emergence of the carbonate platform and were briefly reworked in a shallow marine setting. The basal dolostone bed of the Black River is exposed immediately atop the sandstone.

Stop #2F: Moat Walls at North Entrance to British Fort

The section from here to locality I is within the Orwell Limestone. The basal beds consists of thick-bedded to massive lime mudstones with vertical spar-filled burrows (form - genus Phytopsis) and rare ostracodes. Fossil abundance and diversity increase in the overlying beds, with gastropods (Loxoplocus), corals (Lambeophyllum, Foerstephyllum) and brachiopods appearing. Grain size increases upsection, with sporadic appearance of intraclast grainstones and ripple cross-lamination. Overall this section is similar to the Lowville Limestone of the type Black River Group of the Tug Hill region. The facies pattern here suggests a progression from restricted (tidal or lagoonal?) mud flats (Phytopsis lime mudstones) to more open marine mixed mud/sand shelf environments.

The summit of the moat outcrop exposes a horizon of black chert nodules which can be traced laterally across the road to locality G.

Stop #2G: Ledges extending from service road to lake shore

Watch for poison ivy!

These exposures closely resemble the Chaumont (House Creek Limestone of Fisher, 1977) facies of the Black River type section. Thick-bedded to massive richly fossiliferous lime packstones and wackestones document a normal marine, relatively low energy carbonate shelf environment. In addition to the forms mentioned earlier, the large stromatoporoid (calcsponge) Stromatocerium, the high-spined gastropods Hormotoma and Subulites, the nautiloids Actinoceras and Geisonoceras, plus bryozoans, brachiopods and pelmatozoan material are common. on some bedding surfaces, black chert nodules follow large horizontal burrows. The chertification here is post-depositional and involved dissolution and reprecipitation of siliceous skeletal material (sponge and radiolarian). The uppermost bed in this set of ledges is a black chert bed approximately 2 cms thick. This bed can be traced to the lake shore where a similar section can be seen. Glacial abrasion obscures much of the detail that is exposed on more weathered surfaces.

Stop #2H: Blocks and Quarry Walls by Lake Shore

The quarry was established in 1870 by the Fletcher Marble Co. in an unsuccessful attempt to find a source of "black marble" dimension stone. The quarry is reportedly only 1 meter or so deep. The narrow spit going north was built to load blocks on barges, but evidently no blocks were shipped. The quarried blocks consist of medium to thick-bedded fossiliferous packstones and wackestones with some ripple cross-laminated grainstone beds visible in the north quarry bench. Strophomenid brachiopods, bryozoans, pelmatozoan stems and fragments

of the trilobite Isotelus are present. The environments represented here are similar to those at 2G. As we continue north and walk along the lake shore, more exposures of the upper part of the Orwell can be examined. The bedding surfaces contain abundant opercula of Maclurites logani, and scattered Forstephyllum, Lambeophyllum and Stromatocerium are found. The byssate bivalve Ambonychia is also present.

The transition from the Orwell to overlying Glens Falls Limestone is covered by beach gravels as we continue west along the lake shore.

Stop 2I:

The contact between the Orwell Formation and the basal Glens Falls Limestone is covered by beach gravels. The lower 16 meters of the Glens Falls lies below the first occurrence of Prasopora. Cryptolithus appears approximately 20 meters from the base of the section. Thus, only the uppermost 10 meters of section are time equivalent to the Westport exposures seen at Westport. The Glens Falls at Crown Point consists of the same muddy packstone facies seen at Westport. Limestone beds typically have shelly basal portions which rapidly grade upward into muddy packstones. Thin calcareous shale interbeds define the bedding. This facies is again interpreted as storm surge-ebb current deposits with intervening shale suspension rainout. There is a slight tendency for the bedding style in the lower portion of the section to be more wavy or lenticular, perhaps suggesting that storm wave scour occurred. The upper portion of the section is slightly thinner bedded, and bryozoans become relatively more abundant. Fine examples of the various trace fossils which characterize this facies are to be found on the bedding surfaces, including Chondrites.

Fossils are abundant and rather diverse. Trilobites (usually fragmental) include Isotelus, Flexicalymene and rare Cryptolithus; the brachiopods Sowerbyella, Rafinesquina; Dinorthis and Dalmanella; bryozoans Prasopora, Eridotrypa and Stictopora; plus orthocone cephalopods and pelmatozoan debris. Gastropods, which are so abundant in the underlying Orwell limestone are exceedingly rare in the Glens Falls.

The Glens Falls here records the continuing deepening of the Middle Ordovician shelf that began with the deposition of the Phytopsis lime mudstones at Stop 2F. The shale interbeds and generally more argillaceous character of the Glens Falls document increase in terrigenous mud input, perhaps derived from the rising Taconic Orogenic complex to the east. Quartz and feldspar grains of volcanic origin are also common in insoluble residues of Glens Falls limestones, suggesting increased eruptive activity at this time.

The contrast in terrigenous content of the Chazy group vs. Black River and Trenton Groups is noteworthy. Insoluble residues from Chazy Group carbonates contain abundant, coarse-grained, rather angular quartz and feldspar grains (e.g. Stops 2B and 2D) whereas the Black River and Trenton Groups lack coarse sand-size grains and

contain either volcanic quartz and feldspar (Black River and Trenton Groups) or clay plus volcanics (Trenton Group). This change is likely related to a shift in available clastic course from the slightly emergent cratonic basement to the west that was exposed during Chazy Group deposition to the rising Taconic volcanic/metamorphic complex to the east during Black River-Trenton deposition.

Southern Extension of the Trip:

For those who are proceeding south from Crown Point, we are willing to offer brief additional stops in the upper Cambrian and lower Ordovician Beekmantown Group and Potsdam Sandstone in the vicinity of Ticonderoga, New York. If you wish to return via I87, return to Rts. 9N and 22, proceed south to Ticonderoga and then west on Rt. 74 to I87.

Acknowledgements

Both of us gratefully acknowledge the assistance of Brewster Baldwin of Middlebury College. Many of the ideas presented here were developed by Brewster during his numerous trips to the Crown Point localities with Middlebury students. One of us (BWS) has been fortunate enough to accompany Brewster to the exposures. BWS also acknowledges the support of the Petroleum Research Foundation of the American Chemical Society for support of research on the Chazy Group.

Bibliography

- BALDWIN, B., 1980, Tectonic significance of Mid-Ordovician section at Crown Point, New York: *Northeastern Geology*, v. 2, p. 2-6.
- BALL, M. M., 1967, Carbonate sand bodies of Florida and the Bahamas: *J. Sed. Pet.*, v. 37, p. 556-591.
- BATHURST, R., 1971, Carbonate Sediments and Their Diagenesis: Elsevier, 658 p.
- BIRD, J. and DEWEY, J., 1970, Lithosphere plate-continental margin tectonics and the evolution of the Appalachian Orogen: *Geol. Soc. Amer. Bull.*, v. 81, p. 1031-1060.
- CISNE, J., KARIG, D., RABE, B., and HAY, B., 1982, Topography and tectonics of the Taconic outer trench slope as revealed through gradient analysis of fossil assemblages: *Lethaia*, v. 15, p. 229-246.
- CLARKE, J. M. and SCHUCHERT, C., 1899, Nomenclature of the New York series of geological formations: *Science, New Ser.*, v. 110, p. 876.

- CONRAD, T. A., 1837, First annual report on the Geological Survey of the Third District of the State of New York: Assembly #161, p. 155-186.
- EMMONS, E., 1842, Geology of New York. Part 2, Comprising the Survey of the Second Geological District, 437 p.
- FISHER, D. W., 1968, Geology of the Plattsburg and Rouses Point, New York-Vermont Quadrangles: N.Y.S. Mus. and Science Service Map and Chart Ser. #10, 51 pp.
- _____, 1977, Correlation of the Hadrynian, Cambrian and Ordovician Rocks in New York State: N.Y.S. Mus. and Science Service Map and Chart Ser. #25, 75 pp.
- _____, 1984, Bedrock geology of the Glens Falls-Whitehall region, New York: N.Y.S. Mus. and Science Service Map and Chart Ser. #35, 58 pp.
- HOFFMAN, H., 1963, Ordovician Chazy Group in Southern Quebec: AAPG Bull., v. 47, p. 270-301.
- MATHER, W., 1943, Geology of New York. Part 1, Comprising the Survey of the First Geological District. 653 pp.
- MEHRTENS, C., 1984, Foreland basin sedimentation in the Trenton Group, central New York: N.Y.S.G.A. Fieldtrip Guidebook, 56th Annual Meeting, p. 59-98.
- OXLEY, P. and KAY, M., 1959, Ordovician Chazy series of the Champlain Valley, New York and Vermont: AAPG Bull., v. 43, p. 817-853.
- PURDY, E. G., 1963, Recent calcium carbonate facies of the Great Bahama Bank. 2. Sedimentary Facies: J. Geol., v. 71, p. 472-497.
- REINECK, H. and SINGH, I., 1980, Depositional Sedimentary Environments: 2nd edition, Springer-Verlag.
- SELLECK, B., 1980, A review of the Post-Orogenic history of the Adirondack Mountain Region: Geol. Soc. Amer. Bull., v. 91, p. 120-124.
- _____, 1982, Humid climate vs. arid climate peritidal carbonates: Ordovician of the northern Appalachians: Geol. Soc. Amer., Abstracts, v. 15, p. 92.
- _____, and BOSWORTH, W., 1985, Allochthonous Chazy (Early Medial Ordovician) limestones in Eastern New York: Tectonic and paleoenvironmental interpretation: Amer. Jour. of Sci., v. 285, p. 1-15.

SPEYER, S., 1982, Paleoenvironmental history of the Lower Ordovician-Middle Ordovician boundary in the Lake Champlain basin, Vermont and New York: Geol. Soc. Amer., Abstracts, v. 14.

VANUXEM, L., 1842, Geology of New York. Part 3, Comprising the Survey of the Third Geologic District. 306 pp.

GEOLOGY OF THE WILLSBORO WOLLASTONITE MINE

JAMES F. OLMSTED
S.U.N.Y. Plattsburgh
Plattsburgh, NY 12901

PAUL W. OLLILA
Vassar College
Poughkeepsie, NY

INTRODUCTION

The wollastonite deposits of this region are the world's major source of this important industrial mineral. Several occurrences of coarse wollastonite gneiss that is potential ore are known throughout the Willsboro and Ausable Forks quadrangles but to date only this and the Lewis deposit have been exploited. We have chosen this, now inactive, mine as the site for the trip because of excellent exposure of related rocktypes as well as unmatched display of structural and metamorphic features. The presently active Lewis mine is located at the other end of a fifteen kilometer long belt of metasediments that overlie the Westport anorthosite dome. Topics of particular interest are the mineralogy of the wollastonite unit, petrography of related units, mineralogical and textural relationships at contacts and the structural geology of the metasedimentary belt.

The trip will consist of a walking traverse in which we will study the lower half of the Willsboro metasedimentary belt. We begin at the lower portal of the mine and proceed north about 600 m. where we encounter the base of the "Midsection Anorthosite" a thick sill-like unit that divides the section into lower and upper parts. We will then cross the section in a westerly traverse to a point about a kilometer west of the lower portal where we will examine the wollastonite and the amphibolitic unit at the top of the Westport anorthosite dome. We then return along strike to the mine site where you can collect samples of the ore and related rocks. The entire hike is about three kilometers through wooded terrain but with one exception (a steep descent) it is not particularly difficult.

GEOLOGIC SETTING

Throughout the northeast Adirondack Mountains metasedimentary shelf type deposits are in contact with anorthosite dome-like structures. The infolded metasedimentary rocks include marble, calcsilicates of a variety of compositions, quartzite and gneisses that range from amphibolite to quartzofeldspathic in composition. Many of the latter two are thought to be of volcanic origin although some may have been intrusive. Emplaced into these units are intrusive rocks that range in composition from granite to gabbro and include anorthosite and related rocks. All of these have been subjected to granulite facies metamorphism which has altered the primary petrographic and structural features. Buddington and Whitcomb (1941) indicate the temporal sequence to begin with Grenville metasediments intruded by anorthosite, gabbro and granitic rocks all of which were deformed and metamorphosed. Our mapping indicates the metagabbro to be the younger rocktype. It occurs as dikes and sills and cuts the other three rock types. In this area we have mapped a large metagabbro sill that has intruded the metasediments above the wollastonite gneiss. We will examine its textural and contact relationships with surrounding rocks for the purpose of understanding influence it may have had on their formation.

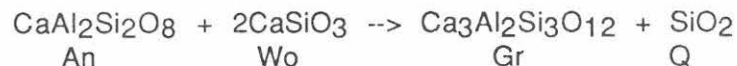
At the Willsboro mine, foliation strikes NNW and dips N about 30 degrees. Rare lineations trend and plunge to the northwest. Additional lineations have been observed at the Deerhead location about four kilometers west, where plunging folds and topography brings anorthosite to the surface beneath the axial region of a keel-like structure. From this point for about one kilometer east of Deerhead, along the belt towards Willsboro the metasediments are missing. It is interpreted that the metasedimentary belt is an isoclinal synform or keel-like structure in which plunge changes direction along strike of the belt. This results in apparent thinning and thickening ("porpoising") of the entire belt along strike.

While deformation and metamorphism associated with the Grenville orogeny has largely transformed original layering lithologic units have survived to a remarkable degree. Figure (1) indicates continuity of the thicker units along strike but in detail smaller units are discontinuous due to faulting, lensing and undoubtedly the "porpoising" noted above. Above the metasedimentary belt is found a thick a thick gabbroic anorthositic gneiss (Figure 2) indicated by Buddington and Whitcomb (1941) as strongly contaminated by metasediments that occur as "layers", "inclusions" and "schlieren" of mafic, garnet rich rock.

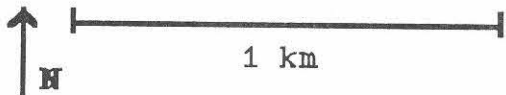
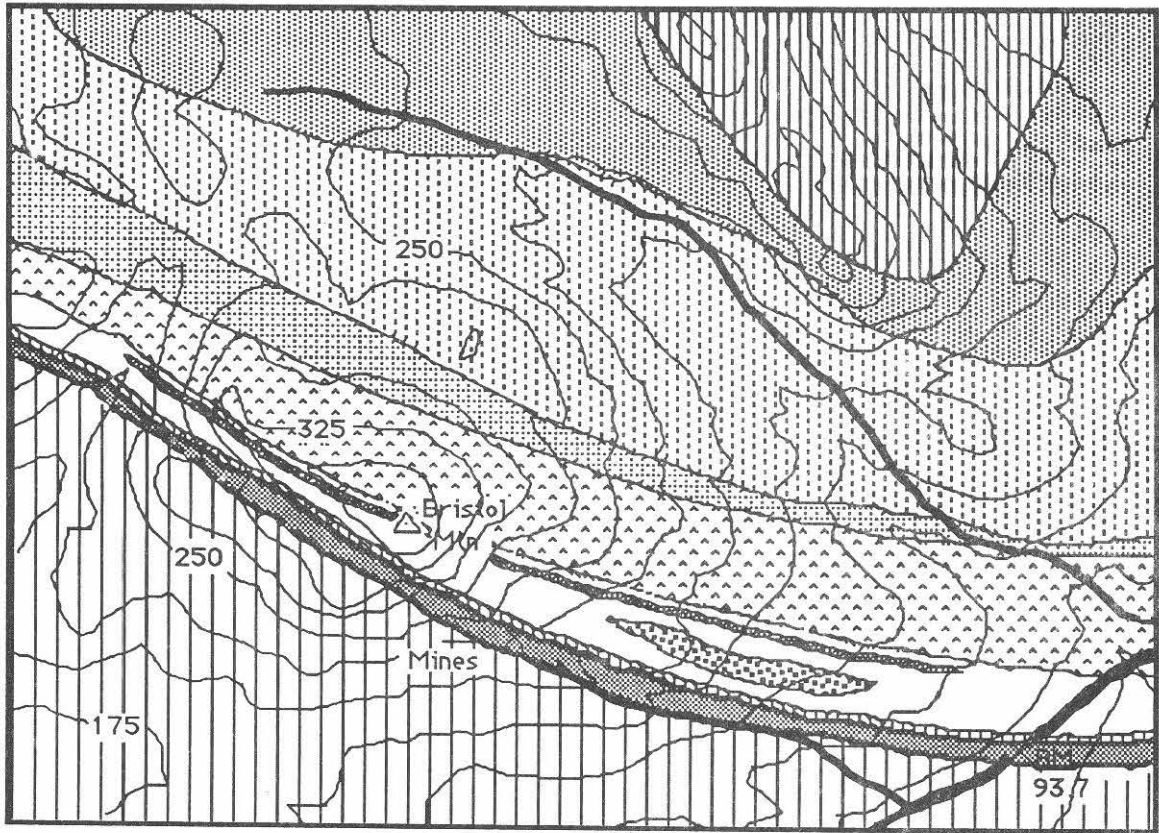
PETROGRAPHY AND MINERALOGY OF THE WILLSBORO MINE AREA

Structurally the lowermost unit of the mine area is the gabbroic anorthosite gneiss of the Westport dome (Figure 2). The rock generally contains large (>5 cm.) dark bluish megacrysts in a lighter bluish gray matrix. DeRudder (1962) has noted that in the mine area the anorthosite is overlain by a mafic rich gneiss that may be a few tens of meters thick. Our mapping has confirmed this but we find that at Deerhead, wollastonite is in contact with anorthosite. We will examine this contact at a point west of the mine area.

The ore consists of wollastonite, grandite garnet (Gr.10 to Gr.90) and calcium rich clinopyroxene (Di.40 to Di.70). The rocks are coarse with foliation defined by orientation of the flattened wollastonite and concentrations of the mafic minerals. The major compositional variation in this unit is the Al/Fe ratio in garnet and Mg/Fe in pyroxene. Within the wollastonite unit the mafic minerals are usually fine granular but garnet is often poikiloblastic. A second occurrence of the mafic phases is skarn-like masses along the edge or occasionally within the ore zone. These consist of grossularitic garnet and diopsidic clinopyroxene with minor quartz and albite. Shape of the skarn bodies ranges from thin (10-20 cm.) tabular masses that extend for several tens of meters along strike to thick (several meters) lenses with greater lateral extent. These are the metamorphic products of reaction between wollastonite and feldspar rich gneisses that are commonly in contact with the ore. The following reaction runs with falling temperature so the skarns are correctly considered to be retrograde.



Immediately above the wollastonite are small units of anorthositic and mafic gneisses. These in turn are overlain by calc-silicate gneisses and amphibolites, mafic and syenitic gneisses that are mixtures of metasedimentary and metaigneous rocks (Figures 2 & 3, Table 1). Major and trace elements (Table 2, Figures 4-6) as well as mineral compositions of these help distinguish the protolith and provide confidence for our field classification. In some exposures we find masses of garnetite (skarn) indicating repetition of units similar to the wollastonite found below. An interesting observation



contour interval 25m

Intrusive igneous rocks

Mixed Gneisses

-  Westport Dome anorthosite
-  gabbroic anorthosite gneiss
-  midsection anorthosite
-  upper anorthositic gneiss
-  metagabbro

-  pyx-gt-wo rock
-  calc-silicate, mafic gneiss
-  pyroxene-plagioclase gneiss
-  quartzite, marble, mixed gneiss
-  syenitic gneiss

Figure 1. Geologic map of the Willsboro wollastonite deposit, Willsboro, N.Y. The map area is located in the northern part of the Willsboro 7.5 by 15 minute quadrangle approximately 4 km southwest of the village of Willsboro.

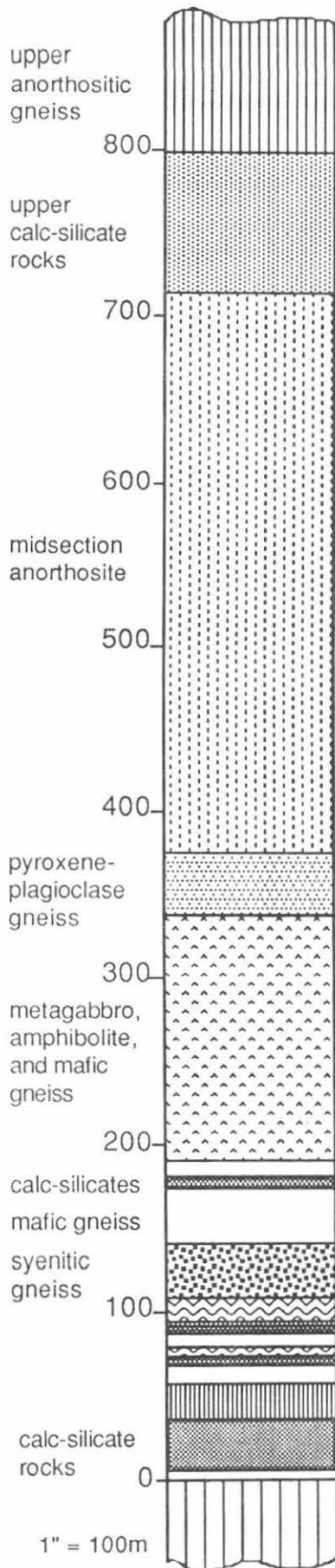


Figure 2. Stratigraphic column for the Willsboro wollastonite deposit. The column on the left is based on Figure 1. The expanded column on the right is based on a tape and compass traverse above the eastern portal at the Willsboro wollastonite mine. All of the calc-silicate rocks in the lower part of the column contain massive layers of grossular-rich garnet. The upper calc-silicate unit includes quartzite, marble, and gray, graphitic, diopside-rich rocks and is unlike the metamorphosed sediments found lower in the section. The mafic gneiss units are heterogeneous and include medium- to coarse-grained amphibolites, medium-grained, hornblende-garnet- pyroxene-plagioclase gneisses, and fine-grained biotite-garnet-hornblende- pyroxene-plagioclase gneisses and granulites. Representative modes are listed in Table 1.

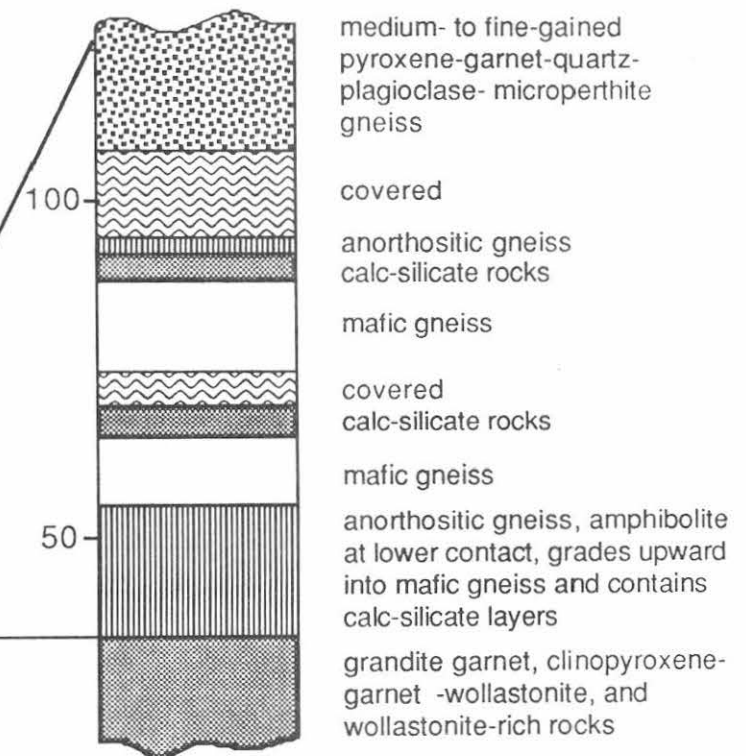


Table 1. Modes of metagabbro, mafic gneiss, and amphibolite associated with the Willsboro wollastonite deposit.

A. Metagabbro (w-27, w-86) and medium- to coarse-grained mafic gneisses that are included in the metagabbro unit shown in Figures 1 and 2.

Sample	w-27	w-86	w-27b	w-20	w-8
plagioclase	41	58	33	40	41
augite	20	4	20	36	2
orthopyroxene	6	7			
hornblende	12	16	34	13	37
biotite	0.2	2		0.6	
garnet	21	12	12	7	5
opaque		1	2	2	0.2
other		0.6	1	2	6

B. Medium- to coarse-grained amphibolites. Samples w-82, w-15, and w-12b are located north of the eastern portal of the Willsboro mine and are within the lower 200m of section shown in figure 2. Sample d138 is from drillcore 81-15.

Sample	w-82	w-15	w-12b	d138
plagioclase	25	38	32	27
augite	1.5	10	2	2
orthopyroxene			5	
hornblende	72	50	56	69
biotite		0.4		
garnet	1.5		4	
opaque			0.2	
other	0.3	0.9	0.6	1.5

C. Fine- to medium grained gneisses and granulites. Samples w-22 and w-24b are located above the middle portal at the Willsboro mine. Samples d132 and d132.5 are from drillcore 81-15. Samples w-81 and w-78 are located above the first portal, within the lower 100m of section shown in Figure 2. Sample w-78 contains bluish-gray plagioclase augen in a fine- to medium-grained, strongly foliated matrix. Sample w-81 is weakly foliated and contains medium-grained augite in a fine grained matrix. The augite grains contain abundant orthopyroxene exsolution lamellae.

Sample	w-22	w-24b	d132	d132.5	w-81	w-78
plagioclase	47	44	46	44	35	46
augite	18	3	13		11	17
orthopyroxene	10	13	13	16	15	
hornblende		36	20	36	23	21
biotite	13	0.2	3	2	5	
garnet		4	1		10	12
opaque	4	0.6	4	2	0.6	4
other	0.4			0.3		0.2

Table 2. Chemical analyses of hornblende-augite-plagioclase gneiss (W-21), metamorphosed gabbros (W-27,W-86), amphibolite (W-82), and mafic gneisses from Willsboro, New York.

Sample	W-27	W-27B	W-21	W-86	W-78	W-81	W-82	W-15
SiO ₂	48.07	46.04	49.20	47.98	47.65	48.15	44.56	48.73
TiO ₂	0.72	2.13	1.02	0.61	2.51	1.95	2.28	1.38
Al ₂ O ₃	18.33	16.47	9.59	21.55	18.20	15.60	15.64	17.98
Fe ₂ O ₃	11.56	13.93	10.21	8.7	12.77	13.66	14.81	11.48
MnO	0.15	0.17	0.15	0.11	0.2	0.18	0.18	0.16
MgO	8.86	6.62	10.54	8.02	3.84	7.68	7.98	6.59
CaO	9.79	11.29	17.85	10.33	10.77	8.83	10.86	9.39
Na ₂ O	2.61	2.87	1.53	2.52	3.54	3.08	2.8	3.47
K ₂ O	0.42	0.49	0.13	0.41	0.6	1.09	1.03	0.75
P ₂ O ₅	0.02	0.02	0.01	0.07	0.43	0.30	0.27	0.21
Total	100.53	100.01	100.21	100.30	100.51	100.53	100.39	100.15

Trace elements (ppm)								
V	108	285	599	63	201	204	269	143
Cr	126	77	252	16	58	80	123	73
Ni	131	86	35	115	27	98	89	86
Zn	98	138	54	71	123	127	113	111
Sr	331	491	169	374	421	279	374	329
Zr	14	28	22	33	158	133	98	103
Nb	0.4	0.8	0.4	1.2	6.6	5	5	3.7
Ba	165	221	22	123	169	329	183	224
La	0	0.4	0	2.9	16	12	5.5	8.5
Ce	1.8	7.4	7.4	9.9	40	34	31	25

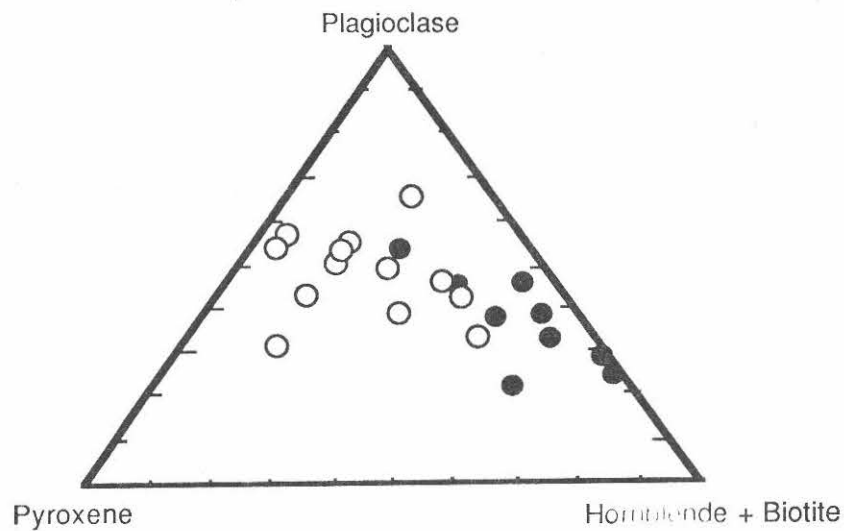


Figure 3. Modes of mafic gneisses and amphibolites from Willsboro, NY plotted on the triangle plagioclase-pyroxene- hornblende + biotite. The samples plotted in black were collected within approximately one meter of a contact with calc-silicate rocks. Other samples were collected at greater distances from contacts with calc-silicate rocks.

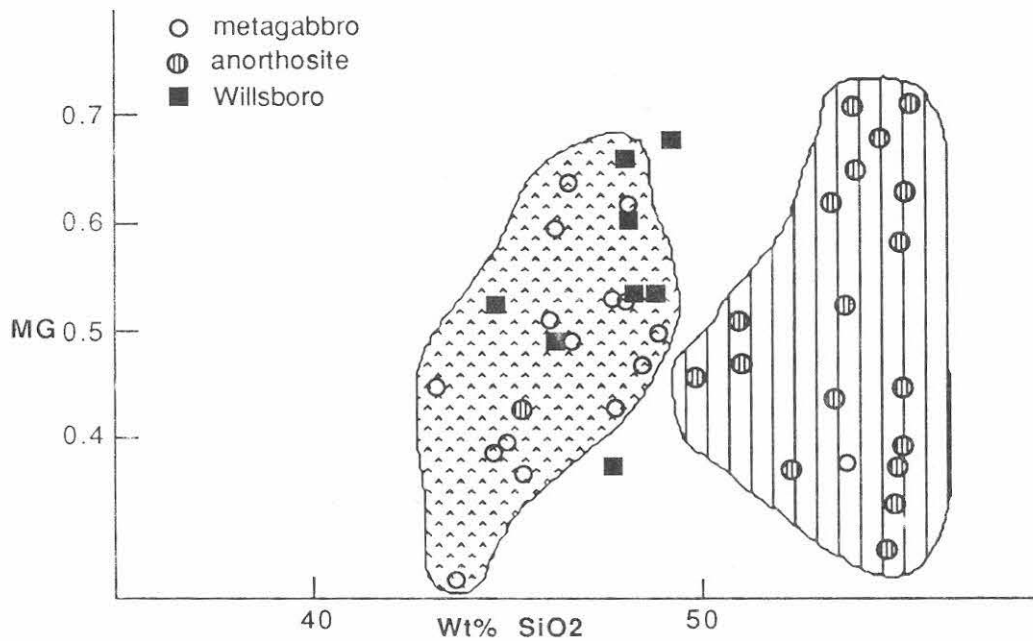


Figure 4. MG (100 Mg/Mg+Fe) versus wt.% SiO₂ for spinel bearing metagabbros, gabbroic anorthosites, and mafic gneisses from Willsboro. The lined pattern on the right encloses 15 of 16 gabbroic and noritic anorthosite analyses from Buddington (1939), Clough (1987), and unpublished analyses from Ollila. The pattern on the left encloses 15 of 16 metagabbro analyses from Buddington (1939), and Gasparik (1980). Analyses of spinel-bearing metagabbros are shown, however, other metagabbros and amphibolites show a similar pattern. Spinel was chosen as a discriminant because it is rare in anorthosite related rocks. Note that six of the eight analyses from Willsboro fall within the metagabbro field. The two analyses that are outside the field are w-78, which contains plagioclase augen and is thought to be anorthosite related and w-21, a calc-silicate gneiss.

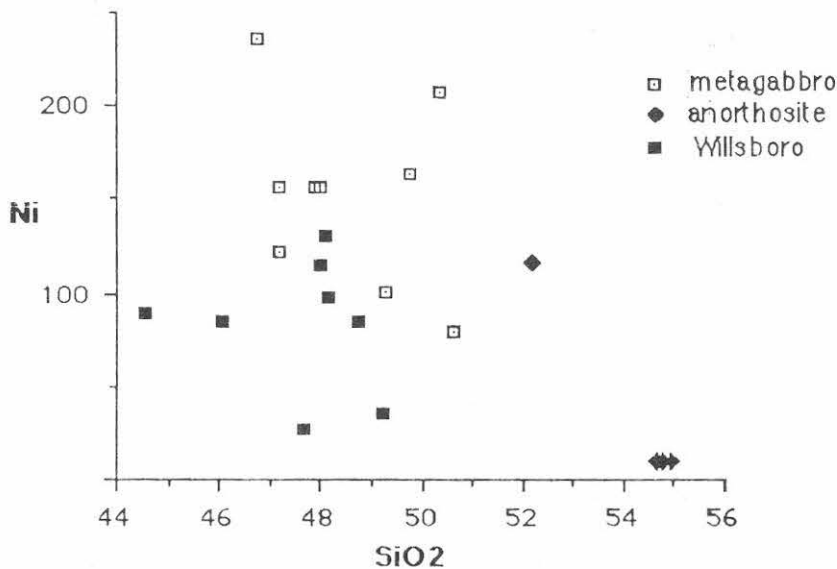


Figure 5. Metagabbro (Buddington, 1939; Clough, 1987), gabbroic anorthosite (Clough, 1987), and mafic gneisses from Willsboro plotted on Ni (ppm) versus wt.% SiO₂. The two Willsboro samples that have low Ni contents are samples w-78 and sample w-21. The other mafic gneisses and amphibolites have Ni contents more typical of metagabbro.

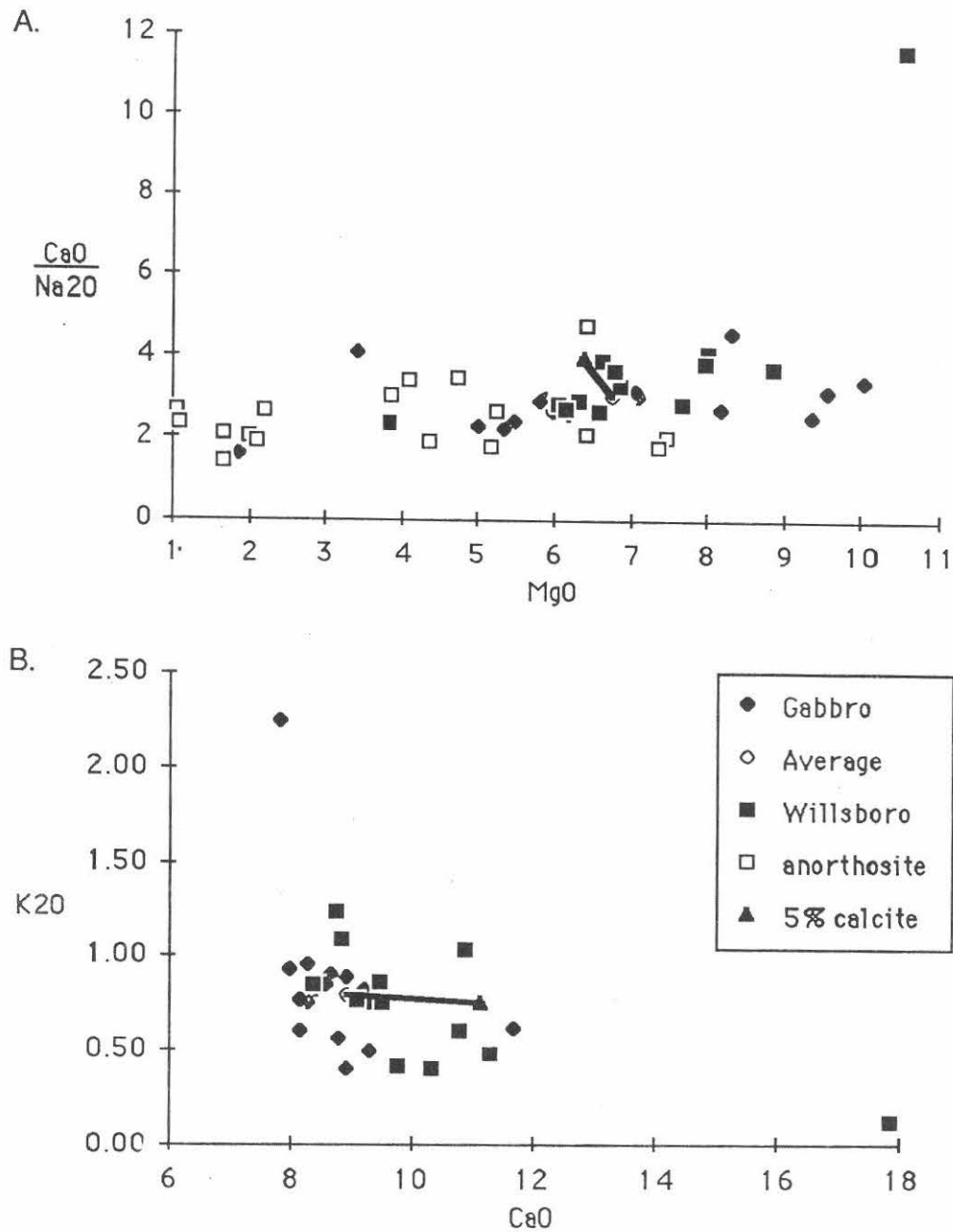


Figure 6. Chemical analyses of rocks from Willsboro, NY, plotted on the diagram CaO/Na₂O vs. MgO and K₂O vs. CaO (adapted from Hollocher, 1985). Gabbroic and noritic anorthosite analyses (n=16) were selected from Buddington (1939), Clough (1987), and unpublished analyses from Ollila. Spinel bearing metagabbro analyses (n=16) are from Buddington (1939) and Gasparik (1980). The average of the 16 metagabbro analyses and a composition determined by adding 5% calcite to the average composition are shown connected by a line. Note that the Willsboro samples either have compositions that closely resemble those of igneous metagabbros, or have compositions that can be explained by the assimilation of only modest amounts of calcite (or wollastonite). The CaO-rich sample in each plot is w-21, a calc-silicate gneiss.

that can be used locally as an exploration tool for wollastonite is that it weathers readily leaving topographic depressions and virtually no outcrop where it occurs near the surface. As a result we are left with these garnetite skarns as sole clues to the presence of wollastonite. Higher in the section we find a metagabbro unit that has been mapped over five kilometers along strike (figures 1 & 2). This unit preserves fine examples of relict igneous texture but grades to amphibolite at lower and upper contacts with metasediments (Figure 3). This supports the notion that a fluid phase was present during the metamorphism of the metagabbro.

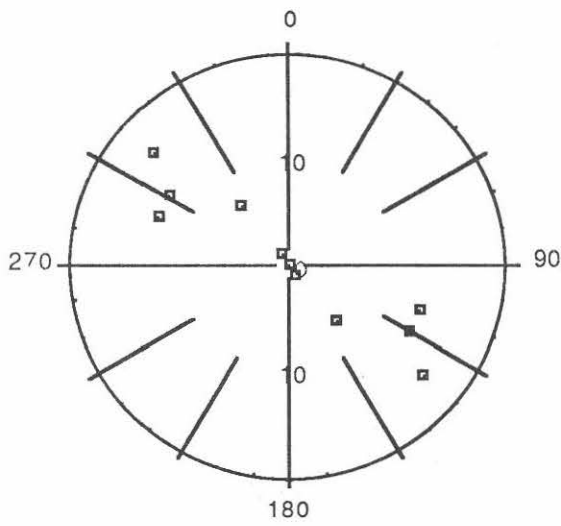
The uppermost unit that we will examine is a thick sill-like body of gabbroic anorthosite gneiss. This extends the entire length of the Willsboro belt and is readily distinguished from the massif anorthosite in both composition and texture. This represents either a contaminated anorthosite intrusive or an unusual intermediate magma composition. Its most distinguishing feature relative to the massif anorthosite is the absence of the blue megacrysts that are so typical of rocks closely related to the massif anorthosite. Its texture is granoblastic with an occasional large almandine poikiloblast. Another interesting feature of this unit is its striking similarity to a sill-like body that occurs in the metasedimentary section surrounding the Jay dome anorthosite some fifteen kilometers west of the present site.

OXYGEN ISOTOPES

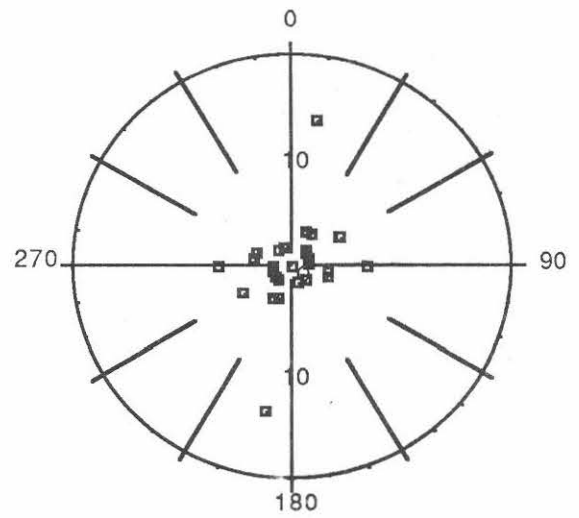
Valley and O'Neil (1982) suggested, on the basis of exceptionally low ^{18}O values, that the Willsboro wollastonite deposit formed at relatively shallow levels (<10 km.). They interpret the wollastonite to be a contact metasomatic deposit produced at the margin of an anorthosite intrusion and, because the low ^{18}O values require involvement of meteoric water, have provided a powerful argument in favor of the shallow intrusion of anorthosite. There are, however, a number of problems associated with the shallow intrusion hypothesis. These have been summarized by Bohlen et al. (1985) and by Ollila et al. (1988). One of the main purposes of this study was to see if other explanations for the low ^{18}O rocks are possible.

The details of Valley and O'Neil's study open a number of interesting questions. In particular, the high ^{18}O gradients within the ore zone and the lack of low ^{18}O plagioclase in anorthositic rocks both here and in highly contaminated anorthositic rocks that overlie the wollastonite deposit (Valley and O'Neil, 1982; Morrison, 1987) seem at odds with the model that Valley and O'Neil have presented.

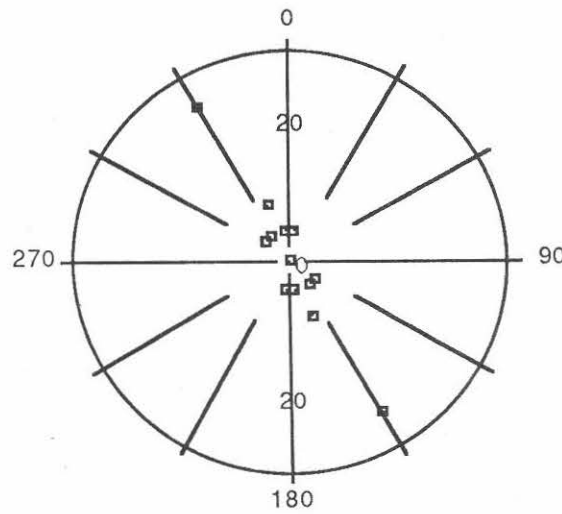
Initially, Ollila et al. (1987) thought that the low ^{18}O values could be explained by a model involving exchange with metamorphic fluids and then further oxygen exchange with late-stage, lower-temperature fluids. The basis for this was the pervasive occurrence of low temperature alteration in associated calc-silicate rocks, the near absence of such alteration in mafic gneisses and anorthositic rocks, and the fact that coexisting minerals analyzed by Valley and O'Neil yielded temperatures of 73°C (Wo-Cpx) and 240°C (Gt-Cpx) according to the thermometers of Mathews et al. (1983) and Bottinga and Javoy (1975). These temperatures are outside the calibrated range of the geothermometers and the uncertainties are extremely large. Consequently, they do not indicate the temperature at which the deposit last equilibrated but do leave open the possibility of low temperature exchange. Kinetic arguments, however, make the model presented above seem unlikely because oxygen isotopic ratios would have to be lowered during the initial metamorphic event to values below what might reasonably be expected during regional metamorphism.



Westport Dome



Central Anorthosite



Northern Anorthosite

Figure 7. Strikes of metagabbro dikes shown on the geologic map of the Willsboro quadrangle (Buddington and Whitcomb, 1945). Frequency % on 10 degree intervals.

An alternate hypothesis is that hydrothermal convection systems involving meteoric water were driven by metagabbro intrusions. This hypothesis is based on the following observations:

- 1) The majority of the mafic gneisses at Willsboro appear to have chemistries more appropriate to metagabbro than anorthosite (Figures 4-6).
- 2) Isotopic data presented by Valley and O'Neil (1982) shows that the only rocks at Willsboro with plagioclase ^{18}O lower than typical for Adirondack igneous rocks are amphibolites that are interlayered with wollastonite ores.
- 3) Modal data (Figure 3) suggests that the calc-silicate rocks acted as conduits for fluids because metaigneous rocks near contacts with calc-silicate rocks are more hydrated. Furthermore the observed low temperature alteration in the calc-silicate rocks demonstrates that they are effective channels for fluids in brittle environments.
- 5) There is a strong correlation between low ^{18}O plagioclase elsewhere in the Marcy anorthosite massif and the occurrence of metagabbro (Taylor, 1969; Morrison, 1987).

An important unanswered question is the circumstances and timing of the intrusion of the metagabbros. Lohead and McLelland (1987) provided evidence that certain metagabbros in the Adirondacks were intruded after a high grade regional metamorphism and that this intrusive event was followed by another metamorphic event.

Metagabbro is far less deformed than anorthosite and metagabbro dikes cut anorthosite and locally anorthositic gneiss. Metagabbro dikes exhibit northwest trends in both the Willsboro quadrangle (Figure 7) and in the Mt. Marcy quadrangle (Adinolfi, 1974). This indicates that the anorthosite was rigid enough to fracture at the time when metagabbro was intruded and suggests that the region experienced NE-SW extension during this time period. Elsewhere, however, anorthositic gneisses and metagabbros are strongly foliated, are concordant, and are deformed together in upright folds. This sort of relationship can be seen in road cuts at the Willsboro exit of the Adirondack Northway (I-87). Ambiguous relationships such as these were also described by Buddington and Whitcomb (1941). These relationships can be explained by intrusion of metagabbro between two metamorphic events or by metagabbros cutting a protoclasic foliation in anorthosite. More field work is necessary to answer this question.

If the metagabbros were intruded at relatively shallow levels after other rocks, including anorthosite, were metamorphosed, the model presented above can provide answers as to why high ^{18}O gradients exist at Willsboro, why anorthositic rocks do not contain low ^{18}O plagioclase, and can explain the spotty occurrence of low ^{18}O plagioclase elsewhere in the Marcy anorthosite massif. While it seems quite possible that low ^{18}O rocks can be explained by the intrusion of metagabbro, the significance of this finding in terms of the intrusion history of anorthositic rocks awaits more knowledge of the temporal relationship between anorthosite and metagabbro.

ECONOMIC GEOLOGY

Coarse potentially recoverable wollastonite has been discovered at four sites along the perimeter of the Westport dome. In all of these the wollastonite is found in contact, or nearly so, with anorthosite. At present only two of these have proven to be economic but its many uses as an industrial mineral make it an attractive target for exploration. Poor exposure due to its solubility and lack of any strong geophysical contrasts make exploration difficult with the result that the major methods of discovery are field mapping and luck.

REFERENCES CITED

- Adinolfi, F. (1974) Joint patterns and the petrology of dikes in the High Peaks region of the Adirondack Mountains. Senior Honors Thesis, University of Massachusetts, 39p.
- Bohlen, S.R., Valley, J.W., and Essene, E.J. (1985) Metamorphism in the Adirondacks. I. Petrology, Pressure and Temperature. *Journal of Petrology*, 26, 971-992.
- Bottinga, Y. and Javoy, M. (1975) Oxygen isotope partitioning among the minerals in igneous and metamorphic rocks. *Reviews of Geophysics and Space Physics*, 13, 401-418.
- Buddington, A.F. (1939) Adirondack igneous rocks and their metamorphism. *Geological Society of America Memoir* 7, 354p.
- Buddington, A.F. and L. Whitcomb (1941) Geology of the Willsboro quadrangle, New York. *New York State Museum Bulletin*, 325, 137p.
- Clough, R. (1987) Geochemistry of anorthosite of the Marcy Massif and an olivine metagabbro body in Moriah, N.Y. Senior Honors Thesis, Middlebury College, Middlebury, Vermont, 55p.
- DeRudder, R.D. (1962) Mineralogy, petrology, and genesis of the Willsboro wollastonite deposit, Willsboro quadrangle, New York. Ph.D. thesis, Indiana University, 156p.
- Gasparik, T. (1980) Geology of the Precambrian rocks between Elizabethtown and Mineville, Eastern Adirondacks, New York. *Geological Society of America Bulletin* 91, 78-88.
- Hollocher, K. (1985) Geochemistry of metamorphosed volcanic rocks in the middle Ordovician Partridge Formation, and amphibole dehydration reactions in the high-grade metamorphic zones of central Massachusetts. Contribution No. 56, Department of Geology and Geography, University of Massachusetts, Amherst, MA., 275p.
- Lochead, A. and McLelland, J. (1987) Evidence for multiple metamorphic events in the Adirondack Mountains, N.Y. *Geological Society of America Abstracts with Programs*, 19, 27.

- Mathews, A., Goldsmith, J.R., and Clayton, R.N. (1983) Oxygen isotope fractionations involving pyroxenes: the calibration of mineral pair geothermometers. *Geochimica et Cosmochimica Acta*, 47, 631-644.
- Morrison, J. and Valley, J.W. (1986) Contamination of the Marcy Anorthosite Massif, Adirondack Mountains, NY: petrologic and isotopic evidence. *Contributions to Mineralogy and Petrology*, 98, 97-108.
- Ollila, P.W., Jaffe, H.W., and Jaffe, E.B. (1988) Pyroxene exsolution: an indicator of high pressure igneous crystallization of pyroxene-bearing quartz syenite gneiss from the High Peaks region of the Adirondack Mountains. *American Mineralogist*, 73, 261-273.
- Ollila, P.W., Greeman, D.A., and Olmsted, J.F. (1987) The geology of the Willsboro wollastonite deposit: shallow versus deep emplacement of Adirondack anorthosite. *Geological Society of America Abstracts with Programs*, 19, 49.
- Taylor, H.P. Jr. (1969) Oxygen isotopic studies of anorthosites with particular reference to the origins of bodies in the Adirondack Mountains, New York. *New York State Museum and Science Service Memoir* 18, 111 - 134.

ROAD LOG

Because there is only one stop on this trip an abbreviated road log will be used beginning at the intersection of NY routes 9 & 22 at exit 33 of the Adirondack Northway (I-87).

Miles	Cumulative	
0.0	0.0	Leaving the intersection head east (south) on NY 22 towards Willsboro.
6.7	6.7	Turn right on Fish and Game Road just after sign indicating Willsboro village limit.
0.3	7.0	Bear right
0.7	7.7	Road left, Continue straight.
0.5	8.2	Bear right on Mtn. View Road at YIELD sign.
0.5	8.7	Joe Rivers Road to right, continue on Mtn. View road.
0.4	9.1	Turn right on unpaved (white mine tailings) road up hill to mine. Park on right if gate is closed or continue up road to first portal.

From the east end of the lower portal of the mine we will climb up over the exposed bedrock, carefully examining the rocktypes as we climb. In the immediate area of the mine they include; wollastonite ore, garnetite, gabbroic anorthosite gneiss, syenitic gneiss and a very mafic appearing calc silicate gneiss. We will point out several structural features as we move up the hill. Higher in the woods we will see evidence of repetition of the wollastonite rock in the form of another garnetite unit. The northernmost extent of the traverse will be indicated by an anorthositic unit that forms a prominent ridge. At this point we turn southwesterly back across the valley where we

encounter more mafic calcsilicates, then up the hill to a large exposure of metagabbro. We will continue southwesterly over Bristol Mountain and down into the next valley where we will examine among other things, the base of the wollastonite unit, its upper contact and the underlying rocks of the Westport Dome. We will then walk easterly along strike of the wollastonite unit past the mine area where you may collect ore samples to your heart's content and back to the cars.

Optional stops may include the westward extension of the Willsboro belt where it crosses the Adirondack Northway and the Deerhead location which is another similar wollastonite occurrence that can provide additional structural insight as well as opportunity to examine other rocktypes in the section.

The following is an abstract of the address by Professor McLelland at the banquet of the Sixtieth annual meeting of the New York State Geological Association, October 8, 1988.

U-Pb Zircon Geochronology of the Adirondack Mts. and Tectonic Implications
McLelland, James M., Geology Dept., Colgate Univ., Hamilton, NY 13346

Zircons from metatonalites in the southern and eastern Adirondacks give Pb-Pb age of 1301 Ma, interpreted as their minimum emplacement age. Metatonalite from the eastern Adirondacks yields an upper intercept age of 1321 ± 60 Ma. It is inferred that these, and intervening metatonalite (1318 ± 20 Ma) northwest of Saratoga Springs, represent a broad zone of ~1300 Ma calcalkaline magmatism. Associated with these units are granodioritic masses (batholiths?) yielding ages of 1235 Ma. Compositionally the metatonalite are similar to the Elzevirian plutons of the Central Metasedimentary Belt (CMB), and it is suggested that both are the result of arc-related magmatism associated with the collision of microplate fragments derived from an early (1800-1600?) supercontinent disrupted during 1450-1350 Ma anorogenic magmatism. This event is believed related to 1415 ± 6 Ma leucogranitic gneiss exposed in the Frontenac Arch. These leucogranitic gneisses crosscut quartzites (zircon ages: 1600-1910 Ma) which must be older than any rock yet recognized in the CMB or Adirondacks and suggest that the Frontenac Terrane has a different history than neighboring terranes.

Marginally calcalkaline leucogranitic gneiss in the Adirondack Lowlands yield U-Pb zircon ages of 1230-1290 Ma and may represent a second Adirondack magmatic arc. Abrupt termination of the leucogranitic gneiss at the Highland-Lowland boundary suggests that the boundary may represent a cryptic suture. Late (~950 Ma) collapse of the orogen probably cropped the Lowlands down to the northwest along this same zone.

Foliated garnet-sillimanite xenoliths in olivine metagabbros dated by U-Pb zircon at 1144 ± 7 Ma may record ~1200-1300 Ma metamorphism accompanying docking associated with the microplates and magmatic arcs described above. The olivine metagabbros appear to belong to the anorogenic, or rift-related, anorthosite-mangerite-charnockite (AMC) magmatism that disrupted eastern portions (Fennoscandia?) of the newly assembled continent at ~1160-1130 Ma. Subsequent closure along S.E. dipping subduction zones resulted in the ~1100-1000 Ma Ottawa phase of the Grenville orogenic cycle. In the Adirondacks this event was accompanied by extreme deformation, doubling of crustal thickness, granulite facies metamorphism, and granitic plutonism at ~1100-1060 Ma. The granites fall into an 1100-1090 Ma suite of hornblende granitic gneiss and magnetite-bearing alaskitic rocks that yield ages of 1070-1060 Ma. These granitic rocks may have supplied substantial heat for the granulite facies metamorphism.

Careful dating of baddeleyite and air abraded zircons from the Marcy anorthosite clearly demonstrate that its emplacement age is somewhat greater than 1110 Ma. A maximum age of the anorthosite is fixed by the crosscutting relationships of sheets of Whiteface type anorthositic gneiss relative to hornblende granitic gneiss dated at 1135 ± 5 Ma. It is concluded that Adirondack anorthosites were emplaced coevally with mangeritic and charnockitic rocks dated at 1130-1160 Ma. The mafic and granitoid suites do not appear to be comagmatic.

This work has been undertaken with the N.Y. Geological Survey and with Jeff Chiarenzelli who performed the age determinations.